Identification and characterisation of progenitor cells for the thymic epithelium

Andrea Ruth Bennett

Thesis presented for the degree of Doctor of Philosophy

University of Edinburgh

2001

EX BIBL. UNIV. EDINBURGH

I declare that the work presented in this thesis is my own,
except where otherwise stated.

Andrea Bennett

To my parents

Acknowledgements

I would like to thank my supervisor Clare Blackburn for giving me this opportunity and for being a great supervisor: thanks for your enthusiasm, guidance and support. Thanks also go to all members of the Blackburn lab, especially Julie Gordon for many hours of embryo dissection, Clare Bennett for help and advice and Alison Farley for numerous coffee breaks. Many other members of the CGR have helped me along the way, special mention goes to the animal house staff for looking after my animals and putting up with my frequent requests. Thank you to the members of my PhD committee: Rick Maizels, Judy Allen and Alexander Medvinsky for helpful advice and discussion.

Special thanks go to Clare for always being there, Al and Julie for nights out and Derek for the early days. Thanks also go to Colin who always believed in me and encouraged me. I would have been unable to work for my PhD without the constant support and unerring love of my parents, and to them I am forever indebted. Finally, thanks to Ray for love, weekends off, stress-busting chocolate, and helping me see the light at the end of the tunnel.

Abstract

The stromal cells of the thymus provide the microenvironments necessary for T-cell maturation and repertoire selection. The thymic stroma consists of distinct subpopulations of epithelial and non-epithelial cells which regulate the development of thymocytes. This work evaluates the hypothesis that the mature epithelial subpopulations present in the adult thymus derive from a progenitor cell population in the thymic primordium marked by two monoclonal antibodies, MTS20 and MTS24. Analysis of cells in the embryonic day 12.5 (E12.5) thymic primordium showed that MTS20 and MTS24 were expressed by approximately 50% of epithelial cells and these cells did not express markers associated with terminally differentiated thymic epithelium. Furthermore, MTS20 and MTS24 were strongly down regulated during thymus ontogeny, and in the adult, reacted only with rare medullary epithelial cells. The MTS20/24$^+$ population purified from E12.5 thymi expressed *whn*, *Pax1*, *Pax9* and *Hoxa3*, transcription factors required during early thymus development.

To assess the functional potential of MTS20/24$^+$ cells, purified E12.5 thymus cell populations were grafted under the kidney capsule of *nude* mice. Immunohistochemical analysis of MTS20/24$^+$ cell grafts demonstrated the presence of mature cortical and medullary thymic epithelium. These grafts were also capable of attracting lymphoid progenitors and of supporting thymocyte differentiation. Furthermore, mature single positive T-cells were present in the periphery of *nude* mice grafted with MTS20/24$^+$ cells indicating that these cells can confer thymus function to athymic recipients. The MTS20/24$^-$ cells from E12.5 thymi could fulfil none of these functions. These data demonstrate that the MTS20/24$^+$ population from the thymic primordium contains progenitor cells that can give rise to the major epithelial populations and generate a functional thymic microenvironment.

Contents

Chapter 1

INTRODUCTION

1.1. The vertebrate immune system

Vertebrate species have advanced immune systems that are able to clear pathogens rapidly and effectively (For an overview of the immune system see Engelhard 1994; Abbas *et al.,* 1997; Parham 2000). The immune system is composed of two arms: the innate immune system and the acquired immune system. Innate immunity, mediated by granulocytes, macrophages and natural killer cells, responds non-specifically to foreign molecules. The acquired immune system can specifically discriminate between pathogens and make appropriate responses. Acquired immunity is mediated by B-lymphocytes and T-lymphocytes, which both display receptors specific for particular foreign antigens on their surface. This specificity results from the diversity of their receptors, which allow recognition of at least 10^8 different molecular structures. The acquired immune system can discriminate between self and non-self, which ensures a response only to foreign molecules. It also exhibits immunological memory, that is, a second encounter with the same antigen induces a heightened immune response. Humoral immunity involves B-lymphocytes which produce antibodies specific for a particular antigenic target and can thus provide a focus for other immunological molecules and cells during pathogen clearance. Cell-mediated immunity involves T-lymphocytes, which are able to recognise pathogens

by virtue of specific T-cell receptors (TCR) on their surface. The TCR binds to fragments of peptide derived from the pathogen. These peptides are displayed on the cell surface in a complex with host major histocompatibility complex (MHC) proteins. Cytotoxic T-cells, distinguished by expression of surface CD8, lyse cells upon recognition of specific MHC Class I-peptide complexes displayed on the surface of infected cells. Helper T-cells, distinguished by surface expression of CD4, are activated by recognition of specific MHC Class II-peptide complexes on specialised antigen-presenting cells (dendritic cells (DC), macrophages or B-cells), and subsequently secrete cytokines to promote differentiation of other immune system cells to aid in the clearance of infection. Thus, T-cells are able to identify and kill infected cells with exquisite specificity.

The majority of T-cells develop within a specialised organ, the thymus (Miller 1961). T-cell progenitors enter the thymus from the bone marrow and subsequently undergo a series of differentiation and selection events before exiting into the periphery as mature naïve T-cells. The selection events within the thymus ensure that the peripheral T-cell repertoire is self-MHC restricted and tolerant to self-antigens. These maturation events occur through interactions between the thymocytes and the stromal cells of the thymus, which include epithelial cells, thymic dendritic cells and macrophages. T-cell development is absolutely dependent on the microenvironment provided by the thymic stroma as, unlike other cells of the immune system, thymocytes cannot be matured and selected *in vitro*.

The steps involved in intra-thymic T-cell development have been elucidated by a large amount of experimental research over the last forty years. Until recently, however, less was known about the cells of the thymic stroma and the role they play in regulating thymocyte development and selection. This chapter reviews the literature on the thymus and intra-thymic T-cell development. Section 1.2 discusses the structure of the thymus and the cells which comprise the thymic stroma. Section 1.3 summarises the maturation and selection of T-cells within the thymus and the

role that the stroma plays in regulating these events. Section 1.4 outlines the development of the thymus and thymic epithelial cell populations during ontogeny and the molecular events controlling thymus organogenesis. Section 1.5 discusses evidence for the idea of 'thymic crosstalk', the interdependence of thymocytes and thymic stromal cells. Section 1.6 summarises current knowledge about *Foxn1*, the gene mutated in *nude* mice, which is required for the development of mature thymic epithelium. Finally, section 1.7 outlines the aims of this project and the experimental approach taken.

1.2. Structure of the thymus

1.2.1. Morphology

The morphology and cellular composition of the mature thymus is illustrated in Figure 1.1 (for reviews of thymus structure see (Kendall 1991; van Ewijk 1991; Boyd *et al.,* 1993; Anderson *et al.,* 1996; van Ewijk *et al.,* 1999). The thymus is an encapsulated, bilobed organ which is situated at the midline above the heart in humans and rodents (Kendall 1991). Each lobe is divided into multiple lobules by fibrous septae or trabeculae which penetrate into the cortex to the cortico-medullary junction (CMJ) forming a subcapsule around each lobule (Boyd *et al.,* 1993). Each lobule is composed of outer cortical and inner medullary epithelial networks which are packed with developing thymocytes (van Ewijk 1991). The thymus is extensively vascularised with capillaries branching throughout the cortex and medulla (Norment and Bevan 2000). The capillaries are surrounded by perivascular spaces (PVS), which contain various accessory cells such as neutrophils, mature T and B

Figure 1.1. Morphology of the thymus
A: Organisation of the thymus into lobules consisting of cortical and medullary epithelium. (From Abbas 1997)

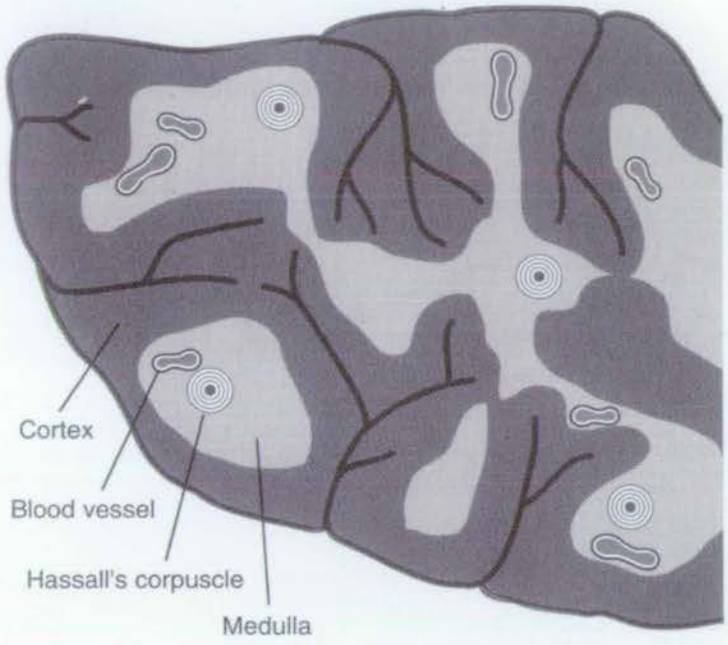

B: Cellular organisation of the thymus (From Parham 2000)

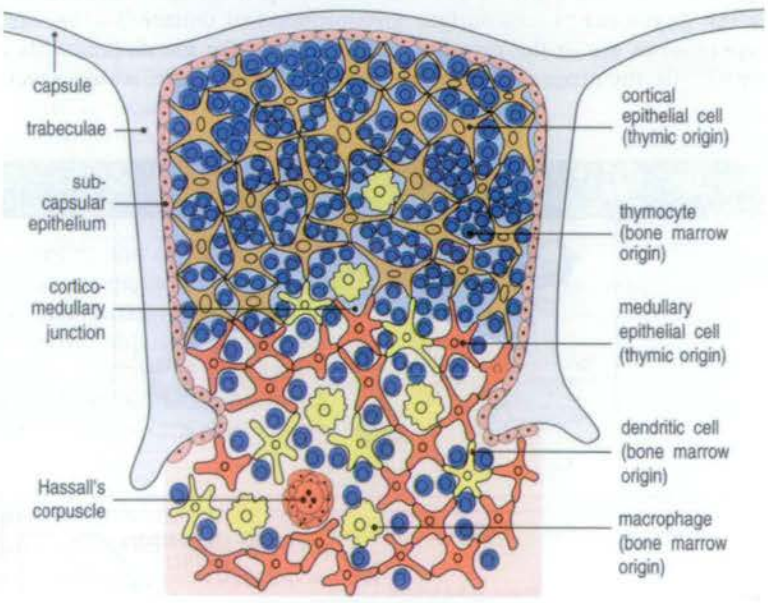

lymphocytes and macrophages (Boyd *et al.,* 1993; Norment and Bevan 2000).

1.2.2. Thymic stromal cells

1.2.2.1. Non-epithelial cells

The majority of stromal cells within the thymus are epithelial cells, however there are also many non-epithelial cell types present: macrophages, dendritic cells, fibroblasts and vascular endothelium (Boyd *et al.,* 1993). Thymic macrophages are found in the connective tissue, cortex and medulla of the thymus, especially at the CMJ (Nabarra and Papiernik 1988). Thymic DCs (or interdigitating cells (IDC)) are present mainly in the medulla of the thymus, also at a higher density at the CMJ (Nabarra and Papiernik 1988). Thymic macrophages and thymic DCs are thought to develop *in situ* from early T-cell precursors which enter the thymus through the vasculature (Ardavin *et al.,* 1993; Ardavin 1997). Thymic macrophages and DCs can be identified by staining with monoclonal antibodies (mAbs) raised against these cell-types from other peripheral lymphoid organs (Brekelmans and van Ewijk 1990). For example, Mac-1 and Mac-2 react with both macrophages and DCs (Nabarra and Papiernik 1988). Thymic macrophages and thymic DCs are MHC Class II positive (Nabarra and Papiernik 1988; Brekelmans and van Ewijk 1990).

The extracellular matrix (ECM) consists of collagens, reticulin fibres and glycoproteins such as laminin and fibronectin (Brekelmans and van Ewijk 1990; Boyd *et al.,* 1993; Anderson *et al.,* 2000). ECM is found in the capsular and septal fibres, in a fine network throughout the cortex and medulla and on thymic nurse cells (see section 1.2.2.2.) (Savino *et al.,* 1993; Anderson *et al.,* 1997). Various antibodies are available which stain different components of the ECM. For example, ER-TR7 recognises fibroblasts and ECM components in the capsule and septa (van Vliet *et*

al., 1984) and MTS 16 recognises basement membrane-associated connective tissue lining the capsule, PVS and blood vessels (Godfrey *et al.*, 1990).

1.2.2.2. Epithelial cells

Ultrastructural examination of the thymus has revealed a large degree of heterogeneity within the thymic epithelial cells (TEC) (Kendall and Boyd 1991). TEC have been classified into 6 types based on descriptions of human thymus (van de Wijngaert *et al.*, 1984). These are as follows:

Type 1 - Subcapsular/perivascular lining. Characterised by well-defined basement membrane which forms a continuous sheet that lines all subcapsular and perivascular regions.

Type 2, 3, 4 - Cortical epithelial cells. Type 2 cells are found primarily in the outer cortex adjacent to the type 1 cells, whereas type 3 and 4 cells form the inner cortex. Types 2 and 3 are very active cells producing cytokines and hormones. Type 4 cells are dying cells which often appear after manipulation of the thymic epithelium.

Type 5 - Medullary epithelial cells, including the CMJ.

Type 6 - Medullary epithelial cells and Hassall's corpuscles.

The outer, cortical epithelium is highly dendritic and is densely packed with thymocytes (Boyd *et al.*, 1993). Within the cortex are thymic nurse cells (TNC), huge epithelial cells that appear to engulf and release large numbers of developing thymocytes (Wekerle *et al.*, 1980; Wekerle and Ketelsen 1980). TNCs are a specialised form of type 2 and type 3 TEC which may provide specific microenvironments needed for thymocyte proliferation or differentiation.

The inner medullary region of the thymus appears tightly packed with voluminous epithelial cells and is loosely packed with thymocytes (Boyd *et al.*, 1993). Hassall's corpuscles (HC) are unique to the thymic medulla (Boyd *et al.*,

1993). They are small clusters or 'swirls' of keratinised cells which are prominent in human but rare in the murine thymus, and whose functional significance is unknown (Boyd *et al.,* 1993).

The epithelial cells of the thymic stroma are unique in that they form three-dimensionally oriented networks (van Ewijk *et al.,* 1999). In most epithelial organs, epithelial cells are arranged in two-dimensional sheets attached to a basement membrane. The 3D network of the thymic stroma creates a sponge like structure through which developing thymocytes can percolate (Figure 1.2) (van Ewijk *et al.,* 1999). The orientation of cortical epithelial cells perpendicular to the thymic capsule is thought to guide the migration of thymocytes from the outer cortex toward the medulla (van Ewijk 1991). This 3D environment is believed to be necessary for developing T-cells to interact with a large variety of stromal cells which direct their differentiation and proliferation.

1.2.2.3. Phenotypic characterisation of thymic epithelial cells

Cytokeratins

All epithelial cells are characterised by a cytoskeletal system of intermediate filaments formed by cytokeratins (CK) (Sun *et al.,* 1979; Tseng *et al.,* 1982). Nineteen human CK polypeptides have now been identified and grouped into two types (Moll *et al.,* 1982). Type I are acidic cytokeratins with low molecular weights between 40 and 56 kDa. Type II cytokeratins are basic, with higher molecular weights between 53 and 68 kDa. The expression of specific keratins appears to correlate with the type of epithelial differentiation: the smaller keratin polypeptides are expressed in almost all epithelia, whilst the larger ones characterise complex or specialised epithelia (Tseng *et al.,* 1982). For example, high molecular weight CKs, such as 3 and 10, are typically expressed in keratinised stratified epithelium and low

Figure 1.2. Scanning electron micrograph of human thymic cortex

Epithelial cells form a 3-dimensional network through which thymocytes migrate. (From von Gaudecker, 1991)

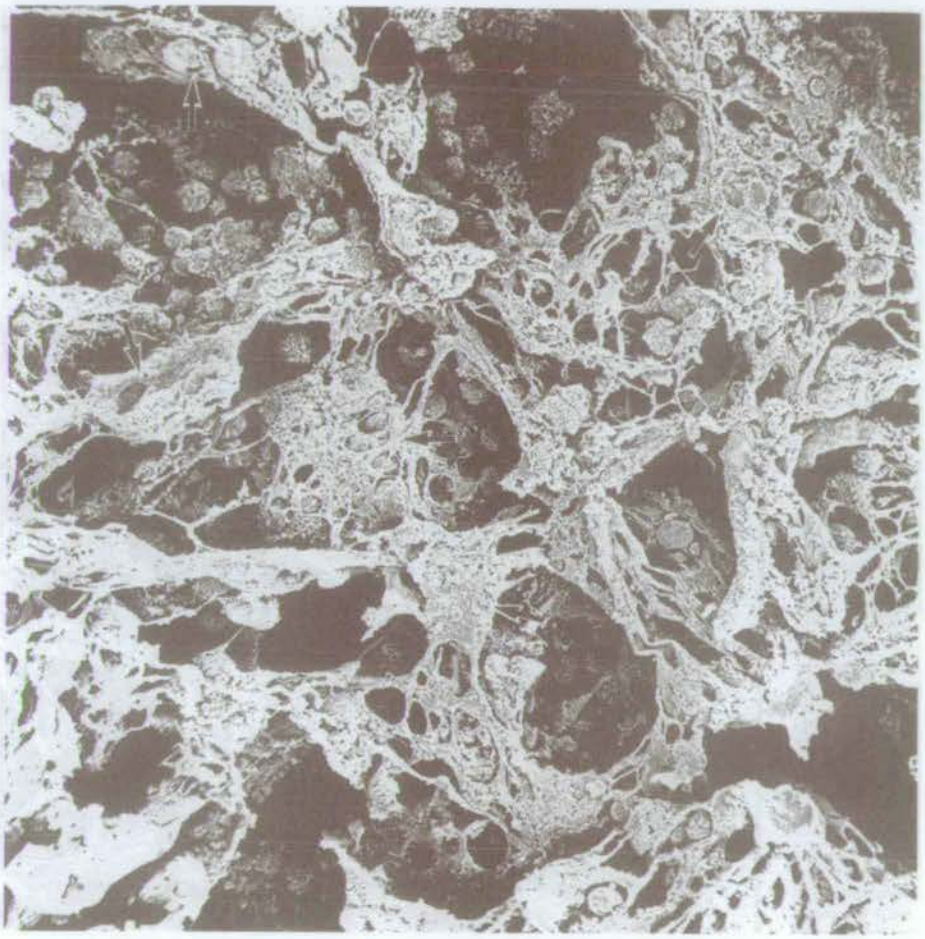

molecular weight CKs, such as 8 and 18, are expressed by simple epithelia (Tseng *et al.,* 1982; Brekelmans and van Ewijk 1990).

Cytokeratin expression in TEC is heterogeneous, and can be used to define subpopulations of TEC (Savino and Dardenne 1988). Generally, cortical TEC resemble 'simple' epithelia expressing CKs of low molecular weight such as CK 8 and 18, whilst medullary TEC express CKs with higher molecular weights such as CK 3, 5, 6 and 10, characteristic of more complex epithelia (Savino and Dardenne 1988; Farr and Braddy 1989; Brekelmans and van Ewijk 1990). One mAb, KL1, exclusively recognises a small subpopulation of medullary TEC characterised by its content of a high molecular weight keratin, 63 kDa (Nicolas *et al.,* 1985). Since epithelial differentiation is known to be associated with the acquisition of high molecular weight keratins, it is suggested that KL1-positive cells may represent a subset of highly differentiated medullary TEC (Nicolas *et al.,* 1985).

A recent study used keratin expression patterns to identify epithelial cell subsets in the mouse and investigate their lineage relationships (Klug *et al.,* 1998). Two subsets of medullary epithelial cells were identified: $K8^-K18^-$ $K5^+K14^+MTS10^+UEA\text{-}1^-$ and $K8^+K18^+K5^-K14^-MTS10^-UEA\text{-}1^+$. In addition, two subsets of cortical epithelial cells were identified: $K8^+K18^+K5^+K14^-MTS10^-UEA\text{-}1^-$ and $K8^+K18^+K5^-K14^-MTS10^-UEA\text{-}1^-$. Analysis of the distribution of these cells in transgenic mice in which T-cell, and therefore TEC development, was arrested at different stages suggested that the cortical $K8^+K5^+$ cells are a precursor subset from which mature cortical $K8^+K5^-$ epithelial cells develop, in a differentiation process concomitant with thymocyte development (Klug *et al.,* 1998). Expression of a cyclin D1 transgene in $K8^+K5^+$ epithelial cells expanded this subset and promoted development of thymic epithelial cells, suggesting that thymic function may be enhanced by manipulating the growth of $K8^+K5^+$ precursor cells (Klug *et al.,* 2000). The lineage relationship of these cortical cell populations to the medullary populations is unknown.

Monoclonal antibodies

Many monoclonal antibodies have been raised against non-lymphoid cells of the thymus in human (Haynes *et al.,* 1984; Ritter *et al.,* 1985), chicken (Wilson *et al.,* 1992), rat (Colic *et al.,* 1988) and mouse (van Vliet *et al.,* 1984; Godfrey *et al.,* 1990). These mAbs have revealed antigenic heterogeneity of the TEC and have been invaluable in analysing the development of the stromal compartments and identifying potentially important new surface molecules (Brekelmans and van Ewijk 1990; van Ewijk 1991; Boyd *et al.,* 1993). Monoclonal antibodies have also been raised against various thymic epithelial cell lines, which provide some indication of the heterogeneity of thymic stromal cells maintained *in vitro* (Farr *et al.,* 1991; Kinebuchi *et al.,* 1991; Naspetti *et al.,* 1997). More recently, single-chain antibodies against thymic stromal components have been isolated from phage display libraries (Palmer *et al.,* 1997; van Ewijk *et al.,* 1997; Ritter and Palmer 1999).

MHC antigens

Antibodies against murine H-2D and H-2K have shown that class I MHC antigens are expressed predominantly in the medullary epithelium of the adult thymus, with weaker reticular cortical epithelial staining in some mouse haplotypes (Rouse *et al.,* 1979; van Ewijk *et al.,* 1980). During thymus development, expression of Class I antigens by TEC commences at embryonic day 16 (E16) (Jenkinson *et al.,* 1981). Class II antibodies such as I-A and I-E show extensive reticular staining in the cortex and a more confluent stain in the medulla. During thymus development, MHC Class II is expressed earlier than Class I, at E13. TNCs also express class I and class II antigens (Wekerle and Ketelsen 1980).

TEC antigens

The reactivities of some of the antibodies produced against TEC were compared in immunohistological studies (Kampinga *et al.,* 1989; Ladyman *et al.,* 1991). Based on their staining patterns in thymus, antibodies were grouped into 'clusters of thymic epithelial staining' (CTES) (Kampinga *et al.,* 1989):

I Pan-epithelial

II Subcapsular/perivascular and medullary TEC including HC and scattered patches in cortex.

III Cortical epithelium.

- IIIA Cortical TEC only
- IIIB cortical and small subset of medullary TEC
- IIIC cortical and subset of leukocytes

IV Medullary TEC including HC.

- IV A Subset of medullary TEC

V HC

XX Miscellaneous.

A summary of some of the murine TEC antibodies which have been produced is shown in Table 1.1. (for more detailed reviews, see (Kampinga *et al.,* 1989; Brekelmans and van Ewijk 1990; Boyd *et al.,* 1993). Further characterisation of many of these mAbs has revealed the cellular location and molecular weight of the antigens they recognise (Kampinga *et al.,* 1989; Ladyman *et al.,* 1991). Most studies have examined mAb expression on TEC by immunohistochemical staining of thymus sections. One report of flow cytometric analysis of TEC showed that epithelial cells are very large and granular compared to thymocytes and so the

Table 1.1. - Thymic epithelial cell monoclonal antibodies

Antibody	Staining Pattern in adult thymus	CTES group	Reference
ER-TR3	cortical and medullary TEC	I	(van Vliet *et al.*, 1984)
ER-TR4	Cortical and isolated medullary TEC	IIIB	
ER-TR5	Medullary TEC	II	
ER-TR7	Fibroblast and ECM in capsule and septa	XX	
MTS 39	Pan-epithelial	I	(Godfrey *et al.*, 1990)
MTS 10	Subcapsule and medulla	II	
MTS 44	Cortex and minor subpop. medulla	IIIB	
MTS 20	Isolated cells or small clusters in medulla	IV A	
MTS 29	Isolated medullary cells	IV A	
MTS 9	Medulla and some cortical TEC, medullary and some cortical thymocytes	XX	
MTS 32	Cortical TEC and thymocytes (Renamed thymic shared antigen-2 (TSA-2))	IIIC	(Vicari *et al.*, 1994; Berzins *et al.*, 1999)
MTS 37	Isolated cortical and medullary TEC and thymocytes	XX	
MTS 35	Minority of medullary TEC and cortical thymocytes. (Renamed Thymic shared antigen-1 (TSA-1))	XX	(MacNeil *et al.*, 1993; Randle *et al.*, 1993)
MTS 16	Basement membrane-associated connective tissue lining capsule, PVS and blood vessels	XX	
4F1	cortical and minor subpop. of medullary TEC and thymocytes	IIIB	(Kanariou *et al.*, 1989; Imami *et al.*, 1992)
IVC4	subcapsular/perivascular and medullary TEC	II	

two populations can easily be distinguished by flow cytometry (Tucek and Boyd 1990). These studies showed unexpected expression of CD4 and Thy-1 on the surface of mouse thymic stroma, localising Thy-1 expression to epithelial cells and CD4 expression to thymic macrophages. Thy-1 is a marker usually associated with thymocytes but has also been found on a variety of other cell types (Tucek and Boyd 1990). Further flow cytometric analysis of thymic stroma reported that some stroma-reactive mAbs have a more extensive distribution than would have been predicted from immunohistology, illustrating the higher sensitivity of flow cytometry (Izon *et al.*, 1994).

The expression patterns of mAbs raised against thymic stroma may provide some indication of the origins of TEC and the functions of different TEC populations. The majority of mAbs which are positive for medullary epithelium also stain the subcapsular region (CTES II) (Boyd *et al.*, 1993). These two areas are physically linked via the trabeculae, which penetrate from the subcapsular region into the medulla. The antigenic similarity indicates that cells in these two areas may derive from a similar origin or may be subject to the same differentiation signals (Boyd *et al.*, 1993). Some mAbs react with determinants expressed on both epithelial cells and thymocytes in the thymus, for example, MTS32 and MTS35 (Godfrey *et al.*, 1990).

The studies described above have demonstrated that the epithelial cells of the thymus are heterogeneous, with respect to morphology and ultrastructure, expression of cytokeratins, and antigenicity (van de Wijngaert *et al.*, 1984; Brekelmans and van Ewijk 1990; Boyd *et al.*, 1993; Naquet *et al.*, 1999; Ritter and Palmer 1999). This heterogeneity has given rise to the hypothesis that each subpopulation of thymic epithelium may be functionally specialised, providing intercellular communication molecules and cytokines appropriate to the phase of T-cell development it directs (Boyd *et al.*, 1993).

1.3. Intra-thymic T-cell development

T-cell progenitors enter the thymus from the bone marrow. In the thymus they differentiate and are subject to the processes of positive and negative selection. Positive selection selects for thymocytes expressing TCRs that recognise self-MHC, while negative selection deletes thymocytes expressing TCRs that recognise self-antigen-derived peptides presented on MHC. Mature naïve T-cells then exit the thymus to seed the periphery. The differentiation pathways of T-cells in the thymus and the lineage relationships between subpopulations of T-cells have been studied extensively and are well understood. (For reviews see von Boehmer 1988; Anderson *et al.,* 1996; Shortman and Wu 1996; Goldrath and Bevan 1999). The main stages in intra-thymic T-cell development are discussed below.

1.3.1. Lymphoid entry into the thymus

T-cell progenitors enter the thymus from the foetal liver during embryonic life and subsequently from the bone marrow during adult life (Dunon and Imhof 1993; Shortman and Wu 1996). The degree of lineage restriction of these cells is unclear but recent studies have identified a lymphoid restricted progenitor in the bone marrow capable of giving rise to T- and B-cells (Kondo *et al.,* 1997). The earliest thymocytes in the adult thymus can be identified by expression of cell surface markers, being c-kit^{+}, Thy-1^{lo}, CD44^{+}, CD4^{lo}, and this cell population can give rise to T, B, NK and dendritic cells (Wu *et al.,* 1991; Shortman and Wu 1996). Recent clonal analyses demonstrated that the majority of progenitors within the foetal thymus were restricted to the T-cell lineage, with only a small number of B or

myeloid lineage-restricted progenitors being present (Kawamoto *et al.,* 1998; Boyd and Chidgey 2000).

In the murine foetal thymus, migrant progenitor cells first enter the primordium around E11-E12, before the thymus is vascularised (Owen and Ritter 1969; Jotereau *et al.,* 1987). Precursor cells migrating to the thymus through the surrounding mesenchymal tissue were observed at E11-E13 (Owen and Ritter 1969; Suniara *et al.,* 1999). These migrant thymic stem cells are c-kit$^+$CD44$^+$CD45$^+$CD34$^+$ (Suniara *et al.,* 1999), and are therefore phenotypically similar to the earliest thymocyte progenitors in the adult thymus. Entry of precursor cells into the murine foetal thymus occurs in two waves (Jotereau *et al.,* 1987; Penit and Vasseur 1989). The first wave enters the thymus between E11 and E13 and gives rise to all thymocytes until just after birth. Those cells entering the thymus after E13 do not begin to differentiate until a week after birth, giving rise to a second wave of thymocytes that replace the first generation. Similar seeding of the avian thymus has also been observed, with three distinct periods of immigration separated by refractory periods (Jotereau and Le Douarin 1982). Precursor cells continue to enter the thymus during adult life, although at a reduced frequency (Dunon and Imhof 1993; Shortman and Wu 1996).

The mechanisms by which precursor cells are attracted to the thymus remain unclear. Evidence that chemoattractant factors produced by the thymus may be involved in this process has come from studies using transfilter migration assays to demonstrate the ability of foetal thymus lobes to attract precursor cells (Jotereau *et al.,* 1980; Fontaine-Perus *et al.,* 1981; Jenkinson *et al.,* 1982).

Molecules with postulated roles in thymus homing include selectins and integrins, in particular, ß1 integrin (Potocnik *et al.,* 2000). CD44 expressed on early thymocyte precursors was implicated in their homing to the thymus (Wu *et al.,* 1993). ß2-microglobulin was reported to play a role in thymus colonisation in avian

embryos (Dunon *et al.,* 1990). However, ß2-microglobulin null mice have normal thymus colonisation by precursor cells (Dunon and Imhof 1993). A novel molecule, Vanin-1, which is expressed by perivascular thymic stromal cells, was reported to regulate adhesion steps involved in thymus homing of precursors (Aurrand-Lions *et al.,* 1996). However, Vanin-1 has subsequently been shown to encode pantetheinase, an enzyme which is widely expressed in mouse tissues, and Vanin-1 null mice have no detectable thymus phenotype (Pitari *et al.,* 2000).

Several chemokines are expressed by TEC and chemokine receptors are expressed by T-cell precursors (Wilkinson *et al.,* 1999). In particular, thymus expressed chemokine (TECK) is strongly expressed by TEC and has chemotactic activity for thymic precursors. However, neutralising antibody to TECK did not inhibit precursor migration (Wilkinson *et al.,* 1999). At present no single factor has been identified which is wholly responsible for the attraction of lymphoid precursors to the thymus. It is likely that other unidentified molecules are involved in chemoattraction in the thymus or that multiple factors may combine to attract precursors to the thymus.

1.3.2. T-cell receptor rearrangement

A schematic representation of T-cell development is shown in figure 1.3. T-cell precursors in the adult murine thymus have germline TCR gene arrangements and are $CD3^-$, $CD8^-$ and $CD4^{lo}$ (Wu *et al.,* 1991). Embryonic T-cell precursors have a similar phenotype, but lack CD4 expression (Shortman and Wu 1996). These cells give rise to cells with the triple-negative (TN) phenotype $CD3^-CD4^-CD8^-$. This TN stage can be further subdivided by expression of CD25 (interleukin-2 receptor) and CD44: $CD25^-CD44^+$ cells precede $CD25^+CD44^+$ cells, which precede $CD25^+CD44^-$ cells (Godfrey *et al.,* 1993).

Figure 1.3. Schematic representation of thymocyte development

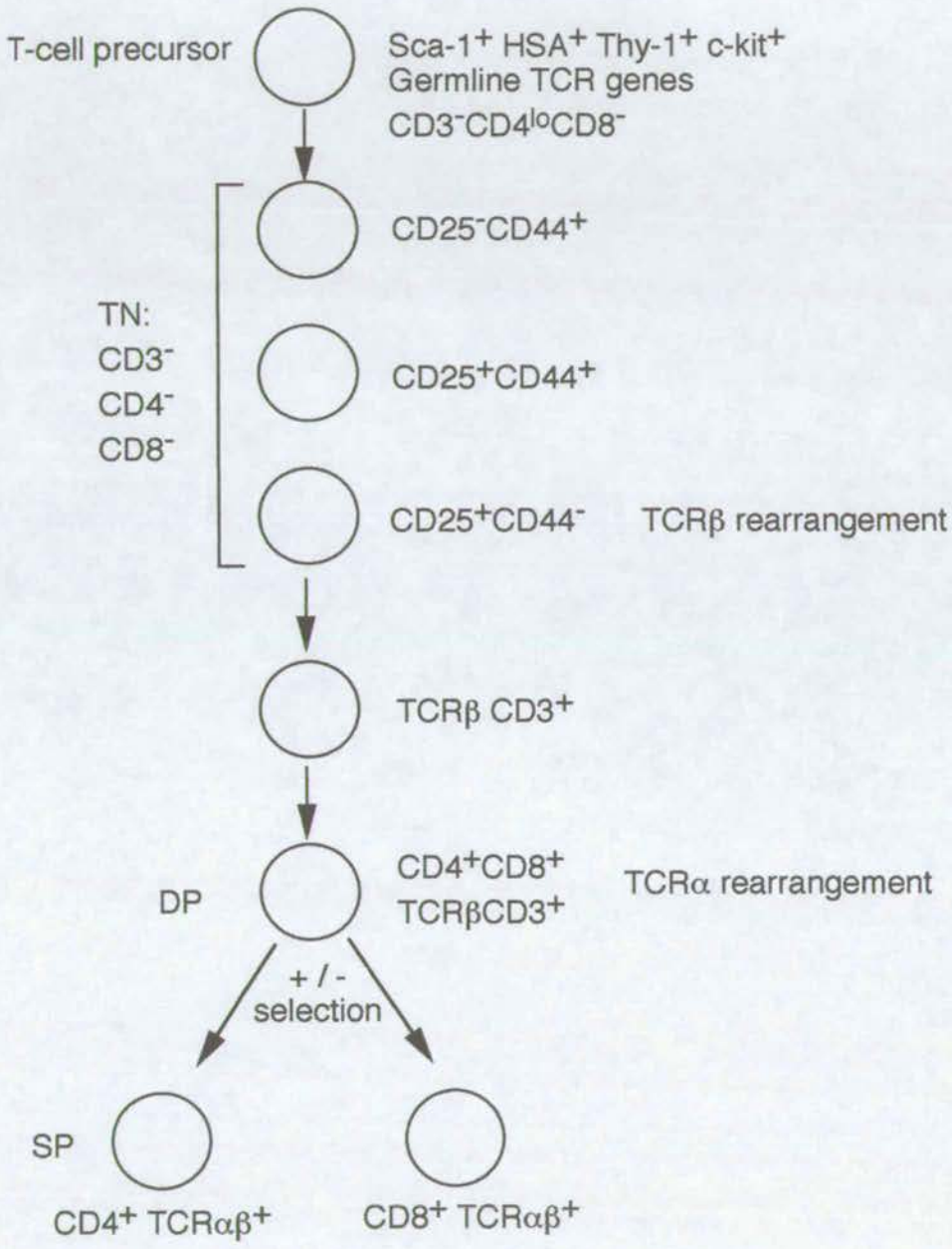

Figure 1.3. Schematic representation of thymocyte development

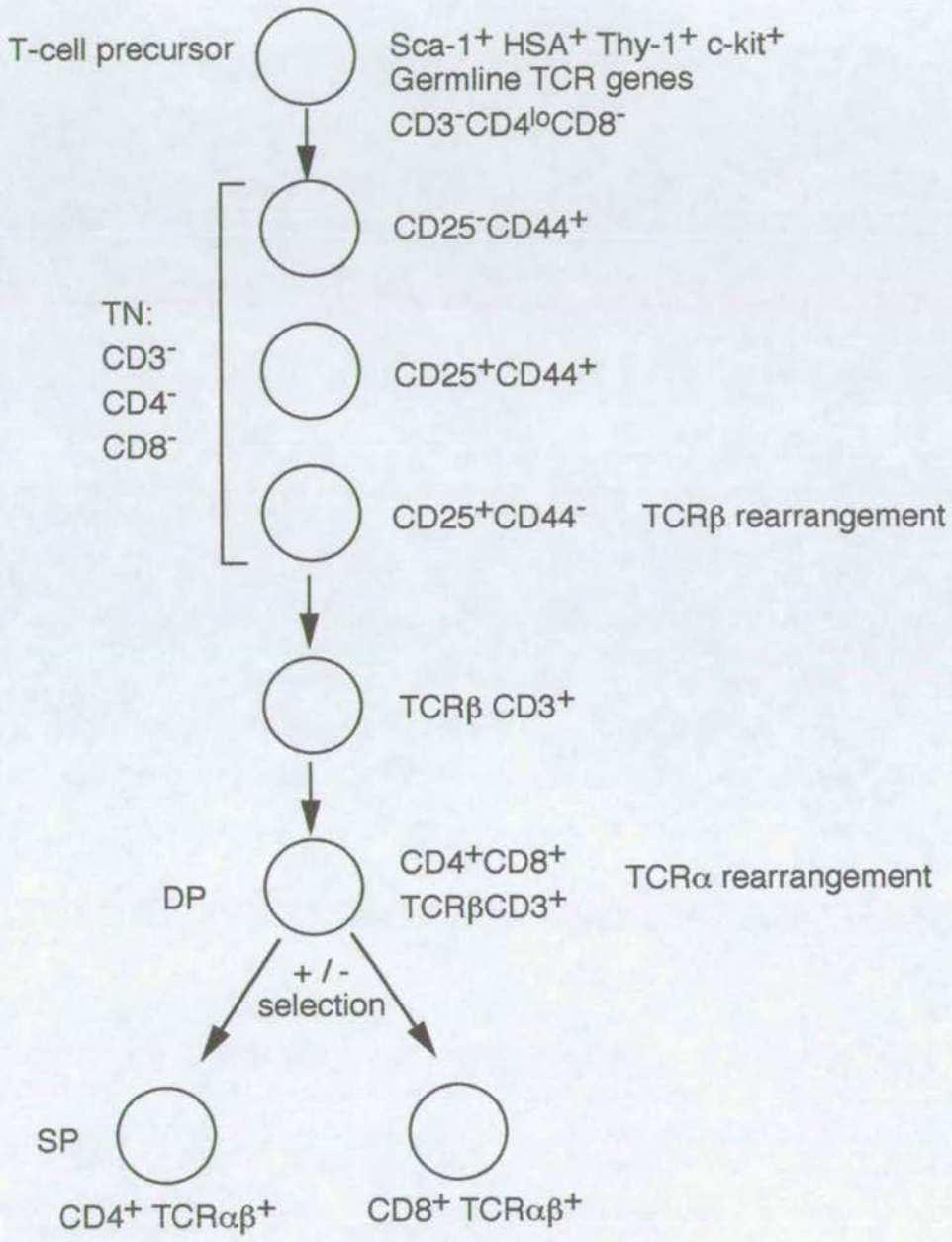

Rearrangement of the genes encoding the α, ß, δ, and γ chains of the TCR provide the structural diversity of TCRs needed to produce T-cells capable of recognising a large variety of antigens (Shortman and Wu 1996). Thymocytes express recombination-activating genes (RAG-1 and RAG-2), which encode recombinase enzymes responsible for catalysing rearrangement (Oettinger *et al.*, 1990). Those thymocytes that make productive rearrangements of δ and γ chain genes result in a CD3 associated δγ heterodimer, which are the first functional cells to be formed in the thymus but account for only 0.5-1% of adult thymocytes (von Boehmer 1988). The majority of thymocytes rearrange the β-chain gene, at the $CD25^{+}CD44^{-}$ stage, to express the β-chain prior to expression of the α-chain. This pre-TCR is thought to recognise an intra-thymic ligand and transmit an activating signal through CD3 that activates Lck, a protein tyrosine kinase (Anderson *et al.*, 1993). This signal transduction selects those thymocytes expressing a β-chain for further maturation and induces expression of CD4 and CD8, giving double positive (DP) $CD4^{+}CD8^{+}$ cells (von Boehmer 1988). This phenotype constitutes 85% of cells in the thymus. Productive TCR α gene rearrangement results in $\alpha ßTCR^{+}CD3^{+}CD4^{+}CD8^{+}$ cells. An estimated 99% of these thymocytes will die in the thymus by apoptosis either because they fail to make productive TCR rearrangements or because they fail to survive thymic selection (see section 1.3.3.). Those thymocytes surviving positive and negative selection develop into single positive cells (SP), expressing either CD4 or CD8, and exit to the periphery (von Boehmer 1988). Recently, $CD4^{+}$ SP T-cells were found to progress through a further seven phenotypic stages in the thymic medulla, defined by expression of Qa-2, HSA, CD69, 3G11 and 6C10, before exit to the periphery (Ge and Chen 1999).

1.3.3. Positive and negative selection

Thymocytes that have rearranged TCR loci undergo selection processes in the thymus to ensure that only thymocytes whose TCRs exhibit self-MHC restriction and self-antigen tolerance are permitted to mature (for reviews see Anderson *et al.*, 1999; Goldrath and Bevan 1999; Laufer *et al.*, 1999; Klein and Kyewski 2000). Positive selection ensures that thymocytes expressing TCRs that bind to self-MHC molecules survive: those cells failing selection die within the thymus by apoptosis. Negative selection eliminates thymocytes which bear a high-affinity receptor for self-MHC or self-peptide plus MHC. These thymocytes would pose the threat of an autoimmune response if allowed to mature.

Positive selection occurs when thymocytes interact with epithelial cells in the thymic cortex expressing MHC-peptide complexes (Laufer *et al.*, 1999). Those cells whose TCR binds to MHC-peptide are rescued from cell death, whilst the majority of $CD4^+CD8^+$ cells will die by apoptosis (Goldrath and Bevan 1999). Negative selection acts to delete any thymocytes whose TCR binds with high affinity to self-peptide antigens in association with self-MHC molecules, presented by thymic dendritic cells or epithelial cells (Laufer *et al.*, 1999). Stromal cells in the thymus process endogenous and exogenous antigens and present them on their cell surface in combination with MHC molecules (Klein and Kyewski 2000).

As positive selection selects thymocytes reactive with self-MHC and negative selection eliminates thymocytes reactive with self-MHC, a mechanism must exist to prevent the entire T-cell repertoire form being eliminated. The affinity model of selection suggests that differences in the affinity of TCRs for self-MHC-peptide complexes determines the outcome of positive and negative selection (Goldrath and Bevan 1999). All thymocytes that can bind to self-MHC-peptide are selected in positive selection, then negative selection eliminates those receptors with high

affinity for self-MHC-peptide, thus leaving only thymocytes with receptors with low affinity for self-MHC-peptide (Laufer *et al.,* 1999). It has been suggested that differences in the thymic stromal cells involved in selection may influence binding of TCRs (Capone *et al.,* 2001). For example, cortical epithelial cells involved in positive selection may express additional molecules that facilitate binding of low affinity TCRs, whereas cells involved in negative selection are only able to bind receptors with high affinity for MHC-peptide (Abbas *et al.,* 1997). A further possibility is that the expression of CD4 and CD8 by thymocytes may influence their affinity for thymic stromal cells. There is evidence that the number of MHC-peptide complexes engaged is also important in selection. Thus, the avidity, the overall stability of the interaction between MHC and TCR, is thought to be important (Abbas *et al.,* 1997). This encompasses not only the affinity of the receptors but the number of receptors involved and their spatial density.

Double-positive thymocytes mature to express either CD8 or CD4 which are specific receptors for MHC Class I and MHC Class II respectively (Goldrath and Bevan 1999). The pairing of coreceptor and TCR expression is thought to be either a stochastic process in which there is a random down-regulation of either CD4 or CD8, or an instructional process where interaction of the TCR with CD4 or CD8 and MHC I or MHC II instructs the cells to differentiate into $CD4^+$ or $CD8^+$ T-cells (Abbas *et al.,* 1997). The majority of evidence seems to support the stochastic model (Owen and Moore 1995), including recent work showing that the transition from DP thymocyte to SP did not require interaction with MHC molecules (Hare *et al.,* 1999).

1.3.4. Regulation of intra-thymic T-cell development

1.3.4.1. Molecular control of T-cell development

The molecular mechanisms regulating thymocyte maturation in the thymus are complex. The identification of many transcription factors, signal transduction molecules and cell surface receptors and the generation of gene knockout mice has proved invaluable in elucidating the mechanisms controlling thymocyte maturation. Figure 1.4. indicates many of the genes involved and the blocks in thymocyte development in various mutant mice.

One of the earliest blocks in thymocyte development is in the Ikaros dominant negative mutant mouse. Ikaros is a zinc finger transcription factor which regulates lymphoid cell fate (Nichogiannopoulou *et al.,* 1998). Ikaros dominant negative mice have an early and complete block in development of all lymphoid cells, suggesting that Ikaros plays an essential role in commitment of HSCs to lymphoid lineages. This is a more severe phenotype than the Ikaros null mice which have a block in precursor entry to the foetal thymus, although 3-5 days after birth some precursors are detected in the thymus. Severely reduced numbers of T-cells are produced during adult life and these have a preferred commitment to the $CD4^+$ lineage, suggesting that Ikaros may also control CD4/CD8 differentiation.

The cytokine IL-7 has essential roles in thymocyte development (Shortman and Wu 1996). IL-7 stimulates the proliferation of immature thymocytes and mature T-cells. It acts on $CD4^-CD8^-$ thymocytes to maintain viability and function, and promotes rearrangement of the ß and γ chain genes (Oosterwegel *et al.,* 1997). IL-$7^{-/-}$ mice have markedly reduced thymocyte numbers although a normal ratio of CD4/CD8 development within these cells, indicating that IL-7 plays a role in proliferation of early thymocytes (von Freeden-Jeffry *et al.,* 1995). IL-$7R^{-/-}$ mice

Figure 1.4. Blocks in thymocyte development in mutant mice

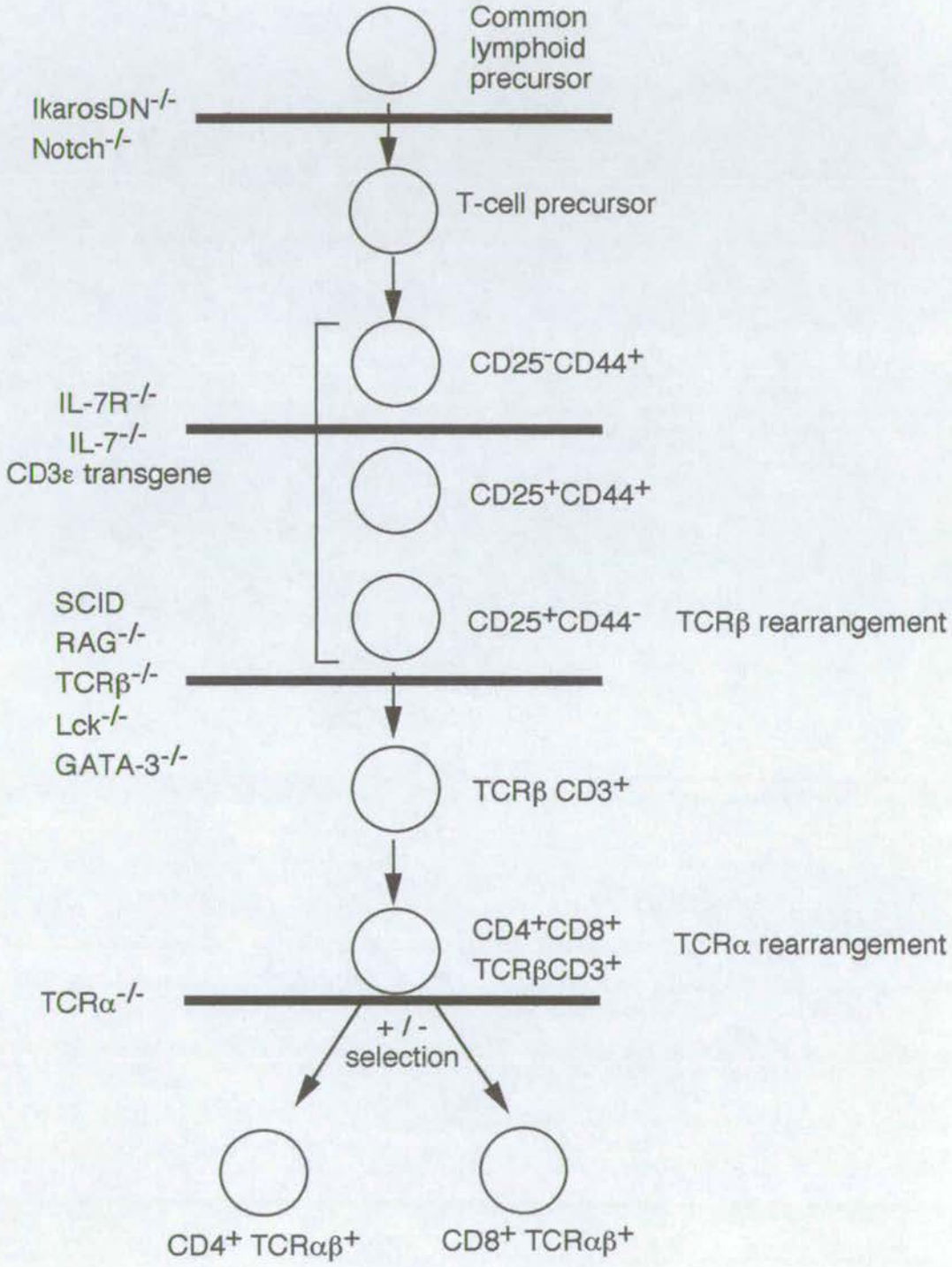

exhibit a profound reduction in number of thymocytes in the thymus and a complete block in T-cell development at the very early $CD25^-$ stage before TCR rearrangement (Peschon *et al.*, 1994).

The role of the Notch receptor and ligand family in T-cell development has been the focus of much attention recently (Osborne and Miele 1999). Notch-1, -2, and -3 are all expressed in thymocytes and the Jagged-1 and -2 ligands are expressed in thymic stromal cells. Notch has been implicated in a variety of roles in thymocyte development. These include regulation of the lineage choice between B cells and T cells, between αß and δγTCR lineages and between $CD4^+$ and $CD8^+$ thymocytes. $Notch^{-/-}$ thymocytes show a complete block at the $CD25^-CD44^+$ stage, however, B cell development is found in the thymus of these mice. A recent report, in which Notch1 is inactivated in immature thymocytes, indicates that Notch1 is not involved in CD4/CD8 lineage commitment, or thymocyte maturation or survival (Wolfer *et al.*, 2001).

Other mice with blocks in the earliest stages of thymocyte development include human CD3ε transgenic mice which are blocked at the $CD25^-CD44^+$ stage (Wang *et al.*, 1994). RAG-1, RAG-2 and SCID mice have arrested thymocyte development at the $CD25^+CD44^-$ stage due to inability to undergo TCR gene rearrangement (Bosma *et al.*, 1983; Schuler *et al.*, 1986; Mombaerts *et al.*, 1992; Shinkai *et al.*, 1992). Mice with mutations in the TCRß-chain or the protein tyrosine kinase, $p56^{lck}$, also have thymocytes blocked at the $CD25^+44^-$ stage, whereas TCR $\alpha^{-/-}$ mice are blocked at the later DP $CD4^+CD8^+$ stage (Palmer *et al.*, 1993). The zinc finger transcription factor GATA-3 which is expressed in thymocytes and mature T-cells, is also essential for thymocyte development (Ting *et al.*, 1996). $GATA\text{-}3^{-/-}$ ES cells can give rise to all erythroid, myeloid and B-cell lineages but cannot give rise to T-cells. Thymocyte development is blocked at the early $CD25^+CD44^-$ stage of development (Ting *et al.*, 1996).

Investigation of mutant mouse strains has thus revealed a great deal about the mechanisms controlling T-cell differentiation. Mice with blocks at particular stages of thymocyte development have also demonstrated the effects of thymocyte development on the thymic stroma (Section 1.5).

1.3.4.2. The role of the thymic stroma in T-cell development

The molecular mechanisms regulating thymocyte development are mediated at least in part by cells of the thymic stroma. An *in vitro* system that reconstructs the thymic microenvironment using defined populations of foetal stromal cell types and thymocytes has proved useful for studying these processes (Anderson *et al.,* 1993; Hare *et al.,* 1999). Reaggregate thymic organ cultures (RTOC) were found to support the maturation of thymocytes from DP to SP mature T-cells, and to support positive selection of T-cells in a manner comparable to thymocyte maturation *in vivo* (Anderson *et al.,* 1993). Using RTOCs, it was found that foetal MHC Class II^+ epithelial cells and foetal mesenchymal cells were necessary for the development of thymocytes from the TN TCR^- stage to the SP TCR^+ stage (Anderson *et al.,* 1993). The mesenchymal support could be substituted by NIH3T3 fibroblasts but not by supernatant from these cells, indicating a cell-contact mediated effect. Recent studies have shown that the latest developmental subpopulation of thymocytes to be dependent on fibroblasts was the $CD25^+CD44^+$ phenotype (Anderson *et al.,* 1997). Mesenchymal cells are thought to have a direct role in thymocyte development by providing an intra-thymic network of fibroblasts and associated ECM which may be necessary for integrin or cytokine interactions with thymocytes (Suniara *et al.,* 2000).

The importance of mesenchyme on thymocyte development was also studied in the foetal thymus at E12.5. Although the E12.5 thymic primordium has been colonised by functionally competent thymocyte precursor cells, it was shown that the

stromal cells of the E12.5 primordium are incapable of supporting T-cell development (Amagai *et al.*, 1995). When foetal thymus was co-cultured with various fibroblast cell lines E12.5 thymus could develop to support full T-cell differentiation, suggesting that a continued interaction with mesenchyme is essential for thymocyte development in the foetal thymus (Itoi and Amagai 1998).

Many adhesion molecules have roles in the intra-thymic development of thymocytes (Patel and Haynes 1993; Reza and Ritter 1994). These adhesion molecules are expressed on thymocytes and interact with ligands on thymic stromal cells or in particular, ligands on ECM molecules in the thymus. Fibronectin is expressed by thymic stromal cells and interacts with members of the ß-1 integrin family, VLA-4, -5 and -6, which are expressed on thymocytes (Sawada *et al.*, 1992). TN thymocytes have been shown to adhere to thymic stromal cells through fibronectin-VLA interactions and this adhesion is thought to have a critical role in inducing or supporting the differentiation of thymocytes (Utsumi *et al.*, 1991). Binding of immature TN thymocytes to laminin via VLA-6 was also reported (Lannes-Vieira *et al.*, 1993; Wadsworth *et al.*, 1993). A conflicting report suggested that merosin but not laminin was expressed in the thymus and interacts with VLA-6 on immature thymocytes (Chang *et al.*, 1993).

Interactions between LFA-1 (a ß-2 integrin) and ICAM-1 are also important for thymocyte development, as addition of antibodies against these molecules to FTOCs resulted in impaired generation of DP thymocytes (Fine and Kruisbeek 1991). Thy-1, expressed on T-lineage cells, supports adhesion of thymocytes to thymic epithelial cells through a heterophilic interaction that can be inhibited by sulfated glycans (Hueber *et al.*, 1992). The mouse homologue of human Ep-CAM, gp40, a homotypic adhesion molecule, is expressed on thymic epithelial cells and thymocytes, with the highest level of expression on immature TN and DP cells (Nelson *et al.*, 1996). gp40 was also detected on thymic dendritic cells indicating that this molecule may mediate adhesion between thymocytes and epithelial cells or

dendritic cells. E-cadherin, one of a family of cell adhesion receptors, is expressed by thymic epithelial cells and thymocytes. Homotypic E-cadherin interactions were shown to be important in thymocyte development and organisation of epithelial cells in RTOC (Muller *et al.*, 1997).

Cytokines are known to play important roles in thymocyte proliferation and differentiation. Many studies have analysed expression of cytokines in thymocyte and thymic stromal cell populations (Carding *et al.*, 1991). In the foetal thymus, MHC Class II^+ epithelial cells were shown to express IL-7 and SCF, whereas foetal mesenchyme was responsible for expression of IL-1α and GM-CSF (Moore *et al.*, 1993). NIH3T3 fibroblasts exhibited the same cytokine expression profile as mesenchymal cells, supporting the idea that fibroblast cells lines can substitute for mesenchyme in thymocyte development (Anderson *et al.*, 1993). Other studies have shown expression of IL-1, IL-3, IL-4, IL-5, IL-6, GM-CSF, IFN-γ and TNF-α in various thymocyte populations and stromal cells (Deman *et al.*, 1996; Montgomery and Dallman 1997). These studies indicate that cytokines produced both by thymocytes and by thymic stromal cells are likely to play important roles in thymocyte maturation.

1.3.4.3. The role of the thymic stroma in T-cell selection

The precise location and temporal relationships of positive and negative selection and the particular stromal cells mediating selection in the thymus has recently been an area of intensive study. The RTOC system was used to investigate the stromal cell requirements for thymocyte positive selection. These studies indicated that MHC II^+ cortical epithelial cells are unique in their ability to support positive selection by providing unidentified differentiation-inducing signals that require sustained cell-surface interactions with epithelial cells (Anderson *et al.*, 1994; Wilkinson *et al.*, 1995; Anderson *et al.*, 1997). Recently it has been shown that only

the initial stages of positive selection, i.e. TCR ligation, are dependent on MHC (Hare *et al.*, 1999). Transgenic mice that express a class II MHC antigen, I-A^b only on cortical epithelial cells have $CD4^+$ cells which have been positively selected but not negatively selected, demonstrating that cortical epithelium is sufficient for positive selection (Laufer *et al.*, 1996). Another investigation using relB-deficient mice, in which medullary epithelium is not present, has shown that positive selection proceeds normally and mature T-cells can exit to the periphery, however, these cells are not negatively selected (DeKoning *et al.*, 1997). A recent study using transgenic mice which express an MHC class I molecule only on cortical epithelial cells has shown that normal numbers of CD8 T-cells develop, however, these cells had not been negatively selected (Capone *et al.*, 2001). These studies demonstrate that cortical epithelium is sufficient for the positive selection of SP T-cells but negative selection mainly occurs on other cell types within the thymus. At present, little is known about the molecular interactions and the accessory molecules provided by cortical epithelial cells which mediate positive selection.

The ability of different stromal cell types to mediate negative selection and the location and temporal relationships between positive and negative selection remain unresolved. It is commonly believed that bone marrow-derived dendritic cells in the medulla of the thymus mediate negative selection by presenting MHC-peptide complexes on their surface. However, in some cases medullary epithelial cells also seem capable of mediating negative selection (Reviewed in (Hare *et al.*, 1999; Naquet *et al.*, 1999; Klein and Kyewski 2000). Furthermore, experiments using TCR transgenic mice have demonstrated that negative selection can occur at any stage of thymocyte development, even mediated by cortical epithelium, depending on the presence of the deleting antigen and the necessary accessory molecules on thymic stroma (Klein and Kyewski 2000). However, TCR transgenic models may be biased in their ability to negatively select thymocytes as TCR expression can be unusually high affecting the avidity of TCR-MHC interactions.

A diverse set of self-peptides is required in the thymus to select a diverse T-cell repertoire. The role of peptide antigens in positive and negative selection has recently been reviewed (Klein and Kyewski 2000). It remains unclear at present whether cortical epithelial cells mediating positive selection present exogenous antigens as well as endogenously derived peptides. A recent study suggested that in the foetal thymus, the onset of positive selection is delayed until extra-thymic proteins, to which self tolerance must be established, have reached the thymus via the vasculature (Fairchild and Waldmann 2000). In negative selection, thymic dendritic cells are highly efficient at taking up and processing exogenous antigens as well as endogenous peptides and presenting them to thymocytes, thus mirroring the extracellular and intracellular array of peptides. Medullary epithelial cells however, are likely only to present endogenously derived antigens. It is believed that thymocytes undergoing negative selection 'scan' medullary stromal cells to ensure interaction with numerous cells expressing distinct peptide profiles.

1.4. Thymus organogenesis and patterning

The development of the thymus during murine embryogenesis has recently been reviewed (Manley 2000). In this review, thymus development was divided into three stages: early organogenesis (E9.5-E11), late organogenesis (E11.5-E15) and late foetal development (E15.5-birth) (Manley 2000). In this section, early organogenesis from E9.5-E11 and early patterning of the thymic primordium from E11.5-E15 are discussed. The following section summarises knowledge about patterning of the thymic stroma via epithelial-thymocyte interactions.

1.4.1. Early organogenesis

In the murine embryo, thymus development begins in the pharyngeal region between E9.5 and E10.5 (Manley 2000). The pharyngeal arches are transient embryonic structures that develop in a cranial to caudal sequence between head and heart and consist of ectoderm-covered bars of mesenchyme (Figure 1.5) (Hogan *et al.*, 1994). These arches are separated by pharyngeal pouches, which are evaginations of the pharyngeal endoderm (Cordier and Haumont 1980). The mesenchymal component of the arches derives from migratory neural crest from the dorsal aspect of the neural tube (Kuratani and Bockman 1990). Studies have indicated roles for all three germ layers, endoderm, neural crest-derived mesenchyme and ectoderm, in thymus organogenesis and these are discussed in detail below.

1.4.1.1. Pharyngeal endoderm

The endoderm of the third pharyngeal pouch appears to be the major contributor to thymic epithelium. Early histological studies in mouse showed that the endoderm from the third pouch buds off from the pharynx at E12 to form the thymic primordium (Smith 1965). Experiments in avian embryos using ectopic transplantations between chick and quail revealed that pharyngeal pouch endoderm alone was sufficient to form thymic epithelium when associated with mesenchyme, and that some cells in the endoderm are specified to the thymic epithelial lineage early in development, before the formation of the third and fourth pharyngeal pouches (Le Douarin and Jotereau 1975). The third pouch endoderm also gives rise to the parathyroid glands at E11.5 which develop along with the thymic primordium and subsequently migrate away from the thymus (Cordier and Haumont 1980) (Figure 1.6).

Figure 1.5. Morphology of the pharyngeal region
(From Hogan et al.1994)

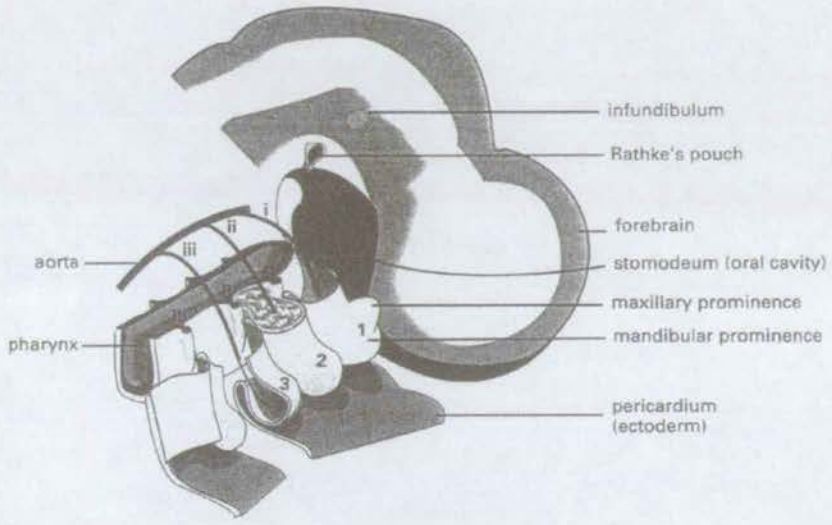

1,2,3: pharyngeal arches
I,II,III: pharyngeal pouches
i, ii, iii: aortic arteries

Figure 1.6. Derivatives of the pharyngeal pouches
(From Manley, 1998)

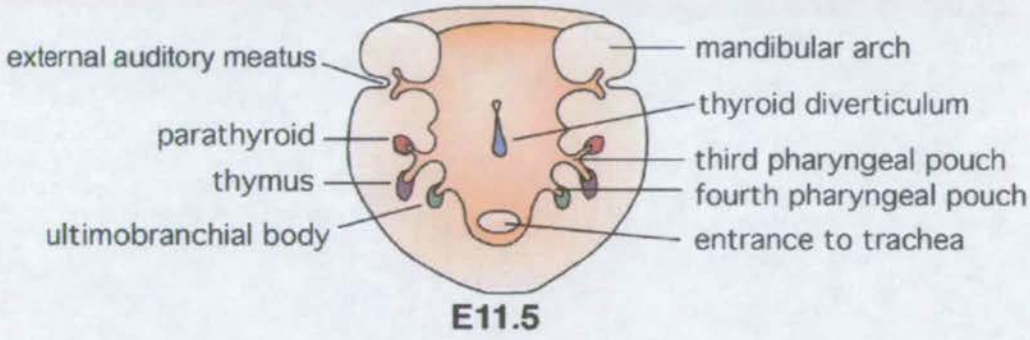

1.4.1.2. Neural crest-derived mesenchyme

Studies have demonstrated the essential role of neural crest-derived mesenchyme in thymus development. Auerbach demonstrated that separation of the mesenchyme from the epithelium in the E12.5 mouse thymus impaired its subsequent development (Auerbach 1960). Lineage analysis experiments using chick-quail chimeras described above, and more recently, transgenic mice with neural crest cells marked with LacZ, have shown that neural crest cells form a mesenchymal capsule around the thymus and the perivascular endothelium of vessels penetrating the thymic stroma (Le Douarin and Jotereau 1975; Jiang *et al.*, 2000). Furthermore, ablation of neural crest in chick resulted in impaired thymus development and function, as well as other associated defects in cardiac, parathyroid and thyroid development (Bockman and Kirby 1984). This group of defects resembles that seen in the human disease DiGeorge syndrome (Amman *et al.*, 1982), indicating that this syndrome may be due to the failure of neural crest to migrate and interact with the surrounding tissues to support development of these organs.

In both mouse and chick, the neural crest-derived mesenchymal component of the thymus can be substituted by mesenchyme from other sites, which can be induced by pharyngeal endoderm to participate fully in thymus development (Auerbach 1960; Le Douarin and Jotereau 1975). Shinohara and Honjo showed that insulin-like growth factors (IGF) -I and -II can replace the effect of the mesenchyme on epithelial differentiation at E12 and that epidermal growth factor (EGF), transforming growth factor-α (TGF-α) or other EGF family members, can replace the mesenchymal role in lobule formation in later embryonic thymi *in vitro* (Shinohara and Honjo 1996; Shinohara and Honjo 1997). These effects by soluble factors are in contrast to a cell-contact dependent effect of mesenchyme upon thymocyte maturation (see section 1.3.4.2) (Anderson *et al.*, 1993).

Mesenchyme appears to have several functional roles in thymus development: an early inductive interaction with the third pouch endoderm to form the thymic primordium (Auerbach 1960), a later role to support continued thymus organogenesis (Shinohara and Honjo 1996; Shinohara and Honjo 1997), and subsequently to form the capsule surrounding the primordium and invasion of the primordium to form blood vessels and septae (Le Douarin and Jotereau 1975). Mesenchyme is also an essential requirement for early thymocyte development in the thymus (Anderson *et al.*, 1993). The importance of the mesenchyme in thymus development is thus clear, however, its precise functions are not well defined and appear to be non-specific as a variety of mesenchymes or fibroblast cells can fulfil these roles.

1.4.1.3. Pharyngeal ectoderm

The physical contribution of ectoderm to thymus organogenesis is controversial as two early histological studies in mice reported different conclusions. The first, in C57BL/6 and AKR strains, showed that although the third pouch endoderm retains an attachment to the ectoderm, there is no evidence for a contribution of ectodermal cells to the thymic epithelium (Smith 1965). The second study in NMRI mice, involved serial sectioning and reconstruction of embryos, and concluded that ectodermal and endodermal components join at E12 to form the thymic primordium (Cordier and Heremans 1975; Cordier and Haumont 1980). This was shown to occur by proliferation of the second arch ectoderm at E10 to form the cervical sinus, and subsequent proliferation of the third cleft ectoderm inwards to contact the endoderm of the third pouch (Figure 1.7.). The ectodermal component pinched off from the ectodermal surface to form the cervical vesicle at E11 and this then covered and wrapped around the third pouch endoderm to form the thymic

Figure 1.7. The pharyngeal region and development of the thymus

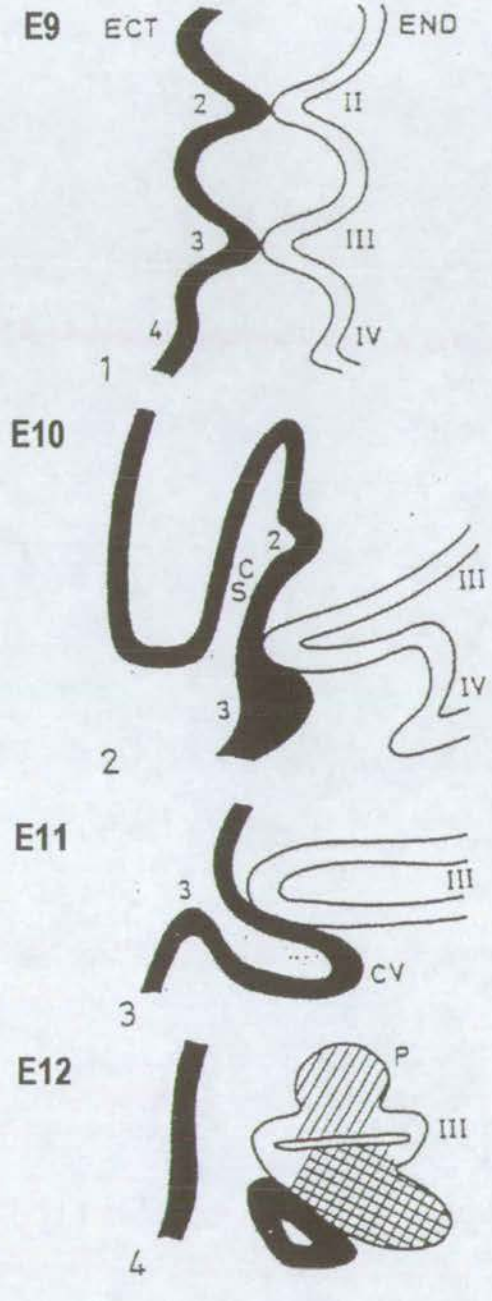

From Cordier (1975).
2,3,4, pahryngeal clefts; II,III,IV, pharyngeal pouches; CS, cervical sinus; CV, cervical vesicle; P, parathyroid; ECT, ectoderm; END, endoderm.

primordium. The thymic epithelium was therefore proposed to have a dual origin in which thymic medulla was formed from endoderm and thymic cortex from ectoderm (Cordier and Haumont 1980). Chick-quail chimera studies appeared to favour the first interpretation as they provided strong evidence that the thymic epithelium derives from endoderm alone (Le Douarin and Jotereau 1975). It is likely that the ectoderm has an inductive effect on endoderm without physically contributing to the thymic epithelium. Some evidence for an inductive effect of ectoderm comes from studies in chick embryos in which pharyngeal ectoderm was removed prior to development of the thymic primordium (Hammond 1954). In this experiment, only a rudimentary thymic primordium formed from the endoderm.

1.4.2. Molecular control of early thymus development

Several transcription factors are known to play important roles in early thymus development. The roles of *Hoxa3*, *Pax1* and *Pax9* will be discussed in detail, followed by an outline of other candidate genes with possible roles in early thymus organogenesis.

1.4.2.1. *Hoxa3*

Hoxa3 is a member of the *Hox* family of transcription factors which contain the antennapedia homeodomain DNA binding motif and function to specify positional information in embryonic development (Reviewed Krumlauf 1994). *Hoxa3* is expressed in the endoderm of the third pharyngeal pouch and the neural crest derived mesenchyme of the third and fourth pharyngeal arches (Manley and Capecchi 1995). *Hoxa3*$^{-/-}$ mutants have numerous pharyngeal defects: complete absence of thymus and parathyroid, reduced thyroid tissue, throat abnormalities and

various heart defects (Chisaka and Capecchi 1991). The exact cause of athymia in *Hoxa3* mutant mice is unclear although it is postulated that *Hoxa3* may regulate down-stream transcription factors (Manley and Capecchi 1995). The *Hoxa3* mutant mouse phenotype is similar to the phenotype seen in DiGeorge patients, however, it has been shown that the defect in the $Hoxa3^{-/-}$ mouse is not due to the amount or distribution of neural crest cells migrating to the arches (Manley and Capecchi 1995).

To determine the role of the *Hoxa3* paralogs, *Hoxb3* and *Hoxd3*, in thymus development, compound mutant mice were made. $Hoxb3^{-/-}Hoxd3^{-/-}$ mice showed no thymus defects (Manley and Capecchi 1998). However, $Hoxa3^{+/-}Hoxb3^{-/-}Hoxd3^{-/-}$ mice showed a failure of the thymic primordia to migrate to their normal positions (Manley and Capecchi 1998). During late foetal development in the mouse, the thymic primordia usually migrate medially, ventrally and caudally before joining at the midline by E15.5. These data suggest that *Hox* genes may play a role in controlling the migration of the thymic primordia.

1.4.2.2. *Pax1*

Pax1, a member of the paired box transcription factor family, is expressed in the endoderm of the third pharyngeal pouch at E10.5 and expression continues as the thymus develops (Wallin *et al.*, 1996). *Pax1* expression is down regulated in the endoderm of the third pharyngeal pouch in $Hoxa3^{-/-}$ embryos (Manley and Capecchi 1995). The role of *Hoxa3* in thymus development may therefore be via its regulation of other transcription factors, particularly *Pax1* (Manley 2000). At E12.5, *Pax1* is expressed throughout the thymic primordium, however, by E14.5 *Pax1* expression is confined to cells in the cortical region (Wallin *et al.*, 1996). As the thymus matures the percentage of cells expressing *Pax1* decreases, such that in the adult thymic cortex only a small number of cells are $Pax1^{+}$. These cells express neither MHC Class II molecules nor ER-TR4, a marker of mature cortical epithelial cells,

suggesting that these *Pax1*$^{+}$ cells may be undifferentiated epithelial precursor cells (Wallin *et al.*, 1996).

Pax1 mutant mice have hypoplastic thymi and a defect in thymocyte maturation and number (Wallin *et al.*, 1996). To investigate the possible genetic interaction between *Hoxa3* and *Pax1*, compound mutants were made (Su and Manley 2000). *Hoxa3*$^{+/-}$*Pax1*$^{-/-}$ mutants displayed more severe thymus defects than *Pax1*$^{-/-}$ single mutants: ectopic thymus lobes, increased thymic hypoplasia and a 10-fold reduction in $CD4^{+}CD8^{+}$ thymocytes, as a result of increased apoptosis of these cells. These results indicate a genetic interaction between *Hoxa3* and *Pax1*, suggesting that they may act together to regulate common down-stream genes.

1.4.2.3. *Pax9*

Another member of the paired box transcription factor family, *Pax9*, which is highly homologous to *Pax1*, is known to have a role in thymus development. *Pax9* is expressed in the pharyngeal pouches and expression is unaffected in the *Pax1* null mouse (Neubaser *et al.*, 1995). *Pax9*$^{-/-}$ mice have a more severe phenotype than *Pax1*$^{-/-}$ mice, with arrested primordia for the thymus and parathyroids (Peters *et al.*, 1998) (K.Pfeffer, Medical Microbiology, University of Munich, Germany, personal communication). Again, the exact role of *Pax9* in thymus development remains unclear. Possible clues to the roles of these transcription factors come from studies in other species. In chick, it has been shown that activation of pharyngeal *Pax1* and *Pax9* expression is an intrinsic property of the endoderm, not requiring induction by other tissues (Muller *et al.*, 1996). This study also showed that *Pax1* and *Pax9* expressing endoderm is highly proliferative and that *Pax1* and *Pax9* may play a role in preventing the fusion of adjacent tissues. In Amphioxus larvae, the *Pax1/Pax9* homologue *AmphiPax1* is down regulated where the pharyngeal pouch endoderm fuses with the surface ectoderm (Holland *et al.*, 1995).

1.4.2.4. Parathyroid development

The *Hoxa3*$^{-/-}$ and *Pax9*$^{-/-}$ mice described above are both aparathyroid in addition to athymic (Chisaka and Capecchi 1991; Peters *et al.*, 1998). The parathyroid develops from the anterior-dorsal segment of the endoderm of the third pharyngeal pouch in close association with the thymus (Cordier and Haumont 1980). A transcription factor specifically expressed in parathyroid has recently been identified: *Glial cells missing2* (*Gcm2*) is a mouse homologue of Drosophila *Gcm* (Kim *et al.*, 1998). *Gcm2*$^{-/-}$ mice completely lack parathyroid glands (Gunther *et al.*, 2000). Recent work in our laboratory has shown that cells at the anterior-dorsal end of the third pharyngeal pouch express *Gcm2* (Gordon *et al.*, 2001) (See Appendix 1). This *Gcm2*-expressing domain does not overlap with a *Foxn1*-expressing domain comprising the remainder of the third pharyngeal pouch. These data show that *Gcm2* and *Foxn1* expression mark two complementary domains in the third pharyngeal pouch that define the parathyroid and thymus primordia (Gordon *et al.*, 2001). *Foxn1* is discussed in section 1.6.

1.4.2.5. Candidate molecules with possible roles in thymus organogenesis

Dissection of the roles of the transcription factors discussed above in thymus organogenesis is beginning to define a transcription factor cascade acting in the endoderm of the third pharyngeal pouch (Figure 1.8.). Many other genes in mouse and chick are expressed in the pharyngeal region or in the thymus itself, such as *fibroblast growth factor-8* (*FGF-8*), *bone morphogenetic protein 4* (*BMP4*), *sonic hedgehog* (*SHH*), and *Nkx-2.8* (Wall and Hogan 1995; Reecy *et al.*, 1997). These signalling molecules and transcription factors may be involved in the initiation of epithelial development and the outgrowth of the thymus from the pharynx. Mice with

Figure 1.8. Formation of the thymic primordium in the mouse
(From Manley 2000)

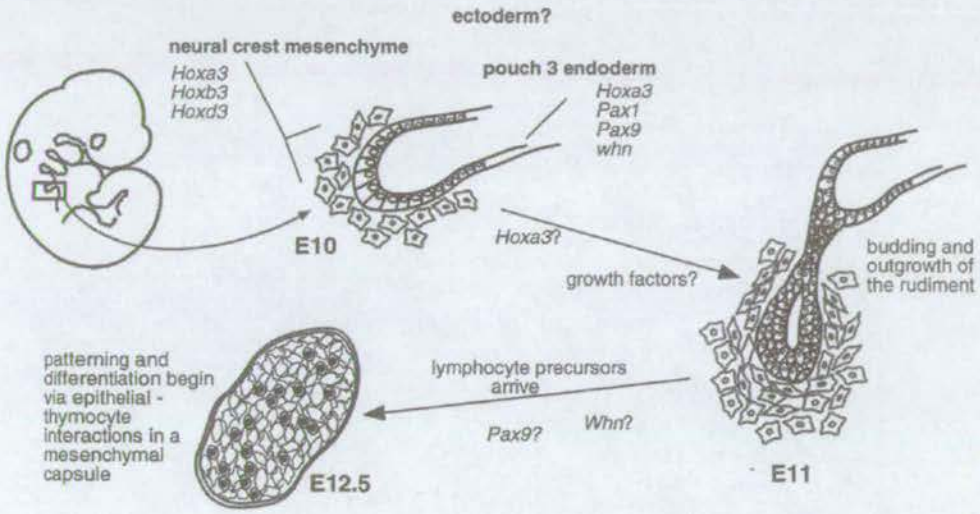

mutations in *FGF-8*, *BMP4* and *SHH* have failed to show any striking thymus phenotypes, either because the mutants are embryonic lethal before thymus development begins or possibly because of redundancy in these gene families (Winnier *et al.*, 1995; Chiang *et al.*, 1996; Meyers *et al.*, 1998). Further investigation of these molecules may provide more details about the control of early thymus organogenesis.

1.4.3. Late organogenesis

By E12.5 in mouse development, bilateral thymic epithelial primordia have formed, which have budded off from the pharynx (Manley 2000). This section outlines the initial stages in patterning of these primordia and the differentiation of thymic epithelial cells. The further development and patterning of the thymic epithelium requires interactions with lymphoid cells, which invade the primordia between E11-E13 (see section 1.5.).

1.4.3.1. Epithelial cell differentiation

Patterning of the thymic epithelial primordium involves differentiation of epithelial cells, resulting in the generation of regional differences within the primordium. Distinct cortical and medullary epithelial areas have been described at E13.5 (van Vliet *et al.*, 1985). As discussed above, mesenchyme is required for inducing thymic epithelial development from E12, including the subsequent expression of MHC molecules (Shinohara and Honjo 1997). The molecular mechanisms controlling differentiation of cells into particular epithelial lineages are unknown.

RelB, a member of the NF-κB family of transcription factors, is required for the differentiation of at least some subpopulations of medullary epithelial cells (Burkly *et al.,* 1995; Weih *et al.,* 1995). *RelB* is expressed in medullary epithelium and dendritic cells, and expression in the thymus does not start until E13.5, suggesting that this is when medulla is first formed (Schmidt-Ullrich *et al.,* 1996).

1.4.3.2. Marker studies

Marker studies, using double immunohistochemical labelling, have revealed thymic epithelial cells which are positive for markers associated with both cortical and medullary epithelium, called 'double positive' cells (Willcox *et al.,* 1987; Kendall *et al.,* 1988; Wilson *et al.,* 1992; Ropke *et al.,* 1995; Von Gaudecker *et al.,* 1997). These 'double positive' cells have been observed in human thymic epithelial tumours, mouse and chicken foetal thymus, human and rat adult thymus and the *nude* mouse thymic rudiment. In primary thymomas, immunofluorescence revealed numerous epithelial cells that are double positive for markers of both cortical and medullary/subcapsular epithelium, in addition to single positive cells (Willcox *et al.,* 1987). These double positive cells were suggested to be common thymic tumour stem cells from which the single positive cells derive. Furthermore, similar double positive cells were observed in the cortex of the normal human thymus, indicating that these could be equivalent epithelial 'stem' cells that can give rise to all the diverse populations of thymic epithelium in normal thymus (Lampert and Ritter 1988; von Gaudecker 1991; Ritter and Boyd 1993; Ritter and Palmer 1999). Additional data supports this concept of a double positive stem cell. Immunocytochemistry of cultured rat thymic fragments showed cells positive for cortical and medullary markers after 6-9 days (Kendall *et al.,* 1988). These cultures were able to form functional thymi when grafted under the kidney capsule of *nude* rats. In normal adult human thymus, double immuno-electron microscopy

demonstrated perivascular epithelial cells in the cortex which labelled with both cortical and medullary/subcapsular markers (Von Gaudecker *et al.*, 1997). Immunocytochemistry of cultured foetal mouse TEC and E14-E16 thymus tissue sections, demonstrated small subpopulations of cells reactive with both cortical and medullary markers (Ropke *et al.*, 1995). Furthermore, double positive cells were reported to comprise the entire thymic microenvironment at day 10 of foetal development (Ritter and Palmer 1999). The localisation of these cells to the pharyngeal endoderm, ectoderm or mesenchyme in early mouse embryos has not been reported, although an endodermal origin would be most likely based on morphological evidence for the origin of the thymus (Le Douarin and Jotereau 1975).

1.4.3.3. The origin of thymic epithelial cells

The origin of the thymic epithelium and the lineage relationships between distinct subpopulations of thymic epithelial cells are unclear. A dual origin for the thymic epithelium, with cortex deriving from ectoderm and medulla from endoderm, was proposed from morphological studies (Cordier and Haumont 1980). However, the marker studies discussed above suggest that a common single progenitor or stem cell may give rise to all thymic epithelial populations (Lampert and Ritter 1988; Ritter and Boyd 1993; Ritter and Palmer 1999). The observation of these double positive epithelial cells and the sparsity of evidence for an ectodermal contribution to the thymus, make the dual origin hypothesis unlikely. However, the observation of double positive epithelial cells does not itself imply the presence of a common stem cell. Purification and lineage analysis of these cells would be necessary to define their potential to give rise to all populations of thymic epithelium. Lineage analysis of germ-layer contributions to the thymus is also warranted to determine the exact origin of the thymic epithelium.

EX BIBL. UNIV. EDINBURGH

1.5. Thymic crosstalk

The microenvironment provided by thymic stromal cells plays a crucial role in thymocyte differentiation and selection. It is now also well established that thymocytes have a profound effect on the morphogenesis of the stromal compartment. This interdependence between thymocytes and thymic stromal cells is termed 'thymic crosstalk' and has been illustrated by various model systems which have shown that disrupted thymocyte development results in a reduced or disrupted thymic stroma (Ritter and Boyd 1993). In the early foetal thymus, the majority of cells are positive for cortical epithelial markers with a few cells positive for medullary epithelial markers present by E13.5 (van Vliet *et al.*, 1985). During further foetal development the regulation of the growth and organisation of cortical and medullary compartments is under the control of developing thymocytes. Thus, crosstalk between thymocytes and thymic stromal cells is essential for correctly organised thymic microenvironments (For reviews see (Ritter and Boyd 1993; van Ewijk *et al.*, 1994; Naquet *et al.*, 1999; van Ewijk *et al.*, 1999).

1.5.1. Medullary epithelial development

The immunosuppressants Cyclosporin A (CsA) and FK506 both block thymic T-cell development between the DP $CD4^+8^+$ stage and the SP $CD4^+$ and $CD8^+$ stage. CsA and FK506 treated mice showed a normal cortical architecture with developing $CD4^+8^+$ thymocytes (Kanariou *et al.*, 1989; Thomson *et al.*, 1991). However, the medulla was reduced to a small remnant, with few lymphocytes, epithelial cells, macrophages and dendritic cells. This indicates that the maturation of SP thymocytes is essential for the formation of normal medullary architecture. This process is

reversible, such that after cessation of CsA treatment, SP thymocytes were observed and with them, the normal medullary epithelial architecture reappeared. Furthermore, following sub-lethal irradiation of the thymus resulting in loss of most thymocytes, collapse of the thymic stromal architecture was observed (Randle-Barrett and Boyd 1995). Post-irradiation, the reorganisation of the stromal microenvironment occurred progressively with thymocyte development, revealed by the restoration of normal patterns of thymic epithelial marker expression.

In TCRα knockout mice, thymocyte development is blocked at the DP stage. These mice showed a normal cortical environment revealed by staining with epithelial markers, but medullary epithelial areas were greatly reduced in size (Palmer *et al.,* 1993). In SCID mice, which cannot rearrange TCR genes and therefore lack DP thymocytes, the medulla comprised a few, small scattered groups of epithelial cells (Shores *et al.,* 1991). The medullary epithelium could be restored to its normal size and architecture by removing the block in T-cell development. Transfer of normal bone marrow cells or mature T-cells into SCID mice restored medullary epithelial cell development (Shores *et al.,* 1991; Surh *et al.,* 1992). RAG-$2^{-/-}$ mice have a similar block in thymocyte development and show a similar disturbance in medullary epithelium which can be restored by transfer of bone marrow or mature T-cells (Hollander *et al.,* 1995). Following bone marrow transfer into SCID or RAG-$2^{-/-}$ mice, the appearance of the first mature SP thymocytes coincided with the appearance of medullary epithelium (Penit *et al.,* 1996). The nature of the interactions regulating medullary organisation are not clear, however a fully assembled TCR-CD3 complex may be required (Shores *et al.,* 1994). These experiments suggest that thymocytes with functional TCR molecules on thymocytes are important for the organisation and maturation of the medullary epithelial compartment and that medullary development can be reconstituted, even at adult stages.

Although transgenic mice lacking $\alpha\beta TCR^+$ thymocytes show disturbed medullary architecture, they do contain scattered medullary cells which are $relB^+$ (Naspetti *et al.,* 1997). Interactions between $relB^+$ epithelial cells and TCR^+ thymocytes are needed for the growth and organisation of medullary compartments (Naspetti *et al.,* 1997). This is consistent with the finding that in foetal thymic lobes treated with deoxyguanosine, which depletes the lobes of all thymocytes, some medullary epithelial cells survived (Ritter and Boyd 1993). These data suggest that a small population of medullary epithelial cells remain in the thymus, even in the absence of maturing T-cells.

1.5.2. Cortical epithelial development

The regulation of cortical epithelium is similarly controlled by thymocytes. A study using mutant mice homozygous for the human CD3-ε transgene, which have a complete block very early in T-cell development at the $CD25^-CD44^+$ stage, showed that these mice fail to develop a medulla and have defective cortical epithelium (Hollander *et al.,* 1995). Wild-type thymocytes could rescue this defect in foetal but not in adult mice suggesting that a developmentally restricted interaction between thymocytes and foetal stromal cells is required for formation of a functional cortex (Hollander *et al.,* 1995). It was noted in these mice that cortical defects included the orientation of cortical TEC parallel to the thymic capsule, as opposed to perpendicular to the capsule as in wild-type mice (van Ewijk *et al.,* 1999). Moreover, the thymi in these mice contained large cysts with absorptive, ciliated and goblet cells, reminiscent of 'classical' epithelial cells. These results indicated that the stromal architecture in CD3ε transgenic mice had fate-shifted, or reverted to a 2D organisation, and further experiments confirmed that thymocytes regulated control of the 3D organisation of the stroma (van Ewijk *et al.,* 1999). Studies comparing the

thymic architecture in CD3ε transgenic, $RAG^{-/-}$ mice and wild-type mice showed that thymocytes regulate stromal organisation in a stepwise manner (van Ewijk *et al.*, 2000). Transplantation of newborn CD3ε transgenic mice with bone marrow from $RAG^{-/-}$ mice restored the 3D organisation of cortical thymic epithelium and induced increased vascularisation and the appearance of TNC into the stroma (van Ewijk *et al.*, 2000). This highlights the importance of the maturation of thymocytes from $CD25^{-}CD44^{+}$ to $CD25^{+}CD44^{-}$ on the organisation of the thymic stroma. Further transplantation of wild-type bone marrow into the $RAG^{-/-}$->CD3ε bone marrow chimaeric mice, resulted in the organisation of medullary, as well as cortical epithelium (van Ewijk *et al.*, 2000). This indicated that the generation of proper cortical microenvironments is a prerequisite for generation of medullary organisation.

A role for high oxygen concentrations in the induction of 3D microenvironments, delivered by the vasculature, was suggested from the above study. *In vitro* culture of thymic lobes has shown that high oxygen conditions, as well as thymocytes, are required for correct microenvironmental architecture (van Ewijk *et al.*, 1999). A recent study has suggested that thymic vasculature may provide additional cues to effect development of the medullary epithelial compartment (Anderson *et al.*, 2000). Vascular elements and medullary TEC developed in a close spatial relationship in wild type and RAG-$2^{-/-}$ thymi.

1.5.3. Shared molecules

Evidence from monoclonal antibodies which recognise antigens on the surface of both thymocytes and stromal cells shows that these cell types share common cell surface molecules. From Table 1.1, it can be seen that MTS 9, MTS 32, MTS 37 and MTS 35 all recognise thymocytes in addition to thymic stromal cells

(Godfrey *et al.,* 1990). MTS35 recognises thymic shared Ag-1, which is expressed on immature thymocytes and a subpopulation of thymic epithelial cells, and was shown, by addition of MTS35 to FTOCs, to regulate early thymocyte development (Randle *et al.,* 1993). Thy-1 is also expressed on both thymocytes and thymic stromal cells (Tucek and Boyd 1990). Shared stromal cell-thymocyte molecules might be involved in homotypic adhesion or heterotypic interactions with complementary ligands or receptors on the opposite cell surface. The molecules might also act as receptors for soluble ligands produced by other stromal cells with the effect of regulating growth and/or differentiation of cells.

1.6. The *Nude* mutation

The *nude* mutation, originally described in 1966 (Flanagan 1966), causes disruption of normal hair growth and congenital athymia and therefore results in severe immunodeficiency (Pantelouris 1968).

1.6.1. The mouse *nude* gene - *Foxn1*

The mouse *nude* gene has been cloned and was named *whn* (*winged-helix nude*) (Nehls *et al.,* 1994) as it is a member of the family of fork-head/winged-helix domain transcription factors. The gene was subsequently renamed *Hfh11* (Segre *et al.,* 1995) and more recently *Foxn1*, in line with new nomenclature for all winged helix / forkhead transcription factors (Kaestner *et al.,* 2000). Forkhead transcription factors are defined by a DNA-binding domain of winged helix structure, and have key roles as transcriptional regulators in embryogenesis, tumorigenesis and the

maintenance of differentiated cell states (Kaufmann and Knochel 1996). For example, hepatocyte nuclear factors 3 (HNF-3), have critical roles in the development of the definitive endoderm germ layer in the mouse (Kaufmann and Knochel 1996).

The *nude* mutation is a single base pair deletion in exon 3, which results in an aberrant transcript encoding a truncated FOXN1 protein that does not contain the characteristic DNA-binding domain (Nehls *et al.,* 1994). A transcriptional activation domain C-terminal to the DNA-binding domain is also essential for the functional FOXN1 protein (Schuddekopf *et al.,* 1996). Disruption of the *Foxn1* gene by homologous recombination, such that a ß-galactosidase-neo cassette was inserted into the third exon of *Foxn1,* confirmed that *Foxn1* is the *nude* gene (Nehls *et al.,* 1996). Expression of *Foxn1* was first detected in the embryo at E9 by RT-PCR (Nehls *et al.,* 1996), however the embryonic expression pattern has not been localised in detail. *Foxn1* is expressed throughout the subcapsular, cortical and medullary epithelial cells at birth and activity remains in the thymus throughout adult life (Nehls *et al.,* 1996).

1.6.2. *Foxn1* in other species

Homologues of the mouse *Foxn1* gene have now been identified in human, rat, bony fish (*Danio rerio* and *Fugu rubripes*), cartilagenous fish (*Scyliorhinus caniculus*), agnathans (*Lampetra planeri*), cephalochordates (*Branchiostoma lanceolatum*) and *Drosophila* (Nehls *et al.,* 1994; Schuddekopf *et al.,* 1996; Schlake *et al.,* 1997; Schorpp *et al.,* 1997; Sugimura *et al.,* 2000). As *Foxn1* is involved in two apparently unrelated differentiation programs in mouse, thymus and hair development, the above homologues were used to examine the evolutionary origin of *Foxn1* (Schuddekopf *et al.,* 1996; Schlake *et al.,* 1997). Bony fish and cartilagenous

fish both develop a thymus but have no hair, whereas, agnathans and cephalochordates have neither thymus nor hair. One copy of a *Foxn1* homologue was found in all these species indicating that in agnathans and cephalochordates the *Foxn1* gene must fulfil a different function. These analyses also indicate that the involvement of *Foxn1* in hair follicle development represents a new function for *Foxn1* in mammals and this is probably due to changes in transcriptional control regions rather than gene duplication. In fact, analysis of the upstream region of the *Foxn1* gene has identified two alternative first exons, transcribed by promoters in a tissue-specific manner (Schorpp *et al.*, 1997). Both promoters appear to be active in skin whereas only the most upstream element is active in thymus. Recent experiments reporting an incomplete rescue of the mutant phenotype in *nude* mice by transgenic expression of *Foxn1*, supports the finding that the *Foxn1* locus is subject to complex transcriptional control (Kurooka *et al.*, 1996). Most of the homologues mentioned above have a very high degree of sequence similarity to the mouse gene especially in the DNA binding domain (80-90% identical). The most recent *Foxn1* homologue to be identified is that in *Drosophila*, *DFoxn1*, and this shares 70% sequence identity with mouse *Foxn1* in the DNA binding domain (Sugimura *et al.*, 2000). The functions of *DFoxn1* appear to be wide-ranging throughout development, particularly in the development of the compound eye, wing veins and bristles.

The identification of a human homologue of the *Foxn1* gene raised the question of whether a *nude* phenotype exists in humans (Schorpp *et al.*, 1997). A recent report detailed the case of two sisters who presented with severe functional T-cell immunodeficiency, congenital alopecia and nail dystrophy (Frank *et al.*, 1999). A homozygous base-pair transition was found in exon 5 of the human *Foxn1* gene which resulted in a nonsense mutation and consequently a complete absence of functional protein. The first affected child died at 12 months and showed a striking impairment of T-cell function. The second child had a bone-marrow transplant which led to immunological reconstitution, including some T-cell function probably due to

mature T-cells from the transplant. This is the first report of a human *nude* phenotype that encompasses both aspects of mutation of the *Foxn1* gene: immunodeficiency and absence of hair.

1.6.3. The role of *Foxn1* in thymus development

The adult *nude* mouse has a non-functional cystic thymic rudiment which remains throughout life. Several studies have aimed to elucidate the morphological defect in *nude* mice and the role of *Foxn1* in thymus organogenesis. The ontogeny of the defect in *nude* mice was examined by a detailed morphological study of the developing thymus (Cordier and Heremans 1975; Cordier and Haumont 1980). These reports concluded that the defect in *nude* embryos was due to the involution of the ectodermal third pharyngeal cleft derived cervical vesicle. The endoderm of the third pouch thus gives rise to a cystic thymic rudiment. The parathyroid glands develop normally from the dorsal region of the pharyngeal endoderm. Since the role of the ectoderm in thymus development is unclear, further analysis is necessary to define the morphological defect in *nude* mice.

Possible genetic interactions between *Hoxa3* and *Foxn1* have been investigated using compound mutant mice. $Hoxa3^{+/-}Foxn1^{-/-}$ showed an identical phenotype to the *nude* mouse, implying no genetic interaction between these transcription factors (Manley 2000). This suggests that *Foxn1* may function in an independent pathway regulating differentiation of thymic epithelial cells.

Monoclonal antibody expression in the *nude* thymic remnant has shown that markers of mature cortical and medullary epithelial cells and MHC antigens are either absent or found only in occasional cells lining the cysts of the *nude* thymus (Jenkinson *et al.*, 1981; Kingston *et al.*, 1984; van Vliet *et al.*, 1985). However, these studies did not include staining with a cytokeratin antibody to define the extent of the

epithelial cell population in the *nude* thymus. A later report showed that most epithelial cells in the *nude* thymic rudiment were positive for the cortical marker MTS 44 and approximately 15% of cells were positive with the medullary marker MTS 10 (Blackburn *et al.,* 1996). A small distinct population of cells appeared both MTS 44 and MTS 10 positive, indicative of 'double positive' epithelial cells discussed in section 1.4.1.4.

To address the nature of the defect in the *nude* thymus, wild type<->*nude* chimaeric mice were made by embryo aggregation (Blackburn *et al.,* 1996). MHC mis-matched mice were used to facilitate tracking of donor and host cells: the *nude* donor cells being H-$2^{k/d}$ and the wild-type host cells being H-2^{b}. All chimaeric animals had functional thymi and produced normal T-cells and some chimeras showed nude skin patches. Analysis of the chimaeric thymic epithelium showed that although some *nude*-derived cells were present in the medulla, they could not form mature epithelial networks, indicating that the *nude* defect could not be rescued by wild-type epithelium or the presence of lymphoid cells (Blackburn *et al.,* 1996). Therefore, the *nude* gene acts cell autonomously and is necessary for the development of mature thymic epithelial subpopulations. The phenotype of those *nude* derived cells remaining in the medulla was examined by reactivity with thymic epithelial antibodies. Surprisingly, *nude* derived cells strongly expressed three markers, MTS 20, 24 and 33, in higher cell numbers than in normal adult thymus. The *nude* thymic rudiment is also comprised of cells expressing these markers (Blackburn *et al.,* 1996). It was hypothesised that the MTS20^{+}, 24^{+}, 33^{+} cell population describes thymic epithelial progenitor cells (TEPC), which in the absence of *nude* are developmentally arrested (Blackburn *et al.,* 1996).

1.6.4. The role of *Foxn1* in skin and hair follicle development

In addition to athymia, the *nude* mouse is further characterised by its hairlessness. However, a detailed morphological study revealed that in fact, *nude* mice are not hairless (Kopf-Maier *et al.*, 1990). The same number of hair bulbs were embedded in the dermis as in normal animals, but in *nude* mice the keratinization processes in both hair follicles and skin epidermis were impaired. This resulted in short, bent hair shafts which only occasionally emerged from the follicles, and highly irregular piles of cornified debris in the epidermis.

Normal hair follicle development begins with a series of interactions between the ectoderm which will give rise to the epidermis and the mesoderm which will give rise to the dermis (review (Hardy 1992)). A dermal papilla is formed in the dermis which then signals to the epidermal cells of the hair matrix to divide. These cells then move up the hair shaft to form hair cells or root sheath cells. Hair growth is cyclical: each follicle proceeds through an active growth phase (anagen) (Figure 1.9.), a regression and shortening phase (catagen) and a resting phase (telogen). The follicle is then reactivated from the base of the resting structure to form a new hair. During mouse embryonic development, the first follicle development is in the whiskers (vibrissa) at E13, whereas the rest of the hair follicles (pelage hairs), start to develop from E14.5 (Kaufman 1992).

Several studies have investigated the role of *Foxn1* during hair follicle and epidermal development. *Foxn1* was expressed in epithelial cells not only in skin but also in developing nails, the nasal passage, tongue, palate and teeth (Lee *et al.*, 1999). A series of experiments investigating the function of *Foxn1* in keratinocytes and hair follicles postulated that *Foxn1* functions to regulate the balance between proliferation and differentiation in epithelial cells (Brissette *et al.*, 1996; Lee *et al.*, 1999; Prowse *et al.*, 1999).

Figure 1.9. Structure of an anagen hair follicle

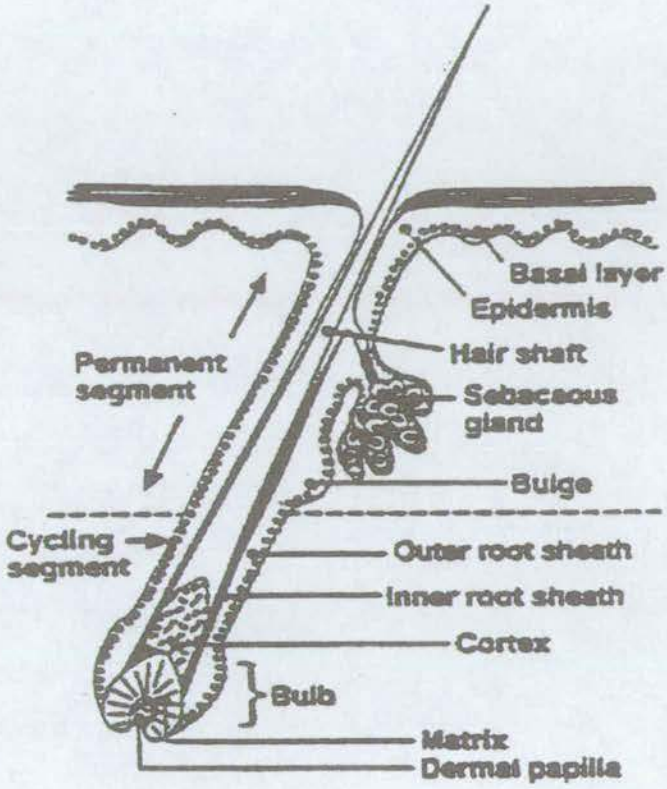

In suprabasal cells of the epidermis and precursor cells of the hair shaft and inner root sheath, *Foxn1* expression was induced at the same time as markers of terminal differentiation appear. Thus, *Foxn1* expression appeared to encompass the transition from the proliferative to post-mitotic state and regulated the initiation of terminal differentiation. In the absence of *Foxn1*, keratinocytes showed an increased propensity to differentiate and ectopic expression of *Foxn1* in epithelia resulted in impaired differentiation and increased proliferation, with hair follicles continually in an abnormal anagen (growth) phase.

Recently *Foxn1* has been shown to function as a transcriptional regulator of keratin genes in hair. Expression of *Foxn1* in HeLa cells induced expression of human hair keratin genes and in mouse *nude* skin, expression of hair keratin genes was severely reduced (Schlake *et al.*, 2000). Genes abnormally expressed in *nude* skin were identified by representational difference analysis (Meier *et al.*, 1999; Meier *et al.*, 1999). *Acidic hair keratin gene 3* (*mHa3*) is usually co-expressed with *Foxn1* in hair follicles but in the absence of *Foxn1*, expression was lost. *Brain and skin serine protease* (*BSSP*) is a novel molecule expressed in the sebaceous gland and outer root sheath of hair follicles. In *nude* skin, its expression was upregulated. These studies are beginning to identify genes involved in the morphological aberrations in *nude* skin, which are targets of *Foxn1* transcriptional regulation.

1.7. Aims and experimental approach

It is clear from the literature that formation of the thymic primordium is directed by pharyngeal pouch endoderm, neural crest-derived mesenchyme and pharyngeal ectoderm (Figure 1.10). Expression of transcription factors, *Hoxa3*, *Pax9* and *Pax1*, in these cells is required for thymus development. Subsequently, the expression of *Foxn1*, and inductive signals from developing thymocytes, are required

Figure 1.10. A progenitor cell for all thymic epithelium?

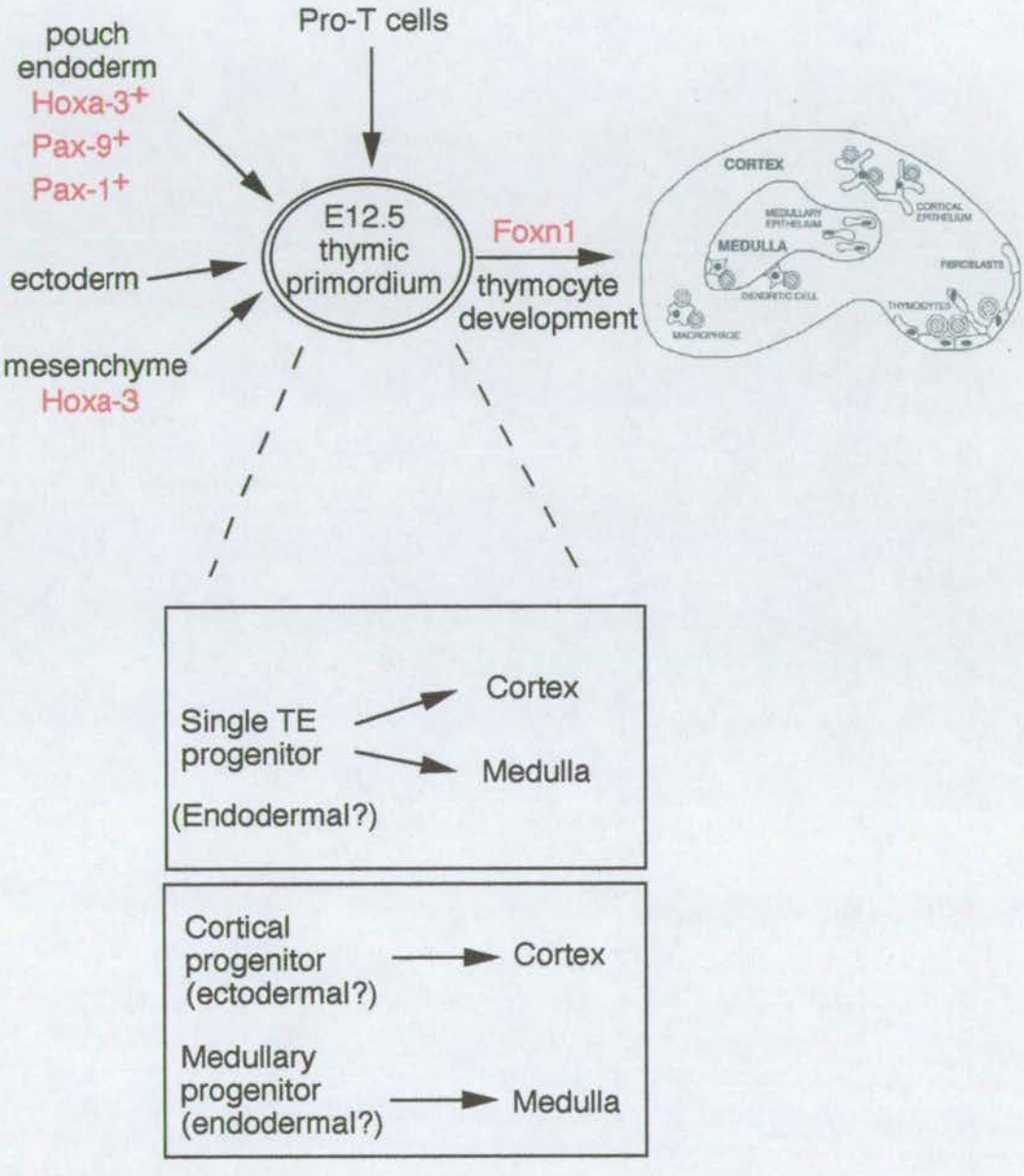

for the differentiation and patterning of epithelial cells in the primordium establishing mature subpopulations of thymic epithelium (TE). However, the origin and lineage relationships between different subpopulations of TE are unclear.

The aim of this thesis was to test the hypothesis that mAbs MTS20 and MTS24, identify thymic epithelial progenitor cells (TEPC) (Blackburn *et al.*, 1996). To investigate this hypothesis, three criteria were established that markers of TEPC should fulfil. Firstly, markers of TEPC should be expressed at a high level during early thymus organogenesis. Secondly, putative TEPC should express markers associated with commitment to the thymic epithelial lineage, but should not display markers associated with mature thymic epithelium. Thirdly, putative TEPC should be able to differentiate into one or more populations of mature thymic epithelium when grown under appropriate conditions. The experiments presented in this thesis investigate whether MTS20$^+$MTS24$^+$ cells from the E12.5 thymic primordium fulfil these criteria.

Chapter three describes the temporal and spatial expression pattern of *Foxn1*, a transcription factor essential for the differentiation of mature TE from precursor cells, throughout thymus development. Chapter four describes the cellular composition of the E12.5 thymic primordium and expression of mAbs MTS20 and MTS24 and other markers of mature TE throughout thymus ontogeny. In chapter five, the lineage commitment of the MTS20/24$^+$ cell population purified from the E12.5 thymic primordium has been investigated by expression of markers of thymic epithelium and transcription factors that are known to be required for thymus organogenesis. Finally, chapter six describes lineage and functional analyses of the E12.5 MTS20/24$^+$ population which investigate the potential of these cells to differentiate into mature TE and provide thymus function *in vivo*.

Chapter 2

MATERIALS AND METHODS

2.1. Materials

Unless otherwise stated, analytical grade chemicals were obtained from either Sigma or BDH Laboratory Supplies (Merc Ltd). Electrophoresis grade agarose was supplied by Flowgen (Sittingbourne, UK). Synthetic oligonucleotides were synthesised by VH Bio Ltd (Newcastle, UK), R&D systems (Oxford, UK) or Oswel DNA service (University of Southampton, UK).

2.1.1. Solutions

1x TAE	0.04M Tris-acetate, 0.001M EDTA
PBS	0.01M phosphate buffer, 0.0027M potassium chloride 0.137M sodium chloride pH 7.4
DEPC treated water	0.1% Diethyl pyrocarbonate in water

Glasgow minimal essential media:

1x GMEM (Gibco)
10% Foetal calf serum (Globepharm, Surrey)
0.25% sodium bicarbonate (Gibco)
0.1% MEM non-essential amino acids (Gibco)
4mM Glutamine (Gibco)
2mM sodium pyruvate (Gibco)
0.1mM 2-mercaptoethanol (Sigma)
Leukemia inhibitory factor (LIF)100U/ml

Dulbecco's modified eagle medium:

1x DMEM (Gibco)
10% foetal calf serum (Globepharm, Surrey)
4mM Glutamine (Gibco)
2mM sodium pyruvate (Gibco)
50U/ml Penicillin (Gibco)
50µg/ml Streptomycin (Gibco)

Eosin solution: 0.02% eosin in dH_20

Fixative for ß-gal staining: 0.2% gluteraldehyde, 1% formaldehyde, 5mM EDTA, 2mM $MgCl_2$, 0.02% NP-40 in PBS

ß-gal staining solution: 1mg/ml X-gal (Promega), 5mM potassium ferrocyanide, 5mM potassium ferricyanide, $MgCl_2$, 0.02% NP-40 in PBS

Cell dissociation mixture: 2mg/ml hyaluronidase, 0.7mg/ml collagenase and 0.05mg/ml deoxyribonuclease in PBS

FACS wash: 10% foetal calf serum in PBS

MACS wash: 0.5% BSA + 2mM EDTA in PBS

2.2. Cell culture

All cell manipulations were carried out in Class II laminar flow sterile hoods (Heraeus) using sterile technique. All cells were incubated at 7% CO_2 at 37°C in a humidified incubator (Heraeus). All solutions were filtered and sterility tested. Cells were grown in tissue culture grade plastic flasks (Corning).

2.2.1. ES cell culture

ES cells were cultured in GMEM media in gelatinised flasks (0.1% gelatin in water). Confluent cultures were passaged by rinsing cells in PBS and incubation in 0.025% trypsin (Gibco). Flasks were tapped to release the cells from the base of the flask and cells were harvested into medium. After centrifugation, the cell pellet was resuspended in fresh medium and replated at 1/10th original density.

2.2.2. Murine embryonic fibroblast (MEF) culture

E13.5 or E14.5 wild type embryos were decapitated, stripped of all their internal organs and all extraembryonic tissue. The remaining tissue was broken into smaller fragments and washed in PBS. The tissue fragments were incubated in 5ml trypsin solution at 37°C for 10 minutes. 10ml of DMEM was added and the solution was drawn through a 10ml syringe to break up the tissue fragments. Subsequently, the solution was drawn through a small gauge needle to create a single cell suspension. The suspension was allowed to stand to allow any large remaining fragments to settle. 2ml of the suspension was transferred into a $25cm^3$ tissue culture flask, topped up with 8ml of medium and incubated at 37°C. The following day, the medium was changed. After 2 days fibroblasts could be seen adhering to the flask. The medium was changed every two days. Upon confluence, the cells were trypsinised and replated at lower densities. When required, the cells were trypsinised, washed in medium and resuspended at the appropriate dilution.

2.2.3. Freezing cells

Cells were trypsinised and resuspended in 10% dimethyl sulphoxide in media. Following centrifugation, the cell pellet from one $25cm^3$ flask was resuspended in 1ml of the same solution and 0.5ml aliquoted into cryotubes (Nunc).

These were placed at -80°C overnight and transferred to a liquid nitrogen cell bank the next day.

2.2.4. Thawing cells

Frozen vials were retrieved and placed in a 37°C water bath. Immediately upon thawing the contents of the vial were transferred into 9.5ml of media and centrifuged. The cell pellet was resuspended in 10mls of media and transferred to a $25cm^3$ flask. The media was changed after 8-16 hours and subsequently maintained as above.

2.3. Histology

2.3.1. Animal maintenance and dissection

All mice were housed and bred within the Centre for Genome Research or the Ann Walker building at the University of Edinburgh according to the provisions of the Animals (Scientific Procedures) Act 1986. Mice were housed in a stabilised environment with a twelve hour light/dark cycle and supplied with food and water *ad libitum*. All animals were culled by the schedule 1 method of cervical dislocation. For the collection of embryos at specific stages of development, matings were set up overnight and females examined for the presence of a vaginal plug the following morning. This was recorded as embryonic day 0.5 (E0.5). Routinely, matings were between C57BL/6 females and CBA males. Pregnant females at the correct stage were sacrificed and the uterus dissected into PBS. Embryos were dissected from the uterus and all extraembryonic tissues removed. The age of the embryo between E9.5 and E11.5 was determined by counting the number of somites. The age of later

embryos was confirmed by morphological criteria. Embryonic thymi were removed from embryos E12.5 to E17.5 by microdissection using a dissecting microscope (Olympus SZ40). Pharyngeal arches were dissected from E9.5 to E11.5 embryos by cutting above the second arch and below the third arch. Adult tissues were dissected free of connective tissue and washed in PBS.

2.3.2. Frozen sections

Freshly dissected tissues or embryos were embedded in OCT compound (Tissue Tek, Miles Inc., USA), snap frozen on dry ice and stored at -80°C. Prior to sectioning, tissue blocks were placed in the cryostat (Anglia scientific, Cryotome 650) to equilibrate to temperature for 30 minutes (-20°C). Sections were cut at 8µm and collected onto glass slides (Chance Propper Ltd) pre-coated with 0.05% Poly-L-Lysine. The sections were air-dried for several hours and stored at -80°C until use.

2.3.3. Hematoxylin and eosin staining

Frozen sections were allowed to equilibrate to room temperature then fixed in 100% acetone (-20°C) for 1 minute. Sections were rinsed in PBS, incubated in Mayer's hematoxylin solution for 1 minute followed by washing in tap water. Sections were then incubated in eosin solution for 3 minutes. After washing in water, sections were air-dried and mounted with DPX.

2.3.4. Immunohistochemistry

Frozen sections were allowed to equilibrate to room temperature then fixed in 100% acetone (-20°C) for 1 minute. Sections were rinsed in PBS and blocked in 10% normal serum in PBS for 30 minutes. For enzymatic detection using horseradish

peroxidase (HRP), endogenous peroxidase activity was blocked prior to antibody binding by incubating sections in 0.3% hydrogen peroxide in methanol for 15 minutes. The primary antibody was applied to the sections at the appropriate concentration and incubated for 1 hour at room temperature. The slides were washed 3 times for 5 minutes in PBS plus 0.05% Tween 20. Following primary antibody incubation, sections were incubated in HRP-conjugated secondary antibody for 1 hour at room temperature followed by three washes for 5 minutes in PBS-Tween. Sections were then incubated in diaminobenzidine (DAB) peroxidase substrate (Sigma FAST DAB tablets) for 3-10 minutes at room temperature. Colour development was monitored and stopped by washing in distilled water. Sections were counterstained in Mayer's hematoxylin for 1 minute, washed in tap water, air dried and mounted in DPX. Staining was examined and photographed under transmitting light using the Vannox AHBT3 microscope (Olympus) and photographed using a C35 AD-4 camera (Olympus).

2.3.5. Immunofluorescence

For immunofluorescence, after primary antibody binding, sections were incubated with fluorescent conjugated secondary antibody in the dark for 1 hour at room temperature followed by 3 washes for 5 minutes with PBS-Tween and a final wash in PBS. Slides were mounted with Fluoromount and examined under the appropriate excitation conditions using the Vannox microscope described above. Some immunofluorescent staining was carried out using the tyramide amplification system (NEN life sciences) which amplifies the signal from antibody binding by depositing numerous flurophore labels onto a bound HRP enzyme. In these cases, tissues sections were initially blocked for endogenous peroxidase activity as above, incubated in the TNB blocking buffer provided for 30 minutes, followed by primary antibody binding, washing and incubation in HRP-conjugated secondary antibody as

described above. After washing sections were incubated in FITC-conjugated tyramide reagent diluted at 1:50 in amplification dilutent provided for 8-10 minutes. After washing, the slides were mounted and examined as above.

2.3.6. Antibodies

Primary antibodies used in immunohistochemical and immunofluorescent studies were MTS20 (IgM) and MTS24 (IgG2a) (rat antibodies provided as hybridoma supernatants by R.Boyd, Monash University Medical School, Melbourne, Australia), MTS 10 (IgM) (rat antibody, Pharmingen, used at 1:50 dilution), 4F1 (IgM) (rat antibody provided as hybridoma supernatant by M.Ritter, Imperial College School of Medicine, London, UK), rabbit anti-cytokeratin (DAKO corporation, used at 1:500 dilution), anti-MHC-Class II (M5114-biotin, used at 1:100), rat anti-Thy-1 (T24, used at 1:100), rat anti-keratin 5 (Covance Research Products, used at 1:1000), rabbit anti-keratin 8 (provided as hybridoma supernatant by E.Richie, University of Texas, USA). Secondary antibodies used were rabbit anti-rat HRP (Sigma, used at 1:750), donkey anti-rabbit HRP (Diagnostics Scotland, used at 1:250), streptavidin FITC (Pharmingen, used at 1:50), rabbit anti-rat FITC (Sigma, used at 1:300), goat anti-rabbit-FITC (Sigma, used at 1:50) and goat anti-rat-PE (Pharmingen, used at 1:50). Control sections with an appropriate isotype-matched primary antibody (rat IgM or rat IgG, Pharmingen) or no primary antibody were included in each experiment.

2.3.7. Staining embryos for ß-gal activity

Freshly dissected embryos were washed in PBS and fixed for 30-60 minutes at 4°C. Samples were washed in PBS + 0.02% NP-40 3 times and incubated in stain solution at 37°C for 4-12 hours. Samples were washed 3 times in PBS NP-40 and

post-fixed in the same fixing solution for 30 minutes. Embryos were examined using Olympus SZ40 dissecting microscope and photographed using a C-35 AD-4 camera. Embryos were stored at 4°C in fix until processed for paraffin embedding and sectioning.

2.3.8. PCR genotyping

For determination of genotype, tail-tips from adult mice or yolk sacs from embryos were digested overnight at 55°C in lysis buffer containing 100mM Tris.HCl pH8.5 (Roche), 5mM EDTA, 0.02% Tween 20, 10 µg/ml Proteinase K (Roche). After vortexing, the sample was diluted 1:10 with water and 5µl added to the PCR reaction mixture. PCR was carried out using primers to the ß-gal cassette or to exon 3 of the *whn* gene. The following conditions were used for PCR: 35 cycles each of 10 sec at 94°C, 10 sec at 53°C, 10 sec at 72°C. PCR products were analysed on a 2% agarose TAE gel with 0.5µg/ml ethidium bromide. 0.5µg of 1kb ladder (Roche) was loaded on the gel as a size standard. Using ß-gal primers, a band of 300 bp was seen in samples containing the ß-gal cassette insertion, and using *whn* primers, a 450 bp band was seen in samples with the endogenous *whn* gene.

PCR reaction mixture:	PCR buffer (Roche) containing: 10mM Tris-HCl, 50mM KCl, 2.5mM MgCl2, 0.1mM dNTP (Roche), 0.1-1µM of each primer, 1U Taq DNA polymerase (Roche)

Primer sequences:

ß-gal primers:	Forward	5' TAA TGG GAT AGG TTA CGT 3'
	Reverse	5' ACA ACG TCG TGA CTG GGA AAA C 3'
whn exon3 primers:	Forward	5' TTC AGC TGC TCG TCG TTT GTG 3'
	Reverse	5' AGA ATT TGG TTG TGT TCC TGG 3'

2.3.9. Paraffin embedding and sectioning

Embryos for paraffin embedding were treated as follows:

70% ethanol	15 minutes
90% ethanol	15 minutes
100% ethanol	15 minutes
100% ethanol	15 minutes
100% ethanol	15 minutes
xylene substitute	15 minutes
xylene substitute	15 minutes
xylene substitute	15 minutes
wax (60°C)	30 minutes
wax (60°C)	30 minutes
wax (60°C)	30 minutes

Xylene substitute and paraffin wax were obtained from Shandon scientific Ltd. Samples were embedded in wax and cooled to 4°C. Sections were cut at 8μm, expanded on water at 40°C, collected onto glass slides and air dried overnight.

2.3.10. Counterstaining

Paraffin sections were counterstained with eosin after ß-gal staining. Sections were dewaxed in xylene substitute for 5 minutes, rehydrated through an ethanol series of 100%, 95%, 70%, 50%, water, then stained in eosin solution for 2 minutes. Sections were dehydrated through ethanol of 70%, 90%, 100%, then cleared in xylene substitute. Sections were then mounted in DPX and examined under a light microscope.

2.4. Flow cytometry and cell sorting

2.4.1. Cell preparation and staining

Freshly dissected tissues were dissociated by incubation at 37°C for 10 minutes in dissociation mixture followed by 10 minutes in 0.025% trypsin at 37°C with agitation. Lymph nodes were squashed under the end of a syringe barrel to release cells and passed through a 70μm cell strainer (Falcon). Cells were washed in FACS wash, counted and resuspended at $1x10^7$ cells per ml. $1x10^6$ or $1x10^5$ cells were incubated with primary antibody for 30 minutes at 4°C, then washed three times with FACS wash. Cells were incubated with secondary antibody for 30 minutes at 4°C then washed three times and resuspended in a final volume of 200μl. For detection of intracellular antigens, cells were treated with fix and perm reagents (Caltag) prior to primary antibody staining.

2.4.2. Flow cytometry

Cells were analysed on a FACScan machine (Becton Dickinson) and staining analysed using Cell Quest software (Becton Dickinson). For analysis, cells were gated to exclude dead cells and red blood cells and to include the population of interest. Antibodies used for flow cytometry were MTS 20, MTS 24, 4F1, anti-cytokeratin (all described above), anti-keratin 5 (from Babco, used at 1:500), anti-keratin 8 (rat antibody provided as hybridoma supernatant by E.Richie, University of Texas, Smithville, USA), anti-H3-P (Juan 1998) (used at 1:100) and rabbit anti-laminin (Sigma, used at 1:200). Secondary antibodies used were goat anti-rat-FITC (Jackson Labs, used at 1:50) and goat anti-rabbit FITC (Sigma, used at 1:500). Directly conjugated antibodies used were CD4-PE (Pharmingen, used at 1:100), CD8-FITC (Pharmingen, used at 1:100), CD3-APC or CD3-Cychrome (Pharmingen, used at 1:100), CD117-FITC (c-kit) (Pharmingen, used at 1:100). Propidium Iodide

(50μg/ml) was used to detect dead cells contaminating the preparations. Controls consisted of unstained cells, cells stained with secondary antibody alone and cells stained with appropriate unreactive isotype-matched primary antibodies.

2.4.3. Fluorescence activated cell sorting (FACS)

Single cell suspensions were prepared and stained as described above in sterile conditions. Sorting was performed on a FACS Star (Becton Dickinson). Aliquots of sorted cell populations were re-analysed by FACS to assess the purity of the sorted populations.

2.4.4. Magnetic cell sorting (MACS)

Adult and E17.5 thymus preparations were depleted of $CD4^+$ and $CD8^+$ cells and double negative thymocytes were prepared from adult thymocyte populations by depletion of $CD4^+$ and $CD8^+$ cells. $1x10^7$ cells were incubated with 80μl of MACS wash and 10μl each of anti-CD4 and anti-CD8 magnetic beads (Miltenyi Biotec) for 15 minutes at 4°C. After washing in MACS wash cells were loaded onto a prewashed CS depletion column held in a MiniMACS magnet (Miltenyi Biotec). The column was washed thoroughly and the effluent containing the cells of interest collected.

2.5. Kidney capsule grafting

2.5.1. Reaggregate cultures

For hanging drop cultures, appropriate numbers of cells were mixed in DMEM media, centrifuged to a pellet and resuspended in 10μl of DMEM media. The

cells were then transferred as a drop to the lid of a sterile bacterial petri dish. The lid was inverted onto the base of the petri dish containing sterile water to prevent evaporation. After culture for 24-48 hours, the cells had reaggregated in the base of the drop.

For RTOC culture, appropriate numbers of cells were mixed in DMEM media, centrifuged to a pellet and excess media was removed. After vortexing to produce a thick cell slurry, the cells were transferred using a fine glass pipette controlled by mouth suction and placed in a drop on a 0.8μm Isopore membrane filter (Millipore) floating on medium in a 6-well tissue culture dish. After culture for 24-48 hours, the cells had reaggregated into a solid structure.

2.5.2. Grafting technique

Female ICRF nu/nu mice were obtained form Harlan UK and kept in isolated, ventilated cages under sterile conditions. Surgical operations were carried out in a Class II flow hood under sterile conditions using a dissection microscope for the grafting procedure. Mice were anaesthetised by intra-peritoneal injection of avertin solution. An incision was made in the flank skin on one side only and the corresponding kidney isolated. A small tear was made in the capsule of the kidney and the reaggregated cells were transferred under the kidney capsule using a glass pipette controlled by mouth suction or fine forceps. A small piece of nitrocellulose filter was also inserted under the capsule at the site of the graft. The kidney was then replaced, the peritoneal cavity sutured and the skin clipped to close the wound.

2.6. Reverse-transcriptase PCR

2.6.1. RNA isolation

Cells or tissue fragments were placed into 500µl of Trizol reagent (Gibco) and incubated at room temperature to allow dissociation of cells. RNA was isolated by adding 100µl chloroform, shaking for 15 seconds followed by centrifugation at 13000rpm for 15 minutes. The upper aqueous phase was removed to a new tube and RNA was precipitated by addition of 250µl of isopropanol and 1µl of RNAse-free glycogen (Roche). After incubation for 10 minutes at room temperature the samples were centrifuged at 13000rpm for 10 minutes. The supernatant was removed and the pellet washed with 1ml of 75% ethanol. After vortexing and centrifugation at 13000rpm for 5 minutes the supernatant was removed and the pellet was airdried for 10 minutes. The pellet was then resuspended in 10µl DEPC treated water and incubated at 55°C for 10 minutes to allow the RNA to resuspend. RNA was then treated with RNase-free DNase I (Roche) at 42°C for 30 minutes to remove any contaminating genomic DNA. The DNase was inactivated by incubation at 75°C for 10 minutes. The RNA was stored at -80°C until use.

2.6.2. cDNA synthesis

cDNA was synthesised using the Reverse-it 1st strand synthesis kit from Advanced Biotechnologies Ltd. The synthesis reaction contained:

1-2µg RNA template

buffer containing 10mM Tris-HCl, 75mM KCl, 3mM MgCl2, 10mM DTT

500µM dNTP mix

5U RNase inhibitor

25U M-MLV reverse transcriptase

0.5 µg oligo dT primer

sterile water to 20µl

The reaction was incubated at 42°C for 60 minutes, followed by 75°C for 10 minutes to inactivate the RT. cDNA was stored at -20°C until use. Equivalent reactions without the reverse transcriptase enzyme were performed for all samples.

2.6.3. PCR

cDNA was normalised for equivalent template amounts by serial dilution and amplification using primers specific to β-actin. Normalised cDNA was serially diluted 3-fold and PCR was performed according to the following protocol:

1µl cDNA

AmpliTaq Gold buffer (PE Applied Biosystems) containing 15mM Tris-HCl, 50mM KCl

2.5mM MgCl2 (PE Applied Biosystems)

0.2mM dNTP mixture (Roche)

0.1-1µM Forward Primer

0.1-1µM Reverse Primer

1U AmpliTaq Gold (PE Applied Biosystems)

sterile water to 20µl

PCR reactions were run in a GeneAmp 9700 thermal cycler (PE Applied Biosystems) according to the following program:

	10 minutes 95°C (hot start)		
denaturation	94°C 20 seconds	}	
annealing	60°C 20 seconds	}	40 cycles
extension	72°C 20 seconds	}	
	72°C 10 minutes		

Following PCR, samples were run on a 2% agarose TAE gel with 0.5µg/ml ethidium bromide. 0.5µg of 1kb ladder (Roche) was loaded on the gel as a size standard. Equivalent reactions with no cDNA template or with the product of the no-reverse transcriptase reaction were run for all samples.

2.6.4. Primer sequences

Primer sequences are as follows:

ß-actin	Forward	5' GTG ACG AGG CCC AGA GCA AGA G 3'
	Reverse	5' AGG GGC CGG ACT CAT CGT ACT C 3'

Expected product size from cDNA: 900bp.

Foxn1	Forward	5' CAG TGT GAC GTC ACA CTT CCA 3'
	Reverse	5' GAA GGC AGG CTG AGA AGA ACA 3'

Expected product size from cDNA: 672bp

Pax1	Forward	5' AGG CCA CGG ATG CAC TCG GTA G 3'
	Reverse	5' AGA TTG GGT CCT TGA AGA ATG C 3'

Expected product size from cDNA: 620bp

Pax9	Forward	5' GCC CAA CGC CAT TCG GCT TCG C 3'
	Reverse	5' CCC GGA TCT CCC AAG CGA AG 3'

Expected product size from cDNA: 247bp

Hoxa3	Forward	5' CCA GAA CCG CCG CAT GAA GTA C 3'
	Reverse	5' GTG GGC AAC TCT CCT GGC TCA C 3'

Expected product size from cDNA: 650bp

Where possible primers were designed to span two or more exons so that amplification from genomic DNA would produce a larger band size than would be expected from cDNA.

2.6.5. Real-time reverse-transcriptase PCR

RNA extraction and cDNA synthesis were as described in section 2.6.1 and 2.6.2. cDNA was serially diluted and PCR was performed according to the following protocol:

2µl cDNA

2µl 1x Lightcycler-DNA Master SYBR Green mixture (Roche) (contains Taq DNA polymerase, reaction buffer, dNTP, SYBR green I dye and 1mM $MgCl_2$)

1mM MgCl2 (Roche)

0.1-1µM Forward Primer

0.1-1µM Reverse Primer

sterile water to 20µl

Each reaction was loaded into a pre-cooled capillary tube, centrifuged at 3000rpm for 5 seconds, loaded into the Lightcycler and run according to the following program:

Denaturation:	95°C for 30 s
Amplification:	95°C for 0 s, 55°C for 5 s, 72°C for 20s, 85°C for 2 s.
	60 cycles
Melting point:	65°C -> 95°C at 0.1°C/s
Cooling:	95°C -> 40°C

Fluorescence was acquired at the end of each amplification cycle at 85°C and throughout the melting point analysis. Following PCR, data was analysed on the Lightcycler data analysis software.

GAPDH primer sequences:

Forward:	5' TGG GAA GCT GGT CAT CAA TGG GAA ACC 3'
Reverse:	5' TCA TGG ATG ACC TTG GCC AGG GG 3'

(*Foxn1* primers as described in section 2.6.4.)

Chapter 3

RESULTS

Expression of *Foxn1* during thymus organogenesis

3.1. Introduction

Foxn1, the gene mutated in *nude* mice, is essential for the differentiation of all mature thymic epithelial subpopulations and for normal skin and hair follicle development (Flanagan 1966; Nehls *et al.,* 1994; Blackburn *et al.,* 1996; Nehls *et al.,* 1996). *Nude* mutant mice retain a non-functional cystic thymic rudiment, resulting in severe immunodeficiency, and a defect in keratinization in the epidermis and hair follicles (Pantelouris 1968; Cordier 1974; Kopf-Maier *et al.,* 1990). *Foxn1* expression is detected in the embryo as early as E9 by RT-PCR (Nehls *et al.,* 1996), however, the embryonic expression pattern has not been localised in detail. In the neonatal thymus, *Foxn1* is expressed throughout the subcapsular, cortical and medullary epithelial cells (Nehls *et al.,* 1996). This chapter describes the investigation of early thymus organogenesis using *Foxn1* as a thymus-specific marker. *Foxn1* expression is analysed by utilising a targeted transgenic mouse line in which ß-gal is placed under the control of the *Foxn1* promoter (Nehls *et al.,* 1996).

The work presented determines the spatial and temporal expression of *Foxn1* during thymus organogenesis, examines the morphology of the cells committed to the thymic epithelial lineage and investigates the morphology of the defect in the *nude* mouse thymus.

In an appendix to this chapter, *Foxn1* expression is examined during skin and hair follicle development in order to determine the temporal and spatial expression profile of *Foxn1* during embryonic hair follicle development and cyclical hair follicle growth.

3.2. Transgenic mouse line

ES cells with a targeted disruption of the *Foxn1* gene were provided by Dr. A.J.H. Smith (CGR, University of Edinburgh) with permission from Dr. T. Boehm (Max-Planck-Institute for Immunobiology, Freiburg, Germany). In these cells an IRES-lacZ-neo cassette was targeted into the third exon of the *Foxn1* gene by homologous recombination, producing a disruption of the *Foxn1* gene and a ß-galactosidase gene under the control of *Foxn1* transcriptional regulatory elements (Nehls *et al.*, 1996). The β-gal cytoplasmic reporter protein can be used to follow *Foxn1* expression. C57BL/6 blastocysts were injected with these ES cells and transferred to the uteri of pseudopregnant mothers by Jane Brennan (CGR, University of Edinburgh). Using coat colour to assess ES cell contribution to offspring, chimaeric males were identified and subsequently test-crossed with C57BL/6 females. Tail DNA genotyping of test-cross offspring indicated transmission of the targeted mutation through the germ line. These male founders were used for backcross matings to provide heterozygous and homozygous animals for analysis.

3.3. *Foxn1* expression during thymus organogenesis

Embryos between E9.5 and E13.5 were taken from matings between $Foxn1^{+/-}$ males and C57BL/6 females. The yolk sacs were dissected from the embryos and kept aside for genotyping. Whole embryos were stained for ß-gal activity and subsequently embedded in paraffin for sectioning. Wild-type littermates were used to control for background ß-gal activity. No background activity was observed in control embryos. At each stage, at least three different litters of embryos were examined to ensure reproducibility of results. Adult thymi were dissected from $Foxn1^{+/-}$ male animals and whole-mount stained.

Expression of ß-gal was first observed in the embryo at E10.5 (35 somite embryos) in the ectoderm covering the second and third pharyngeal arches (Figure 3.1.A,B). Para-sagittal sections through the arches revealed punctate staining, indicating very low-level expression, in the ectoderm overlying the arches and in the pericardium surrounding the developing heart, which is also ectodermal in origin (Figure 3.1.C,D). The level and distribution of expression in E10.5 embryos was slightly variable between embryos, ranging from expression localised primarily in ectoderm overlying pharyngeal arch three, to expression encompassing ectoderm overlying pharyngeal arches one to three.

At E11.25 (40-44 somites), ß-gal expression remained in some ectodermal cells covering the arches and was for the first time observed in the endoderm of the third pharyngeal pouch (Figure 3.2.A-D). At this stage, the endodermal cells of the pouch can be clearly delineated from the surrounding mesenchyme and range from one cell layer near the pharynx to several cell layers towards the heart (Figure 3.2.D). β-gal expression was first observed in those cells at the ventral end of the pharyngeal endoderm.

Figure 3.1. β -gal expression in the developing pharyngeal region of E10.5 (35 somites) β-gal/*Foxn1*$^{+/-}$ embryos

A: Whole embryo showing β-gal expression in pharyngeal arch ectoderm.

B: High magnification of β-gal staining in pharyngeal arch ectoderm.

C: Para-sagittal section through the pharyngeal arches showing β-gal in ectodermal cells overlying the arches and pericardium.

D: High magnification of section through pharyngeal arches showing β-gal staining in pharyngeal ectoderm.

A and B show β-gal whole mount stained embryos, C and D show paraffin wax sections through the pharyngeal region of β-gal whole mount stained embryos counterstained with eosin.

Figure 3.2. β-gal expression in the developing pharyngeal region of E11.25 (42 somites) β-gal/*Foxn1*$^{+/-}$ embryos

A: Whole embryo showing β-gal expression in pharyngeal arch ectoderm.

B: Magnification of arch area from A.

C: Para-sagittal section through pharynx showing β-gal expression in pharyngeal arch ectoderm and in third pharyngeal pouch endoderm.

D: Magnification of third pharyngeal pouch endoderm. β-gal expression is first observed in cells at the ventral end of the pouch.

A and B show β-gal whole mount stained embryos, C and D show paraffin wax sections through the pharyngeal region of β-gal whole mount stained embryos counterstained with eosin.

In all figures, anterior is up, ventral to the left. H, heart; I, II, III, IV, first, second, third and fourth pharyngeal arches; 2, 3, second and third pharyngeal pouches; arrows in 3.1.C and 3.2.C indicate ectodermal β-gal expression.

Scale bars: 3.1A, 3.2A, 1mm; 3.1B, 3.2B, 200μm; 3.1C, 3.2C, 3.1D, 3.2D, 100μm.

Figure 3.1.

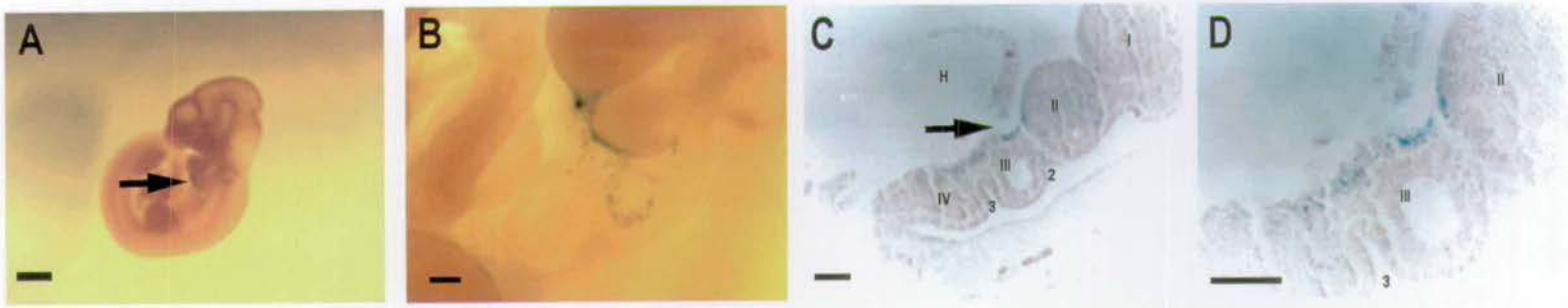

Figure 3.2.

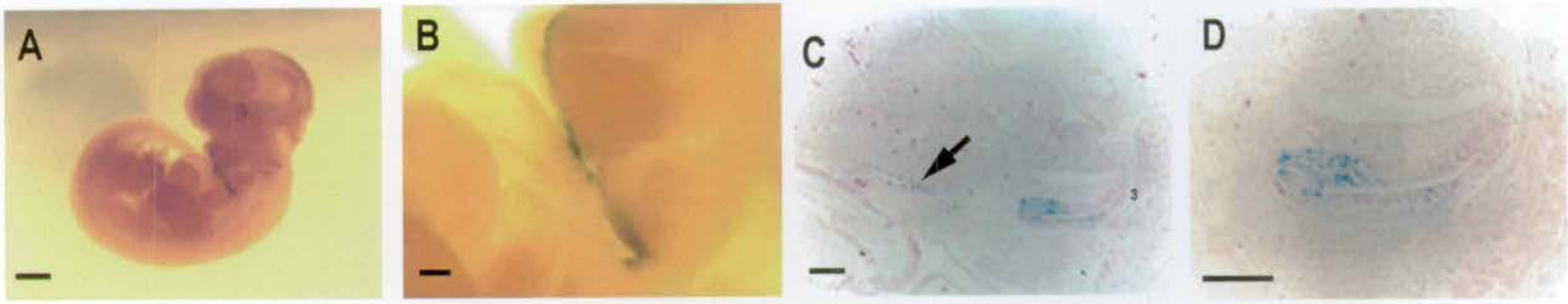

By E11.5, expression was no longer seen in the ectoderm of the arches, however, strong ß-gal expression was observed in the third pharyngeal pouch (Figure 3.3.A-E). In the ventral portion of the pouch, the onset of *Foxn1* expression appeared to coincide with a rapid proliferation of cells and a change in morphology of the endodermal cells from a single columnar epithelial layer to more rounded cells in a three-dimensional net ork (Figure 3.3.E). At the dorsal end of the pouch, the cells remain in a single cell layer and lack ß-gal expression (Figure 3.3.E). There also appeared to be low-level expression of ß-gal in a few cells in the surrounding mesenchyme close to the pouch. This expression was variable between embryos and may be due to leaching of the ß-gal stain.

At E12.5, the two thymic primordia are clearly visible in a ventral view of the embryo (Figure 3.4.A). Para-sagittal sections show considerable proliferation and outgrowth of the *Foxn1*-expressing cells (Figure 3.4.B). A few cells at the dorsal end of the pouch do not express ß-gal. In a magnified section of the thymic primordium, the morphology of the cells can be seen: an outer layer of elongated cells surrounds the inner mass of rounder cells (Figure 3.4.C). The majority of cells appear to be ß-gal$^+$, except for a few cells at the dorsal end of the pouch, and the primordium is surrounded by a thin mesenchymal capsule in some areas. The central cavity of the primordium has almost closed.

Figure 3.5.A-C shows ventral views of embryos at E11.5, E12.5 and E13.5 stained for ß-gal activity. The thymic primordia are clearly visible and as development proceeds the two lobes migrate medially and ventrally towards the developing heart. Expression of ß-gal continues throughout the thymic epithelium during subsequent foetal development and during adult life (data not shown and Figure 3.6).

Figure 3.3. β-gal expression in the pharyngeal region of E11.5 β-gal/*Foxn1*$^{+/-}$ embryos

A: Whole embryo showing β-gal expression confined to the third pharyngeal pouch.

B: High magnification of β-gal expression in third pharyngeal pouch.

C: β-gal expression in E11.5 embryo 'cleared' to show bilateral pouches.

D: Para-sagittal section through pharyngeal region showing strong β-gal expression in endoderm of third pouch.

E: High magnification of β-gal expression in third pharyngeal pouch endoderm.

A, B, C show β-gal whole mount stained embryos, anterior to the right, ventral is up; D and E show paraffin wax sections through the pharyngeal region of β-gal whole mount stained embryos counterstained with eosin. In D and E, anterior is up, ventral to the left.

Figure 3.4. β-gal expression in the E12.5 thymic primordium of β-gal/*Foxn1*$^{+/-}$ embryos

A: Ventral view of E12.5 embryo showing β-gal expression in bilateral thymic primordia.

B: Para-sagittal section through E12.5 embryo showing β-gal expression in all cells of thymic primordium.

C: High magnification of E12.5 thymic primordia. Arrow points to capsule surrounding the thymus.

A is β-gal whole mount stained embryo, anterior is up. B and C show paraffin wax sections through the thymic primordium of β-gal whole mount stained embryos counterstained with eosin. In B and C, anterior is up, ventral to the left.

H, heart; 3, third pharyngeal pouch.

Scale bars: 3.3A, 3.4A, 1mm; 3.3B, 500μm; 3.3C, 200μm; 3.3D, 3.3E, 3.4B, 100μm; 3.4C, 50μm.

Figure 3.3.

Figure 3.4.

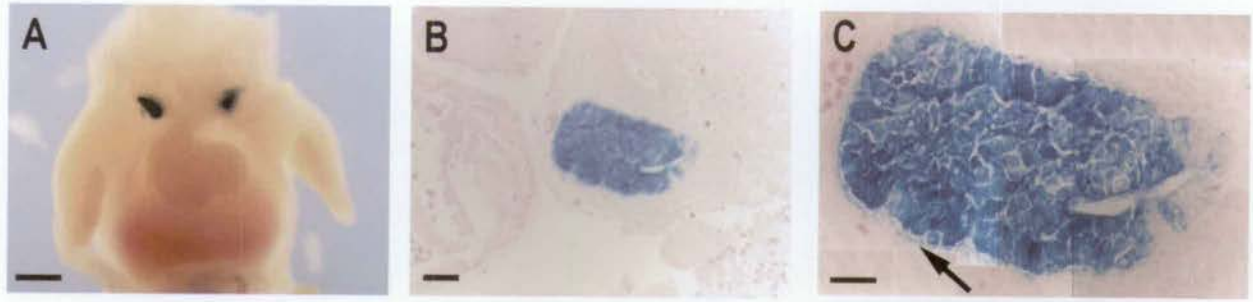

Figure 3.5. β-gal expression in thymic primordia of β-gal/*Foxn1*$^{+/-}$ embryos

A: Ventral view of an E11.5 embryo showing β-gal expression in bilateral thymic primordia.

B: Ventral view of E12.5 embryo showing β-gal expression in bilateral thymic primordia.

C: Ventral view of E13.5 embryo showing β-gal expression in bilateral thymic primordia.

As development proceeds the two primordia migrate medially and laterally and will subsequently join at E15.5. A, B and C show ventral views of decapitated β–gal whole mount stained embryos, anterior is up.

Figure 3.6. β-gal expression in the thymus of an adult β-gal/*Foxn1*$^{+/-}$ mouse.

β–gal is expressed uniformly throughout the adult thymus. A thymus was dissected from a six-week old mouse and whole mount stained.

Scale bars: 3.5A, 3.5B, 3.6, 1mm; 3.5C, 2mm.

Figure 3.5.

Figure 3.6.

These data demonstrate that *Foxn1* is transiently expressed in the ectoderm overlying the pharyngeal arches and surrounding the heart at E10.5 until E11.5. *Foxn1* expression commences in the endoderm of the third pharyngeal pouch at E11.25 and is coincident with proliferation and outgrowth of the $Foxn1^{+}$ endodermal cells at the ventral end of the pouch. *Foxn1* expression continues in thymic epithelial cells throughout foetal and adult life.

3.4. Analysis of thymus organogenesis in *nude* mice

Male $Foxn1^{+/-}$ mice were crossed with female $Foxn1^{+/-}$ mice and embryos from E11 to E13.5 were dissected. The genotype of the embryos was determined by PCR from the yolk sac of each embryo and homozygous embryos were analysed for ß-gal activity. The $Foxn1^{-/-}$ homozygote animals recapitulate the *nude* mutant mouse, as both alleles of the *Foxn1* gene are disrupted (Nehls *et al.*, 1996). This enables us to use ß-gal expression as a marker for cells committed to the thymic lineage whilst examining the morphological defect that occurs in the *nude* mutant mouse.

Whole-mount staining and subsequent para-sagittal sectioning of E11 to E11.5 $Foxn1^{-/-}$ embryos revealed an identical pattern of ß-gal activity in the ectoderm and endoderm as in the heterozygote embryos (Figure 3.7.A,B). At E11.5, the ventral portion of the endoderm had begun to proliferate as in the heterozygotes (Figure 3.7.B). Between E12 and E13 however, the morphology of the ß-gal expressing cells was markedly different to the heterozygous embryos. The normal proliferation and outgrowth of cells appeared to be arrested at E12.5 (Figure 3.7.C) and no further proliferation of ß-gal expressing cells occurred (Figure 3.7.D). By E13.5, the normal heterozygous thymic primordium was approximately four times the size of the cluster of ß-gal expressing cells in the $Foxn1^{-/-}$ embryo (Figure 3.7.D,E). The cells in

Figure 3.7. β-gal expression in β-gal/*Foxn1*$^{-/-}$ embryos during thymus development

A: Para-sagittal section through pharyngeal region of E11.25 *Foxn1*$^{-/-}$ embryo showing β-gal expression in ectoderm of arches and endoderm of third pharyngeal pouch.

B: Para-sagittal section through pharynx of E11.5 *Foxn1*$^{-/-}$ embryo showing β-gal expression in endoderm of third pharyngeal pouch and proliferation of cells at ventral end of pouch.

C: Para-sagittal section through E12.5 *Foxn1*$^{-/-}$ embryo showing β-gal expression in the arrested thymic primordium.

D: Para-sagittal section through E13.5 *Foxn1*$^{-/-}$ embryo showing β-gal expression in the thymic rudiment.

E: Para-saggital section through E13.5 *Foxn1*$^{+/-}$ embryo showing β-gal expression in the normal embryonic thymus. Note the large size of the thymus in *Foxn1*$^{+/-}$ embryo compared to the *Foxn1*$^{-/-}$ embryo in D.

F: Higher magnification of E13.5 thymic primordia from *Foxn1*$^{-/-}$ embryos.

All figures show paraffin wax sections through the pharyngeal region of β-gal whole mount stained embryos, counterstained with eosin.

In all figures anterior is up, ventral to the left. 3, third pharyngeal pouch; H, heart.

Scale bars: all 100μm.

Figure 3.7.

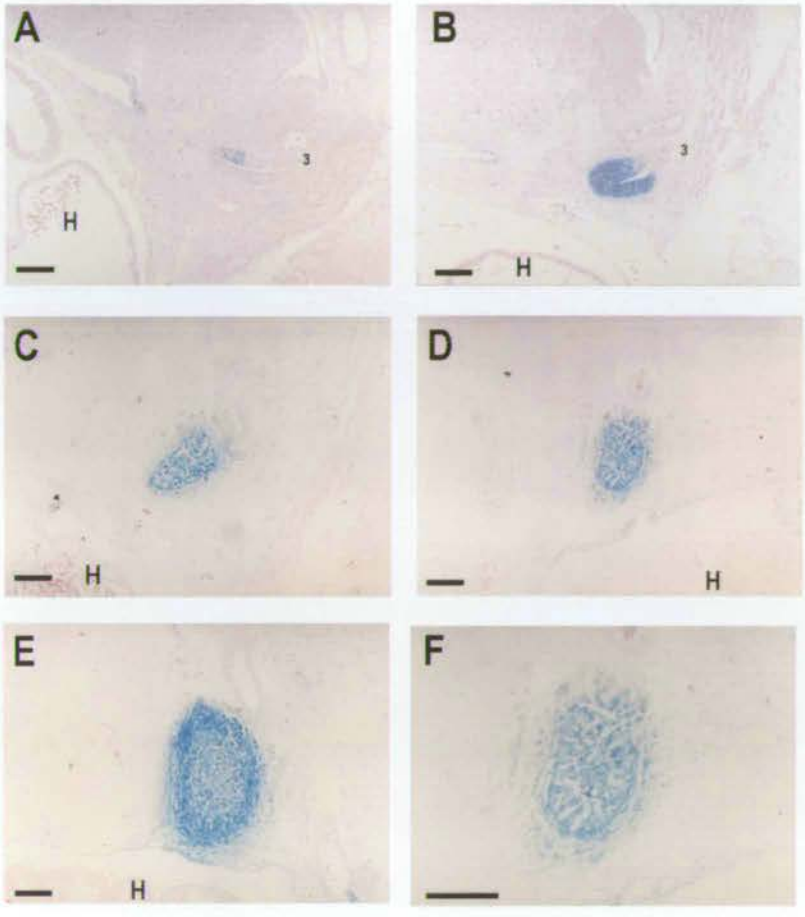

the E13.5 *Foxn1*$^{-/-}$ thymic rudiment were less densely packed with large intercellular spaces and some mesenchymal cells surrounding the *Foxn1*$^{-/-}$ rudiment appeared to express low levels of β-gal (Figure 3.7.F).

These data demonstrate that in *Foxn1*$^{-/-}$ embryos, thymus development proceeds normally until E12, when the usual proliferation and outgrowth of cells from the endoderm of the third pharyngeal pouch appears to be arrested. No subsequent development of the thymus occurs leaving a small cystic thymic rudiment.

3.5. Discussion

The use of the transgenic mouse line reported in this study provides distinct advantages over alternative methods of gene expression analysis. The ß-gal reporter is expressed in the cytoplasm of cells and is therefore more easily observable than FOXN1 protein detection or mRNA detection which would be localised to the nuclei. This line of mice has been used in two published studies investigating thymus development and hair follicle development, and has been shown to be a specific and sensitive marker of *Foxn1* expression (Nehls *et al.,* 1996; Lee *et al.,* 1999). Comparison of ß-gal expression with mRNA detection by non-radioactive *in situ* hybridisation and protein detection by immunohistochemistry showed identical results (Lee *et al.,* 1999). In our laboratory, non-radioactive *in situ* hybridisation has confirmed that the expression pattern of *Foxn1* in the thymic primordium at E11.5 and E12.5 corresponds to that seen with the ß-gal transgenic mouse line (J.Gordon, CGR, University of Edinburgh, personal communication).

Foxn1 expression during thymus development

The data presented showed that *Foxn1* was expressed in some ectodermal cells of the pharyngeal region at E10.5, but by E11.5 expression was confined to the endodermal cells of the third pharyngeal pouch. These cells proliferated to become the thymic primordia by E12.5 and *Foxn1* expression continued in the thymus throughout subsequent development.

The transient ectodermal expression in cells overlying the pharyngeal arches was of low level and variable between embryos. This variability may have been due to slight age differences between embryos or differences in stain penetration or incubation time. Characterisation of *Foxn1* expression by radioactive *in situ* hybridisation did not reveal any ectodermal expression (T.Boehm, Max-Planck-Institute for Immunobiology, Freiburg, Germany, personal communication). It is likely that this discrepancy is due to differences in the sensitivity of the two techniques.

With respect to thymus development, the main site of *Foxn1* expression is in the endoderm of the third pharyngeal pouch, beginning at E11.25 and increasing thereafter. The onset of *Foxn1* expression in these cells appears to coincide with a huge proliferation of the ventral portion of the pouch and a change in morphology of the cells. Prior to the onset of *Foxn1* expression the pharyngeal pouch consists of a single layer of columnar-type epithelial cells. The *Foxn1* expressing cells at E11.5 become rounder and form a three dimensional network of cells rather than a layer of epithelium. At the tapered dorsal end of the pouch the cells do not express *Foxn1*. These are the cells from which the parathyroid will form at E11.5, although no morphological evidence of formation of the parathyroid could be seen. This is likely to be due to the plane of sectioning as the parathyroid primordium forms from only a few cell widths in the centre of the cranial surface of the pouch (Cordier and Haumont 1980). Recent work in our laboratory has shown, through analysis of the

expression of *Gcm2*, a parathyroid specific transcription factor (Gunther *et al.*, 2000), that the cells at the anterior-dorsal end of the pouch are destined to become parathyroid and that the *Foxn1*-expressing and *Gcm2*-expressing domains are mutually exclusive (Gordon *et al.*, 2001) (See Appendix 1). By E12.5 the thymic primordium has formed and there has been a huge proliferation of *Foxn1* expressing cells and outgrowth of cells ventrally. The cavity of the pouch has almost closed and the thymus has separated from the pharynx.

At E11.5 some cells in the surrounding mesenchyme appeared to express low levels of ß-gal although this expression was variable between embryos. It is likely that this may be due to leaching of the ß-gal stain although it is also possible that some cells in the surrounding mesenchyme may transiently express *Foxn1* at low levels as an inductive activity from mesenchyme is essential for thymus development (Auerbach 1960; Le Douarin and Jotereau 1975).

The data presented support a primarily endodermal origin for the thymic epithelium as shown previously in avian embryogenesis (Le Douarin and Jotereau 1975). Neural crest derived mesenchyme plays an essential role in thymus development both by an inductive interaction early in development and later, by surrounding the thymus to form the capsule and invading the primordium to form the septae and blood vessels (Auerbach 1960; Le Douarin and Jotereau 1975; Bockman and Kirby 1984). In this study, mesenchyme can be observed surrounding the developing thymus at all stages and is usually $Foxn1^-$. An ectodermal contribution to the thymus cannot be excluded by this study, however no evidence of any ectodermal cells, either $Foxn1^+$ or $Foxn1^-$ can be seen migrating to or interacting with the developing thymic primordium. In contrast to earlier studies, no evidence of the ectoderm derived cervical vesicle enclosing the endoderm at E11.5-12 is observed (Cordier and Heremans 1975; Cordier and Haumont 1980)

With respect to a possible ectodermal contribution to the thymus, transverse sectioning of embryos demonstrated that between E9.5 and E10.5 the endoderm of the third pharyngeal pouch is in close contact with the pharyngeal ectoderm (J.Gordon, CGR, University of Edinburgh, personal communication) (Manley 2000). Transverse sectioning of ß-gal stained *Foxn1*$^{+/-}$ embryos would provide further details on the expression of *Foxn1* in pharyngeal ectoderm and its possible contribution to thymus development. Definitive lineage analysis studies in the mouse are needed to resolve the issue of an ectodermal contribution to the thymus and these studies are currently underway (J.Gordon, V.Wilson, N.Manley and C.Blackburn, CGR, University of Edinburgh, and Medical College of Georgia, Augusta, Georgia, personal communication).

Analysis of thymus organogenesis in *nude* mice

The data presented indicate that the development of the thymic primordium in *Foxn1*$^{-/-}$ mice is arrested at E12. Before this time the morphology of the pharyngeal pouch and surrounding mesenchyme is indistinguishable from heterozygous embryos. By E12.5-13 however, the morphology of the primordium is vastly changed. Proliferation is limited such that subsequently the primordium barely increases in size and the cells are less densely packed with larger intercellular spaces. This is likely to be the start of the development of cystic structures which characterise the adult *nude* thymic remnant (Cordier 1974).

From this present study, however, it is difficult to determine the precise morphological defect that occurs in *nude* mice. Previous analyses have proposed that the mutation is ectodermal in origin (Cordier and Heremans 1975; Cordier and Haumont 1980). These studies showed that at E10.5-11, the ectoderm of the third pharyngeal cleft, which has formed the cervical vesicle, involutes instead of developing further, and subsequently results in failure of the ectoderm to induce

differentiation of the endoderm (Cordier and Haumont 1980). Since no contribution of pharyngeal arch ectoderm was observed in *Foxn1*$^{+/-}$ or *Foxn1*$^{-/-}$ embryos in the present investigation, the reported ectodermal failure in *nude* mice cannot be confirmed. However, since *Foxn1* expression appears to be confined to the endoderm, and *Foxn1* acts cell-autonomously, *Foxn1*$^{-/-}$ embryos must have an intrinsic defect in the endoderm resulting in developmental arrest of the primordium (Blackburn *et al.,* 1996). This does not preclude an intrinsic defect in the ectoderm as well. Direct lineage analysis is required to determine the exact origin of the thymic primordium in normal and *nude* embryos and assess the nature of the thymus defect in *nude* embryos.

Foxn1 function

In hair follicle development, *Foxn1* appears to function as a transcriptional regulator of hair keratin genes (Meier *et al.,* 1999; Schlake *et al.,* 2000). Although no targets of *Foxn1* function have been reported in the thymus, it is likely that *Foxn1* also regulates keratin gene expression in thymic epithelial cells. Numerous studies have shown that patterns of cytokeratin expression can define specific subsets of thymic epithelium (Nicolas *et al.,* 1985; Savino and Dardenne 1988; Farr and Braddy 1989). More recently, studies have shown that cortical TE cells progress from precursors expressing K8 and K5 to mature cortical TE cells which are $K8^{+}K5^{-}$ (Klug *et al.,* 1998; Klug *et al.,* 2000). A possible role for *Foxn1* might be the transcriptional regulation of these keratin genes leading to differentiation of TE cells. It is likely that *Foxn1* may regulate multiple down-stream targets and identification of these target genes will allow further investigation of *Foxn1* function and thymic epithelial cell differentiation.

Appendix to Chapter 3

Foxn1 expression in developing hair follicles and skin

To determine the onset of *Foxn1* expression in the developing skin and hair follicles, $Foxn1^{+/-}$ embryos between E14.5 and E16.5 were whole-mount stained for ß-gal activity followed by sectioning. During embryonic development, ß-gal activity was observed at E14.5 (the first time point assessed) in the vibrissae, the developing nasal region and mouth, the nail primordia, eyebrows, and the skin around the ear and tail (Figure 3.8.A,B). By E15.5, expression was elevated in the sites mentioned and weak ß-gal staining was observed in the pelage follicles covering most of the head and body (Figure 3.8.C,D). At E16.5, strong ß-gal expression was evident over the whole of the skin surface (Figure 3.8.E,F). Subsequent sectioning of E16.5 embryos revealed strong expression of β-gal in the vibrissae, the epidermis of the skin and the developing nail beds (Figure 3.9.A,B).

To localise *Foxn1* activity in mature hair follicles and skin, flank and facial skin biopsies from newborn and adult heterozygotes were whole mount stained for β-gal activity and sectioned. Whole mount preparations of adult skin showed the large hair bulbs of the vibrissae deep below the skin surface, and the smaller pelage hair follicles, staining intensely for ß-gal (Figure 3.10.A,B). Sectioning through newborn skin demonstrated $Foxn1^{+}$ cells in the epidermis and in the hair follicles (Figure 3.11.A-D). Expression of ß-gal appeared to be stronger in the hair follicles than in the epidermis (Figure 3.11.A,B). Within the hair follicles, ß-gal was most strongly expressed in the hair shaft but was also observed in some cells in the surrounding inner root sheath (IRS) and some cells in the outer root sheath (ORS) (Figure 3.11.B-D). No expression was detected in the hair bulb matrix.

Figure 3.8. β-gal expression in the skin and hair of late gestation β-gal/*Foxn1*$^{+/-}$ embryos

A: Head of E14.5 embryo showing β-gal expression in vibrissae, nasal region and mouth, eye brows and skin around the developing ear.

B: Trunk of E14.5 embryo showing β -gal expression in nail primordia and tail tip.

C: Head of E15.5 embryo showing elevated levels of β -gal expression in vibrissae, nasal region and mouth, eye brows and skin around the developing ear.

D: Trunk of E15.5 embryo showing β -gal expression beginning in pelage follicles covering the body.

E: Head of E16.5 embryo showing increased expression of β -gal in skin and hair follicles.

F: Trunk of E16.5 embryo showing strong β -gal expression in all pelage hairs.

A- F show β-gal whole mount stained embryos, in B, D and F anterior is up, ventral to the left.

Figure 3.9. β-gal expression in E16.5 skin and hair follicles from β-gal/*Foxn1*$^{+/-}$ embryos

A: Cross-section through face skin showing β-gal expression in vibrissae and in epidermis of skin.

B: Section through limb of E16.5 embryo showing β-gal expression in nail primordia.

A and B show paraffin wax sections through β-gal whole mount stained embryos counterstained with eosin.

Scale bars: Figure 3.8, 1mm; Figure 3.9, 100μm.

Figure 3.8.

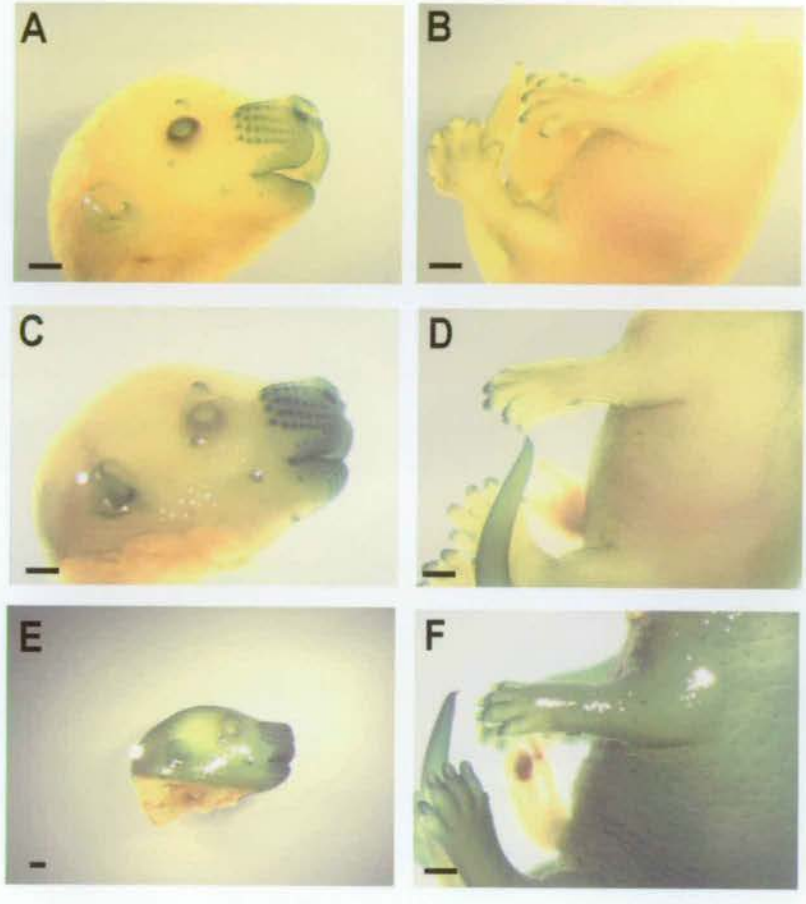

Figure 3.9.

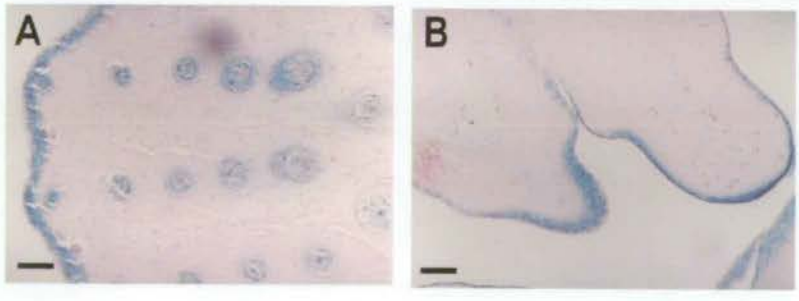

Figure 3.10. Whole mount β-gal expression in hair and skin from adult β-gal/*Foxn1*$^{+/-}$ mice

A: Adult vibrissae skin preparation showing β-gal in vibrissae follicles. Arrow points to vibrissa follicle bulb.

B: Adult pelage skin preparation showing β -gal expression in pelage follicles and in epidermis. Arrow points to pelage follicles and arrowhead points to epidermal staining.

A and B show β-gal whole mount stained skin preparations.

Figure 3.11. β-gal expression in sections of skin and hair from adult β-gal/*Foxn1*$^{+/-}$ mice

A: Cross-section through facial skin showing β -gal expression in vibrissae and in epidermis of skin.

B: Longitudinal section through pelage hair and skin showing β-gal expression in hair follicles and epidermis. In the hair follicle β-gal expression is confined to the hair shaft, and the inner root sheath. Arrow points to epidermal expression.

C: Longitudinal section through developing hair follicle showing β-gal expression in hair shaft but not in hair bulb matrix.

D: Cross-section through hair follicle showing β-gal expression in the hair shaft and inner root sheath.

A - D show paraffin wax sections through β-gal whole mount stained skin preparations counterstained with eosin.

IRS, inner root sheath; HS, hair shaft; m, hair bulb matrix.

Scale bars: Figure 3.10, 1mm; Figure 3.11, 100μm.

Figure 3.10.

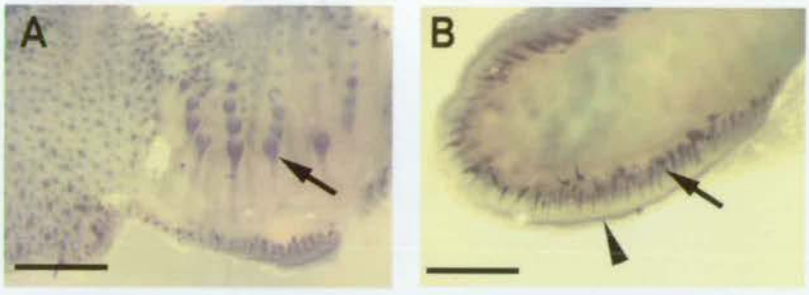

Figure 3.11.

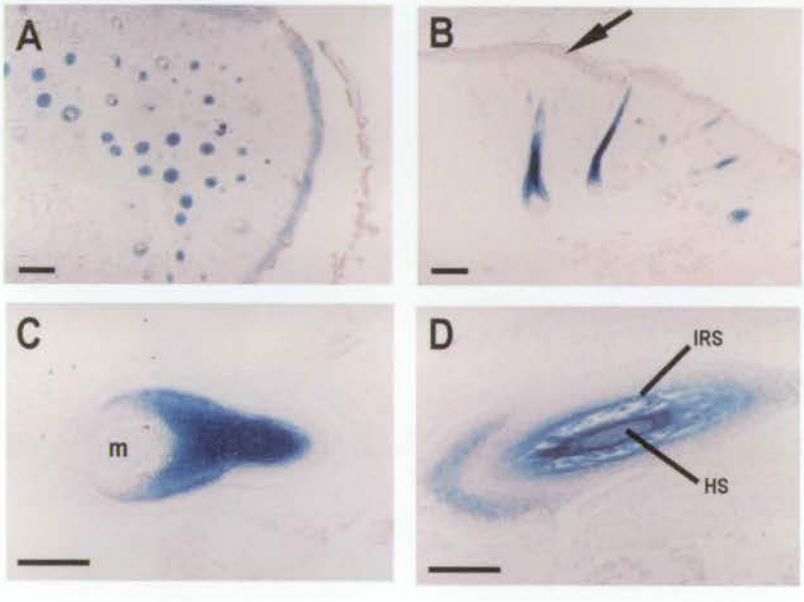

Discussion

The data presented have demonstrated that *Foxn1* is expressed at E14.5 in the vibrissae, the skin of the head and the nail primordia. By E16.5, *Foxn1* expression was observed in all pelage and vibrissae follicles and skin. In collaboration with Dr B.C.Powell, (Child Health Research Institute, Adelaide, Australia) a more detailed analysis of *Foxn1* expression in hair follicles was carried out using radioactive *in situ* hybridisation. These data described the expression of *Foxn1* and *histone H3*, a marker of proliferating cells (Chou *et al.*, 1990), during the cyclical growth and renewal of hair follicles, looking at follicles during embryonic development, during anagen, catagen and second anagen.

As these studies were being completed a report was published in the literature describing a similar analysis of *Foxn1* expression during skin and hair development using the same *Foxn1*/ß-gal transgenic mouse line (Lee *et al.*, 1999). The three studies mentioned are mainly in agreement about the pattern of expression of *Foxn1* during skin and hair follicle development. However, there are a few discrepancies. Lee *et al.* observed the first low-level expression of ß-gal in the embryo at E13 in the nasal region and at E13.5 in the vibrissae and nail primordia (Lee *et al.*, 1999), indicating that *Foxn1* expression in these sites appears slightly earlier than considered in the analysis presented here. In the mature hair follicle, ß-gal expression was reported throughout the IRS and in some cells of the ORS, primarily near the base of the follicle (Lee *et al.*, 1999). Our ß-gal expression is in agreement with these observations. However, our radioactive *in situ* hybridisation data showed no expression of *Foxn1* in the ORS cells or in the Henle and Huxley layers of the IRS and only low-level expression in the IRS cuticle (B.Powell, Child Health Research Institute, Adelaide, Australia, personal communication). A further study, again using radioactive *in situ* hybridisation, reported *Foxn1* expression in the ORS but not in the

IRS (Meier *et al.*, 1999). These discrepancies may be partially explained by differences in the sensitivity of the techniques used: ß-gal detection may be more sensitive than radioactive *in situ* hybridisation or there may be some leaching of ß-gal into the adjacent tissues. However, this does not explain the discrepancy between the two sets of radioactive *in situ* data, leaving the expression of *Foxn1* in the IRS and ORS in some doubt.

Lee *et al.* propose that *Foxn1* expression is associated with the onset of terminal differentiation in skin and hair follicles (Lee *et al.*, 1999). Protein expression of the differentiation markers keratin-1 and involucrin appeared at a similar time as the onset of ß-gal expression in epidermis (Lee *et al.*, 1999); however, these markers were not co-localised to the same cells, which would be necessary as *Foxn1* acts cell-autonomously (Blackburn *et al.*, 1996). In the hair follicle, the expression of ß-gal in progenitor cells undergoing differentiation into hair and IRS cells is suggested to correlate *Foxn1* with the onset of terminal differentiation (Lee *et al.*, 1999). Using Ki-67 as a marker of proliferating cells, some rare ß-gal-expressing cells in the skin and hair follicle were found to be proliferating (Lee *et al.*, 1999). Our data indicate that *Foxn1* is expressed in both proliferating and differentiating cells in the hair follicle and suggest that the extent of *Foxn1* expression in proliferating cells in more widespread than Lee *et al.* observed (B.Powell, Child Health Research Institute, Adelaide, Australia, personal communication). The co-localisation between ß-gal and Ki-67 was shown by antibody staining on ß-gal stained sections (Lee *et al.*, 1999). Our previous attempts to show antibody binding on ß-gal stained sections of hair follicles, demonstrated that the ß-gal staining severely impaired the binding of the antibody to the sections resulting in a reduced expression pattern and no co-localisation (data not shown). This may explain the reduced co-localisation of *Foxn1* and Ki-67 seen by Lee *et al.* compared to our data.

Furthermore, our data on *Foxn1* expression in the E11.5-E12.5 thymic primordium, suggest that the onset of *Foxn1* expression coincides with a huge

increase in proliferation of the *Foxn1* expressing cells, along with the onset of differentiation of these cells into mature thymic epithelium. Previous experiments have shown by BrdU labelling, that at E15.5, 74% of thymic epithelial cells are in cycle (Anderson *et al.,* 1998), and data presented in this thesis shows that at E12.5, around 98% of cells in the thymic primordium are in cycle (see section 4.3 and Figure 4.2.F).

In conclusion, it appears likely that *Foxn1* is expressed in both proliferative and differentiative phases of hair follicle development and thymus development. In hair follicle development, *Foxn1* appears to function as a transcriptional regulator of hair keratin genes (Meier *et al.,* 1999; Schlake *et al.,* 2000), which is consistent with the phenotype of the *nude* mutant mouse, displaying impaired keratinization of the epidermis and hair follicles. Furthermore, other genes which are abnormally expressed in *nude* skin are being identified (Meier *et al.,* 1999). It is possible that *Foxn1* may have multiple functions and may regulate multiple down-stream targets. Further analysis of genes involved in hair follicle development is required to determine the down-stream targets of *Foxn1* regulation.

Chapter 4

RESULTS

Characterisation of thymic epithelial cells during ontogeny

4.1. Introduction

Cells committed to thymic epithelial lineages but unable to express the *nude* gene, *Foxn1,* express the determinants recognised by two mAbs, MTS20 and MTS24, in both *nude*-wildtype chimaeras and the *nude* thymic remnant (Blackburn *et al.,* 1996). Therefore, cells marked by these two mAbs may be thymic epithelial progenitor cells (TEPC), which are developmentally arrested in the absence of *Foxn1* (Blackburn *et al.,* 1996). The aim of this work is to test the hypothesis that MTS20 and MTS24 mark progenitor cells for the thymic epithelium. Firstly, this chapter describes characterisation of the cellular composition of the E12.5 thymic primordium by flow cytometric analysis. Secondly, it describes the expression of the antibodies, MTS20 and MTS24, and other markers of TE, throughout thymus

ontogeny from E12.5 - adult, by flow cytometry and immunochemical staining of tissue sections. In an appendix to this chapter, MTS20 and MTS24 expression is analysed in skin and hair follicles of wild type and *nude* adult mice by immunohistochemistry.

4.2. Antibodies

MTS20 and MTS24 were raised in rat against mouse thymic stromal cell suspensions as part of a panel of monoclonal antibodies designated 'Mouse thymic stromal' (MTS) (See Table 1.1.) (Godfrey *et al.,* 1990) (R.Boyd, Monash University Medical School, Prahan, Melbourne, personal communication). Initial characterisation of these antibodies was conducted by immunohistochemical staining of adult thymus sections: both MTS20 and MTS24 recognised isolated epithelial cells or clusters of epithelial cells in the thymus medulla (Godfrey *et al.,* 1990) (R.Boyd, Monash University Medical School, Prahan, Melbourne, personal communication). MTS20 staining was described as granular and extracellular suggesting that this mAb recognised a secretory molecule (Godfrey *et al.,* 1990). Enhanced MTS20 staining was reported on foetal mouse thymus sections (D.Godfrey, Monash University Medical School, Prahan, Melbourne, PhD thesis). MTS10, another member of the MTS Ab panel, is specific for medullary and subcapsular epithelium (Godfrey *et al.,* 1990). 4F1 is a rat antibody raised against mouse thymic stroma, which reacts with cortical epithelium and a minor subpopulation of medullary epithelial cells (Kanariou *et al.,* 1989). In this study, MTS10 and 4F1 are used as markers of mature medullary and cortical thymic epithelium respectively.

4.3. Characterisation of the E12.5 thymic primordium

The cellular composition of the E12.5 thymic primordium was analysed by flow cytometry of dissociated cells. For flow cytometry, $1x10^5$ cells were used for each antibody and each experiment was repeated at least 3 times, unless otherwise stated. In each experiment, 10,000 events (cells) were counted.

The dissected E12.5 thymi were elongated structures varying between 300-600μm in length and 150-250μm in width (Figure 4.1.A). Some dissected thymic lobes had an attached parathyroid gland at the anterior end of the thymus (Figure 4.1.B). Each E12.5 thymus lobe was estimated to contain approximately 5,000 cells, based on counting dissociated cells.

The light scatter profile of the dissociated E12.5 thymic primordium cells demonstrated the diversity in size and granularity of these cells (Figure 4.2.A). Forward-scatter (FSC) is a measure of cell size and side-scatter (SSC) is a measure of cell complexity. Cells could be divided into two populations based on light scatter: R1, large granular cells (57% of total population) and R2, smaller and less granular cells (27% of total population). The remaining cells mainly in the bottom left corner of the plot were either dead cells (as detected by staining with propidium iodide, data not shown) or red blood cells (as detected by staining with anti-TER119, data not shown) and were not included in the gates.

The proportion of epithelial cells in the E12.5 thymic primordium was determined by staining with a pan-cytokeratin (CK) antibody, since cytokeratins are present in all epithelial cells (Nicolas *et al.,* 1985). For flow cytometric staining with anti-cytokeratin antibodies, cells were fixed and permeabilised prior to staining to allow intracellular penetration of antibody. Flow cytometry revealed that 90% of R1

Figure 4.1. Thymi dissected from E12.5 wild-type embryos

A: E12.5 thymi are between 300-600μm in length.

B: E12.5 thymi with attached parathyroid glands.

Thymi were dissected from embryos using a dissection microscope and fine forceps. In A, thymi are photographed with a microscope graticule.

Scale bars: A, 1mm; B, 200μm. P, parathyroid.

Figure 4.1.

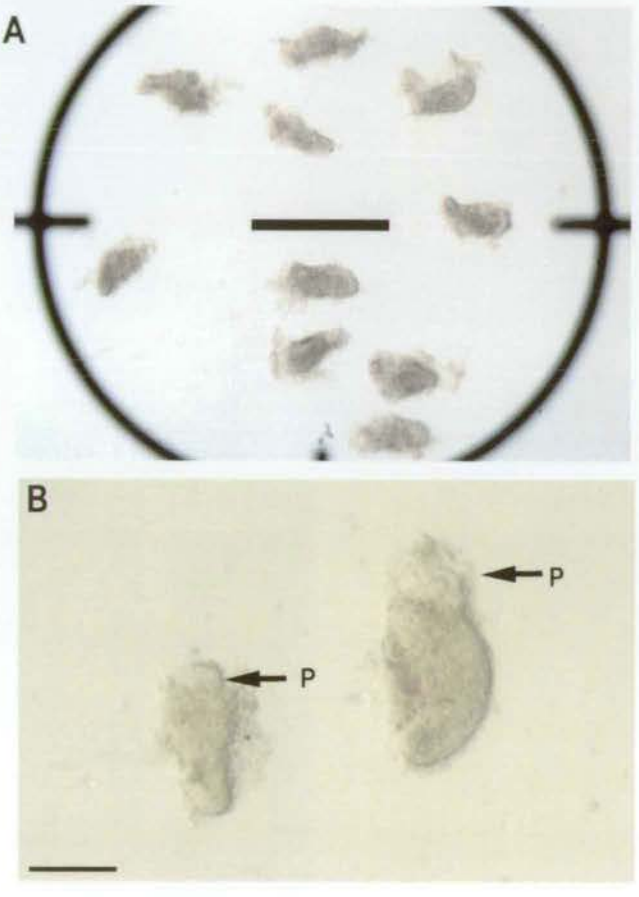

Figure 4.2. Flow cytometric analysis of keratin expression in E12.5 thymus cells

A: Light scatter profile of E12.5 thymus cells showing R1 and R2 gates on large and small cells respectively. R1 contains 57% of the total population and R2 contains 27% of the total population.

B: 90% of cells in R1 stain with cytokeratin antibody

C: 75% of cells in R2 stain with cytokeratin antibody

D: 40% of total cells express K8. The majority of $K8^+$ cells fall into R1.

E: 20% of total cells express K5. The majority of $K5^+$ cells fall into R1.

F: Double-labelling of total cells with keratin 5 and 8 reveals that all $K5^+$ cells are $K8^+$.

Thymi were dissected from E12.5 wild-type embryos and dissociated to a single cell suspension. 1 $x10^6$ cells were stained with the appropriate antibody and analysed by flow cytometry. Histograms in B-F represent staining on total cell population ie. R1 + R2. The data presented is representative of 2 separate experiments. 10,000 events were collected for each experiment. The dotted line in histograms represents cells stained with an isotype control antibody to show the unstained cells. The solid line represents staining with the test antibody. The percentage of cells stained is the proportion of antibody positive cells in M1 minus the proportion of isotype-control cells in M1. Right hand panel of D and E, show FSC-SSC profile of cells in M1 of histograms.

Figure 4.2.

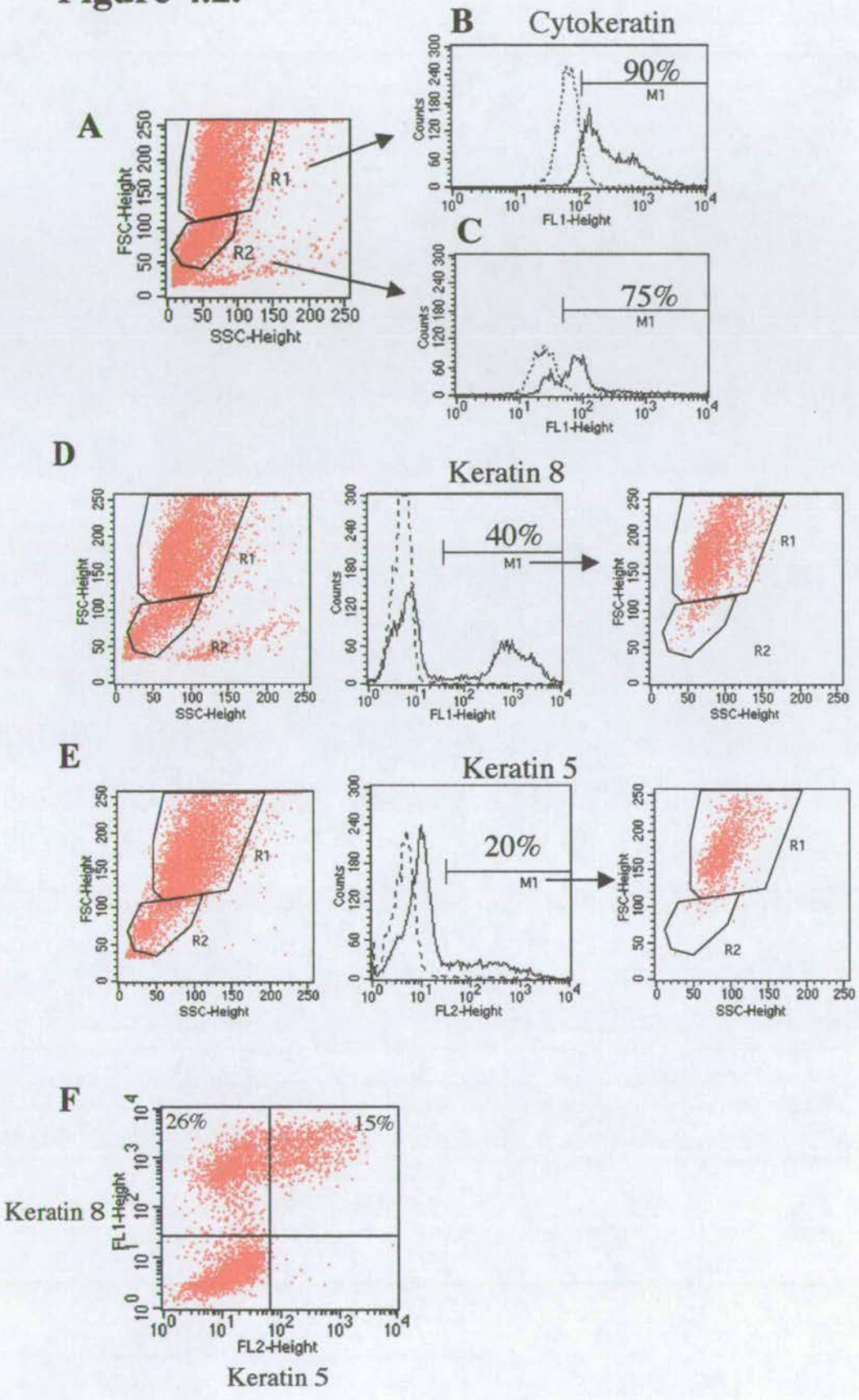
A
B
Cytokeratin
90%
M1
R1
R2
FSC-Height
SSC-Height
Counts
FL1-Height
C
75%
M1
D
Keratin 8
40%
M1
E
Keratin 5
20%
M1
FL2-Height
F
26%
15%
Keratin 8
FL1-Height
FL2-Height
Keratin 5

cells were CK^+ and 75% of R2 cells were CK^+ (Figure 4.2.B,C). This indicated that approximately 75% of the total cells in the E12.5 primordium were epithelial. The cytokeratin staining observed in these cells varied in intensity as indicated by the FL1-height on Figure 4.2.B and C: cells in R1 were cytokeratin$^{bright/med}$ whereas those in R2 were cytokeratin^{dull}. The differences in the intensity of staining may reflect the maturation or differentiation status of the individual cells within the primordium. To further characterise the expression of specific keratins within the E12.5 thymic primordium, cells were stained with antibodies against keratin 8 (K8) and keratin 5 (K5). 40% of E12.5 thymus cells stained with K8 and 20% stained with K5 (Figure 4.2.D,E). The $K8^+$ and $K5^+$ cells were mainly within gate R1. Furthermore, double labelling of E12.5 cells with both antibodies demonstrated that all $K5^+$ cells were also $K8^+$ (Figure 4.2.F). Therefore, approximately 20% of E12.5 thymus cells are $K8^+K5^+$, 20% are $K8^+K5^-$ and the remainder are $K8^-K5^-$.

The proportion of cycling cells in the E12.5 thymus was measured by staining dissociated cells with an antibody against phosphorylated histone H3 (anti-H3-P) (Juan *et al.,* 1998). For flow cytometric analysis with this antibody, cells were fixed and permeabilised prior to staining to allow intracellular penetration of the antibody. Figure 4.3A shows that 98% of cells stained with anti-H3-P, indicating that the majority of cells in the thymic primordium were proliferating.

The extracellular matrix molecule laminin, is largely produced by and associated with mesenchymal cells within and surrounding the thymic epithelium (Lannes-Vieira *et al.,* 1993; Savino *et al.,* 1993). To estimate the proportion of mesenchymal cells within the E12.5 primordium, cells were stained with an antibody against laminin. 15-20% of E12.5 thymus cells expressed laminin (Figure 4.3.B). The light scatter profile of the cells in this experiment appears different to the profiles in the other experiments due to a difference in the set-up of the flow cytometer for this analysis. The R1 and R2 populations were still clearly visible and

Figure 4.3. Flow cytometric analysis of E12.5 thymus cells

A: 98% of cells are positive with phospho-histone H3 antibody.

B: 19% of cells express laminin. The majority of laminin$^+$ cells are in R1.

C: 6% of cells express c-kit. The majority of these cells are in R1.

Thymi were dissected from E12.5 wild-type embryos and dissociated to a single cell suspension. 1 x10^6 cells were stained with the appropriate antibody and analysed by flow cytometry. Histograms in A-C represent staining on total cell population ie. R1 + R2. The data presented is representative of 2 separate experiments except Figure 4.3.B which is one single experiment. Data in B is from a different experiment to that in A and C. 10,000 events were collected for each experiment. The dotted line in histograms represents cells stained with an isotype control antibody to show the unstained cells. The solid line represents staining with the test antibody. The percentage of cells stained is the proportion of antibody positive cells in M1 minus the proportion of isotype-control cells in M1. Right hand panels show FSC-SSC profile of cells in M1 of histograms.

Figure 4.3.

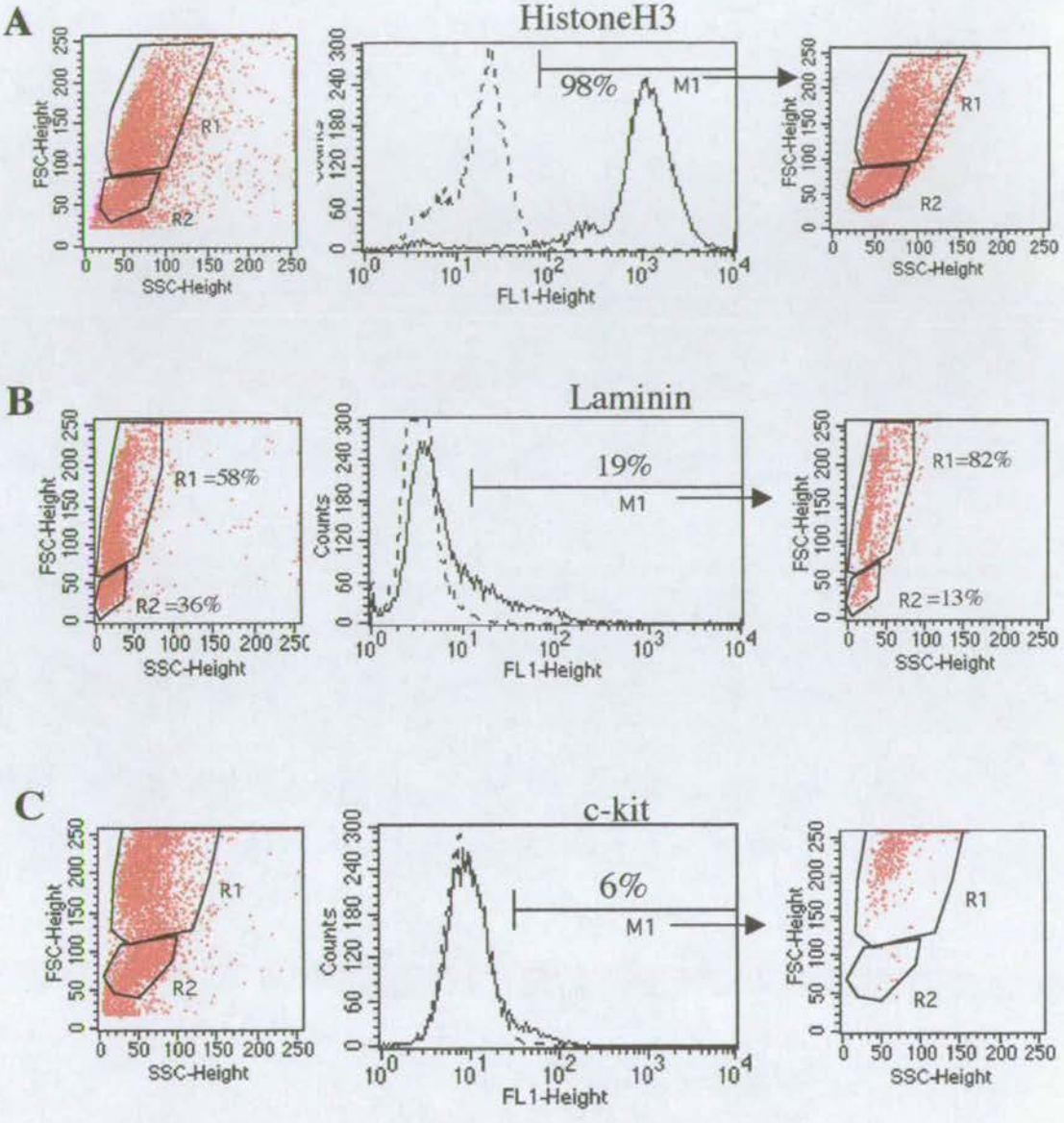
A
HistoneH3
98%
M1
R1
R2
FSC-Height
SSC-Height
FL1-Height
Counts
B
Laminin
19%
M1
R1 =58%
R2 =36%
R1=82%
R2 =13%
C
c-kit
6%
M1
R1
R2

are marked on the plot. The laminin$^+$ cells are predominantly in R1.

c-kit (or CD117), a tyrosine kinase receptor, is a marker of multipotent HSCs and is also expressed on the most immature subset of thymocytes within the foetal thymus (Matsuzaki *et al.*, 1993; Kondo *et al.*, 1997; Kawamoto *et al.*, 1998). Staining with anti-c-kit antibody was used to determine whether T-cell progenitors were present within the thymic primordium at E12.5. Figure 4.3.C shows that approximately 6% of cells in the E12.5 primordium were c-kit$^+$ and these were large cells predominantly in R1.

4.4. Expression of MTS20 and MTS24 during thymus ontogeny

To determine the expression pattern of MTS20, MTS24 and other markers of mature thymic epithelial populations during thymogenesis, thymi were dissected from embryos at E12.5-E14.5, E17.5, and from adult mice. The cells were dissociated, counted, and $1x10^5$ cells were stained with each antibody. In each experiment, 10,000 events (or cells) were counted and each experiment was repeated at least 3 times, unless otherwise stated. The number of cells positive for a particular marker is expressed as a percentage of positive cells out of 10,000 events counted. Therefore, the proportion of positive cells can be compared between different samples.

In the E12.5 thymic primordium, MTS20 and MTS24 stained an average of 34% and 35% of cells respectively (Table 4.1), and MTS20 and MTS24 in combination stained 42% of cells, indicating that MTS20 and MTS24 react with determinants on the same cells (Figure 4.4.A). 4F1, a marker associated with mature cortical epithelium (Kanariou *et al.*, 1989), reacted with approximately 37% of cells in the primordium (Figure 4.4.B bottom panel, and Table 4.1).

Figure 4.4. Expression of anti-epithelial mAbs on E12.5 thymus cells by flow cytometry

A: MTS20 stains approximately 38% of cells in the E12.5 thymic primordium. MTS24 stains approximately 43% of cells in the E12.5 thymic primordium. MTS20 and MTS24 together stain 42% of cells in the E12.5 thymic primordium, indicating that MTS20 and MTS24 react with determinants on the same cells.

B: The light scatter profile of the cells show that 86% of $MTS20^+$ and $MTS24^+$ cells are in gate R1 (large cells), whereas 75% of $4F1^+$ cells are in gate R2 (small cells), indicating that the E12.5 $MTS20/24^+$ and $4F1^+$ cell populations are largely distinct.

Thymi were dissected from E12.5 wild-type embryos and dissociated to a single cell suspension. 1 $x10^6$ cells were stained with the appropriate antibody and analysed by flow cytometry. 10,000 events were collected for each experiment. Data presented in A are from 1 experiment only, data in B are from experiment 1 of 4 separate experiments (Table 4.1). Histograms in A and B represent staining on total cell population, ie. R1 + R2. The dotted line in histograms represents cells stained with an isotype control antibody. The solid line represents staining with the test antibody. The percentage of cells stained is the proportion of antibody positive cells in M1 minus the proportion of isotype-control cells in M1. Left hand panels in B show FSC-SSC profile of total cell population and R1 and R2 regions. Right hand panels in B show FSC-SSC profile of cells in M1 of histograms and percentages of those cells in R1 and R2.

Figure 4.4.

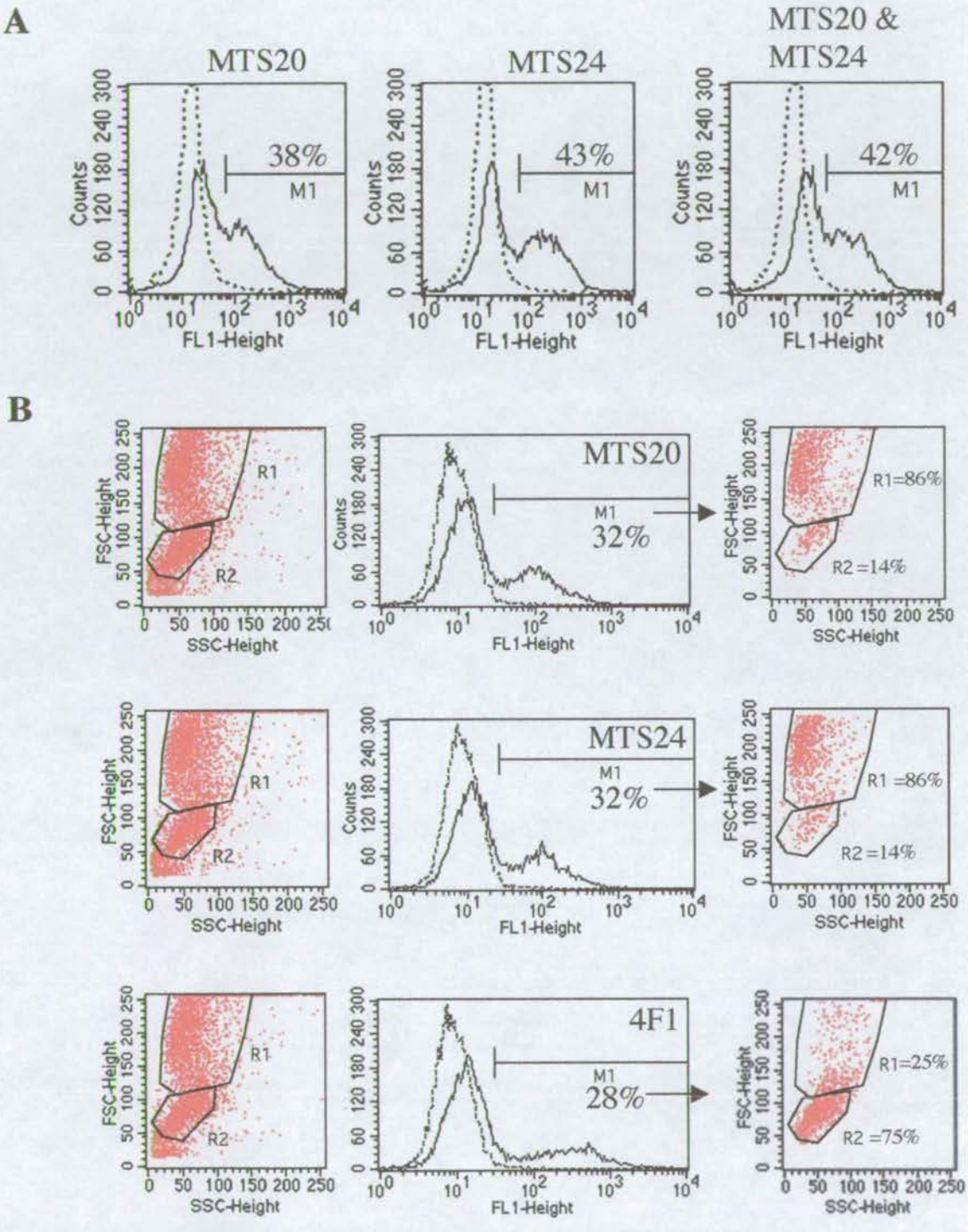
A
MTS20
MTS24
MTS20 &
MTS24
38%
43%
42%
M1
Counts
FL1-Height
B
R1
R2
FSC-Height
SSC-Height
MTS20
MTS24
4F1
32%
28%
R1=86%
R2=14%
R1=25%
R2=75%

Table 4.1. Expression of anti-epithelial mAbs in E12.5 thymi by flow cytometry

mAb	Exp.1 (%)	Exp.2 (%)	Exp.3 (%)	Exp.4 (%)	Mean (%)	SD (%)
MTS20	32	44	24	37	34	8.4
MTS24	32	44	23	42	35	9.7
4F1	28	35	42	42	37	6.7

Thymi were dissected from E12.5 wild-type embryos and dissociated to a single cell suspension. 1 $x10^6$ cells were stained with the appropriate antibody and analysed by flow cytometry. Figures refer to percentage of cells stained with each mAb in each flow cytometry experiment minus isotype-control antibody staining. SD, standard deviation.

Approximately 86% of MTS20$^+$ and MTS24$^+$ cells were in R1 (large cells), whereas 75% of 4F1$^+$ cells were in R2 (small cells) (Figure 4.4.B). The E12.5 MTS20/24$^+$ and 4F1$^+$ cell populations were therefore largely distinct, based on the light scatter profile of the cells. Collectively, these data indicate that there are three distinct epithelial populations in the E12.5 thymic primordium: MTS20/24$^+$4F1$^-$, MTS20/24$^-$4F1$^+$ and MTS20/24$^-$4F1$^-$.

At E13.5, MTS24 stained 30% of thymus cells, a similar proportion to the E12.5 primordium, however, MTS20 staining had decreased to 20% of thymus cells (Figure 4.5.B and Table 4.2). At E14.5, only 9% of thymus cells were MTS20$^+$ and MTS24 staining had decreased to 17% of thymus cells (Figure 4.5C and Table 4.2). E17.5 and adult thymus preparations were enriched for epithelial cells prior to staining by MACS depletion of all DP and SP thymocytes. At E17.5, only 1-2% of these enriched thymic epithelial cells reacted with MTS20 and MTS24, and approximately 1% of the adult epithelium-enriched thymus preparation stained with MTS20 and MTS24 (Figure 4.5.D,E and Table 4.2). These data show that the proportion of MTS20 and MTS24 expressing cells in the thymus was down regulated during thymus ontogeny. Figure 4.5 also shows the light scatter profile of the cells at each stage of development. Whereas at E12.5 the cells fell naturally into two populations based on size, from E13.5 onwards the cells appeared as a single population spread along the size axis.

The expression patterns of MTS20 and MTS24 during thymus development were confirmed by immunohistochemical staining of thymus sections and compared with the expression patterns of MTS10 and 4F1, markers associated with mature medullary and cortical epithelium respectively. At E12.5, cytokeratin staining was evident throughout much of the primordium at varying levels of intensity, reflecting the pattern seen by flow cytometric analysis (Figure 4.6.A). MTS20 and MTS24 showed weak staining on cells throughout the E12.5 thymic primordium (Figure

Figure 4.5. Flow cytometric analysis of MTS20 and MTS24 during thymogenesis from E12.5 - adult

A: MTS20 and MTS24 each stain 32% of cells in the E12.5 primordium.

B: MTS20 stains 23% of cells and MTS24 stains 31% of cells in the E13.5 thymus.

C: MTS20 stains 8% of cells and MTS24 stains 18% of cells in the E14.5 thymus.

D: MTS20 and MTS24 stain between 1-2% of cells in E17.5 thymi after depletion of DP and SP thymocytes.

E: MTS20 and MTS24 stain between 0.5 and 1.5% of cells in adult thymi after depletion of DP and SP thymocytes.

Thymi were dissected from wild-type embryos between E12.5 and E17.5 and adult mice, and dissociated to a single cell suspension. E17.5 and adult thymus preparations were depleted of single positive and double positive thymocytes by CD4/CD8 MACS depletion. 1 $x10^6$ cells were stained with the appropriate antibody and analysed by flow cytometry. Data presented are representative of 3 separate experiments, except at E12.5 where data is from one of four experiments. 10,000 events were collected for each experiment. The dotted line in histograms represents cells stained with an isotype control antibody to show the unstained cells. The solid line represents staining with the test antibody. The percentage of cells stained is the proportion of antibody positive cells in M1 minus the proportion of isotype-control cells in M1.

Figure 4.5.

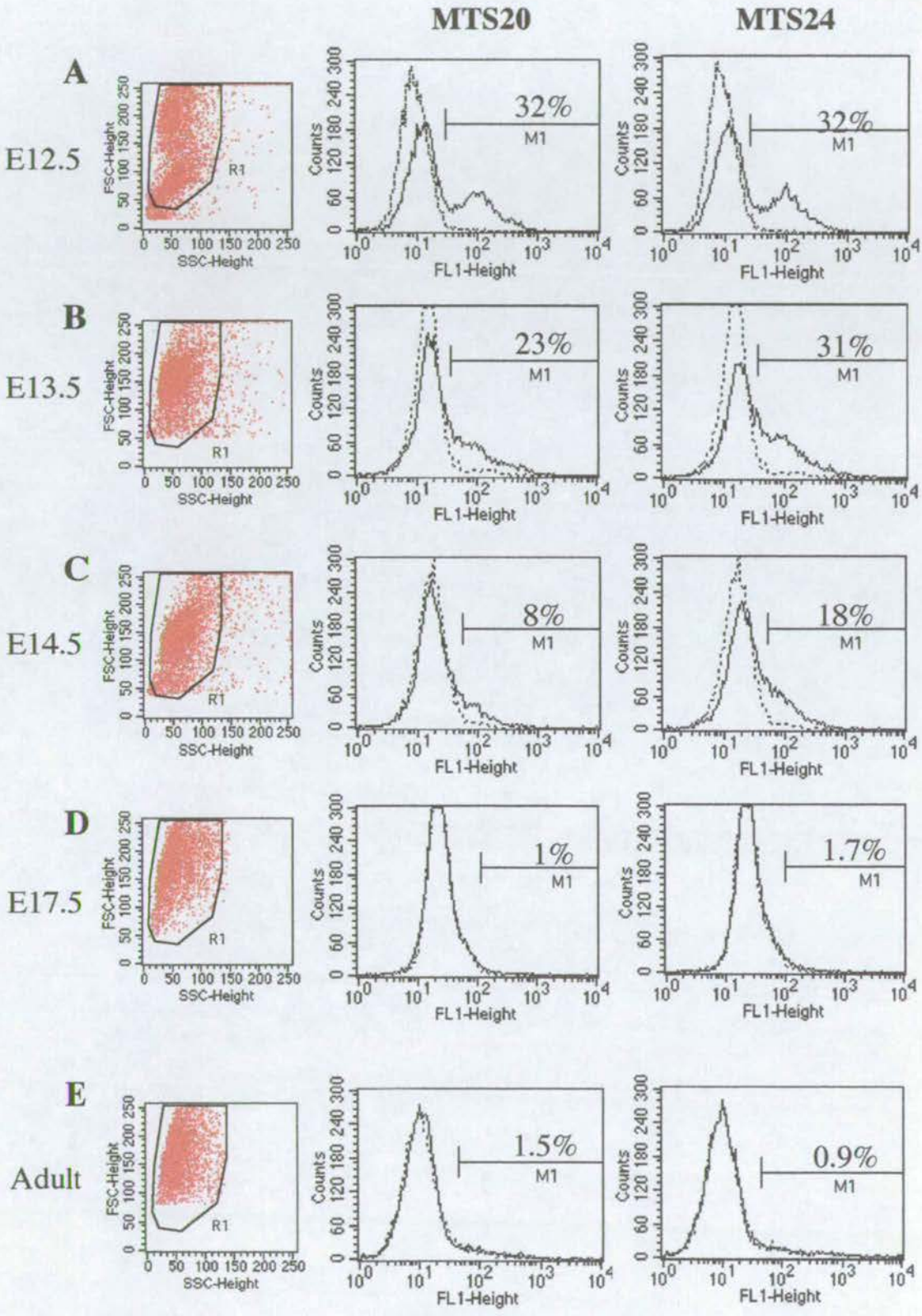
MTS20
MTS24
A
E12.5
B
E13.5
C
E14.5
D
E17.5
E
Adult
FSC-Height
SSC-Height
R1
Counts
FL1-Height
M1
32%
32%
23%
31%
8%
18%
1%
1.7%
1.5%
0.9%

Table 4.2. Expression of MTS20 and MTS24 during thymus ontogeny

mAb	Exp.1 (%)	Exp.2 (%)	Exp.3 (%)	Mean (%)	SD
E13.5 MTS20	23	16	21	20	3.6
E13.5 MTS24	31	27	32	30	2.6
E14.5 MTS20	8	10	8	9	1.2
E14.5 MTS24	18	15	19	17	2.1
E17.5 MTS20	1	0.7	1.2	1	0.3
E17.5 MTS24	1.7	1.5	1.5	1.6	0.1
Adult MTS20	1.5	1.6	1.0	1.4	0.3
Adult MTS24	0.9	1.2	0.7	0.9	0.3

Thymi were dissected from wild-type E13.5 to E17.5 embryos and adult mice and dissociated to a single cell suspension. 1 x10^6 cells were stained with the appropriate antibody and analysed by flow cytometry. Figures refer to percentage of cells stained with each mAb in each flow cytometry experiment minus isotype-control antibody staining. SD, standard deviation.

Figure 4.6. Expression of anti-epithelial mAbs in E12.5 thymus by immunohistochemistry on frozen sections

A: Cytokeratin staining in the E12.5 thymic primordium

B: MTS10 stains a small foci of cells in the centre of the E12.5 thymic primordium.

C: MTS20 stains the majority of cells at a low level.

D: MTS24 stains the majority of cells at a low level.

E: Isotype control antibody does not react with cells in the primordium however, the edge of the section appears fluorescent.

E12.5 thymi were snap frozen and 7µm frozen sections cut. Sections were stained with the appropriate antibody followed by FITC-conjugated secondary antibody, and visualised under appropriate excitation conditions. Not serial sections.

Scale bars: all 100µm.

Figure 4.6.

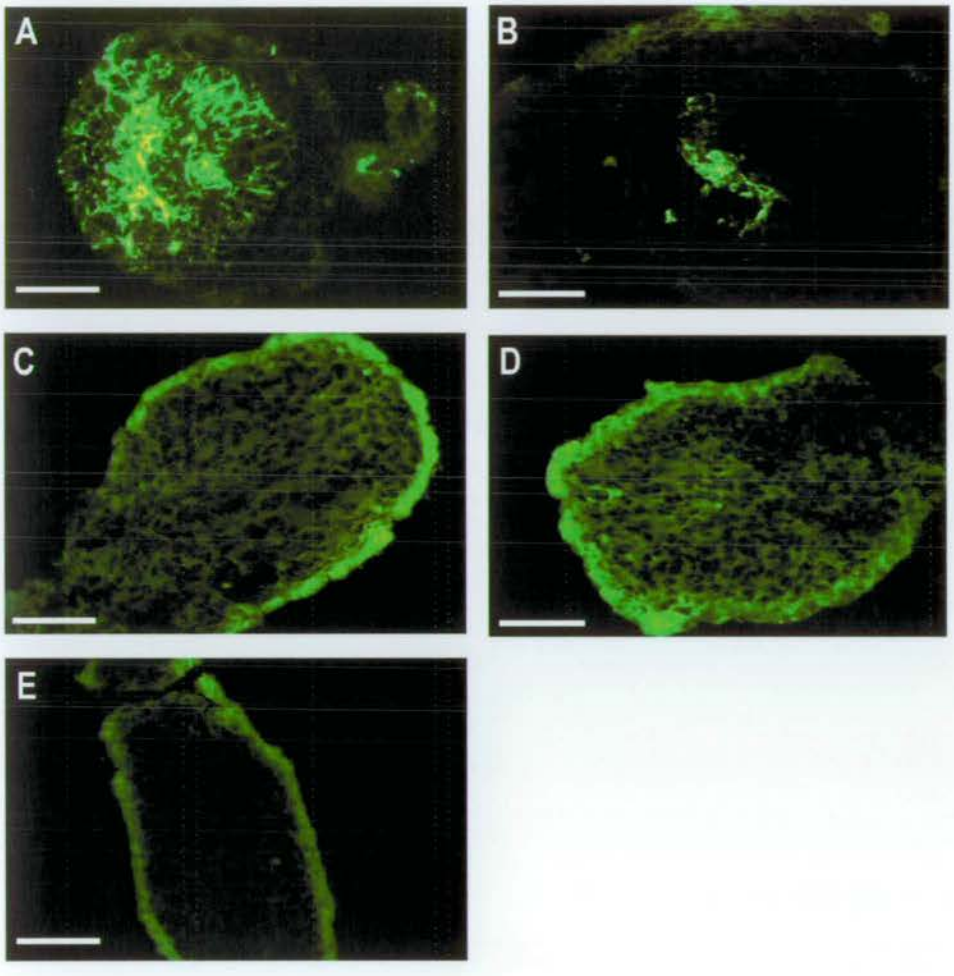

4.6.C, D). Staining with an isotype control antibody (IgM) showed no reactivity with cells within the thymic primordium, however, the edges of the section stained strongly (Figure 4.6.E). This edge effect was also observed in sections stained with the secondary antibody only (data not shown) indicating trapping of the FITC-conjugated secondary antibody at the edges of the section. MTS10, a marker of mature medullary epithelium (Godfrey *et al.,* 1990), stained a small focus of cells in the centre of the E12.5 primordium (Figure 4.6.B), although this was not present on all sections, indicating that only a few central cells in the primordium were MTS10$^+$. MTS10 could not be used to analyse cells by flow cytometry as it detects an intracellular antigen but is also fixation sensitive, preventing the use of the fixation and permeabilisation reagents usually used for intracellular staining. It was therefore not possible to quantitate MTS10$^+$ cells.

At E13.5, weak staining was observed with MTS20 and MTS24 in cells within the thymic primordium (Figure 4.7.C,D). Scattered cells throughout the E13.5 thymus were 4F1$^+$ and a few small central clusters of MTS10$^+$ cells were observed (Figure 4.7.A,B). At E14.5 no staining could be detected with MTS20 and MTS24 in the thymus above background levels (Figure 4.7.H,I,J). Flow cytometric analysis showed that 18% of E14.5 thymus cells were MTS24$^+$ (Figure 4.5.C.), however, the level of fluorescence was very low indicating weak staining which may be below the level of detection in immunofluorescent studies. At E14.5, numerous MTS10$^+$ patches of cells were observed in the thymus surrounded by predominantly 4F1$^+$ cells (Figure 4.7.F,G).

At E17.5, no staining was observed in the thymus with MTS20 or MTS24 (Figure 4.8.C,D), however, in the adult thymus, individual cells or clusters of cells stained strongly with these mAbs in keeping with the published expression pattern (Figure 4.8.H,I,M,N) (Godfrey *et al.,* 1990). In the adult thymus, the MTS20 and MTS24 staining co-localised with cytokeratin expression demonstrating that the

Figure 4.7. Expression of anti-epithelial mAbs in E13.5 and E14.5 thymi by immunohistochemistry on frozen sections

A: E13.5 thymus section stained with 4F1.

B: E13.5 thymus section stained with MTS10.

C: E13.5 thymus section stained with MTS20.

D: E13.5 thymus section stained with MTS24.

E: E13.5 thymus sections stained with isotype-control antibody.

F: E14.5 thymus section stained with 4F1.

G: E14.5 thymus section stained with MTS10.

H: E14.5 thymus section stained with MTS20.

I: E14.5 thymus section stained with MTS24.

J: E14.5 thymus section stained with isotype-control antibody.

E13.5 and E14.5 thymi were snap frozen and 7μm frozen sections cut. Sections were stained with the appropriate antibody followed by FITC-conjugated secondary antibody, and visualised under appropriate excitation conditions. Not serial sections.

Scale bars: all 100μm

Figure 4.7.

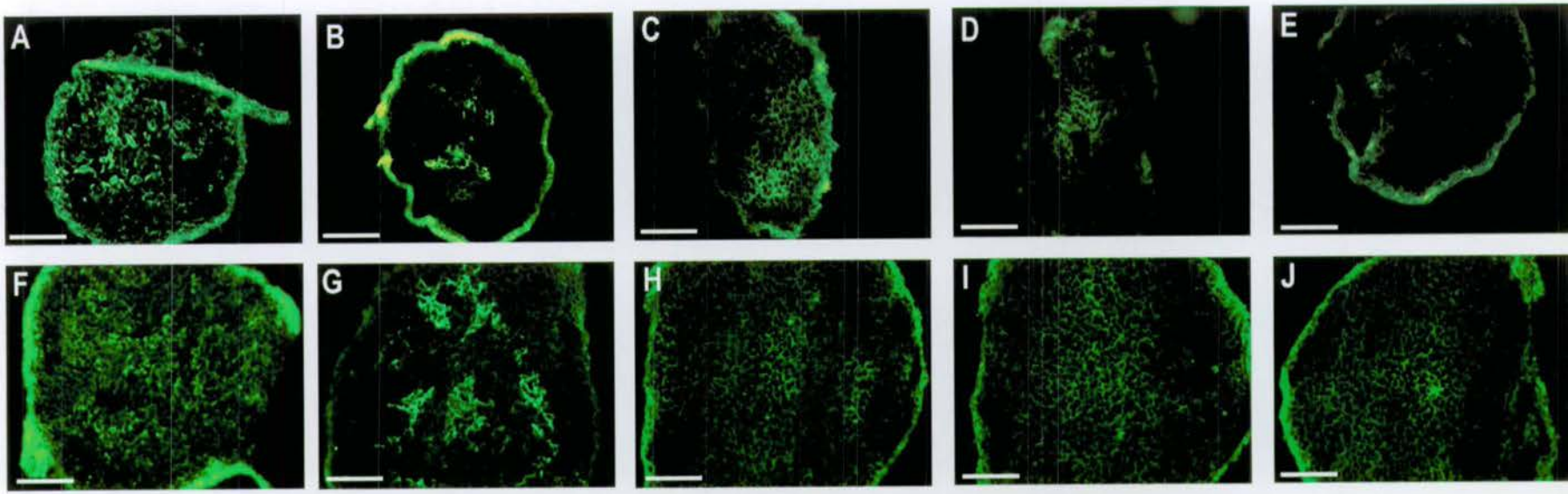

Figure 4.8. Expression of anti-epithelial mAbs in E17.5 and adult thymi by immunohistochemistry on frozen sections

A: E17.5 thymus section stained with MTS10.

B: E17.5 thymus section stained with 4F1.

C: E17.5 thymus section stained with MTS20.

D: E17.5 thymus section stained with MTS24.

E: E17.5 thymus sections stained with isotype-control antibody.

F: Adult thymus section stained with MTS10.

G: Adult thymus section stained with 4F1.

H: Adult thymus section stained with MTS20.

I: Adult thymus section stained with MTS24.

J: Adult thymus section stained with isotype-control antibody.

K: Adult thymus section stained with anti-cytokeratin antibody.

L: Adult thymus section double stained with anti-cytokeratin FITC (green) and MTS24-PE (red).

M: High magnification of MTS20$^+$ cell in adult thymus.

N: High magnification of MTS24$^+$ cell in adult thymus.

E17.5 and adult thymi were snap frozen and 7μm frozen sections cut. Sections were stained with the appropriate antibody followed by FITC-conjugated secondary antibody, and visualised under appropriate excitation conditions. Not serial sections.

Scale bars: All 100μm. M, medulla; C, cortex; arrowheads in H and I indicate positive cells in adult thymus; arrow in L indicates double-positive cell.

Figure 4.8.

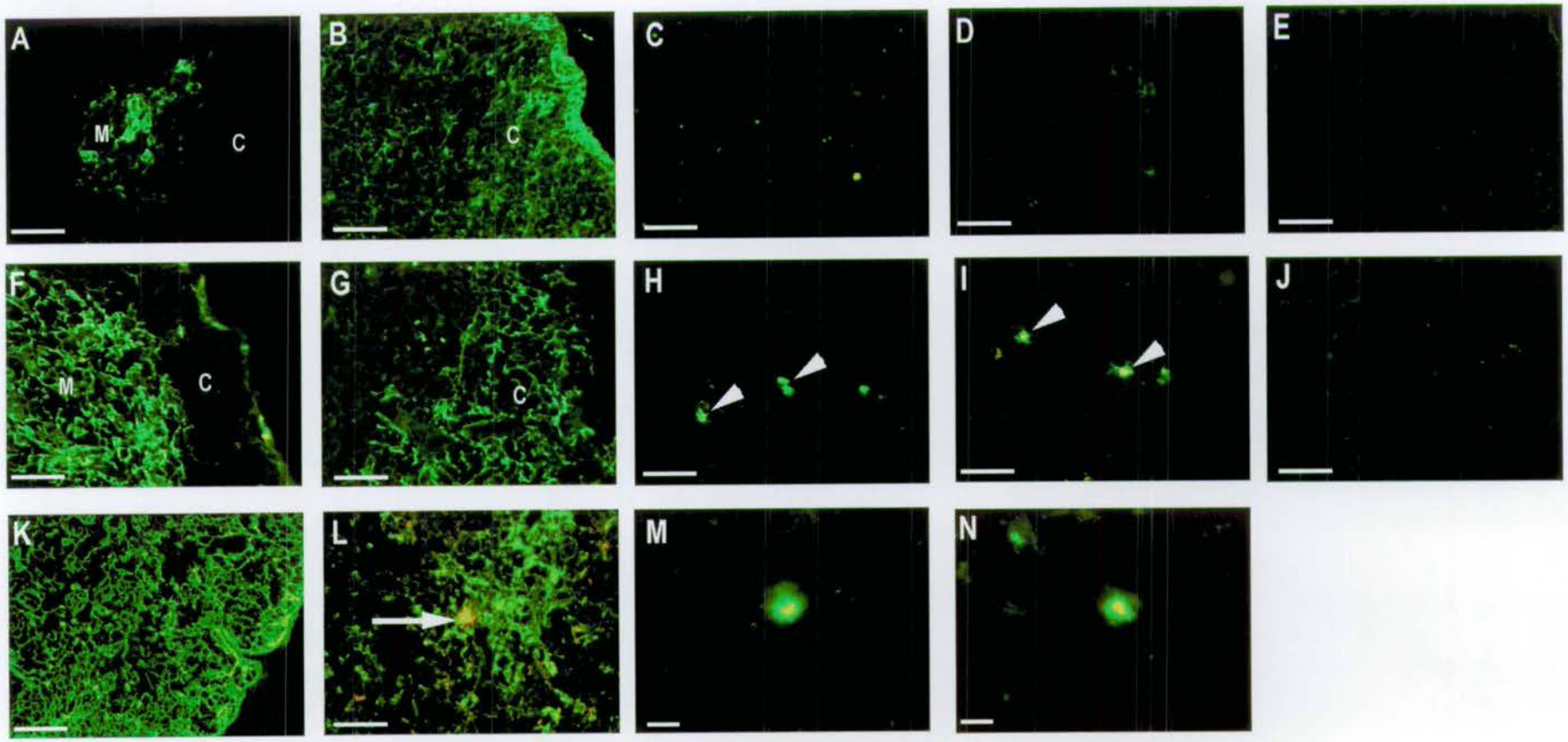

MTS20$^+$ and MTS24$^+$ cells are epithelial (data not shown and Figure 4.8.L). At E17.5, 4F1$^+$ cortical epithelial cells and MTS10$^+$ medullary epithelial cells were observed in a pattern similar to the mature adult thymus, with central medullary epithelial islands surrounded by cortical epithelium (Figure 4.8.A,B,F,G).

Collectively, these data support the flow cytometry data, showing that a large proportion of cells in the early thymic primordium are MTS20/24$^+$ and that, as thymogenesis proceeds, the proportion of cells expressing these determinants declines. Down regulation of MTS20 and MTS24 determinants corresponds with increasing expression of markers associated with mature thymic epithelial subpopulations.

MTS20 and MTS24 expression was also analysed in the pharyngeal region prior to formation of the thymic primordium. A segment of embryo containing the second, third and fourth pharyngeal arches and pouches was dissected from embryos at E9.5, E10.5 and E11.5. Figure 4.9.A shows the approximate area dissected from an E10.5 embryo. Flow cytometric analysis revealed that at E9.5, approximately 5% of cells were MTS20$^+$ and 12% of cells were MTS24$^+$ (Figure 4.9.B and Table 4.3). At E10.5 6-7% of cells were both MTS20$^+$ and MTS24$^+$ (Figure 4.9.C and Table 4.3). The E9.5 and E10.5 MTS20$^+$ and MTS24$^+$ cells were distributed throughout the total cell population (Figure 4.9.B,C.). At E11.5 between 0.5 and 1% of cells stained with MTS20 and MTS24 (Figure 4.9.D and Table 4.3). Table 4.3 presents the individual data from three experiments showing that the low amount of staining detected was reproducible over several experiments. The statistical significance of these results was tested using the Kolmogorov-Smirnov test for the analysis of histograms (Young 1977). The MTS20 and MTS24 staining at E9.5 and E10.5 was significant above background in all experiments ($p<0.001$). However, at E11.5 only one experiment of the three showed statistically significant staining above the isotype control antibody (Table 4.3).

Figure 4.9. Expression of MTS20 and MTS24 in the pharyngeal arch region by flow cytometry

A: E10.5 embryo marked to show area dissected in these experiments

B: MTS20 stains 5% of cells and MTS24 stains 12% of cells in the E9.5 pharyngeal arch region. The $MTS20^+$ and $MTS24^+$ cells are evenly distributed throughout the total cell population.

C: MTS20 stains 7% of cells and MTS24 stains 6% of cells in the E10.5 pharyngeal arch region. The $MTS20^+$ and $MTS24^+$ cells are evenly distributed throughout the total cell population.

D: MTS20 and MTS24 stain 0.5-1% of cells in the E11.5 pharyngeal arch region.

Scale bar in A represents 1mm.

Thepharyngeal region was dissected from E9.5-E11.5 wild-type embryos and dissociated to a single cell suspension. 1 $x10^6$ cells were stained with the appropriate antibody and analysed by flow cytometry. Histograms in C represent staining on total cell population ie. R1 + R2. Data presented are representative of 3 separate experiments (Table 4.3). 10,000 events were collected for each experiment. The dotted line in histograms represents cells stained with an isotype control antibody to show the unstained cells. The solid line represents staining with the test antibody. The percentage of cells stained is the proportion of antibody positive cells in M1 minus the proportion of isotype control cells in M1. Right hand panels in B and C show FSC-SSC profile of cells in M1 of histograms.

Figure 4.9.

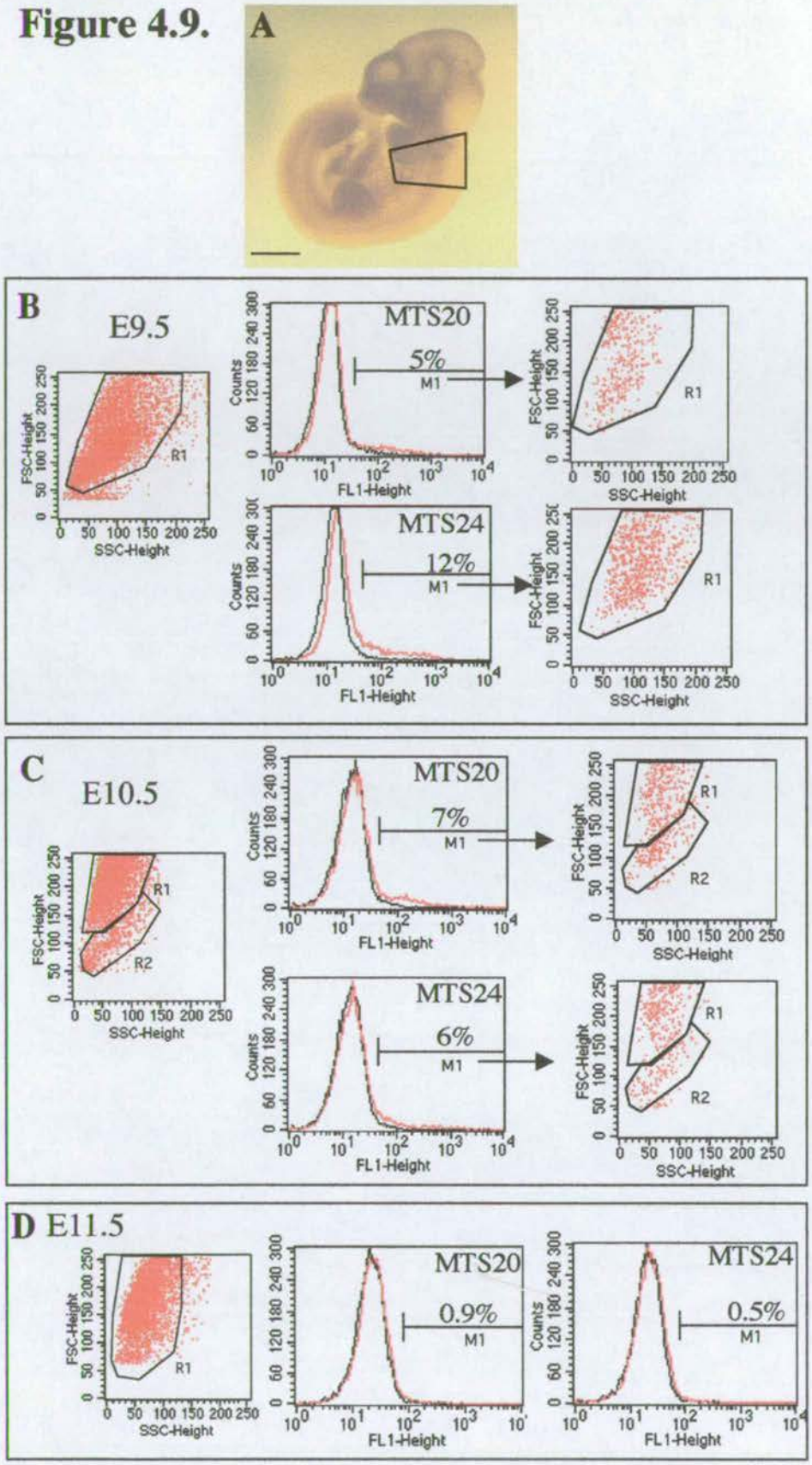
A
B
E9.5
MTS20
5%
M1
MTS24
12%
M1
R1
FSC-Height
SSC-Height
Counts
FL1-Height
C
E10.5
MTS20
7%
M1
MTS24
6%
M1
R1
R2
D E11.5
MTS20
0.9%
M1
MTS24
0.5%
M1

Table 4.3. Expression of MTS20 and MTS24 by flow cytometry in the pharyngeal arch region of embryos

Experiment	Exp.1 (%)	Exp.2 (%)	Exp.3 (%)	Mean (%)	SD (%)
E9.5 MTS20	5	6	4.6	5.2	0.7
E9.5 MTS24	5.4	12	5.9	7.8	3.7
E10.5 MTS20	7	6	7	6.7	0.6
E10.5 MTS24	6	7	8	7	1
E11.5 MTS20	0.3[a]	0.9[a]	1.7[b]	1	0.7
E11.5 MTS24	0[a]	0.5[a]	1.5[c]	0.7	0.8

The pharyngeal region was dissected from wild-type E9.5 to E11.5 embryos and dissociated to a single cell suspension. 1 $x10^6$ cells were stained with the appropriate antibody and analysed by flow cytometry. Figures refer to percentage of cells stained with each mAb in each flow cytometry experiment. [a]Antibody staining compared to isotype control $p>0.1$; [b]Antibody staining compared to isotype control $p<0.001$; [c]Antibody staining compared to isotype control $p<0.05$.

These data identified a small but significant population of cells in the E9.5 and E10.5 pharyngeal region that expressed MTS20 and MTS24 determinants. At E11.5, some staining was observed with MTS20 and MTS24, however, this staining was not statistically significant.

4.5 Discussion

In order to evaluate the hypothesis that MTS20 and MTS24 mark a TEPC population in the E12.5 thymic primordium, the cellular composition of the early thymic primordium has been characterised and the expression patterns of MTS20, MTS24 and other markers of mature thymic epithelium have been analysed throughout thymus development. These data constitute the first detailed analysis of the E12.5 thymic primordium and show that it consists of three phenotypically distinguishable populations of epithelium, one of which is MTS20/24$^+$, as well as non-epithelial cells such as c-kit$^+$ haemato-lymphoid cells and laminin$^+$ fibroblast cells. Furthermore, these data demonstrate that the determinants recognised by MTS20 and MTS24 are present in the pharyngeal region prior to thymus development and are down regulated during thymus ontogeny.

Cellular composition of the E12.5 thymic primordium

In the present studies, E12.5 was the earliest stage in mouse embryonic development at which a discrete thymus could be dissected from the embryo. Until recently, investigation of the phenotype of cells within the murine embryonic thymus has only begun at E13.5 or later in ontogeny (Jenkinson *et al.,* 1981; van Vliet *et al.,* 1985; Ropke *et al.,* 1995; Anderson *et al.,* 1998). Recent studies have analysed the

E12.5 primordium by immunohistochemical staining of tissue sections (Suniara *et al.*, 1999; Suniara *et al.*, 2000). These experiments demonstrated that the thymus at this stage consists of epithelium surrounded by a mesenchymal capsule, although mesenchymal cells had not yet invaded the epithelium (Suniara *et al.*, 2000). No further characterisation of the epithelium was reported. These studies in BALB/C embryos report different sizes for the E12.5 primordium dissected: 30μm diameter (Suniara *et al.*, 2000) and 200-300μm diameter (Suniara *et al.*, 2000). The data presented here show that the E12.5 primordium from C57BL/6 embryos varied between 300-600μm in length. However, the elongated morphology of the thymus and the observation of attached parathyroid glands indicate that the stage of the embryos used in this study is equivalent to those used in Suniara et al. (2000). It is probable that variations in the timing of embryo dissection and strain differences between C57BL/6 and BALB/C mice account for the difference in the reported size of the thymic primordium. As each E12.5 thymus lobe contained approximately 5,000 cells, thymi were routinely dissected from 80-100 embryos to obtain enough cells for one flow cytometry experiment.

The data presented here demonstrate that the E12.5 thymic primordium comprised approximately 75% epithelial cells. Furthermore, approximately 20% of cells were $K8^+K5^+$ and a further 20% were $K8^+$ $K5^-$. Klug et al. (1998) have shown that subpopulations of epithelial cells within the thymus can be defined by expression of these cytokeratins. They suggest that cortical epithelial cells proceed from a $K8^+K5^+$ precursor phenotype to $K8^+K5^-$ mature cortical epithelial cells (Klug *et al.*, 1998). Klug et al. did not present an analysis of keratin expression during thymic ontogeny and their data do not address the phenotype of precursor cells for medullary epithelium. The data presented here show that 20% of E12.5 thymic primordium cells are of equivalent phenotype to the putative cortical precursor cell and would be consistent with the 20% of $K8^+K5^-$ cells being either mature cortical epithelium or simple epithelial progenitors. The $K8^+K5^+$ precursor cells may be

common precursors for cortical and medullary epithelial cells. Alternatively, medullary epithelial precursors may express other keratins (Klug *et al.,* 1998). For example, in the thymi of CD3ε transgenic mice, which lack mature T-cells and an organised medullary compartment, a subset of medullary epithelial cells express K14 (Klug *et al.,* 1998).

The majority of cells in the E12.5 thymic primordium were actively proliferating. This high proportion of cycling cells was consistent with the data presented in chapter three showing a large increase in size and cellularity of the thymic primordium between E11.5 and E12.5. It is also consistent with a previous study showing a decline in proliferation of thymic epithelial cells during thymus ontogeny (Anderson *et al.,* 1998). This study showed that at E15, 74% of cells were in cycle, which declined to 63% by E16 and 34% by E18.

15-20% of E12.5 thymus cells expressed the extracellular matrix molecule laminin, indicating the presence of mesenchymal fibroblast cells, although thymic epithelial cells also express specific laminin family members in the thymus (Kim *et al.,* 2000). 6% of cells in the E12.5 thymic primordium were c-kit$^+$, indicating colonisation of the primordium by haemato-lymphoid progenitor cells. This is consistent with previous work demonstrating that colonisation of the third pharyngeal pouch begins as early as E11 (Penit and Vasseur 1989) and localising c-kit$^+$ cells within the E12.5 thymic primordium (Suniara *et al.,* 1999). These cells had migrated to the thymus through the surrounding mesenchyme, as the thymus was not yet vascularised at E12.5 (Suniara *et al.,* 1999).

The cells of the E12.5 thymus could be divided into distinct populations based on size and granularity of the cells. Moreover, three phenotypically distinct populations were observed: MTS20/24$^+$4F1$^-$ cells comprised approximately 35% of total E12.5 thymus cells, MTS20/24$^-$4F1$^+$ cells comprised approximately 35% of total cells and MTS20/24$^-$4F1$^-$ cells comprised approximately 30% of cells. The

latter population likely contained the mesenchymal fibroblast cells and haemato-lymphoid cells identified and a remaining 5-10% of epithelial cells which are MTS20/24$^-$4F1$^-$. These are likely to be cells committed to the parathyroid lineage, as the parathyroid remains joined to the thymus until E13-13.5 (Cordier and Haumont 1980; Suniara *et al.,* 2000). Indeed, a parathyroid gland could be observed attached to most dissected E12.5 thymi.

Immunohistochemical staining of E12.5 thymus sections generally supported this phenotype analysis, however problems were encountered with the reactivity of secondary antibody reagents on early thymus sections. In general, the thymic stromal cells exhibited high auto-fluorescence when viewed under the microscope. Furthermore, trapping of the secondary antibody, particularly at the edges of the section, gave a high background level of fluorescence. These problems prevented a definitive phenotypic analysis from immunohistochemical staining, particularly in the case of MTS20 and MTS24 where the mAbs exhibit weak reactivity with their target cells. The flow cytometric analysis provided a more sensitive and reproducible demonstration of the phenotype of E12.5 thymus cells.

Immunohistochemical staining of E12.5 thymus sections clearly demonstrated that a small focus of cells stained with MTS10, a marker associated with medullary thymic epithelium (Godfrey *et al.,* 1990). MTS10 could not be used in flow cytometry analysis due to fixation sensitivity, preventing analysis of the light scatter profile of MTS10$^+$ cells. It is possible that the MTS10$^+$ cells reside in any of the three defined epithelial populations described here. Previously, marker studies have described 'double positive' epithelial cells which stain with markers associated with both cortical and medullary epithelium (Willcox *et al.,* 1987; Wilson *et al.,* 1992; Ropke *et al.,* 1995; Von Gaudecker *et al.,* 1997). These cells have been found in thymic epithelial tumours, and in normal foetal and adult thymus in human and mouse, and have been suggested to be common precursor cells for cortical and medullary epithelium (von Gaudecker 1991; Ritter and Boyd 1993; Ritter and Palmer

1999). It is possible that the MTS10$^+$ cells observed here in the E12.5 thymic primordium are also 4F1$^+$: these cells would be an equivalent double positive cell population. This 'double positive' population would be distinct from the MTS20/24$^+$ population in the E12.5 thymic primordium based on the light scatter profile of cells. It is possible that either the MTS20/24$^+$ cell population or a 'double positive' cell population may contain progenitor cells for the thymic epithelium. Alternatively the MTS20/24$^+$ cell population in the E12.5 thymic primordium may give rise to 'double positive' epithelial cells which can then differentiate into either cortical or medullary epithelium.

Expression of MTS20/24 during thymogenesis

The flow cytometric data presented demonstrate that MTS20/24$^+$ cells are numerous in the early thymic primordium at E12.5 and E13.5 and the proportion of cells expressing these markers declines as development proceeds. MTS20 and MTS24 staining on thymic primordium cells was relatively weak, exhibiting low fluorescence levels. Immunohistochemical staining of sections also showed weak expression of MTS20/24 in the foetal thymus. However, in adult thymus sections, where these mAbs react with rare single cells or clusters of cells, MTS20/24 staining was bright on these cells. The results presented here for MTS20 are consistent with the immunohistochemical localisation of MTS20 during thymogenesis reported previously from E13.5 onwards (D.Godfrey, Monash University Medical School, Prahan, Australia, PhD thesis). The expression of MTS24 has not previously been analysed during thymus development.

At E12.5, MTS20 and MTS24 stained a similar proportion of cells. Moreover, when used in combination to stain E12.5 thymus cells, MTS20/24 staining was observed on a similar proportion of cells as when stained singly, indicating that MTS20 and MTS24 react with determinants on the same cells.

However, at E13.5 and E14.5, MTS24 stained a greater proportion of cells than MTS20. This indicates that expression of the determinant recognised by MTS20 is down regulated earlier in thymus development than the determinant recognised by MTS24.

Immunofluorescence on sections of thymus revealed scattered cells throughout the E12.5 primordium which were $4F1^+$, a marker associated with cortical epithelial cells, and a small focus of $MTS10^+$ cells, a marker associated with medullary epithelial cells. This is the first demonstration that cells with a medullary phenotype are present at E12.5 and indicates that some differentiation of epithelial cells into cortical and medullary populations has occurred by E12.5. As thymus development proceeded, the medullary foci expanded to resemble the adult pattern of medullary islands surrounded by cortical epithelium by E17.5. This medullary expansion is concomitant with thymocyte development as interactions with maturing thymocytes are required for the expansion and organisation of medullary compartments (Surh *et al.,* 1992; Penit *et al.,* 1996; Naspetti *et al.,* 1997). Medullary expansion occurs rapidly at E17.5 when the first DP and SP thymocytes appear (Naquet *et al.,* 1999).

Some cells in the pharyngeal region of the E9.5 and E10.5 embryo stain with MTS20 and MTS24. The exact localisation of these cells has not been determined in this study. However, MTS24 expression has been localised to the endoderm of the third pharyngeal pouch at E11.5 by confocal microscopy (Jason Gill, Monash University Medical School, Prahan, Australia, personal communication). Little or no staining could be detected in the E11.5 pharyngeal region in this study by flow cytometry: this is likely to be due to the large volume of tissue dissected from the embryo at this stage masking low level expression of these antibodies. The tissue dissected in these experiments contained pharyngeal arches 2, 3 and 4, and corresponding tissue from the dorsal region of the embryo including neural tube. At E11.5 this amounted to a large volume of tissue, of which the 3rd pharyngeal pouch

would have comprised a tiny part. Expression of MTS20 and MTS24 in the pharyngeal region would be consistent with the presence of some cells committed to thymic epithelial lineages before formation of the thymic primordium, as has been shown in chick (Le Douarin and Jotereau 1975). The presence of MTS20/24$^+$ cells in the endoderm of the third pharyngeal pouch would also be consistent with the thymic epithelium originating from this region as shown in chick (Le Douarin and Jotereau 1975) and suggested from the pattern of *Foxn1* expression described in chapter 3.

Summary

The data presented in this chapter have phenotypically defined the populations of cells present in the E12.5 thymic primordium. Epithelial cells comprised approximately 75% of the total cells at E12.5: some cells expressed markers associated with mature cortical (4F1$^+$) and medullary (MTS10$^+$) epithelium, while around 40% of epithelial cells were MTS20/24$^+$4F1$^-$. The proportion of MTS20/24$^+$ cells declined markedly during thymogenesis and in the adult thymus, only rare cells expressed MTS20/24 (approximately 1%). MTS20/24$^+$ cells were also detected in the pharyngeal region of the embryo prior to thymus formation. These data are consistent with the pattern of expression expected of markers of TEPC: they should be expressed by a significant proportion of cells in the early thymic primordium. The observation of some MTS20/24$^+$ cells in the pharyngeal region at E9.5-E10.5 might indicate that some cells are committed to the thymic epithelial lineage early in ontogeny prior to thymus development. The continued expression of MTS20/24 on cells in the adult thymus might suggest a residual TEPC population that remains in the thymus throughout adult life. Alternatively, the MTS20/24$^-$ population present at E12.5, in which putative 'double positive' precursor cells might reside, could contain progenitors for the entire TE, or the MTS20/24$^+$ and the MTS20/24$^-$ populations could contain separate progenitors for medullary epithelium

and cortical epithelium respectively. The experiments presented in chapters five and six address these possibilities.

Appendix to Chapter 4

Expression of MTS20/24 in skin and hair follicles

A panel of adult mouse tissues was screened by immunohistochemical staining on sections to ascertain the wider expression pattern of MTS20 and MTS24. Most tissues analysed were negative for MTS20 and MTS24 staining (heart, liver, lung, kidney and spleen) (data not shown), consistent with the published data for MTS20, except for the absence of staining in kidney (Godfrey *et al.,* 1990). MTS24 staining has since been localised to the epithelia of the kidney and lung (J.Gill, Monash University Medical School, Prahan, Australia, personal communication). In the present study, staining was observed in epidermal epithelium, as reported for MTS20 in the original characterisation (Godfrey *et al.,* 1990), and in hair follicles. MTS20 and MTS24 appeared to have near identical expression patterns in the skin and hair follicles, as would be expected from their expression on the same cells in the thymus. MTS20 and MTS24 reacted weakly with cells throughout the epidermis and with cells in the IRS of the hair follicle (Figure 4.10). Expression of MTS10, previously reported to stain the stratum basal of the epidermis (Godfrey *et al.,* 1990), was also observed in hair follicles: MTS10 strongly stained the basal layer of cells in the epidermis and cells throughout the IRS and ORS in the hair follicle (Figure 4.11.).

As MTS20 and MTS24 are expressed in the thymic remnant of *nude* mice at enhanced levels (Blackburn *et al.,* 1996), sections of skin from *nude* mice were analysed to determine if the absence of *Foxn1* affected the expression of MTS20/24 in skin and hair follicles. MTS20 and MTS24 exhibited a similar pattern of expression in *nude* skin and hair follicles as in wild type, however, staining with both mAbs was more

Figure 4.10. Immunohistochemical staining of wax sections of wild-type skin and hair follicles with MTS20 and MTS24

A: MTS20 is expressed in the epidermal cell layer and the hair canal.

B: Section through a hair follicle showing weak MTS20 staining in the hair shaft.

C: Cross-section through a hair follicle showing MTS20 in the inner cuticles of the IRS.

D: MTS24 is expressed in epidermal cells and the hair canal.

E: MTS24 expression is localised to a single layer of cells lining the hair shaft.

F: Cross-section through a follicle showing MTS24 expression in the IRS.

Adult vibrissae skin preparations were embedded in paraffin wax and sectioned. The sections were stained with the appropriate antibody followed by a HRP-conjugated secondary antibody and visualised using DAB substrate (brown colour). Sections were counterstained with hematoxylin.

Arrows in A and D show epidermal staining. Arrowheads in A, B, D, E, show staining in the hair canal. Scale bars: A, B, D, E, G,H, 100μm; C, F, I, 50μm.

Figure 4.10.

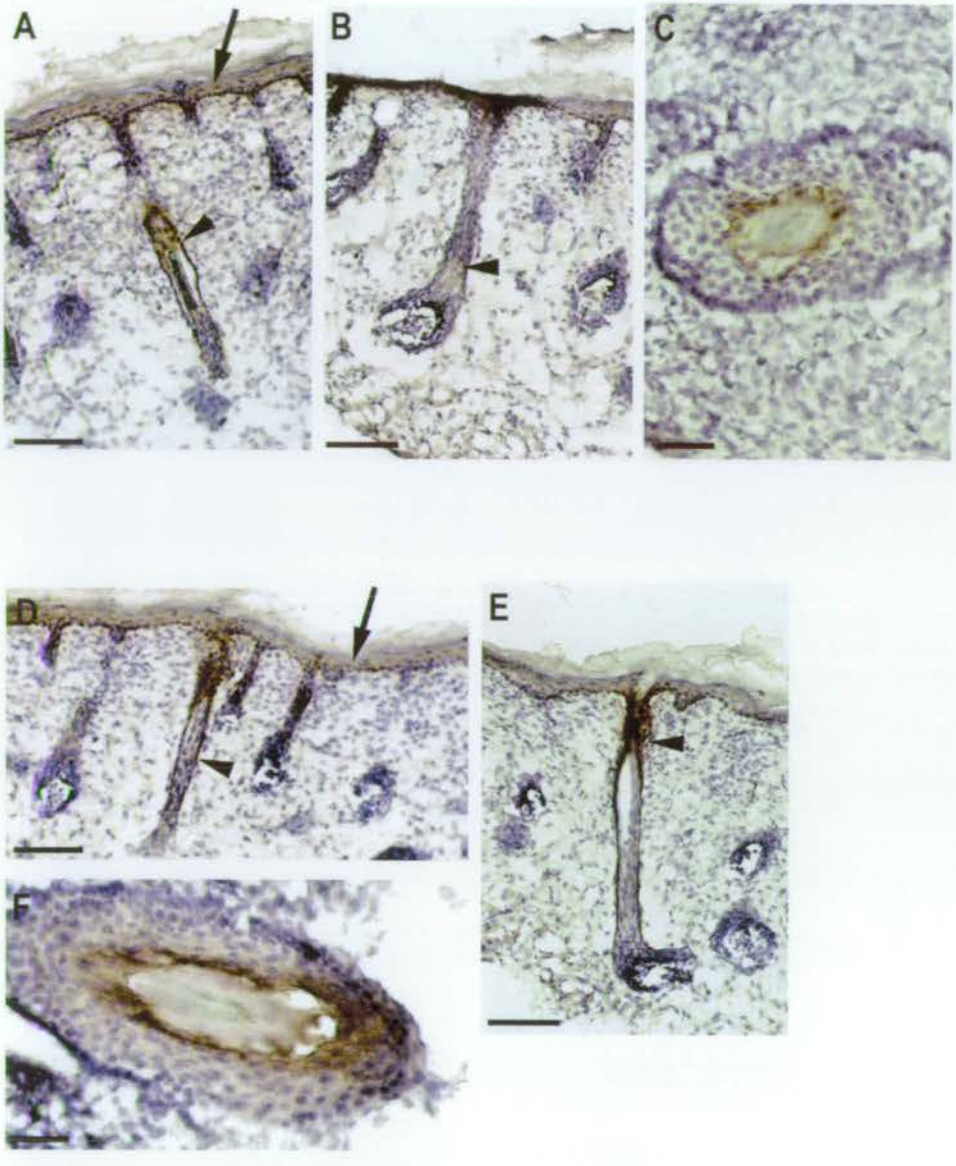

Figure 4.11. Immunohistochemical staining of wax sections of wild-type skin and hair follicles with MTS10 and isotype-control antibodies

A: MTS10 is strongly expressed in the basal layer of the epidermis and in the hair canal.

B: High magnification of the basal layer of the epidermis.

C: Cross-section through a hair follicle showing MTS10 expression widely distributed throughout the IRS and ORS.

D-E: Isotype-control antibody shows no reactivity on skin and hair follicles.

Adult vibrissae skin preparations were embedded in paraffin wax and sectioned. The sections were stained with the appropriate antibody followed by a HRP-conjugated secondary antibody and visualised using DAB substrate (brown colour). Sections were counterstained with hematoxylin.

Arrow in A points to basal epidermal cells and arrowhead in A shows staining in the hair canal. Scale bars: A, D, E, 100μm; B, C, 50μm.

Figure 4.11.

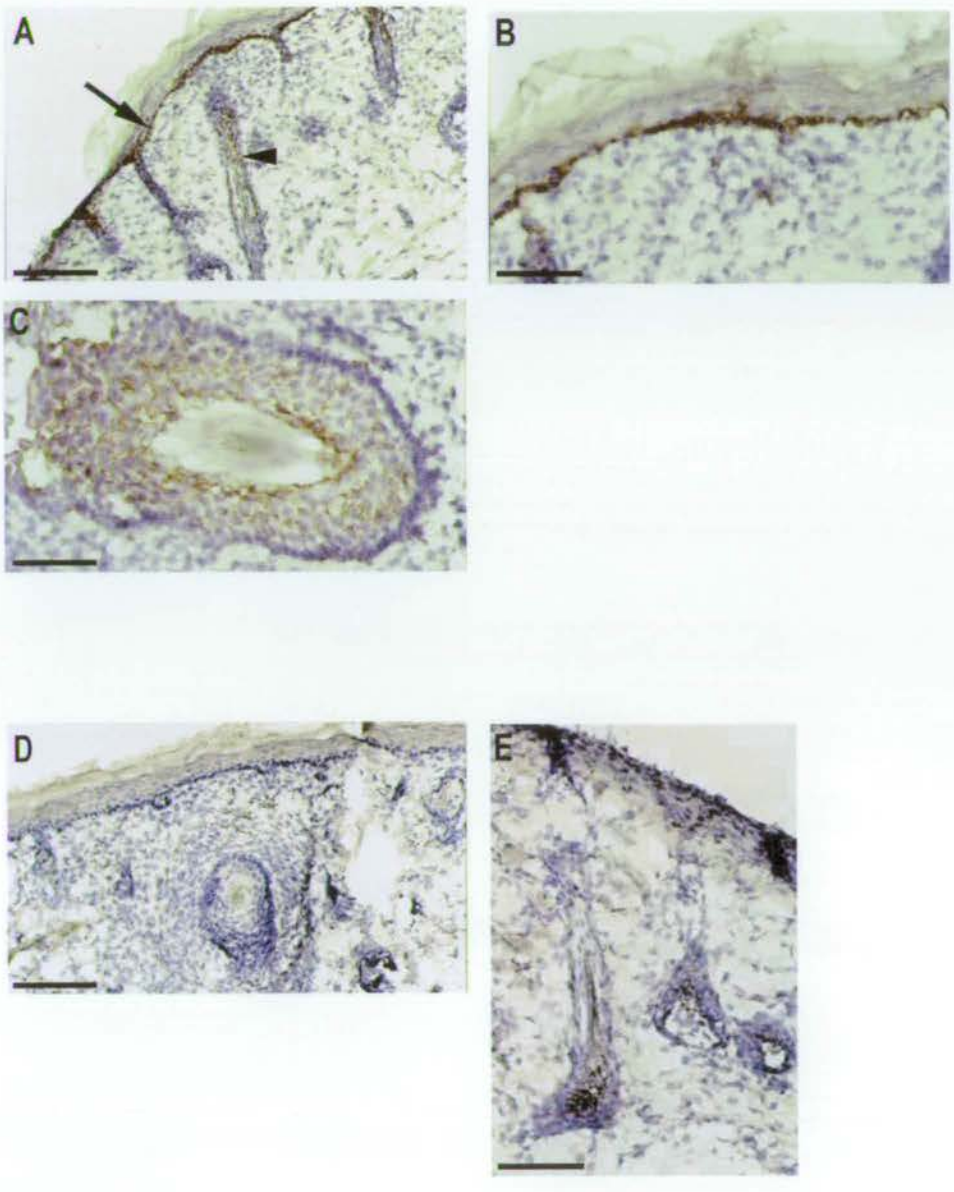

intense in *nude* hair follicles (Figure 4.12). MTS10 also showed an enhanced level of staining in *nude* hair follicles, particularly in cells of the ORS (Figure 4.13).

Discussion

MTS20 expression was previously reported in epithelia of the epidermis, uterus, vagina, bladder, kidney, salivary gland and trachea (Godfrey *et al.*, 1990). MTS24 expression has been shown in many epithelia including vagina, uterus, bladder, kidney, lung, salivary gland and lactating breast (J.Gill, Monash University Medical School, Prahan, Australia, personal communication). The data presented here show that MTS20, MTS24 and MTS10 have specific expression patterns in skin epidermis and root sheath cells of the hair follicle. Comparison of the ß-gal/*Foxn1* expression pattern and mAb expression indicated that MTS20 and MTS24 are likely to be expressed by some *Foxn1*$^{+}$ cells in the epidermis and IRS cells, although *Foxn1* is expressed more widely than MTS20/24. Co-localisation of ß-gal/*Foxn1* and MTS20/24 was attempted but the ß-gal staining blocked subsequent binding of the mAbs to the sections. In the absence of *Foxn1*, in *nude* skin biopsies, MTS20 and MTS24 expression was stronger particularly in the IRS cells. MTS10 expression was also enhanced in *nude* hair follicles. These results suggest that *Foxn1* and the molecules recognised by these mAbs may function in the same genetic pathway. It is unlikely that upregulation of expression of these antigens in *nude* skin is directly due to the absence of *Foxn1* as *Foxn1* functions as a transcriptional activator, not a repressor (Schuddekopf *et al.*, 1996). Therefore, upregulation of these antigens may be an indirect effect of the abnormal differentiation of the skin and hair follicles in *nude* mice.

Figure 4.12. Immunohistochemical staining of wax sections of *nude* skin and hair follicles with MTS20 and MTS24

A: MTS20 is expressed in the hair canal.

B: Cross-section through a hair follicle showing MTS20 expression in the cuticle of the IRS.

C: Cross section through vibrissae follicles showing MTS20 staining epidermis and hair canals but not hair bulbs.

D: Longitudinal section through a vibrissae hair follicle showing MTS20 expression in the IRS cells.

E: MTS24 is expressed in epidermis and the hair canal.

F: Cross-section through a follicle showing strong MTS24 staining in the IRS cuticle.

G: Slanting cross-section through vibrissae follicles showing MTS24 expression in epidermis and hair canals but not in hair bulbs.

H: Longitudinal section through a vibrissae follicle showing MTS24 expression in IRS cells.

Adult vibrissae skin preparations from *nude* mice were embedded in paraffin wax and sectioned. The sections were stained with the appropriate antibody followed by a HRP-conjugated secondary antibody and visualised using DAB substrate (brown colour). Sections were counterstained with hematoxylin.

Scale bars: A, C, D, E, G, H, 200μm; B, F, 100μm.

Figure 4.12.

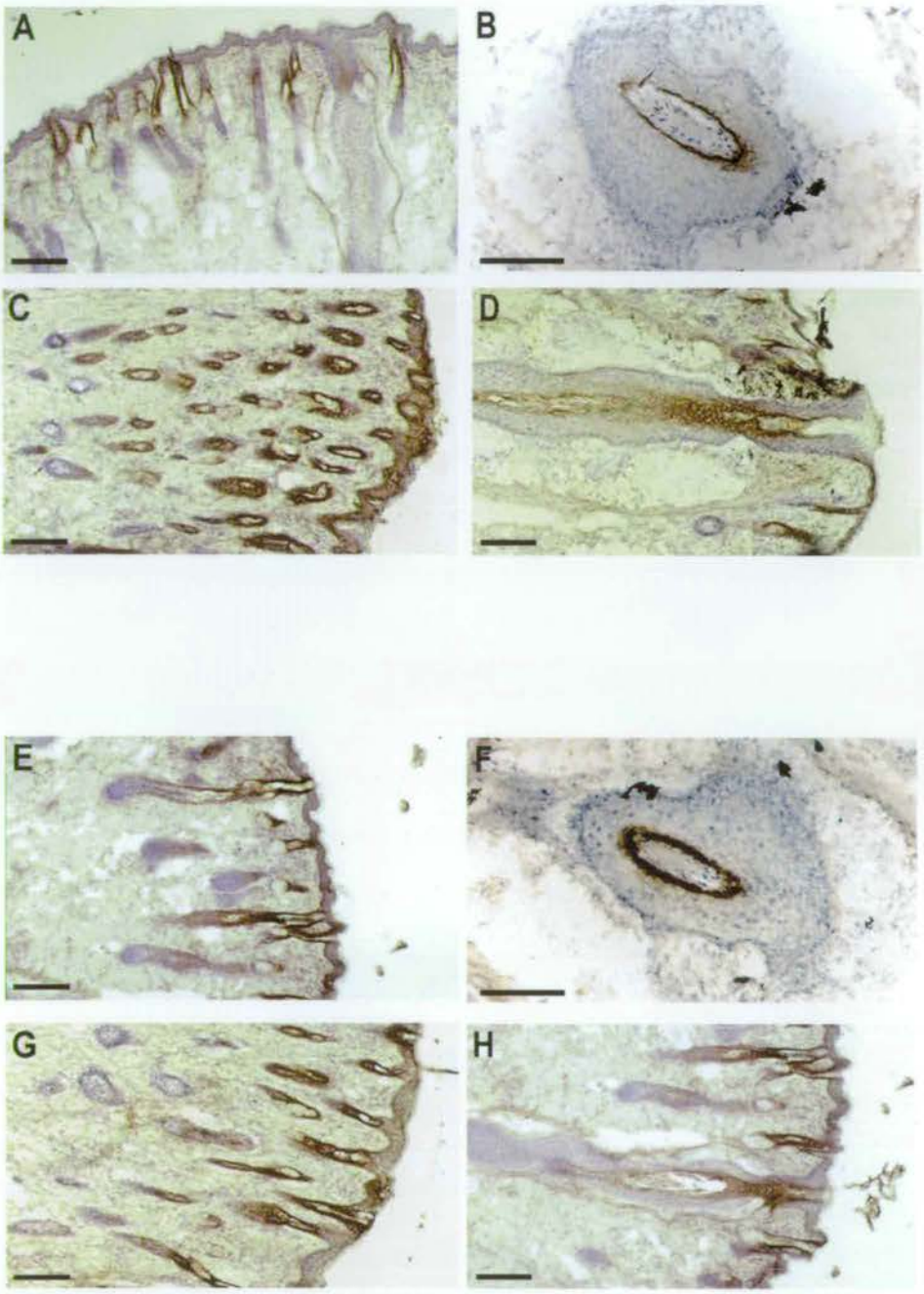

Figure 4.13. Immunohistochemical staining of wax sections of *nude* skin and hair follicles with MTS10 and isotype-control antibodies

A: MTS10 expression in *nude* hair follicles and epidermis.

B: MTS10 expression is confined to the basal epidermal cells and ORS cells of the follicle.

C: Longitudinal section of a follicle showing MTS10 expression in ORS cells along the length of the follicle.

D: Cross-section through a follicle showing MTS10 localised to the ORS cells.

E and F: Isotype control antibody shows no reactivity with *nude* hair and skin.

Adult vibrissae skin preparations from *nude* mice were embedded in paraffin wax and sectioned. The sections were stained with the appropriate antibody followed by a HRP-conjugated secondary antibody and visualised using DAB substrate (brown colour). Sections were counterstained with hematoxylin.

Arrow in B points to basal epidermal cells. ORS, outer root sheath.

Scale bars: all 100μm.

Figure 4.13.

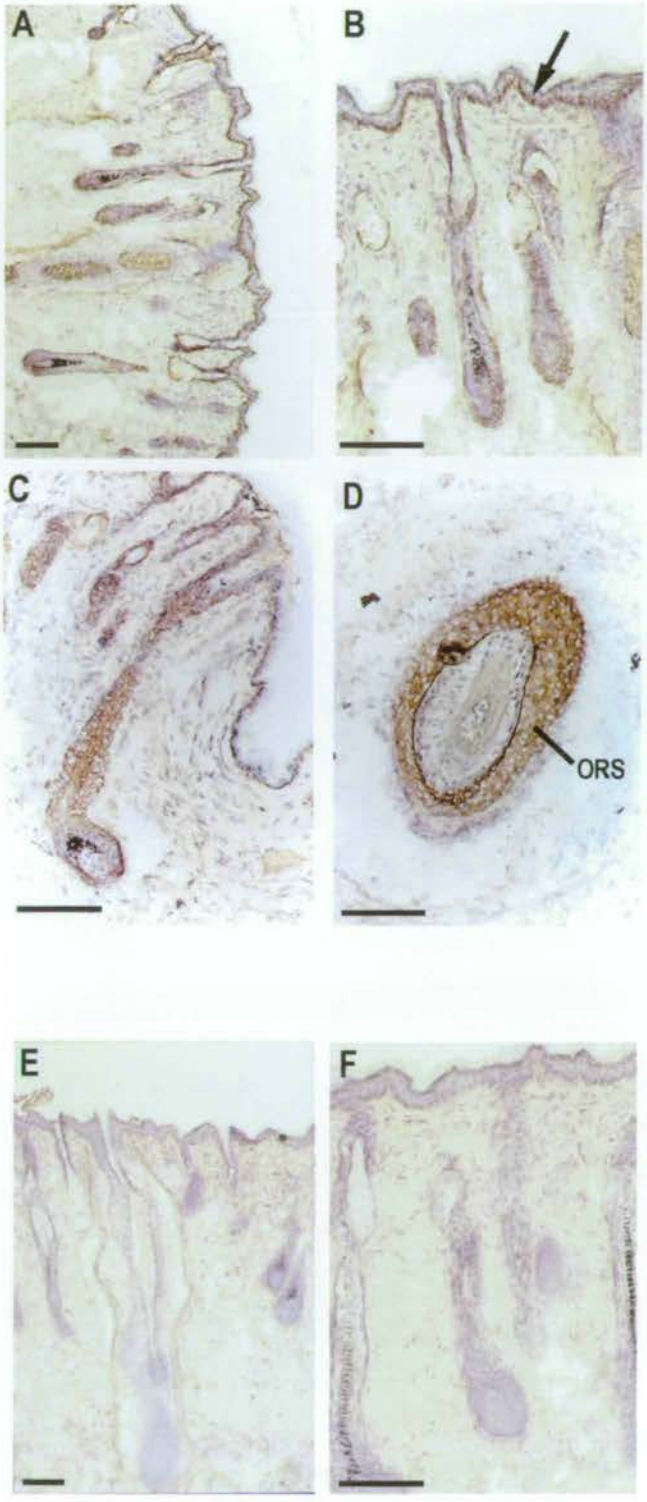

Chapter 5

RESULTS

Characterisation of MTS20/24$^+$ cells from the E12.5 thymic primordium

5.1 Introduction

The aim of this work is to test the hypothesis that MTS20 and MTS24 mark TEPC, which require the transcription factor *Foxn1* to differentiate. Alternatively, the MTS20/24$^+$ cell population could be a *Foxn1*-independent thymic epithelial population. Thymic epithelial progenitor cells should express markers or genes associated with commitment to the thymic epithelial lineage, but not markers of mature, differentiated thymic epithelial cells, or only low levels of these markers. To evaluate the hypothesis that MTS20 and MTS24 are markers of TEPC, purified MTS20/24$^+$ cells from the E12.5 thymic primordium were characterised phenotypically. Freshly purified MTS20/24$^+$ cells were stained with antibodies

against keratins and other thymic epithelial cell subpopulations and analysed for expression of transcription factors associated with thymus development by RT-PCR.

5.2 Fluorescence activated cell sorting

For phenotypic analyses, dissociated E12.5 thymus cells were purified into two populations by fluorescence activated cell sorting (FACS): MTS20/24^{+} cells, which comprise approximately 30% of total E12.5 thymus cells, and MTS20/24^{-} cells which comprise approximately 70% of total E12.5 thymus cells (section 4.4). Figure 5.1 shows typical results from a FACS sort. 39% of E12.5 thymus cells expressed MTS20/24 compared to the isotype control antibody (Figure 5.1.A). Following FACS sorting, small amounts of the sorted cells were reanalysed to check the purity of the sort (Figure 5.1.B). The purified MTS20/24^{-} cell population was routinely greater than 98% pure and the purified MTS20/24^{+} cell population was routinely greater than 95% pure.

Figure 5.1. Fluorescence activated cell sorting of MTS20/24^{+} cells from E12.5 thymi

A: Dissociated E12.5 thymi cells stained with isotype control antibody and with MTS20 and MTS24. 39% of cells positive for MTS20/24 are sorted by FACS.

B: Assessment of purity of the sorted cell populations following sorting. Routinely, MTS20/24^{-} cells were 98-100% pure and MTS20/24^{+} cells were 95-98% pure.

Thymi were dissected from E12.5 wild-type embryos, dissociated to a single cell suspension and stained with the appropriate antibody followed by a FITC-conjugated secondary antibody. Cells were sorted into MTS20/24^{+} and MTS20/24^{-} populations and following sorting, small samples of cells from each population were checked on the FACScan for purity.

Representative of 20 experiments. Figures are percentage of cells in region M1.

Figure 5.1.A

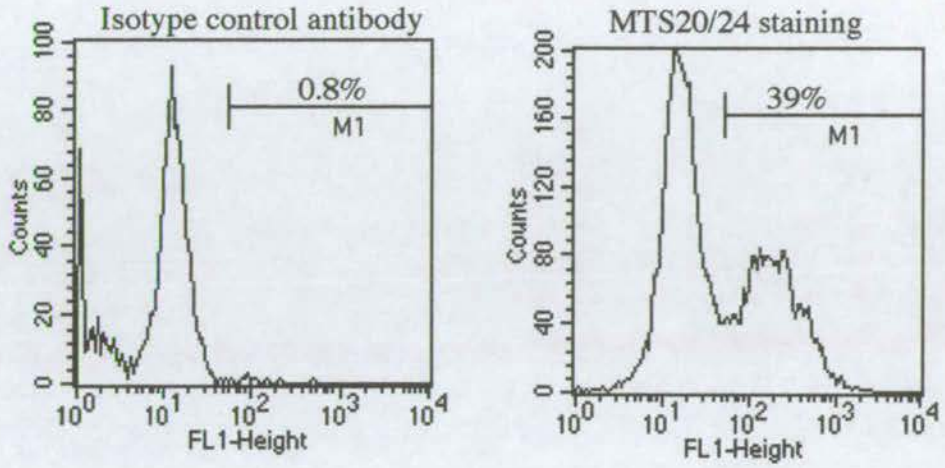

Figure 5.1.B

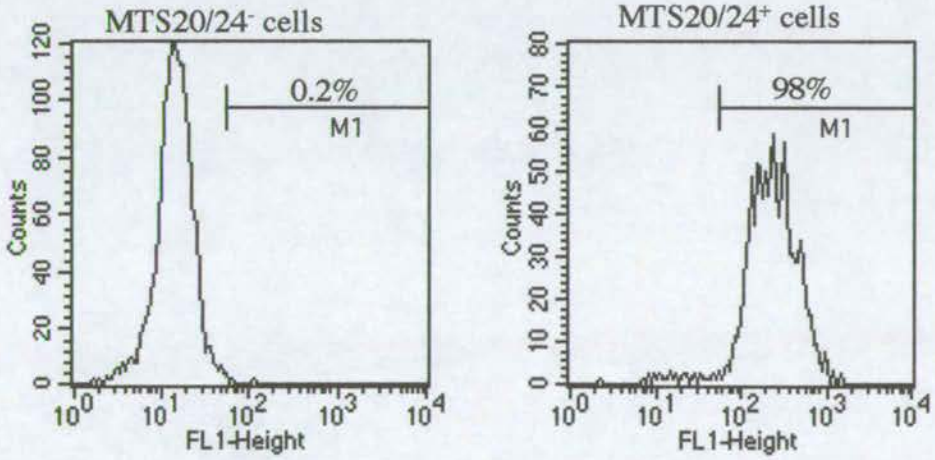

5.3. Characterisation of MTS20/24$^+$ cells

All epithelial cells express keratins and patterns of keratin expression have been used to define different populations of thymic epithelial cells (Savino and Dardenne 1988; Farr and Braddy 1989). Based on keratin expression, two populations of medullary epithelial cells have been identified in the adult thymus: K8$^-$K18$^-$K5$^+$K14$^+$MTS10$^+$UEA-1$^-$ and K8$^+$K18$^+$K5$^-$K14$^-$MTS10$^-$UEA-1$^+$ (Klug *et al.*, 1998). Two populations of epithelial cells have also been defined in the cortex: the major population is K8$^+$K18$^+$K5$^-$K14$^-$MTS10$^-$UEA-1$^-$, and a minor population is K8$^+$K18$^+$K5$^+$K14$^-$MTS10$^-$UEA-1$^-$ (Klug *et al.*, 1998). This latter K8$^+$K5$^+$ population was suggested to be a precursor population for cortical epithelium, which differentiates into K8$^+$K5$^-$ cortical epithelium (Klug *et al.*, 1998).

To characterise the keratin phenotype of the MTS20/24$^+$ cell population from the E12.5 thymic primordium, frozen sections of freshly purified cells were immunostained with anti-cytokeratin. Freshly purified cells were also stained with specific keratins and analysed by flow cytometry. The majority of MTS20/24$^+$ cells were CK$^+$ (Figure 5.2.B). Furthermore, 97% of MTS20/24$^+$ cells expressed K8 and 46% expressed K5 (Figure 5.2.F,G), indicating that approximately 50% of MTS20/24$^+$ cells are K8$^+$K5$^+$.

TEPC should be undifferentiated immature cells which do not express markers associated with mature differentiated thymic epithelium, or express only low levels of these markers. The expression of 4F1, which is associated with cortical epithelium, and MTS10, which is associated with medullary epithelium was analysed on frozen sections of freshly purified MTS20/24$^+$ cells. Neither 4F1 nor MTS10 were detected on MTS20/24$^+$ cells (Figure 5.2.B,C).

These analyses demonstrate that all E12.5 MTS20/24$^+$ cells express keratins and 50% of them are K5$^+$K8$^+$, similar to the putative cortical precursor cells

Figure 5.2. Expression of anti-thymic epithelial antibodies on purified E12.5 MTS20/24$^+$ cells

A: The majority of MTS20/24$^+$ cells express pan-cytokeratin

B: MTS20/24$^+$ cells do not express 4F1

C: MTS20/24$^+$ cells do not express MTS10

D: Isotype-control antibody on MTS20/24$^+$ cells

In A-D, freshly purified E12.5 MTS20/24$^+$ cells were snap frozen and sectioned prior to antibody staining. Representative of three experiments. The sections shown are not serial. Scale bars: all 100μm

E: 46% of freshly purified MTS20/24$^+$ cells are K5$^+$

F: 97% of freshly purified MTS20/24$^+$ cells are K8$^+$.

In E and F, freshly purified E12.5 MTS20/24$^+$ cells were re-incubated with K5 and K8 antibodies, followed by a PE-conjugated secondary antibody and analysed by flow cytometry. Dotted line represents isotype-control antibody, solid line indicates test antibody. Figure is percentage of positive cells in region M1 minus the percentage of isotype-control cells in M1.

Figure 5.2.

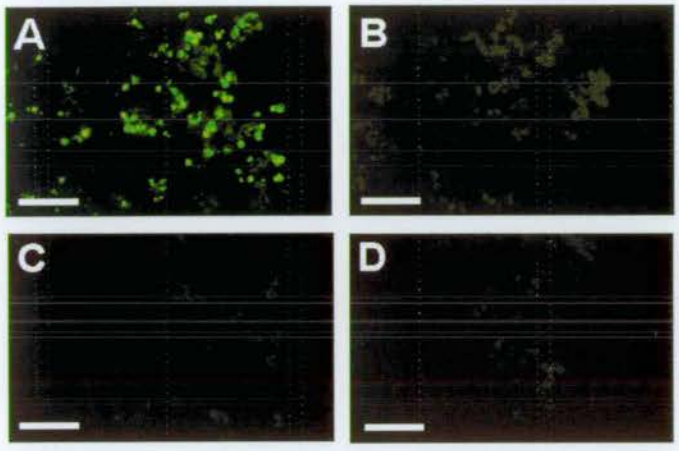
A
B
C
D

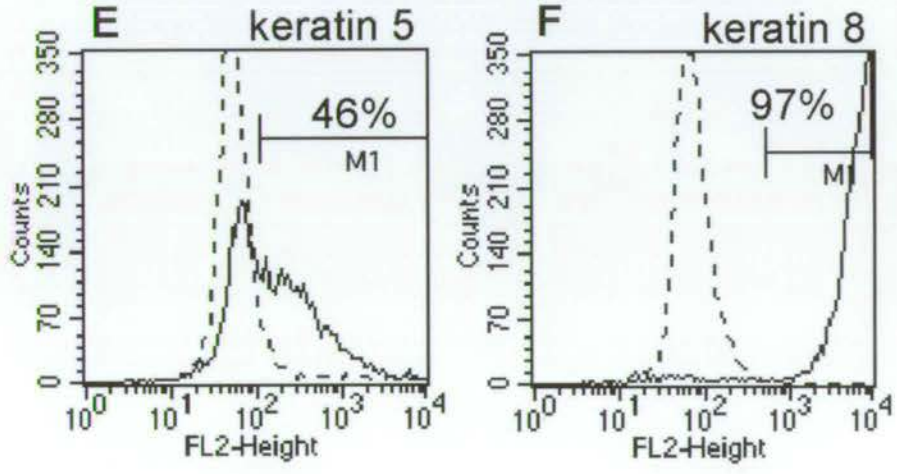
E
keratin 5
46%
M1
Counts
0
70
140
210
280
350
10^0
10^1
10^2
10^3
10^4
FL2-Height
F
keratin 8
97%
M1
Counts
0
70
140
210
280
350
10^0
10^1
10^2
10^3
10^4
FL2-Height

identified recently (Klug *et al.*, 1998). MTS20/24$^+$ cells did not express 4F1 or MTS10, markers associated with mature thymic epithelium. These data indicate that E12.5 MTS20/24$^+$ cells are committed to the thymic epithelial lineage but are phenotypically immature, and are consistent with TEPC residing in the MTS20/24$^+$ cell population.

5.4. Transcription factor gene expression in MTS20/24$^+$ cells

Developmental commitment and stem/progenitor cell fate are regulated by transcription factors (Slack 2000; Watt and Hogan 2000). The expression of transcription factors associated with thymus development was analysed in MTS20/24$^+$ cells by RT-PCR. Expression of *Foxn1*, *Hoxa3*, *Pax9* and *Pax1* was investigated, as mutant analysis had indicated important roles for these transcription factors in thymus development. The forkhead/winged-helix transcription factor *Foxn1*, the gene mutated in *nude* mice (Nehls *et al.*, 1994; Nehls *et al.*, 1996), is required cell-autonomously for the differentiation of mature thymic epithelial populations from thymic progenitor cells (Blackburn *et al.*, 1996). *Hoxa3* is expressed in the third pharyngeal pouch endoderm and the neural crest-derived mesenchyme of the third and fourth pharyngeal arches; *Hoxa3*$^{-/-}$ mice are athymic (Manley and Capecchi 1995). *Pax9* is expressed in the endoderm of the third pharyngeal pouch; *Pax9*$^{-/-}$ mice are athymic (Neubaser *et al.*, 1995; Peters *et al.*, 1998). *Pax1* is expressed in the third pharyngeal pouch endoderm and expression continues in the developing thymus (Wallin *et al.*, 1996); *Pax1*$^{-/-}$ mice have hypoplastic thymi and defects in thymocyte development (Wallin *et al.*, 1996).

Transcription factor expression in MTS20/24$^+$ cells was analysed by reverse-transcriptase-PCR. PCR was carried out on serial dilutions of cDNA to semi-quantitatively analyse the expression of genes in these populations using specific primers as detailed in section 2.6.4. *ß-actin* was used as an internal control for reverse transcription and PCR. Each PCR reaction was repeated at least 3 times. Comparison of the intensity of product bands between the diluted samples allows a semi-quantitative analysis of the amount of specific product in each sample.

MTS20/24$^+$ cells purified from E12.5 thymi expressed *Foxn1*, *Pax1*, *Pax9* and *Hoxa3* (Figure 5.3.). Expression of these transcription factors was also detected in MTS20/24$^-$ cells, although at much lower levels (Figure 5.3.). Amplification of *β-actin* produced consistently high levels of product in each diluted sample and demonstrated that equivalent amounts of cDNA template were present in the MTS20/24$^+$ and MTS20/24$^-$ cell samples. *Foxn1* was expressed in both cell populations; however, expression was approximately 100-fold lower in the MTS20/24$^-$ cell population compared to the MTS20/24$^+$ cell population, as product was detectable in 1/100 dilution of MTS20/24$^+$ cDNA, but only in undiluted MTS20/24$^-$ cDNA. *Pax1* was expressed in both E12.5 cell populations, with *Pax1* expression in MTS20/24$^+$ cells between 10-100-fold higher than in MTS20/24$^-$ cells. *Pax9* expression was detected in both cell populations and was approximately 10-fold lower in MTS20/24$^-$ cells than MTS20/24$^+$ cells. *Hoxa3* was detected in MTS20/24$^+$ cells and MTS20/24$^-$ cells. Expression of *Hoxa3* in MTS20/24$^-$ cells was approximately 10-fold lower than MTS20/24$^+$ cells.

These data demonstrate that the E12.5 MTS20/24$^+$ cell population expresses *Foxn1*, *Pax1*, *Pax9* and *Hoxa3*, all of which are known to be involved in thymus development. The expression of these transcription factors in MTS20/24$^+$ cells is consistent with the hypothesis that MTS20 and MTS24 mark TEPC.

Figure 5.3. Transcription factor gene expression in E12.5 MTS20/24^{+} and MTS20/24^{-} cells by RT-PCR

E12.5 MTS20/24^{+} cells express *Foxn1*, *Pax1*, *Pax9* and *Hoxa3*, transcription factors with important roles in early thymus development. MTS20/24^{-} cells also express these transcription factors although at much lower levels.

Total RNA and cDNA were prepared from freshly purified E12.5 thymus cells and RT-PCR performed on serially diluted cDNA template using gene specific primers. Products were run on a 2% agarose gel and visualised by ethidium bromide staining. 1, 1/10 and 1/100 refer to the dilution of the cDNA template. neg, no template control.

Figure 5.3.

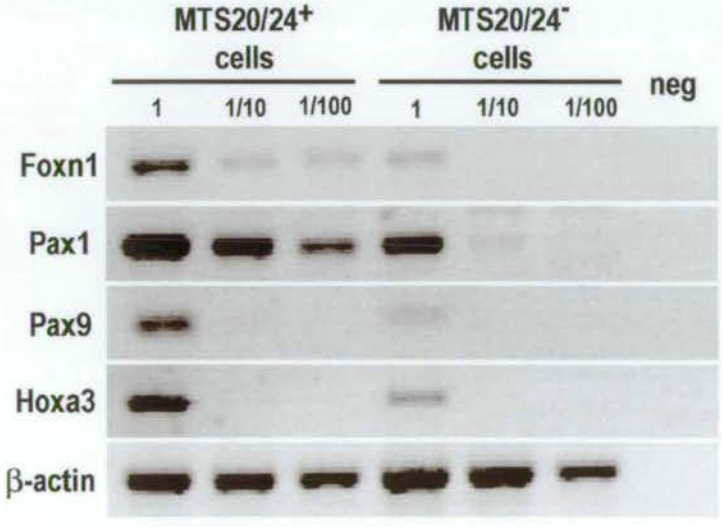
MTS20/24+ cells
MTS20/24- cells
neg
1
1/10
1/100
1
1/10
1/100
Foxn1
Pax1
Pax9
Hoxa3
β-actin

5.5. Real-time reverse-transcriptase PCR

Real-time RT-PCR was used to quantify the amount of *Foxn1* cDNA present in MTS20/24$^+$ and MTS20/24$^-$ cells. This technique measures product formation during PCR by including SYBR Green I dye in the reaction, which fluoresces upon binding to double stranded DNA. The fluorescence of each cDNA sample is continuously monitored throughout the reaction, resulting in a real-time amplification curve. Amplification is recorded using primers which amplify a standard control gene present in equal amounts in all samples, and primers for the genes under test. The log-linear phase of the reaction is identified for the standard, and a standard curve obtained which can then be used to quantitate the relative expression of other genes in the starting material. SYBR Green I dye can also bind to any non-specific double stranded DNA which forms during the reaction, such as primer-dimers. To ensure accurate measurement of the amount of PCR product, the fluorescence of the reaction is read at the end of each cycle at a temperature above which the non-specific DNA has denatured and below the melting temperature of the specific PCR product. The Lightcycler analysis software was used to analyse the data in these experiments. Glyceraldehyde-3-phosphate dehydrogenase (GAPDH) primers were used as the standard in these experiments.

Prior to quantitative analysis, PCR reaction conditions were optimised. Firstly, the $MgCl_2$ concentration in the reaction was optimised for the primer pairs, GAPDH and *Foxn1*. Concentrations of 1mM, 2mM and 3mM $MgCl_2$ were tested and 2mM was found to be optimal for both primer pairs. Secondly, the melting points of the non-specific double stranded DNA and the specific products were determined by melting point analysis. Figure 5.4 shows amplification curves and melting point analysis for GAPDH and *Foxn1* in serially diluted whole E12.5 thymus cDNA with 2mM $MgCl_2$. The melting curve analysis for the GAPDH reactions show that non-

Figure 5.4. Real-time RT-PCR optimisation experiments

A: Real-time amplification curve for GAPDH on whole E12.5 thymus cDNA

B: Real-time amplification curve for *Foxn1* on whole E12.5 thymus cDNA

C: Melting point analysis for GAPDH. GAPDH product melts at 89°C, whereas non-specific products melt at 81°C.

D: Melting point analysis for *Foxn1*. *Foxn1* specific product melts at 91°C.

Thymi were dissected fromE12.5 embryos and total RNA extracted. CDNA was synthesised and RT-PCR was performed on serial dilutions of cDNA in the presence of SYBR Green I dye. The fluorescence was measured after each cycle in the Lightcycler. A and B are real-time amplification curves showing increasing fluorescence with cycle number. Following amplification, samples were heated slowly to determine the melting point of the products formed. C and D show change in fluorescence with increasing temperature.

Figure 5.4.

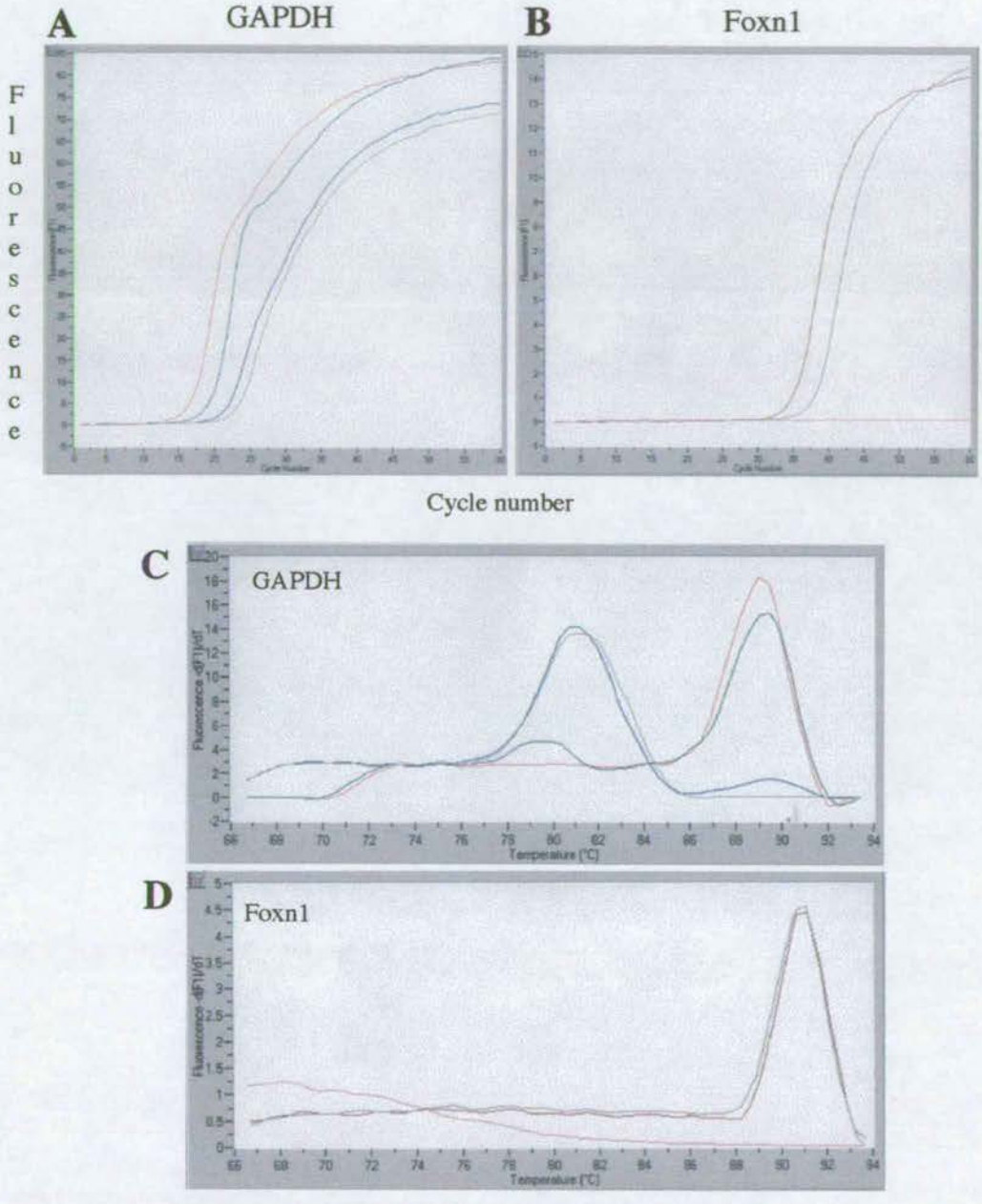
A
GAPDH
B
Foxn1
Fluorescence
Cycle number
C
GAPDH
D
Foxn1
Temperature (°C)
GAPDH:
Neat cDNA
1:10 dilution
1:100 dilution
No CDNA
Foxn1:
Neat cDNA
1:10 dilution
No cDNA

specific double stranded DNA melts at 81°C, whereas specific product melts at 89°C (Figure 5.4.C). An appropriate temperature above the non-specific product melting point and below specific product melting point at which to record fluorescence was 85°C. The melting curve analysis for *Foxn1* reactions shows that no non-specific product has formed (Figure 5.4.D). The specific *Foxn1* product melts at 91°C, so the chosen temperature of 85°C for fluorescence measurement is below the melting point of the *Foxn1* product.

After these initial optimisation experiments, one experiment was performed on serially diluted cDNA from MTS20/24$^+$ and MTS20/24$^-$ cells with GAPDH and *Foxn1* primers. The fluorescence was measured after each PCR cycle at 85°C and a 2mM concentration of $MgCl_2$ was used in the reactions. Background fluorescence was removed by setting a noise band on the amplification curve of the GAPDH reaction. The log-linear portion of the amplification curve was then identified and a standard curve drawn for each sample based on the known dilutions of the template (Figure 5.5.). From these standard curves, the relative concentration of *Foxn1* in each sample was determined. Expression of *Foxn1* in MTS20/24$^+$ cells was 100-fold more than in MTS20/24$^-$ cells (Table 5.1.).

Figure 5.5 Real-time RT-PCR analysis - Determination of standard curves for GAPDH in MTS20/24$^+$ and MTS20/24$^-$ cells.

A: Identification of log-linear region, setting of noise band and drawing of standard curve for MTS20/24$^+$ cell samples.

B: Identification of log-linear region, setting of noise band and drawing of standard curve for MTS20/24$^-$ cell samples.

Following PCR amplification, the log-linear region of the GAPDH amplification curve is identified and a noise band is drawn through the log-linear region. A standard curve is then calculated for GPADH in each sample against which the relative concentration of other cDNAs can be determined.

Figure 5.5.

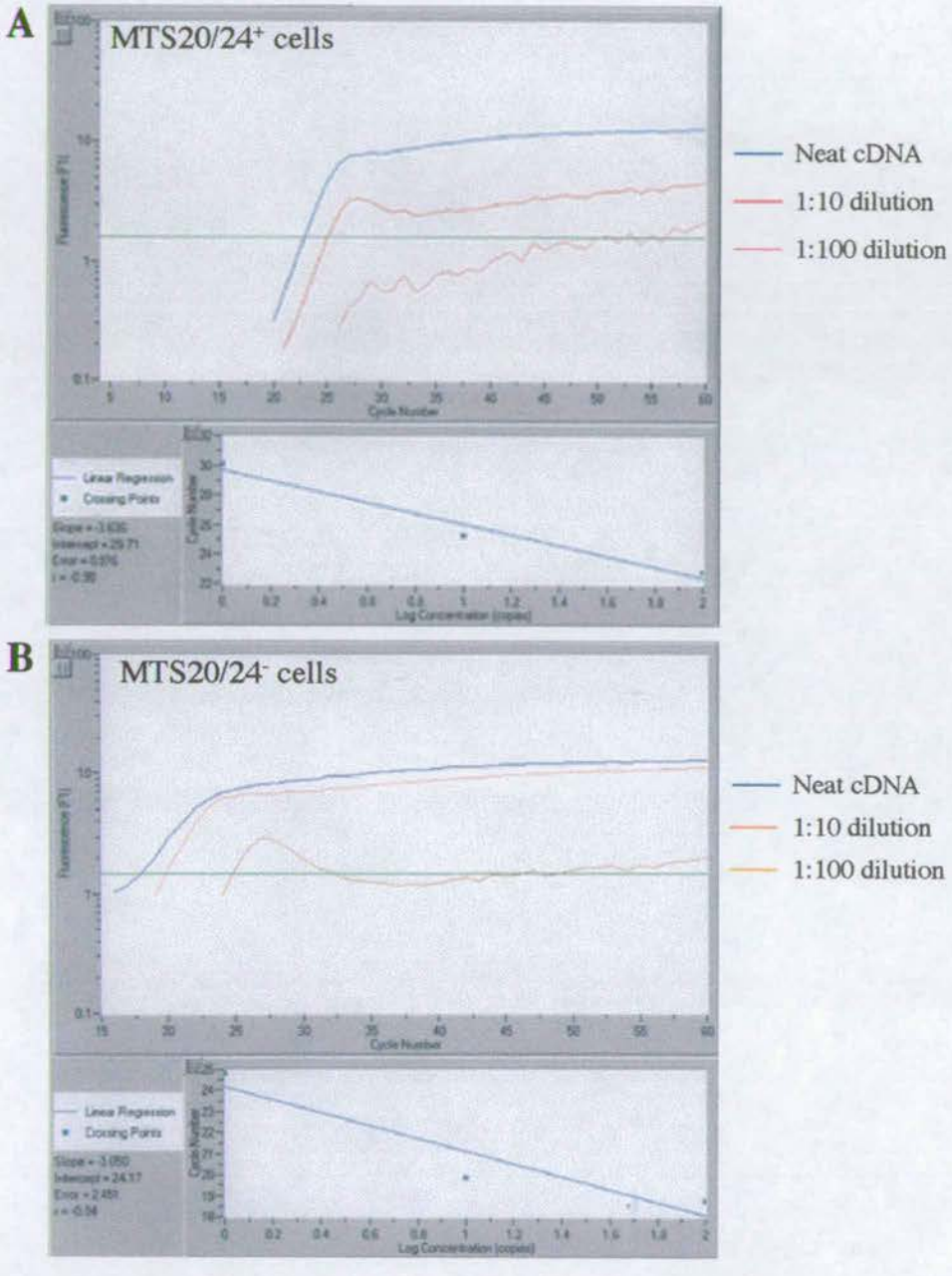
A
MTS20/24+ cells
Neat cDNA
1:10 dilution
1:100 dilution
Cycle Number
Linear Regression
Crossing Points
Log Concentration (copies)
B
MTS20/24- cells
Neat cDNA
1:10 dilution
1:100 dilution
Cycle Number
Linear Regression
Crossing Points
Log Concentration (copies)

Table 5.1. Quantification of *Foxn1* expression in E12.5 MTS20/24$^+$ cells using real-time RT-PCR

Sample	GAPDH (no. of copies)	*Foxn1* (no. of copies)
MTS20/24$^+$ cells	100	0.016
MTS20/24$^-$ cells	100	0.00013
MTS20/24$^+$ cells	10	0.00062
MTS20/24$^-$ cells	10	0.0000084

From standard curves for GAPDH expression, the relative number of copies of *Foxn1* in the samples can be determined. Compared to 100 copies of GAPDH, expression of *Foxn1* in MTS20/24$^+$ cells is 100-fold higher than in MTS20/24$^-$ cells. Compared to 10 copies of GAPDH, expression of *Foxn1* in MTS20/24$^+$ cells is 100-fold higher than in MTS20/24$^-$ cells.

5.6 Discussion

This chapter describes the phenotypic characterisation of the MTS20/24$^+$ cell population from E12.5 thymi. Freshly purified E12.5 MTS20/24$^+$ cells expressed cytokeratin but did not express 4F1 or MTS10, markers associated with differentiated cortical and medullary thymic epithelium respectively. This confirms that the MTS20/24$^+$ population and the 4F1$^+$ population from E12.5 thymi are distinct (section 4.4.). These data also show that the MTS10$^+$ population identified by immunohistochemistry on E12.5 thymus sections (section 4.4.) does not overlap with the MTS20/24$^+$ population.

Approximately 50% of MTS20/24$^+$ cells were K8$^+$K5$^+$ and 50% were K8$^+$K5$^-$ Previous experiments have suggested that K8$^+$K5$^+$ thymic epithelial cells are cortical precursor cells which give rise to K8$^+$K5$^-$ mature cortical thymic epithelial cells (Klug *et al.*, 1998; Klug *et al.*, 2000). These experiments did not investigate keratin expression in medullary precursor cells or the expression of keratins during thymic ontogeny. The data presented here show that 50% of the E12.5 MTS20/24$^+$ cell population comprises putative K8$^+$K5$^+$ cortical precursor cells. The K8$^+$K5$^+$ cells may be common precursor cells for both cortical and medullary thymic epithelium. Alternatively, medullary precursor cells with a different cytokeratin phenotype may be present within the E12.5 thymic primordium, either in the MTS20/24$^+$ or the MTS20/24$^-$ population.

The transcription factors *Foxn1, Pax1, Pax9* and *Hoxa3* were expressed in the E12.5 MTS20/24$^+$ cell population. These transcription factors were also expressed in the MTS20/24$^-$ population albeit at lower levels. This is not unexpected as the MTS20/24$^-$ population may contain differentiating progeny and mature thymic epithelial cells which continue to express these transcription factors. *Foxn1* expression is maintained in differentiated epithelial cells throughout thymus

development and in the adult thymus (section 3.3 and (Nehls *et al.*, 1996)). *Pax1* is expressed in a significant fraction of E14.5 thymus cells and is progressively down regulated during thymus development (Wallin *et al.*, 1996). In the adult thymus, *Pax1* is expressed in a low number of cortical epithelial cells which are phenotypically undifferentiated, and consequently, *Pax1* has been suggested to be a marker of thymic epithelial precursor cells (Wallin *et al.*, 1996). It is possible that MTS20/24 and *Pax1* mark TEPC as MTS20/24$^+$ cells express high levels of *Pax1* compared to MTS20/24$^-$ cells. However, the *Pax1*$^+$ and MTS20/24$^+$ cells are located in different regions of the adult thymus: *Pax1*$^+$ cells are located within the cortex (Wallin *et al.*, 1996), whereas MTS20/24$^+$ cells are located in the medulla (Godfrey *et al.*, 1990). *Pax9* is expressed in thymic epithelial cells throughout foetal development and in adult thymus (Peters *et al.*, 1995). *Hoxa3* is expressed by thymic epithelial cells at E15.5 and in adult thymus, by RT-PCR (N.Manley, Medical College of Georgia, Augusta, USA, personal communication), indicating that *Hoxa3* is expressed in differentiated epithelial cells. Expression of these transcription factors would therefore be expected in differentiating thymic epithelial cells which may be present in the MTS20/24$^-$ cell population, as well as in TEPC.

Semi-quantitative RT-PCR analysis estimated that MTS20/24$^+$ cells expressed 100-fold more *Foxn1* than MTS20/24$^-$ cells. The quantification of *Foxn1* expression by real-time RT-PCR also showed that MTS20/24$^+$ cells expressed 100-fold more *Foxn1* than MTS20/24$^-$ cells. This indicates that *Foxn1* expression is between 10- and 100-fold greater in MTS20/24$^+$ cells than in MTS20/24$^-$ cells. However, only one quantitative experiment was performed in this analysis. The real-time RT-PCR analysis would need to be repeated at least three times to ensure accurate and reproducible results.

A possible source of error in all experiments in which cell populations are isolated by FACS, is contamination within the populations due to the impurity of the sort. The generally accepted minimum purity for FACS is 95%. In the experiments

presented here, all populations of sorted cells were checked for purity prior to further use. MTS20/24$^+$ cell populations were always at least 95-98% pure and MTS20/24$^-$ cell populations were between 98-100% pure. In the immunohistochemical staining experiments, MTS20/24$^-$ cells contaminating the MTS20/24$^+$ cell population might have been revealed by 4F1$^+$ or MTS10$^+$ cells in the MTS20/24$^+$ population. In the RT-PCR analysis, MTS20/24$^-$ cell contamination of the MTS20/24$^+$ population would be unlikely to be responsible for the expression observed in the MTS20/24$^+$ samples, as this was stronger than in the MTS20/24$^-$ cell samples in all cases. Contamination of MTS20/24$^+$ cells within the MTS20/24$^-$ cell fraction may be responsible for the observed transcription factor expression in MTS20/24$^-$ cell samples. This is particularly relevant where the observed expression of genes in the MTS20/24$^-$ cell sample is at a low level, as in the case of *Foxn1*, *Pax9* and *Hoxa3*. However, this would not affect the overall conclusions of this experiment concerning the expression of transcription factors in MTS20/24$^+$ cells.

To further analyse the phenotype and lineage commitment of the E12.5 MTS20/24$^+$ cell population, single cell RT-PCR studies could be employed to investigate other markers, including transcription factors and signalling molecules, that might be expressed in TEPC. For example, IGF is able to support the development of the early thymic primordium in the absence of mesenchyme, suggesting that TEPC might express IGF receptors (Shinohara and Honjo 1997). The RelB transcription factor might be expressed by TEPC as it is necessary for the differentiation of a subset of medullary epithelial cells (Burkly *et al.*, 1995; Schmidt-Ullrich *et al.*, 1996). The Wnt signalling pathway has been implicated in the transcriptional control of stem/progenitor cell fate in other organs (Watt and Hogan 2000) so components of this pathway might be expressed by TEPC. These analyses would also identify new markers which identify the MTS20/24$^+$ cell population in the E12.5 thymic primordium and allow investigation of the heterogeneity of the

MTS20/24$^+$ population by defining subpopulations of cells within the MTS20/24$^+$ population.

In conclusion, this work has shown that the MTS20/24$^+$ cell population from the E12.5 thymic primordium expresses keratin but does not express markers associated with mature differentiated thymic epithelium. Furthermore, MTS20/24$^+$ cells express transcription factors associated with thymus development. These data indicate that MTS20/24$^+$ cells are committed to the thymic epithelial lineage and are therefore consistent with the hypothesis that the MTS20/24$^+$ population contains TEPC.

Chapter 6

RESULTS

Investigation of the functional potential of thymic epithelial subpopulations

6.1. Introduction

The work presented in this chapter aimed to determine, through lineage and functional analyses, whether the MTS20/24$^+$ cell population from E12.5 thymi are TEPC. The data presented in chapters 4 and 5 demonstrated that the expression profile of MTS20 and MTS24 are consistent with those expected of TEPC markers and that the MTS20/24$^+$ cell population is committed to the thymic epithelial lineage. These data are therefore consistent with the MTS20/24$^+$ cell population containing progenitor cells for the thymic epithelium, but would also be consistent with the MTS20/24$^+$ cell population being a *Foxn1*-independent thymic epithelial population. TEPC could alternatively reside within the MTS20/24$^-$ cell population or the MTS20/24$^+$ and MTS20/24$^-$ populations could contain separate progenitor cells, one

for the cortical epithelium and one for the medullary epithelium. Direct assessment of the differentiative potential of the MTS20/24$^+$ and MTS20/24$^-$ cell populations has been tested in this chapter.

6.2. The kidney capsule grafting model

The differentiation potential of MTS20/24$^+$ and MTS20/24$^-$ cells from E12.5 thymi was investigated using an experimental model based on RTOC (Anderson *et al.*, 1993). Defined numbers of purified MTS20/24$^+$ or MTS20/24$^-$ cells, either with or without fibroblast cells and thymocytes, were cultured *in vitro* for 1-2 days to permit reaggregation, then grafted under the kidney capsule of congenitally athymic *nude* mice. An overview of the experimental protocol is shown in Figure 6.1. Kidney capsule grafting has been utilised extensively as a model system in which cells can grow and differentiate in an enclosed physiological environment (Bogden *et al.*, 1979; Zinkernagel *et al.*, 1980; Chen and Kosco 1993). As *nude* mice are congenitally athymic, with few peripheral T-cells (Pantelouris 1968) but a normal hemato-lymphoid compartment, grafting of thymi into *nude* recipients has been used extensively to study T-cell development, specificity, and tolerance induction (Zinkernagel *et al.*, 1980; Hoffmann *et al.*, 1992). In the experiments presented below, grafting under the kidney capsule of *nude* recipient mice provided a sensitive assay for development of thymus function which was monitored by the development of peripheral T-cells.

In preliminary experiments, the optimal *in vitro* culture conditions for aggregating E12.5 thymus cells were investigated. Firstly, purified E12.5 thymus cell populations were cultured in hanging drops to allow aggregation. Cell numbers between 3,000 and 10,000 cells were tested and in all cases the cells appeared to form tiny aggregates in the base of the drop. For the grafting procedure, the cells

Figure 6.1. Kidney capsule grafting protocol

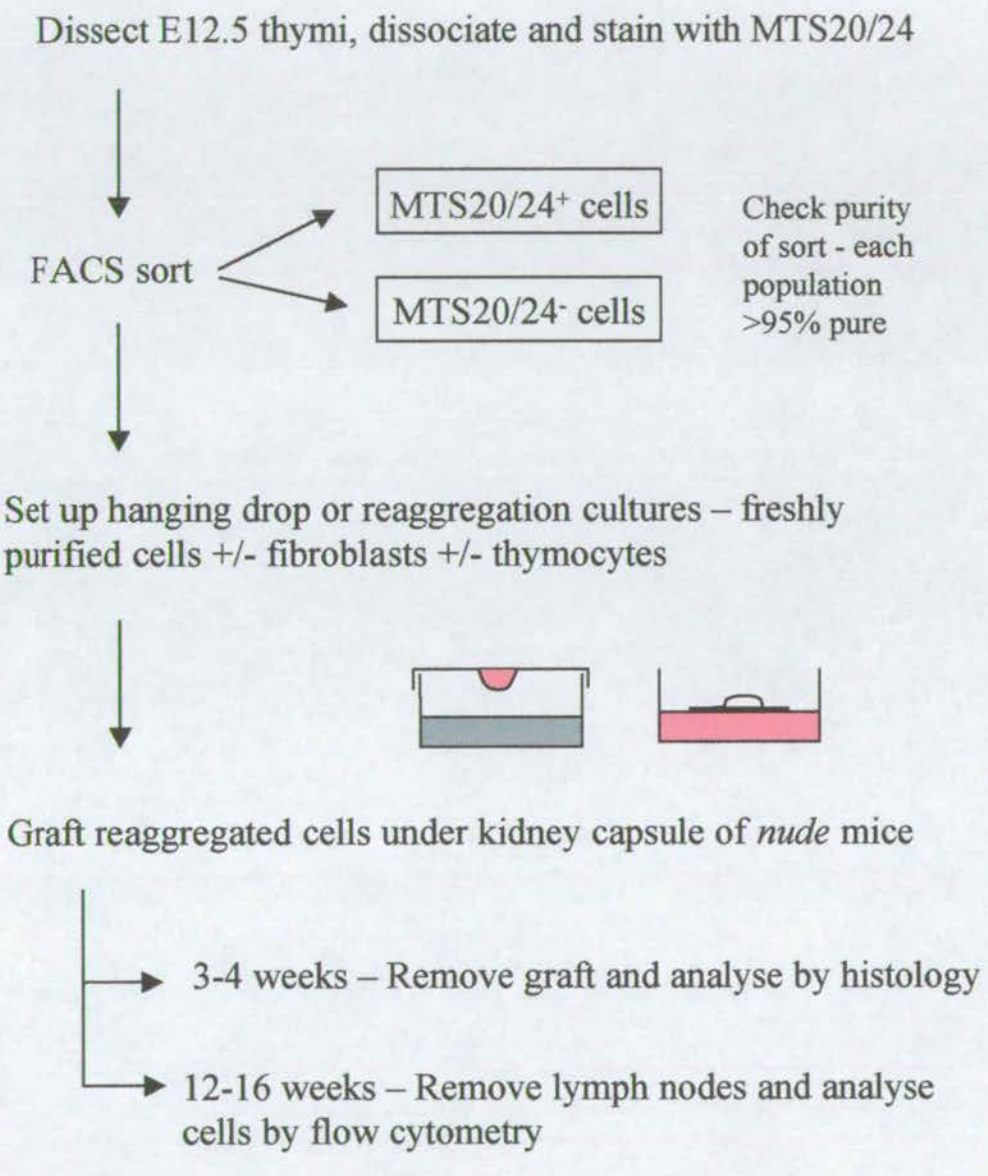

were drawn into a fine glass pipette in a small volume of medium and transferred under the kidney capsule. In a preliminary experiment, where 10,000 whole thymus cells were grafted, no evidence of grafted cells could be observed under the kidney capsule at four weeks after grafting. This method was therefore not suitable for lineage studies, where recovery of the graft is necessary, but was used for long-term reconstitution experiments for grafting small numbers of cells.

Further experiments tested a model based on reaggregate foetal thymic organ culture, RTOC, (Anderson *et al.,* 1993) in which the cells were mixed in a tiny volume of media and the resulting cell slurry placed in a single drop onto a filter floating on media. After 24-48 hours, the cells had reaggregated into a solid structure which could be lifted from the filter using fine forceps and implanted under the kidney capsule. Experiments were performed to establish the optimal cell numbers required for reaggregation. The minimum number of cells which would routinely reaggregate was 100,000. To aid identification of the site of the graft under the kidney capsule, a small piece of nitrocellulose filter was inserted under the capsule adjacent to the reaggregated cells. This method allowed the cells to be transferred as a single cohesive structure and had the advantage of re-establishing a three-dimensionally oriented structure within the graft, similar to the structure within the normal thymus.

A preliminary experiment, in which 100,000 whole thymus cells were reaggregated and grafted under the kidney capsule of a *nude* mouse, demonstrated that a robust graft was present after four weeks. This time was based on RTOCs maintained *in vitro*, which showed development of $CD4^+$ or $CD8^+$ SP T-cells after nine days and showed normal cortical and medullary architecture within the RTOCs (Anderson *et al.,* 1993) (G.Anderson, Department of Anatomy, University of Birmingham, UK, personal communication). In the experiments described here, grafts were left 3-4 weeks before analysis, as the E12.5 epithelial cells used were more immature than the E14.5 cells used above in RTOCs and the reaggregates were

not supplied with T-cell precursors. Circulating T-cell precursors in the recipient mouse would be required to reach the graft under the kidney capsule. This method of reaggregation was used for all lineage studies where grafts needed to be recovered, and in some long-term reconstitution experiments where large numbers of cells were grafted.

Fibroblast cells were included in the grafts for two reasons. Firstly, fibroblast cells are required for both early thymus organogenesis and thymocyte development (Auerbach 1960; Le Douarin and Jotereau 1975; Bockman and Kirby 1984; Anderson *et al.,* 1993; Shinohara and Honjo 1996; Anderson *et al.,* 1997; Itoi and Amagai 1998; Suniara *et al.,* 2000). Secondly, fibroblast cells were used as carrier cells in experiments using the RTOC reaggregation method, as RTOCs required approximately 100,000 cells for successful reaggregation. Initial experiments used the NIH3T3 fibroblast cell line maintained *in vitro* as the source of fibroblast cells as this had been used in RTOC experiments previously (Anderson *et al.,* 1993; Anderson *et al.,* 1997). However grafting of these cells under the kidney capsule resulted in uncontrolled proliferation of NIH3T3 cells and the formation of abdominal cysts often resulting in the premature death of the mouse. Subsequently, primary murine embryonic fibroblasts (MEFs) grown out from E13.5 or E14.5 wild-type embryos were found to be suitable for use in *in vivo* grafting.

To investigate the lineage potential of MTS20/24^{+} and MTS20/24^{-} cells, short-term grafts were established. Here, between 12,500 and 80,000 freshly purified cells were mixed with 100,000 MEFs, reaggregated using the RTOC method and grafted under the kidney capsule of *nude* mice. After 3-4 weeks the kidneys were removed and the grafts recovered and analysed by histology and immunofluorescence. Control experiments consisted of mice grafted with whole E12.5 thymus lobes or MEFs alone.

To investigate the functional potential of the MTS20/24$^+$ and MTS20/24$^-$ populations, long-term grafts were established in which freshly purified cells were either grafted alone or with added fibroblast cells. In experiments with cell numbers below 100,000 total cells, the hanging drop method of reaggregation was used. In experiments with cell numbers above 100,000 total cells, the RTOC method of reaggregation was used. Long-term grafts were left for 12-16 weeks before removal of the lymph nodes from the grafted recipient mice and analysis of the lymph node cells by flow cytometry. The axillary, inguinal and popliteal lymph nodes were dissected. Control mice were grafted with whole E12.5 thymus lobes, dissociated and reaggregated whole E12.5 thymus cells or fibroblasts only.

6.3. Lineage potential of MTS20/24$^+$ cells

Freshly purified MTS20/24$^+$ cells from the E12.5 thymic primordium are keratin$^+$, 4F1$^-$ and MTS10$^-$ (See figure 5.2). To assess the lineage potential of cells from the E12.5 thymic primordium, RTOCs were established and analysed at two time points: immediately prior to, and three weeks after, grafting. To assess the status of MTS20/24$^+$ cells prior to grafting, RTOCs were established with 60,000 MTS20/24$^+$ cells and 60,000 MEFs. After 48 hours, the reaggregates were snap frozen, cryosectioned and stained with anti-TE mAbs. Within the reaggregates, numerous patches of cells were keratin$^+$ (Figure 6.2.B), indicating that the MTS20/24$^+$ cells within the reaggregates had grouped into epithelial patches surrounded by keratin$^-$ fibroblasts. Staining with 4F1, a marker associated with cortical epithelium, revealed patches of 4F1$^+$ cells within the reaggregate (Figure 6.2.C.). Staining with MTS10, a marker associated with medullary epithelium, revealed the presence of scattered MTS10$^+$ cells throughout the reaggregate (Figure 6.2.D.). The extent of staining with 4F1 and MTS10 was less than the keratin$^+$ areas.

Figure 6.2. Analysis of E12.5 MTS20/24$^+$ cell reaggregates after 48 hour culture

A: Hematoxylin and eosin stained section of MTS20/24$^+$ cell reaggregate

B: Section of MTS20/24$^+$ cell reaggregate stained for cytokeratin

C: Section of MTS20/24$^+$ cell reaggregate stained with 4F1, a marker of cortical epithelium

D: Section of MTS20/24$^+$ cell reaggregate stained with MTS10, a marker of medullary epithelium

E: Section of MTS20/24$^+$ cell reaggregate stained for MHC Class II

F: Section of MTS20/24$^+$ cell reaggregate stained with an isotype-control antibody

Thymi were dissected from E12.5 embryos, dissociated to a single cell suspension and stained with MTS20 and MTS24. Following purification of the MTS20/24$^+$ population, MTS20/24$^+$ cells were mixed with murine embryonic fibroblasts and reaggregated using the FTOC method. After 48 hours in culture, reaggregates were snap frozen, sectioned and stained with the appropriate antibodies.

Scale bars: All 100μm. Not serial sections.

Figure 6.2.

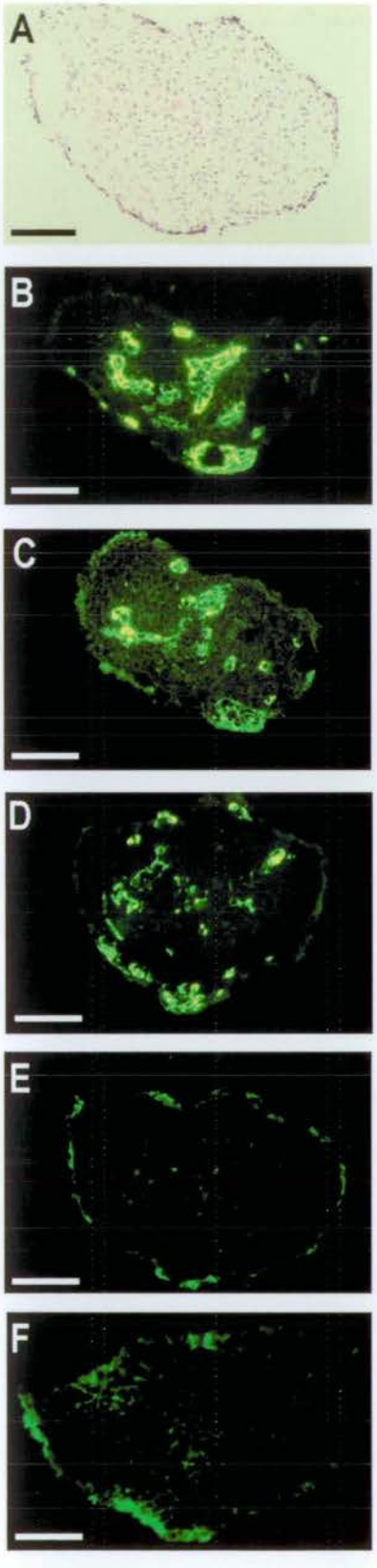

No MHC Class II positive cells were present within the reaggregates (Figure 6.2.E.). Control experiments demonstrated, by flow cytometry, that MEFs did not express keratin or 4F1 (data not shown). The presence of $4F1^+$ and $MTS10^+$ cells within the reaggregates indicated that some $MTS20/24^+$ epithelial cells had started to express markers of differentiated epithelial cells by 48 hours in reaggregate culture in the absence of T-cells.

To investigate the potential of $MTS20/24^+$ cells to differentiate into populations of mature thymic epithelium and form a thymus, short-term grafts were established with between 12,500 and 80,000 freshly purified $MTS20/24^+$ or $MTS20/24^-$ E12.5 cells and 100,000 MEFs (Table 6.1.). Dissociated E12.5 thymus cells were stained with both MTS20 and MTS24 and purified by FACS as described in Section 5.2. The purity of the sorted cells used in these experiments was consistently greater than 95%. Cells were reaggregated using the RTOC method and grafted under the kidney capsule of *nude* mice. After 3-4 weeks the mice were sacrificed and the kidney removed. The kidneys were examined macroscopically and photographed before embedding for frozen sectioning and analysis by immunohistochemistry.

In mice grafted with $MTS20/24^+$ cells (n=3, A, B, C), robust grafts were observed in all cases. Macroscopically the grafts consisted of a rounded clump of whitish coloured cells located near or on the nitrocellulose filter and measuring approximately 2-3mm in length (Figure 6.3). This was estimated to be at least five times the size of the cell reaggregate initially grafted. The presence of numerous blood vessels surrounding the graft indicated that the graft had become vascularised.

Hematoxylin and eosin stained sections of these grafts revealed a cellular morphology similar to that of a normal neonatal thymus with areas of densely stained cells surrounding patches of lighter staining cells, reminiscent of normal cortical and

Table 6.1. Numbers of cells in short-term grafts for lineage analysis

Mouse	No. of thymus cells	No. of MEFs
A	8 x10^4 MTS20/24$^+$ cells	1 x10^5
B	1.25 x10^4 MTS20/24$^+$ cells	1 x10^5
C	1.25 x10^4 MTS20/24$^+$ cells	1 x10^5
D	2.5 x10^4 MTS20/24$^-$ cells	1 x10^5
E	1.25 x10^4 MTS20/24$^-$ cells	1 x10^5
F	1.25 x10^4 MTS20/24$^-$ cells	1 x10^5
G, H, I	E12.5 whole thymus lobe (~5x10^3 cells)	0
J, K, L	0	1 x10^5

Mice B,C,E and F were grafted on the same day with cells from the same FACS sort. Mouse A and mouse D and groups G,H,I and J,K,L were all grafted on different days with cells from different experiments. Cells were mixed together in the numbers indicated and reaggregated *in vitro* for 24-36 hours using the RTOC method, before grafting under the kidney capsule of *nude* mice. Recipient mice were sacrificed after 3-4 weeks and the grafts analysed.

Figure 6.3. E12.5 MTS20/24$^+$ cell grafts under the kidney capsule

Purified MTS20/24$^+$ cells from E12.5 thymi were mixed with MEFs, reaggregated in culture for 48 hours and grafted under the kidney capsule of *nude* mice. In all expeiments a small piece of nitrocellulose filter was inserted along with the graft to mark the graft site. After 4 weeks, the kidneys were removed and photographed.

Arrows indicate grafted cells. In kidneys from Mouse B and Mouse C, the small piece of filter used to mark the site of the graft is visible.

Scale bars: all 1mm.

Figure 6.3.

Mouse A

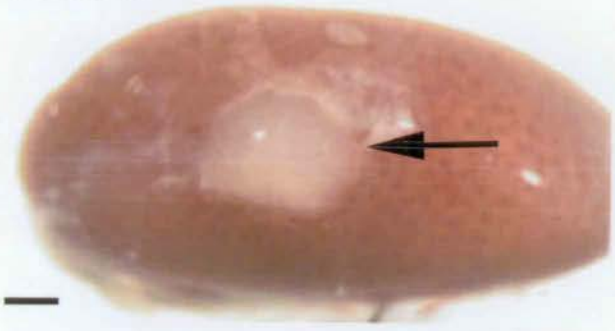

Mouse B

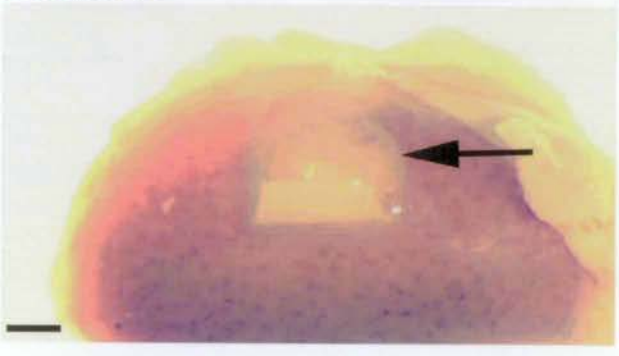

Mouse C

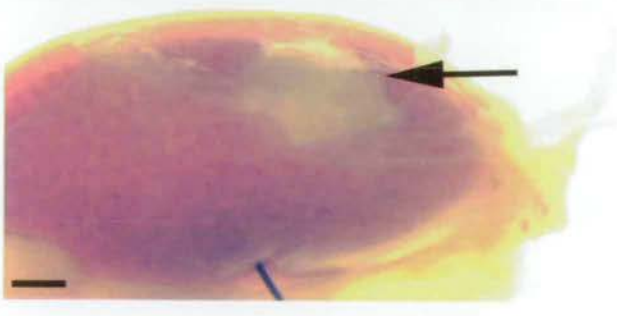

Figure 6.4. Histology of E12.5 MTS20/24^{+} cells grafted under the kidney capsule of *nude* mice

A: Section through graft from Mouse B (Figure 6.3.)

B: Section through graft from Mouse C (Figure 6.3.)

Grafts and kidneys were snap frozen and sections were cut through the grafts. The sections were stained with hematoxylin and eosin to show the histology of the cells within the grafts.

k, kidney; g, graft; arrow indicates filter used to mark site of graft, arrowhead in A indicates a blood vessel penetrating the graft.

Scale bars: all 200μm

Figure 6.4.

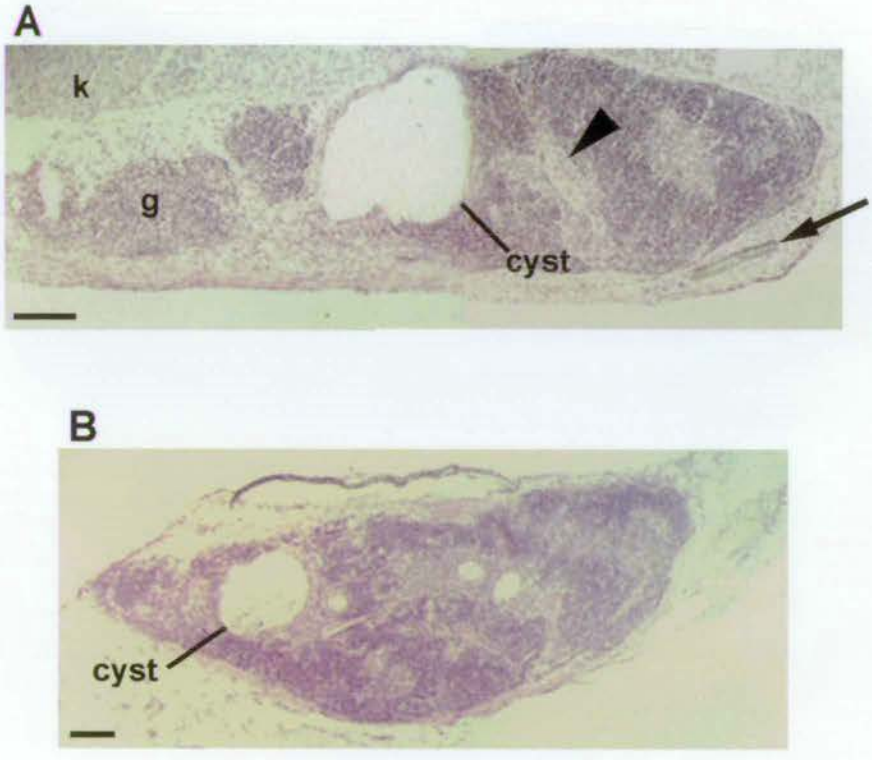

medullary epithelial architecture (Figure 6.4). The darkly staining cells within the grafts were of lymphoid appearance. Blood vessels were observed penetrating the grafts, confirming that vascularisation had commenced, and all grafts contained a central cyst-like structure which rarely contained cells (Figure 6.4).

Immunohistochemical analysis on serial sections of the MTS20/24$^+$ cell grafts showed extensive networks of cytokeratin-positive epithelium throughout each graft (Figure 6.5.B). The majority of this epithelium weakly expressed MHC Class II and stronger expression of MHC Class II was observed in some patches of epithelium (Figure 6.5.C). The majority of the epithelium was positive for 4F1, marking cortical epithelium, and small central patches of epithelium were positive for MTS10, marking medullary epithelium (Figure 6.5.D, E). Comparison of figures 6.5.D and E reveals that the area of MTS10$^+$ medullary epithelium corresponds to a 4F1$^-$ area. Furthermore, the area of strongest MHC Class II expression corresponds to the area of MTS10 expression (Figure 6.5.C,E.), indicating that MHC Class II is most strongly expressed in medullary epithelium in keeping with the reports of others (Rouse *et al.*, 1979; van Ewijk *et al.*, 1980).

The staining patterns of 4F1 and MTS10 also correspond to the darker and lighter stained patches of cells in the hematoxylin and eosin stained section (Figure 6.5.A), consistent with the cortical epithelium being densely packed with thymocytes and the medullary epithelium containing fewer thymocytes. The lymphoid cells within the grafts were positive for Thy-1 (Figure 6.5.F) and negative for B220 (data not shown) indicating that they were T-lineage cells. Since no T-cell precursors were present in the grafts, this data indicates that the MTS20/24$^+$ cell graft can attract T-lineage cells.

Figure 6.5. Immunohistochemical staining of frozen sections of E12.5 MTS20/24$^+$ cell graft from Mouse B

A: Hematoxylin and eosin stained section

B: MTS20/24$^+$ cell graft stained for cytokeratin expression

C: MTS20/24$^+$ cell graft stained for MHC Class II expression

D: MTS20/24$^+$ cell graft stained for expression of 4F1, a marker of cortical epithelium

E: MTS20/24$^+$ cell graft stained for expression of MTS10, a marker of medullary epithelium

F: MTS20/24$^+$ cell graft stained for Thy-1 expression

G: MTS20/24$^+$ cell graft stained with an isotype-control antibody

E12.5 MTS20/24$^+$ cell grafts and kidneys were removed from the host nude mice after four weeks and the grafts were snap frozen. Sections were stained with the appropriate antibody followed by an FITC-conjugated secondary antibody.

m, medulla; c, cortex; box in A is area shown in B-G, serial sections.

Scale bars: All 100μm

Figure 6.5.

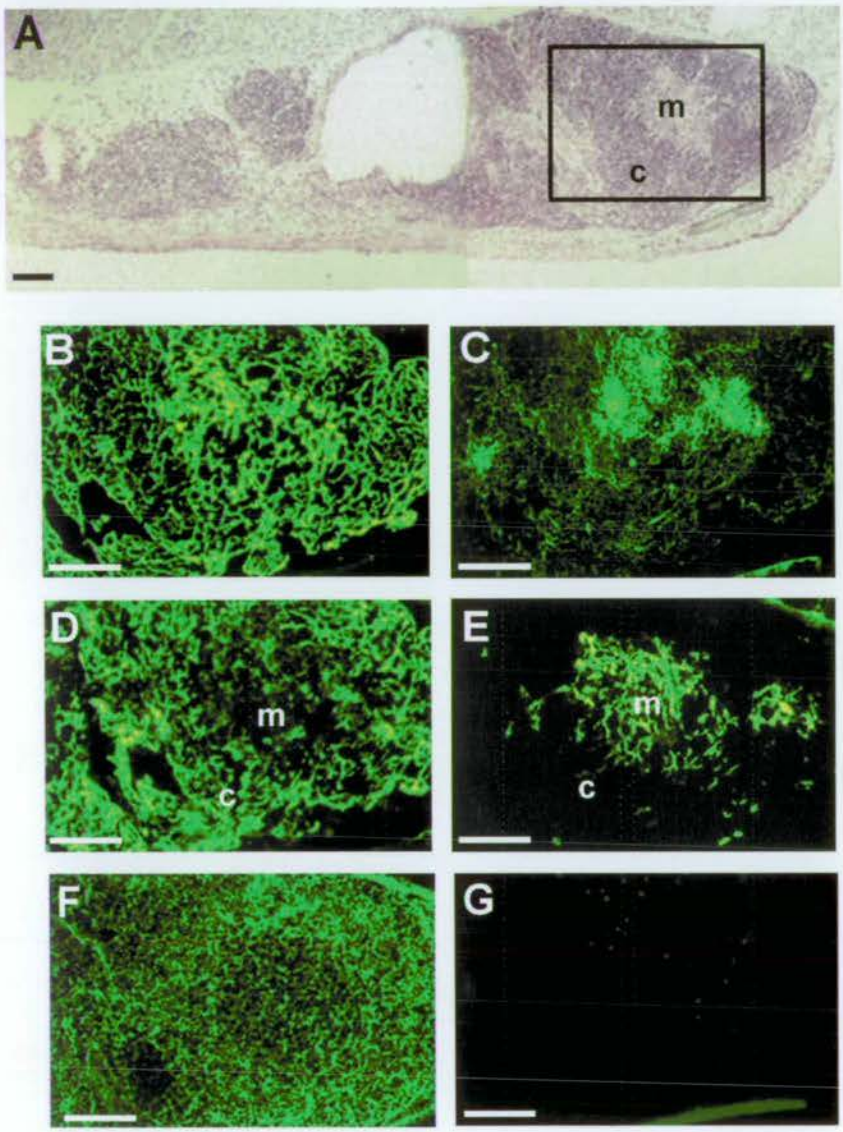

In mice grafted with MTS20/24$^-$ cells and MEFs (n=3,D,E,F), no evidence of any grafted cells was observed under the kidney capsule after four weeks, although the site of the graft was clearly marked by a piece of filter in all cases (Figure 6.6). In control experiments, mice grafted with whole E12.5 thymus lobes (n=3,G,H,I) contained robust grafts in all cases. Sectioning and immunohistochemical analysis of these grafts revealed normal thymus histology with cytokeratin positive epithelium encompassing MTS10$^+$ areas of medullary epithelium and 4F1$^+$ areas of cortical epithelium (Figure 6.7.C,E,F). These grafts also contained MHC Class II$^+$ epithelium (Figure 6.7.D) and Thy-1$^+$ T-lineage cells (Figure 6.7.G). In mice grafted with fibroblasts only, 1 out of 3 mice (J) contained a graft at the site of the filter. Sectioning of this graft revealed cells with an adipocytic morphology (Figure 6.7.I,J), and no evidence of epithelial cells. The remaining 2 mice (K, L) showed no evidence of grafted cells under the kidney capsule.

As thymocytes are required for TE development, the inability of MTS20/24$^-$ cells to survive when grafted under the kidney capsule may have been because MTS20/24$^-$ cells were unable to attract T-cell progenitors to the graft. Although the MTS20/24$^-$ cell population contained some lymphoid progenitor cells (approximately 6% of total E12.5 thymus cells (section 4.3)), it is possible that this small population could not maintain survival of the epithelial cells. To test this, a further six short-term grafts were established with MTS20/24$^+$ or MTS20/24$^-$ cells mixed with MEFs and with the addition of immature CD4$^-$CD8$^-$ thymocytes purified from adult thymocyte preparations (Table 6.2.).

Figure 6.6. E12.5 MTS20/24$^-$ cell grafts after 4 weeks under the kidney capsule of *nude* mice

Purified MTS20/24$^-$ cells from E12.5 thymi were mixed with MEFs, reaggregated in culture for 48 hours and grafted under the kidney capsule of *nude* mice. After 4 weeks, the kidneys were removed and photographed.

No cells could be seen at the site of the graft after 4 weeks.

Arrows indicate filter under kidney capsule which marks the site of the graft

Scale bars: All 1mm.

Figure 6.6.

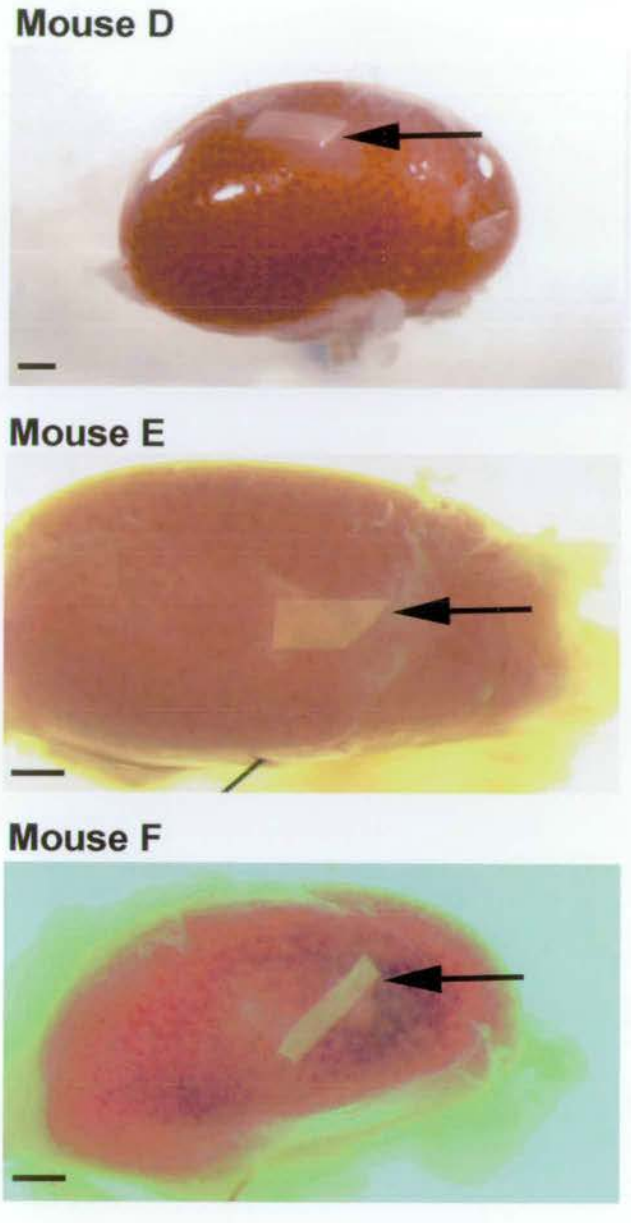

Figure 6.7. Histology of whole E12.5 thymus lobes and murine embryonic fibroblasts alone grafted under the kidney capsule of *nude* mice for 4 weeks

A: Hematoxylin and eosin stained section of whole thymus lobe grafted under the kidney capsule

B: Higher magnification of thymus graft

C: Whole lobe graft stained for cytokeratin expression

D: Whole lobe graft stained for MHC Class II expression

E: Whole lobe graft stained with 4F1 marking cortical epithelium

F: Whole lobe graft stained with MTS10 marking medullary epithelium

G: Whole lobe graft stained for Thy-1 expression

H: Whole lobe graft stained with isotype-control antibody

I: Hematoxylin and eosin stained section of MEF only graft under the kidney capsule

J: Higher magnification of MEF only graft

Whole E12.5 thymi or reaggregated MEFs were grafted under the kidney capusle of nude mice. After 4 weeks the kidneys were removed and snap frozen. Sections were stained with hematoxylina nd eosin or the appropriate antibodies. k, kidney; g, graft.

Scale bars: 6.7.A,I, 200μm; 6.7.B-H,J, 100μm

Figure 6.7.

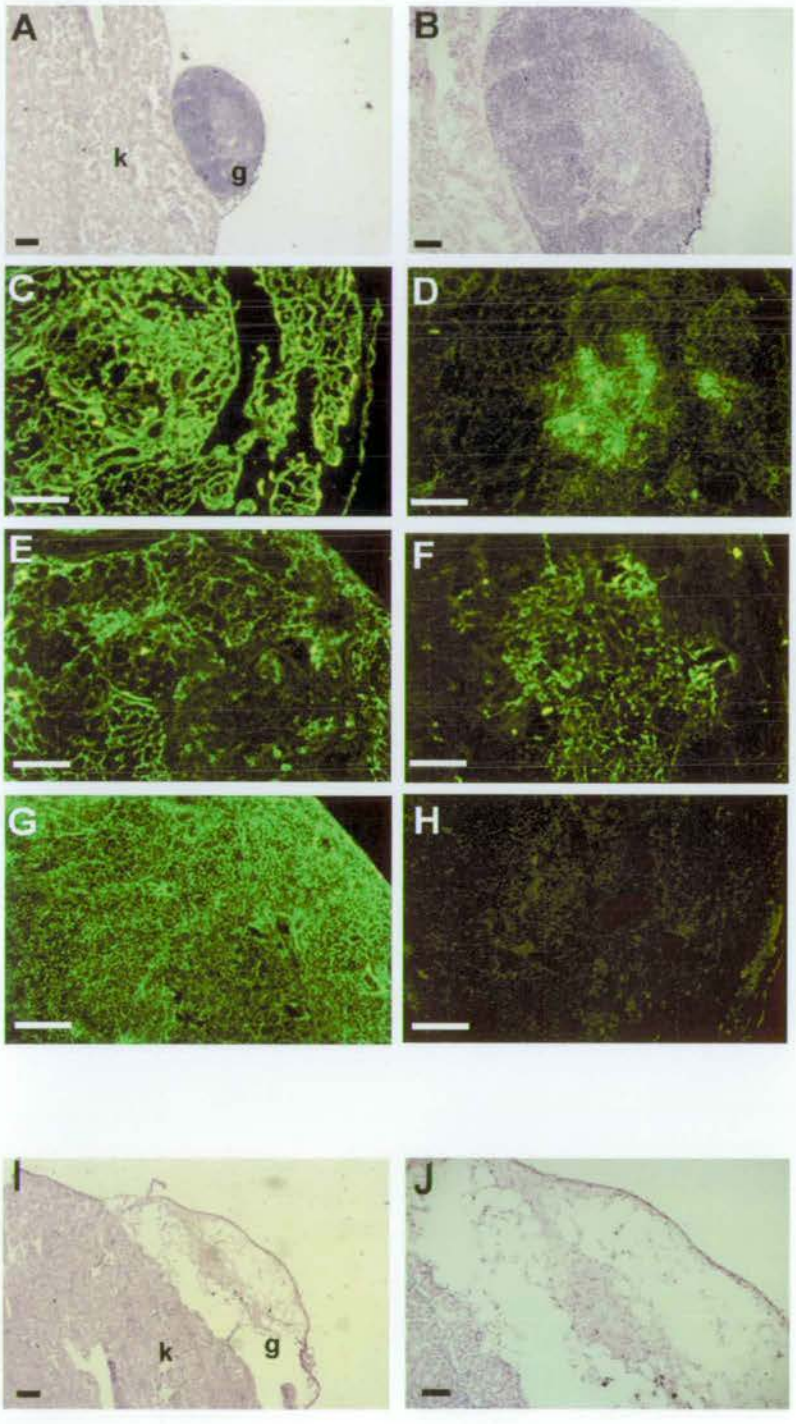

Table 6.2 Numbers of cells in short-term grafts including immature $CD4^-CD8^-$ thymocytes.

Mouse	No. of thymus cells	No. of MEFs	No. of $CD4^-CD8^-$ thymocytes
A	8×10^4 $MTS20/24^+$ cells	1×10^5	1×10^5
B	1.25×10^4 $MTS20/24^+$ cells	1×10^5	1×10^5
C	1.25×10^4 $MTS20/24^+$ cells	1×10^5	1×10^5
D	2.5×10^4 $MTS20/24^-$ cells	1×10^5	1×10^5
E	1.25×10^4 $MTS20/24^-$ cells	1×10^5	1×10^5
F	1.25×10^4 $MTS20/24^-$ cells	1×10^5	1×10^5

Mice B,C,E and F were grafted on the same day with cells from the same FACS sort. Mouse A and mouse D were grafted on different days with cells from different experiments. Cells were mixed together in the numbers indicated and reaggregated *in vitro* for 24-36 hours using the RTOC method, before grafting under the kidney capsule of *nude* mice. Recipient mice were sacrificed after 3-4 weeks and the grafts analysed.

Three weeks after grafting, the kidneys were analysed for the presence of the grafts. Robust grafts were recovered from all mice grafted with MTS20/24$^+$ cells (n=3) (Figure 6.8.A). One graft was analysed histologically: immunostaining revealed the presence of cortical and medullary epithelium (Figure 6.8.C-G), similar to that in MTS20/24$^+$ cell grafts without thymocytes. However, no grafts were observed in the MTS20/24$^-$ cell recipient mice (Figure 6.8. B). These data suggest that MTS20/24$^-$ cells could not survive when grafted under the kidney capsule of *nude* mice, even when supplied with immature thymocytes.

In summary, these data show that cells within the purified MTS20/24$^+$ population from E12.5 thymi can differentiate into cells expressing markers associated with mature cortical (4F1$^+$) thymic epithelium and mature medullary (MTS10$^+$) thymic epithelium. MTS20/24$^+$ cells or their progeny can also attract T-lineage cells and can initiate vascularisation of the grafts. Purified MTS20/24$^-$ cells could not fulfil these functions. Therefore, the MTS20/24$^+$ population contains progenitor cells which can differentiate into the major subpopulations of thymic epithelium.

Figure 6.8. Grafts of MTS20/24$^+$ and MTS20/24$^-$ cells with CD4$^-$CD8$^-$ thymocytes

A: MTS20/24$^+$ cell graft supplied with CD4$^-$CD8$^-$ thymocytes under the kidney capsule

B: Kidney from *nude* mouse grafted with MTS20/24$^-$ cells and CD4$^-$CD8$^-$ thymocytes

C: Hematoxylin and eosin stained section of MTS20/24$^+$ cell graft

D: MTS20/24$^+$ cell graft stained for cytokeratin

E: MTS20/24$^+$ cell graft stained with 4F1

F: MTS20/24$^+$ cell graft stained with MTS10

G: MTS20/24$^+$ cell graft stained with an isotype-control antibody

Purified E12.5 thymus cells were mixed with MEFs and thymocytes, reaggregated and grafted under the kidney capsule of *nude* mice. After 4 weeks the kidneys were removed and photographed (A and B). Frozen sections through the grafts were taken and stained with hematoxylin and eosin or the appropriate antibodies (C-G). Arrow in A indicates graft, arrow in B indicates filter used to mark site of the graft. C-G are serial sections. Scale bars: A,B, 1mm; C-G, 100μm.

Figure 6.8.

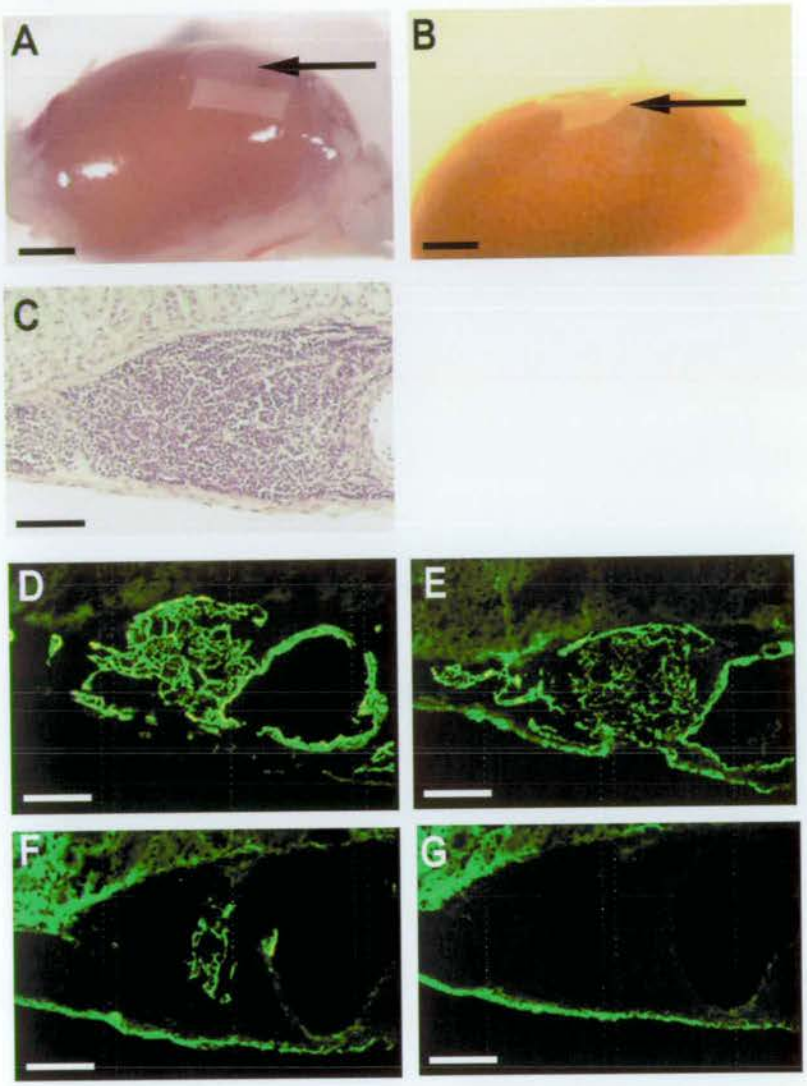

6.4. Functional potential of MTS20/24$^+$ cells

6.4.1. Ability to support thymocyte development

To test the functional potential of the MTS20/24$^+$ cell population, two experimental series were set up. Firstly, the development of thymocytes was analysed in two of the grafts from the previous experiment, in which purified MTS20/24$^+$ cells were mixed with MEFs and CD4$^-$CD8$^-$ thymocytes (Table 6.2) and grafted under the kidney capsule of *nude* mice. After 3 weeks, the grafts were removed and the thymocytes released from the grafts. The thymocytes were stained for flow cytometry with antibodies against CD3, CD4 and CD8. The data was analysed after gating on the lymphocyte population in the FSC-SSC profile (Figure 6.9.A). The results showed that CD4$^+$ and CD8$^+$ single-positive T-cells and CD4$^+$CD8$^+$ double-positive T-cells were present in the grafts and that the distribution of the CD4$^+$, CD8$^+$ and CD4$^+$CD8$^+$ subsets was identical to that of a normal adult thymus (Figure 6.9.B,C). These data show that the MTS20/24$^+$ cell grafts could provide a thymic microenvironment sufficient to support the differentiation of immature CD4$^-$CD8$^-$ thymocytes into single-positive T-cells.

6.4.2. Ability to support peripheral T-cell development

Secondly, the presence of peripheral T-cells was analysed in long-term grafted recipient mice. Grafts were established containing between 500-5000 MTS20/24$^+$ cells or 500-160,000 MTS20/24$^-$ cells either with or without fibroblasts (Table 6.3.). After 12-16 weeks, the recipient *nude* mice were sacrificed and the axillary, inguinal and popliteal lymph nodes were removed. $1x10^6$ cells recovered from these lymph nodes were analysed by flow cytometry with antibodies against CD3, CD4 and CD8. Data from $1x10^4$ cells were collected and gated for the

Figure 6.9. Phenotypic analysis of thymocyte development within MTS20/24$^+$ cell grafts supplied with CD4$^-$CD8$^-$ thymocytes.

A: Light scatter profile of cells obtained from MTS20/24$^+$ cells graft supplied with CD4$^-$CD8$^-$ thymocytes. R1 is the gate applied for the lymphocyte population.

B: Flow cytometric analysis of lymphocytes from MTS20/24$^+$ cell grafts showing development of CD4$^+$ cells, CD8$^+$ cells and CD4$^+$ CD8$^+$ cells.

C: Flow cytometric analysis of thymocytes from normal adult thymus (Taken from Abbas 1997).

Purified E12.5 MTS20/24$^+$ cells were mixed with MEFs and CD4$^-$CD8$^-$ thymocytes, reaggregated and grafted under the kidney capsule of *nude* mice. After 4 weeks the kidneys were removed and the cells were released from the grafts. These cells were stained with CD4 and CD8 and analysed by flow cytometry.

Figures refer to percentage of cells in each quadrant.

Figure 6.9.A

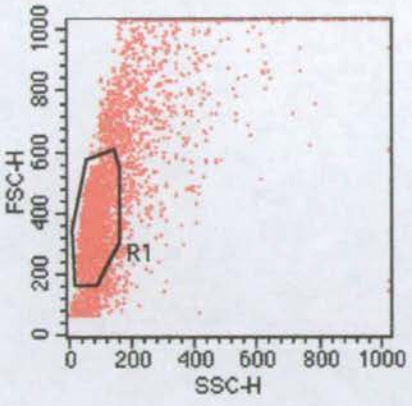

Figure 6.9.B

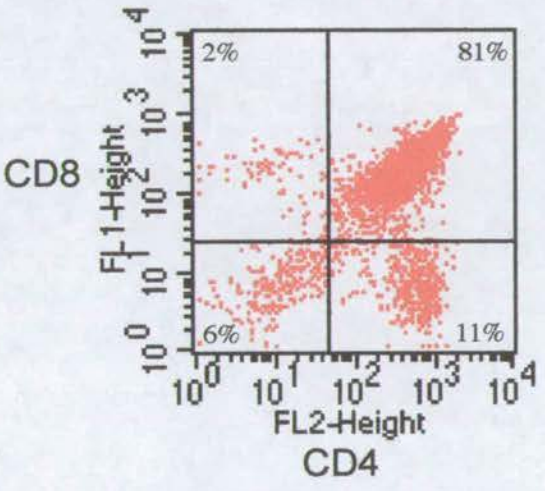

Figure 6.9.C. (Taken from Abbas 1997)

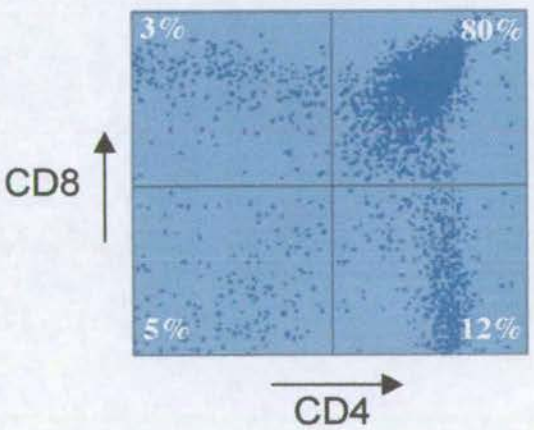

Table 6.3. Numbers of cells in long-term grafts for functional analysis

Cells were mixed together in the numbers indicated and reaggregated *in vitro* for 24-36 hours before grafting under the kidney capsule of *nude* mice. Recipient mice were sacrificed after 12-16 weeks and the lymph node cells analysed for the presence of T-cells. Scoring of successful reconstitution of thymus function was based on T-cell numbers in recipient mice exceeding two standard deviations from the mean of the ungrafted *nude* population.

Nude mice were obtained and grafted in two separate experiments (marked Exp.1 and Exp.2). Mice grafted on the same date were grafted with cells from the same FACS sort.

D & R, dissociated and reaggregated whole E12.5 thymus cells. *indicates grafts which were cultured overnight using the hanging drop method. ^indicates the use of NIH3T3 cells instead of MEFs. [a], at E12.5, two thymic lobes contain approximately 10,000 cells, thus 2,900 MTS20/24^{+} or 7,100 MTS20/24^{-} cells constitute one embryonic thymus-equivalent (embryo-equivalent).

Table 6.3. Numbers of cells in long-term grafts for functional analysis

Mouse, exp. date and no.	No. of thymus cells	[a]Embryo-equivalent	No. of fibroblasts	Exp. No.
A* (22/09/99-1)	5×10^2 MTS20/24$^+$ cells	0.17	0	1
B* (22/09/99-1)	5×10^2 MTS20/24$^+$ cells	0.17	1×10^3	1
C (24/03/00-2)	5×10^2 MTS20/24$^+$ cells	0.17	2×10^5	2
D (24/03/00-2)	5×10^2 MTS20/24$^+$ cells	0.17	2×10^5	2
E* (23/03/99-1)	1×10^3 MTS20/24$^+$ cells	0.34	^1×10^3	1
F (12/05/00-2)	1×10^3 MTS20/24$^+$ cells	0.34	2×10^5	2
G* (28/10/99-1)	5×10^3 MTS20/24$^+$ cells	1.72	0	1
H (24/03/00-2)	5×10^2 MTS20/24$^-$ cells	0.07	2×10^5	2
I (11/05/00-2)	5×10^2 MTS20/24$^-$ cells	0.07	2×10^5	2
J (24/03/00-2)	1×10^3 MTS20/24$^-$ cells	0.14	2×10^5	2
K* (28/10/99-1)	1×10^4 MTS20/24$^-$ cells	1.41	0	1
L* (26/03/99-1)	1×10^4 MTS20/24$^-$ cells	1.41	^4×10^3	1
M (05/07/00-2)	1.6×10^5MTS20/24$^-$ cells	22.5	1×10^5	2
N* (22/09/99-1)	1×10^4 d & r	1	1×10^3	1
O* (22/09/99-1)	1×10^4 d & r	1	1×10^3	1
P* (28/10/99-1)	1×10^4 d & r	1	0	1
Q* (29/09/99-1)	1×10^4 d & r	1	0	1
R* (29/09/99-1)	1×10^4 d & r	1	0	1
S* (29/09/99-1)	1×10^4 d & r	1	0	1
T* (26/03/99-1)	1×10^4 d & r	1	0	1
U* (26/03/99-1)	1×10^4 d & r	1	0	1
V (03/03/00-2)	1×10^5 d & r	10	0	2

lymphocyte population for subsequent analysis (See Figure 6.9.A). Mice in which T-cell numbers exceeded two standard deviations from the mean of the ungrafted *nude* population were taken as having successful grafts. This scoring criterion was directly reflected by the presence of $CD4^+$ and $CD8^+$ T-cell populations in contour plots set at 60% probability and 5% threshold. Controls were provided by ungrafted wild-type mice, ungrafted *nude* mice, *nude* mice grafted with two whole E12.5 thymus lobes, *nude* mice grafted with dissociated and reaggregated whole E12.5 thymus cells (see Table 6.3) and *nude* mice grafted with 2 $x10^5$ MEFs only.

6.4.2.1. Analysis of control mice

The lymph nodes of ungrafted wild-type mice contained $CD4^+$ and $CD8^+$ T-cell populations (n=12) whereas ungrafted *nude* mice had no distinct T-cell populations in their lymph nodes (n=15) (Figure 6.10). In ungrafted wild-type mice, the $CD3^+CD4^+$ T-cell population varied between 17-43% of the total lymphocyte population (mean=33%) and the $CD3^+CD8^+$ T-cell population varied between 15-29% of the total lymphocyte population (mean=21%). In ungrafted *nude* mice, few lymph node cells were positive for these markers: the $CD3^+CD4^+$ cell population varied between 0.1-4.9% of the total lymphocyte population (mean=2.0%) and the $CD3^+CD8^+$ cell population varied between 0-5% of the total lymphocyte population (mean=1.4%).

In mice grafted with two whole E12.5 thymus lobes (one embryonic thymus equivalent, see Table 6.3.), all recipients had $CD4^+$ T-cell populations and 6 out of 7 had $CD8^+$ T-cell populations in their lymph nodes (n=7) (Figure 6.11.A). The $CD4^+$ T-cells recovered from these mice varied between 22-61% of total lymphocytes (mean=37%), similar to the proportion found in the lymph nodes of wild-type mice. The $CD8^+$ T-cells recovered from these mice varied between 3-14% of total

Figure 6.10. Analysis of T-cell populations in lymph nodes of wild-type and ungrafted *nude* mice

A: $CD4^+$ and $CD8^+$ profiles in 3 representative wild-type mice. $CD4^+$ T-cells comprised approximately 33% and $CD8^+$ T-cells comprised approximately 21% of total lymphocytes.

B: $CD4^+$ and $CD8^+$ profiles in 3 representative *nude* mice. $CD4^+$ T-cells comprised approximately 2% and $CD8^+$ T-cells comprised approximately 1.4% of total lymphocytes.

The axillary, inguinal and popliteal lymph nodes were removed from wild-type and *nude* mice, cells were released and stained with CD3, CD4 and CD8 antibodies. Presence of $CD4^+$ and $CD8^+$ T-cell populations was analysed by flow cytometry.

Plots on the left-hand side show CD3 on the x-axis and CD4 on the y-axis. Plots on the right-hand side show CD3 on the x-axis and CD8 on the y-axis. $CD4^+$ and $CD8^+$ T-cell populations are in the top-right quadrant of plots and the figures refer to the percentage of $CD3^+CD4^+$ or $CD3^+CD8^+$ cells out of total gated lymphocytes.

Figure 6.10.A

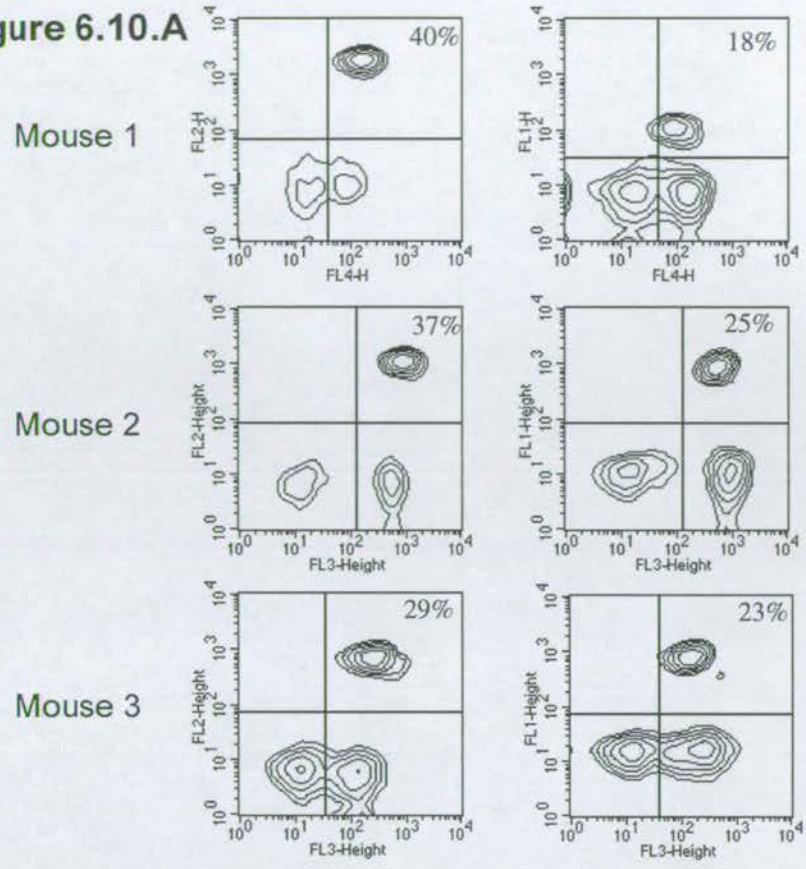

Figure 6.10.B

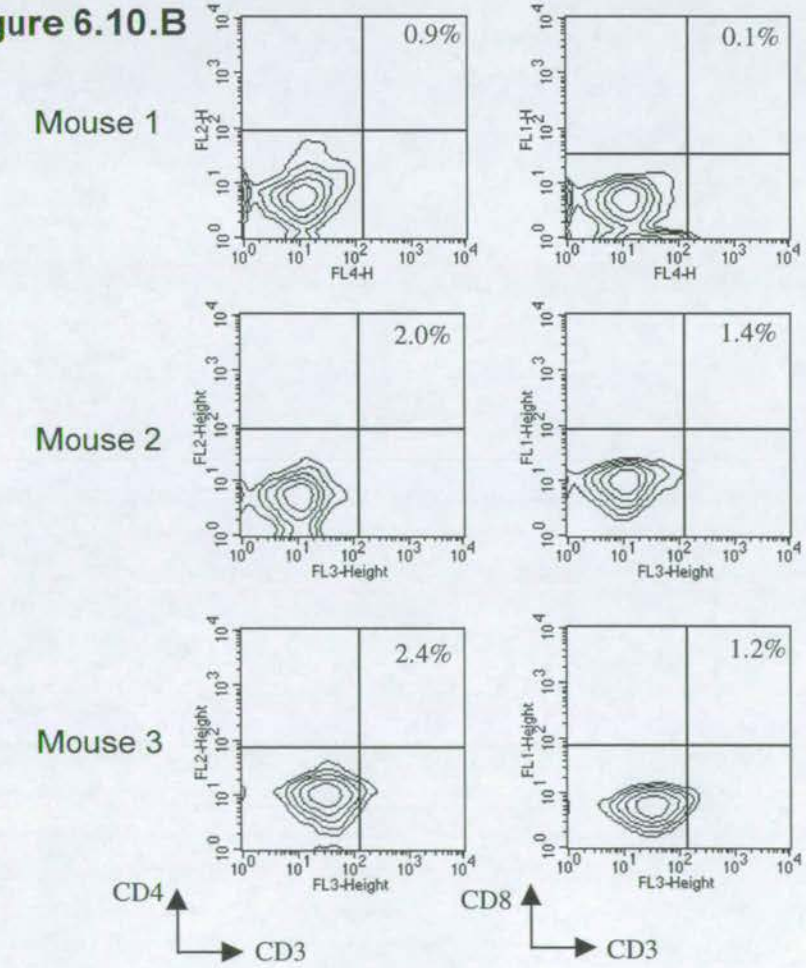

Figure 6.11. Analysis of T-cell populations in lymph nodes of *nude* mice grafted with two whole E12.5 thymus lobes or dissociated and reaggregated whole E12.5 thymus cells.

A: $CD4^+$ and $CD8^+$ profiles in 3 representative *nude* mice grafted with two whole E12.5 thymus lobes. $CD4^+$ T-cells comprised approximately 37% and $CD8^+$ T-cells comprised approximately 10% of total lymphocytes.

B: $CD4^+$ and $CD8^+$ profiles in 3 representative *nude* mice grafted with dissociated and reaggregated whole E12.5 thymus cells. 5/9 recipients contained $CD4^+$ T-cells whereas none of the recipient mice contained $CD8^+$ T-cells. In the five mice which contained $CD4^+$ T-cell populations, these cells comprised approximately 13% of total lymphocytes.

The axillary, inguinal and popliteal lymph nodes were removed from *nude* mice 12-16 weeks after grafting with whole E12.5 thymi or dissociated and reaggregated whole E12.5 thymus cells. Lymph node cells were released and stained with CD3, CD4 and CD8 antibodies. Presence of $CD4^+$ and $CD8^+$ T-cell populations was analysed by flow cytometry.

Plots on the left-hand side show CD3 on the x-axis and CD4 on the y-axis. Plots on the right-hand side show CD3 on the x-axis and CD8 on the y-axis. $CD4^+$ and $CD8^+$ T-cell populations are in the top-right quadrant of plots and the figures refer to the percentage of $CD3^+CD4^+$ or $CD3^+CD8^+$ cells out of total gated lymphocytes.

Figure 6.11.A

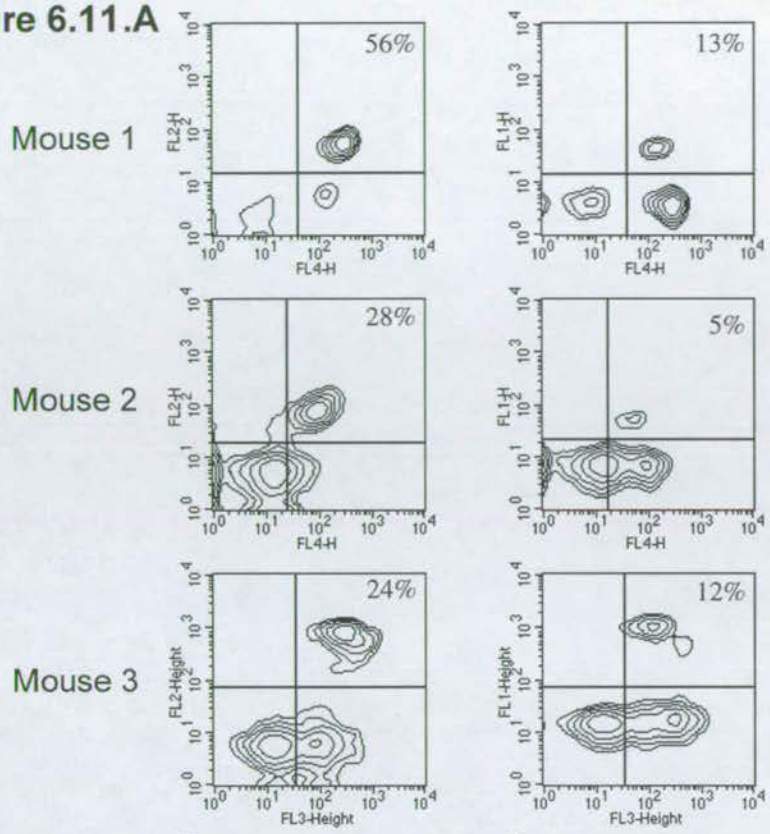

Figure 6.11.B

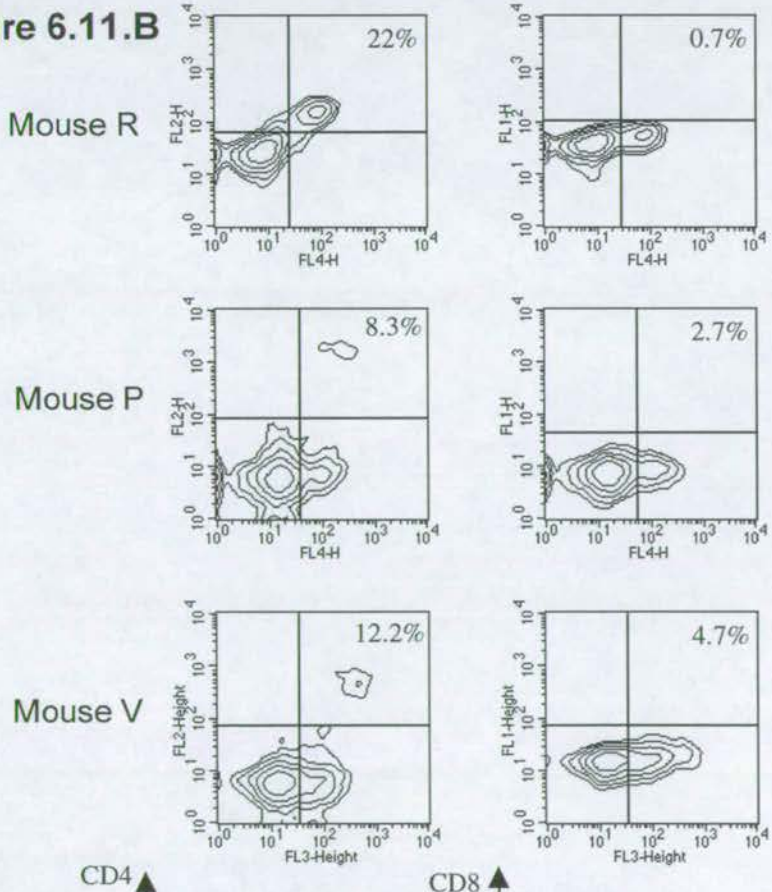

lymphocytes (mean=9.7%), less than the proportion found in wild-type mice but substantially greater populations than those in ungrafted *nude* mice.

In mice grafted with 10,000 (1 embryo-equivalent) (n=8) or 100,000 (10 embryo-equivalents) (n=1) dissociated and reaggregated whole E12.5 thymus cells, $CD4^+$ T-cell populations were found in the lymph nodes of 5 out of 9 recipient mice (Figure 6.11.B). $CD8^+$ T-cell populations were not found in any recipients. The $CD4^+$ T-cells found in the five successful grafted mice comprised 7-22% of total lymphocytes (mean=13%). The four mice in which $CD4^+$ T-cell populations could not be found were mice N, Q, S and T (See table 6.3).

Recipient mice grafted with 2×10^5 MEF cells alone did not contain distinct T-cell populations in their lymph nodes (n=3) (Figure 6.12). The mean $CD4^+$ T-cell population in these mice was 1.7% of total lymphocytes and the mean $CD8^+$ T-cell population was 1.1% of total lymphocytes.

6.4.2.2. Analysis of experimental mice

In mice grafted with 500-5,000 MTS20/24$^+$ cells (0.2-1.7 embryo-equivalents), distinct $CD4^+$ T-cell populations were present in the lymph nodes of 6 out of 7 recipients, and $CD8^+$ T-cells populations were present in the lymph nodes of 5 out of 7 recipients (Figure 6.13.). The $CD4^+$ T-cells populations recovered from these mice varied between 8-17% of total lymphocytes (mean=11%), and the $CD8^+$ T-cell populations varied between 4-14% (mean=9.4%). The one recipient mouse in which no T-cells were found was grafted with 1×10^3 MTS20/24$^+$ cells + 2×10^5 MEFs (Mouse F).

In recipient mice grafted with 500-160,000 MTS20/24$^-$ cells (0.1-22.5 embryo-equivalents), only one of six recipient mice contained distinct T-cell populations in its lymph nodes (Mouse K) (Figure 6.14). However, the T-cell

Figure 6.12. Analysis of T-cell populations in lymph nodes of *nude* mice grafted with MEFs only

No distinct T-cell populations were observed in nude mice grafted with MEFs only (n=3). $CD4^+$ T-cells comprised 1.7% of total lymphocytes and $CD8^+$ T-cells comprised 1.1% of total lymphocytes.

The axillary, inguinal and popliteal lymph nodes were removed from *nude* mice 12-16 weeks after grafting with MEFs only. Lymph node cells were released and stained with CD3, CD4 and CD8 antibodies. Presence of $CD4^+$ and $CD8^+$ T-cell populations was analysed by flow cytometry.

Plots on the left-hand side show CD3 on the x-axis and CD4 on the y-axis. Plots on the right-hand side show CD3 on the x-axis and CD8 on the y-axis. $CD4^+$ and $CD8^+$ T-cell populations are in the top-right quadrant of plots and the figures refer to the percentage of $CD3^+CD4^+$ or $CD3^+CD8^+$ cells out of total gated lymphocytes.

Figure 6.12.

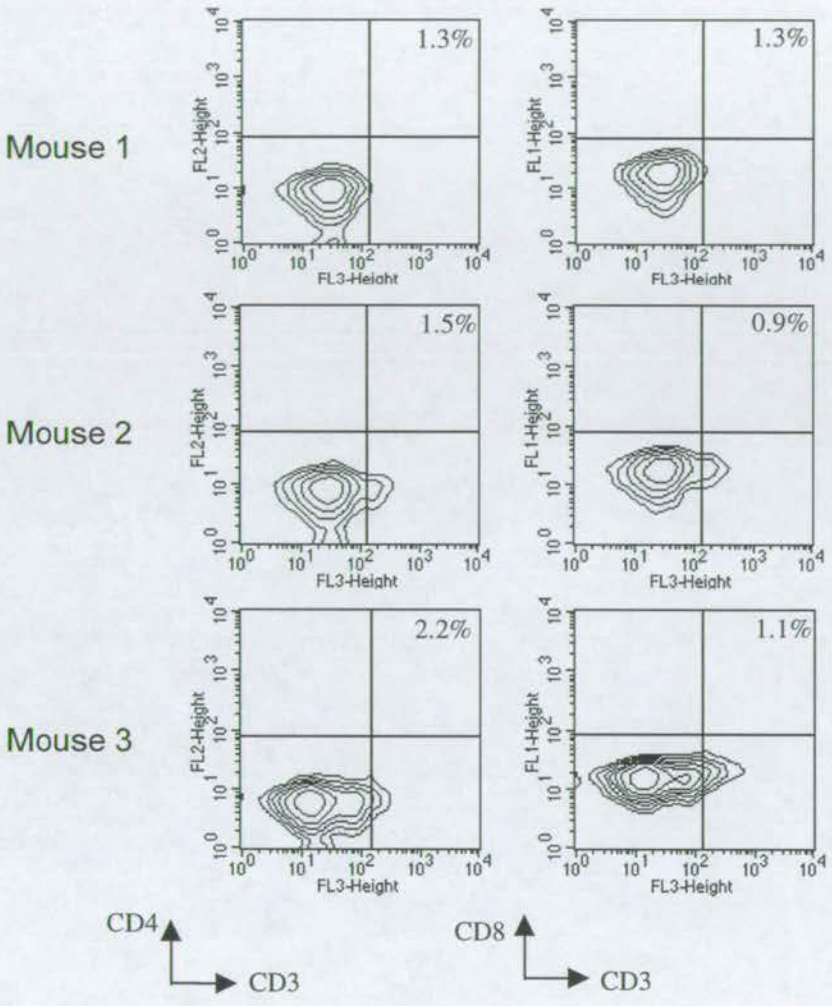
Mouse 1
Mouse 2
Mouse 3
1.3%
1.3%
1.5%
0.9%
2.2%
1.1%
FL2-Height
FL1-Height
FL3-Height
CD4
CD3
CD8
CD3

Figure 6.13. Analysis of T-cell populations in lymph nodes of *nude* mice grafted with MTS20/24$^+$ cells

6/7 recipient mice grafted with MTS20/24$^+$ cells contained CD4$^+$ T-cells and 5/7 contained CD8$^+$ T-cells. CD4$^+$ T-cells comprised approximately 11% of total lymphocytes and CD8$^+$ T-cells comprised approximately 9.4% of total lymphocytes.

The axillary, inguinal and popliteal lymph nodes were removed from *nude* mice 12-16 weeks after grafting with E12.5 MTS20/24$^+$ cells. Lymph node cells were released and stained with CD3, CD4 and CD8 antibodies. Presence of CD4$^+$ and CD8$^+$ T-cell populations was analysed by flow cytometry.

Plots on the left-hand side show CD3 on the x-axis and CD4 on the y-axis. Plots on the right-hand side show CD3 on the x-axis and CD8 on the y-axis. CD4$^+$ and CD8$^+$ T-cell populations are in the top-right quadrant of plots and the figures refer to the percentage of CD3$^+$CD4$^+$ or CD3$^+$CD8$^+$ cells out of total gated lymphocytes.

Figure 6.13.

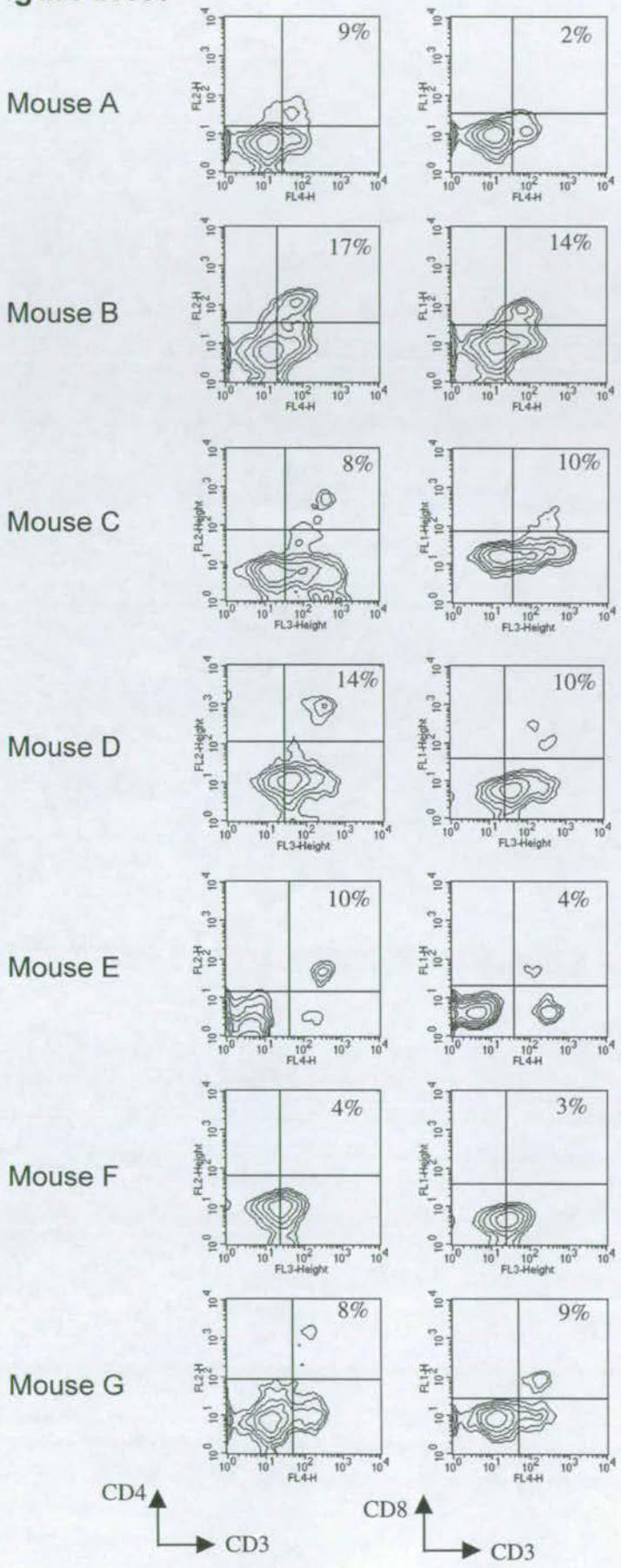
Mouse A
9%
2%
Mouse B
17%
14%
Mouse C
8%
10%
Mouse D
14%
10%
Mouse E
10%
4%
Mouse F
4%
3%
Mouse G
8%
9%
FL4-H
FL2-H
FL1-H
FL3-Height
FL2-Height
FL1-Height
CD4
CD3
CD8
CD3

Figure 6.14. Analysis of T-cell populations in lymph nodes of *nude* mice grafted with MTS20/24$^-$ cells

Only 1/6 recipient mice grafted with MTS20/24$^-$ cells contained distinct T-cells populations in its lymph nodes. CD4$^+$ T-cells comprised 4% of total lymphocytes and CD8$^+$ T-cells comprised 5% of total lymphocytes. The remaining five recipient mice had no distinct T-cell populations in their lymph nodes.

The axillary, inguinal and popliteal lymph nodes were removed from *nude* mice 12-16 weeks after grafting with E12.5 MTS20/24$^-$ cells. Lymph node cells were released and stained with CD3, CD4 and CD8 antibodies. Presence of CD4$^+$ and CD8$^+$ T-cell populations was analysed by flow cytometry.

Plots on the left-hand side show CD3 on the x-axis and CD4 on the y-axis. Plots on the right-hand side show CD3 on the x-axis and CD8 on the y-axis. CD4$^+$ and CD8$^+$ T-cell populations are in the top-right quadrant of plots and the figures refer to the percentage of CD3$^+$CD4$^+$ or CD3$^+$CD8$^+$ cells out of total gated lymphocytes.

Figure 6.14.

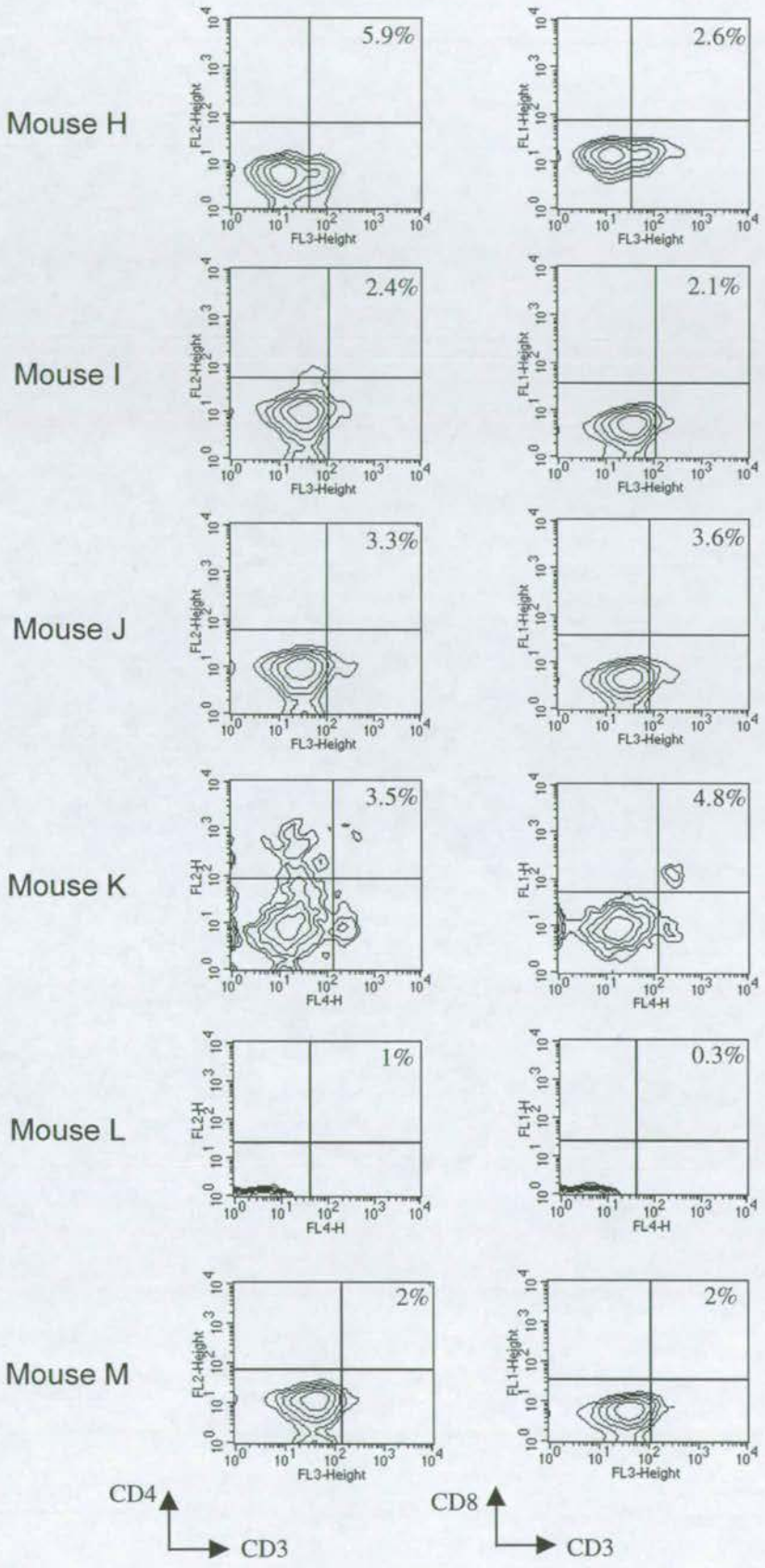
Mouse H
5.9%
2.6%
Mouse I
2.4%
2.1%
Mouse J
3.3%
3.6%
Mouse K
3.5%
4.8%
Mouse L
1%
0.3%
Mouse M
2%
2%
FL2-Height
FL1-Height
FL3-Height
FL4-H
CD4
CD3
CD8
CD3

populations comprised only 3% ($CD4^+$) and 5% ($CD8^+$) of total lymphocytes. The remaining five recipient mice had no distinct T-cell populations in their lymph nodes.

6.4.2.3. Statistical analysis of peripheral T-cell numbers

For statistical analysis of the differences in T-cell numbers between ungrafted *nude* mice and grafted recipients, the actual number of T-cells per 10^6 lymph node cells was used. Figure 6.15 shows the number of $CD4^+$ T-cells and $CD8^+$ T-cells per 10^6 lymph node cells in each experimental mouse of the two separate experiments. Table 6.4 shows the mean numbers of T-cells per 10^6 lymph node cells for each group of mice in total (Exp.1 and Exp.2). The Mann-Whitney U-test, for testing non-parametric independent samples (Dytham 1999), was used to analyse the statistical significance of differences between the mean T-cell populations. Statistical analysis was performed using the Prism statistics package. All mice in each group were included in the statistical analysis.

The mean number of T-cells in mice grafted with $MTS20/24^+$ cells was significantly greater than those in ungrafted *nude* mice ($p=0.0006$ for $CD4^+$, $p=0.011$ for $CD8^+$), whereas T-cell numbers in recipients grafted with $MTS20/24^-$ cells were not significantly different to ungrafted *nude* mice ($p>0.6$ for $CD4^+$, $p>0.2$ for $CD8^+$). Recipient mice which received grafts of two whole E12.5 thymus lobes had significantly greater T-cell populations than ungrafted *nude* mice ($p=0.0002$ for $CD4^+$, $p=0.01$ for $CD8^+$). Mean T-cell numbers in all recipients grafted with dissociated and reaggregated whole E12.5 thymus cells were significantly different to ungrafted *nude* mice for $CD4^+$ T-cells but not for $CD8^+$ T-cells ($p=0.02$ for $CD4^+$, $p>0.4$ for $CD8^+$). T-cell numbers in recipients grafted with MEFs alone were not significantly different to ungrafted *nude* mice ($p>0.5$ for $CD4^+$, $p>0.9$ for $CD8^+$).

Figure 6.15. Scatter graphs of T-cell numbers in each experimental mouse of two separate experiments.

A: Scatter graph of $CD4^+$ and $CD8^+$ T-cells in lymph nodes of wild-type, ungrafted *nude* and whole lobe grafted recipient mice.

B: Scatter graph of $CD4^+$ T-cells in lymph nodes of ungrafted *nude*, $MTS20/24^+$ cell grafted, $MTS20/24^-$ cell grafted, d & r grafted, and MEF only grafted recipient mice.

C: Scatter graph of $CD8^+$ T-cells in lymph nodes of ungrafted *nude*, $MTS20/24^+$ cell grafted, $MTS20/24^-$ cell grafted, d & r grafted, and MEF only grafted recipient mice.

Lymph nodes were removed from wild-type or *nude* mice grafted with cells as shown and the lymph node cells were stained with CD3, CD4 and CD8. Flow cytometry revealed the number of actual $CD4^+$ and $CD8^+$ T-cells in the lymph nodes of each mouse. Mice marked in red are from Experiment 1 and mice marked in yellow are from experiment 2. Figures on the y-axis are numbers of T-cell per 10^6 lymph node cells. LN, lymph nodes; d & r, dissociated and reaggregated whole E12.5 thymus cells.

Figure 6.15.

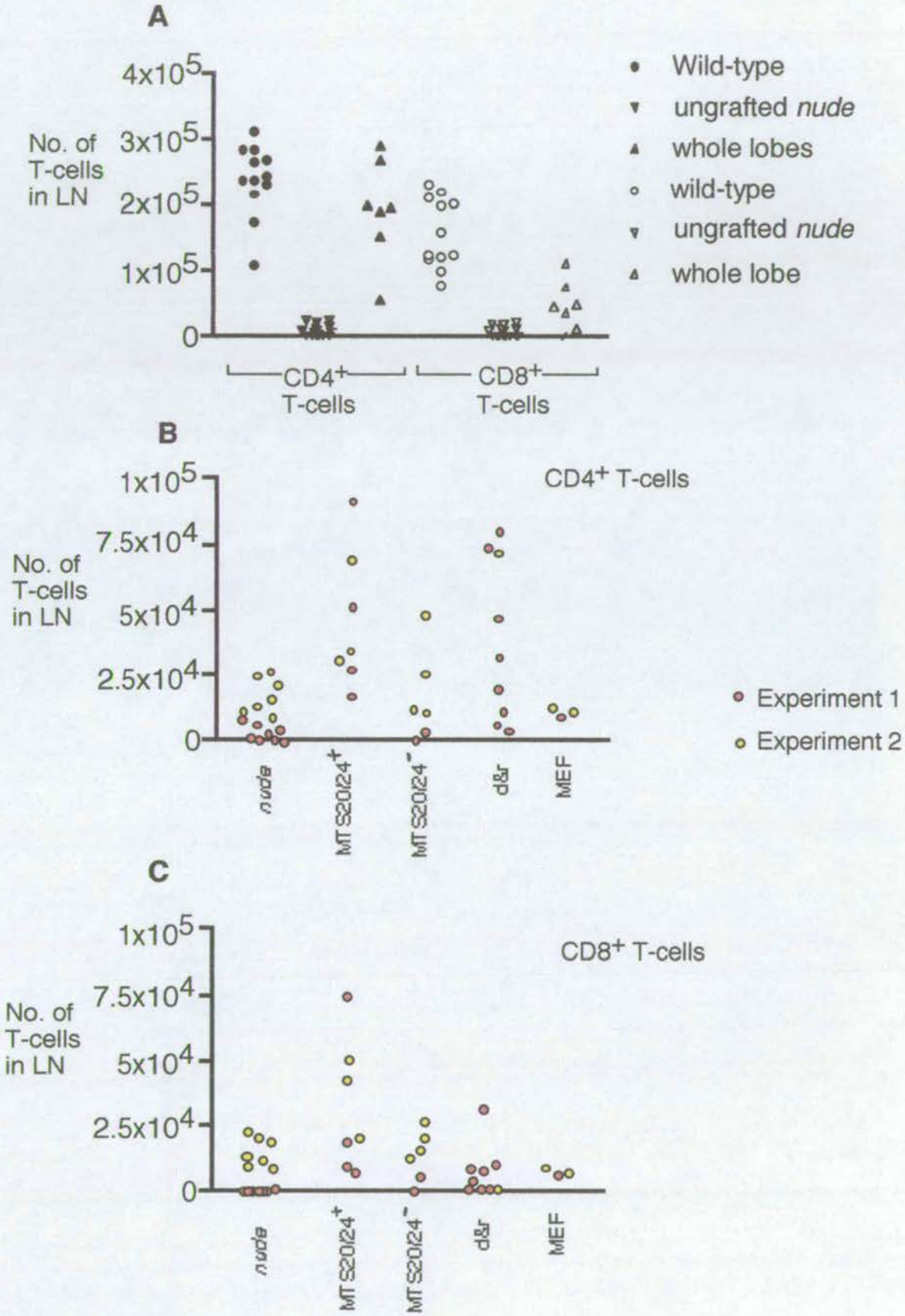
A
4x10^5
3x10^5
2x10^5
1x10^5
0
No. of T-cells in LN
CD4+ T-cells
CD8+ T-cells
Wild-type
ungrafted nude
whole lobes
wild-type
ungrafted nude
whole lobe
B
CD4+ T-cells
1x10^5
7.5x10^4
5x10^4
2.5x10^4
0
No. of T-cells in LN
nude
MTS20/24+
MTS20/24-
d&r
MEF
Experiment 1
Experiment 2
C
CD8+ T-cells
1x10^5
7.5x10^4
5x10^4
2.5x10^4
0
No. of T-cells in LN
nude
MTS20/24+
MTS20/24-
d&r
MEF

Table 6.4. Analysis of T-cells in lymph nodes of grafted *nude* recipient mice

Graft	no. of mice analysed	mean $CD4^+$ cells/10^6 LN cells (± s.e.m)	mean $CD8^+$ cells/10^6 LN cells (± s.e.m)
E12.5 $MTS20/24^+$ cells	n=7	$4.6x10^{4\,a}$ ($\pm 9.9x10^3$)	$3.3x10^{4\,a}$ ($\pm 9.1x10^3$)
E12.5 $MTS20/24^-$ cells	n=6	$1.6x10^{4\,b}$ ($\pm 7.2x10^3$)	$1.3x10^{4\,b}$ ($\pm 4x10^3$)
Ungrafted *nude*	n=15	$1.0x10^4$ ($\pm 2.3x10^3$)	$7.4x10^3$ ($\pm 2x10^3$)
Ungrafted wild-type	n=12	$2.4x10^5$ ($\pm 1.6x10^4$)	$1.6x10^5$ ($\pm 1.5x10^4$)
2 whole E12.5 thymus lobes	n=7	$1.9x10^{5\,c}$ ($\pm 2.9x10^4$)	$4.9x10^{4\,c}$ ($\pm 1.4x10^4$)
Dissociated and reaggregated E12.5 thymus	n=9	$3.8x10^{4\,d}$ ($1.0x10^4$)	$7.8x10^{3\,d}$ ($3.2x10^3$)
MEF only	n=3	$1.1x10^{4\,e}$ ($9.8x10^2$)	$7.7x10^{3\,e}$ ($9.6x10^2$)

LN, lymph node; s.e.m, standard error of mean.

Statistical analyses include data from all mice in each group.

[a] $MTS20/24^+$ recipients versus ungrafted *nude*, p=0.0006 for $CD4^+$, p=0.011 for $CD8^+$. [b] $MTS20/24^-$ recipients versus ungrafted *nude*, p>0.6 for $CD4^+$, p>0.2 for $CD8^+$. [c] whole lobe recipients versus ungrafted *nude*, p=0.0002 for $CD4^+$, p=0.010 for $CD8^+$. [d] dissociated and reaggregated E12.5 thymus recipients versus *nude*, p=0.02 for $CD4^+$, p>0.4 for $CD8^+$. [e] MEF only recipients versus *nude*, p>0.5 for $CD4^+$, p>0.9 for $CD8^+$.

In conclusion, this work has shown that significant T-cell populations were present in the periphery of mice grafted with MTS20/24$^+$ cells, whereas no significant T-cell populations were found in recipients grafted with MTS20/24$^-$ cells. These data demonstrate that as few as 500 MTS20/24$^+$ cells purified from E12.5 thymus and grafted under the kidney capsule of *nude* mice can support T-cell maturation and export to the periphery *in vivo*. The equivalent MTS20/24$^-$ cell population could not support T-cell development. This indicates the functional maturity of the differentiated epithelial subpopulations within MTS20/24$^+$ cell grafts and demonstrates that the MTS20/24$^+$ cell population is sufficient to generate a functional thymus.

6.5. Discussion

In this chapter, the use of an *in vivo* model system to assess the lineage and functional potential of subpopulations of thymic stromal cells purified from E12.5 thymi has been described. In this system, defined numbers of purified thymus cell populations were reaggregated in culture, either alone or mixed with fibroblasts and/or thymocytes, and grafted under the kidney capsule of *nude* mice. The potential of the grafted stromal cells to differentiate into mature epithelial lineages and the capacity of the grafts to support T-cell development was assessed. The data presented have demonstrated that MTS20/24$^+$ cells purified from E12.5 thymi can differentiate into MHC Class II$^+$ cortical and medullary thymic epithelium, attract lymphoid progenitor cells, initiate vascularisation of the graft and support maturation and differentiation of T-cells which can exit the graft to populate the peripheral T-cell pool. The equivalent MTS20/24$^-$ cell population from E12.5 thymi is unable to form a functional thymus *in vivo*, even with the addition of fibroblasts and DN

thymocytes. These data demonstrate that the MTS20/24$^+$ population from E12.5 thymi contains progenitor cells for the major cortical and medullary thymic epithelial cell populations, and strongly suggest that the MTS20/24$^-$ cell population does not contain any progenitor cells.

Lineage potential of MTS20/24$^+$ cells

Analysis of MTS20/24$^+$ cells after RTOC, demonstrated that these cells start to express markers of differentiated thymic epithelium by as early as 48 hours, even in the absence of lymphoid cells. This indicates the capacity of the MTS20/24$^+$ cell population to differentiate *in vitro* and suggests that differentiation is initiated independently of interactions with lymphoid cells. It is possible that FACS sorting these cells using the MTS20 and MTS24 antibodies hyperactivates the cells and stimulates them to differentiate rapidly.

Immunohistochemical analysis of MTS20/24$^+$ cell grafts demonstrated that cells within the MTS20/24$^+$ population were able to differentiate into cortical and medullary epithelium, both with and without the addition of DN thymocytes. MTS20/24$^+$ cell grafts were organised into an apparently normal thymic architecture, consisting of clearly distinguishable cortical and medullary regions and containing numerous T-lineage lymphocytes. The epithelial networks were MHC Class II$^+$, indicative of mature thymic epithelium and important functionally for thymocyte differentiation and selection. The grafts had also been invaded by numerous blood vessels indicating the ability of cells within the MTS20/24$^+$ population to initiate vascularisation. A distinguishing feature of these grafts was the presence of a central cyst-like structure not present in normal thymi. The cysts were lined by 4F1$^+$ epithelial cells and occasionally contained Thy-1$^+$ lymphoid cells. Similar cysts were observed in the thymi of CD3ε transgenic mice (van Ewijk *et al.*, 1999; van Ewijk *et al.*, 2000). These cysts contained classical epithelial cells such as absorptive cells,

ciliated cells and goblet cells on a basement membrane, suggesting that the arrest of early T-cell development reverts the usual 3-D stromal architecture back into a 2-D organisation (van Ewijk *et al.,* 1999; van Ewijk *et al.,* 2000). The cysts present in the MTS20/24^{+} cell grafts might be areas in which cells have differentiated into classical epithelial cell types instead of thymic epithelium, possibly because these areas have not come into contact with developing thymocytes.

No grafts were found in recipients grafted with MTS20/24^{-} cells either with or without the addition of DN thymocytes. This suggests that the E12.5 MTS20/24^{-} cell population was unable to survive or differentiate *in vivo*. The MTS20/24^{-} cell population from E12.5 thymi is comprised of approximately 50% 4F1^{+} epithelial cells, and 50% 4F1^{-} cells, which include epithelial cells, mesenchymal fibroblast cells, lymphoid progenitor cells and parathyroid-lineage cells (see sections 4.3 and 4.4). Previous reports have suggested that cortical epithelium alone is sufficient to support the generation of single positive T-cells (Laufer *et al.,* 1996; DeKoning *et al.,* 1997; Ge and Chen 2000; Capone *et al.,* 2001). We might therefore have expected that the MTS20/24^{-} cell population could form mature cortical epithelial networks and support thymocyte development. Its inability to do so suggests that MTS20/24^{+} cells may be further required during epithelial development to support the survival and growth of mature or differentiating cortical thymic epithelium. Alternatively, the 4F1^{+} cells in the E12.5 thymic primordium may not be thymic epithelial cells, however, this is unlikely given the data in chapter 4.3 and 4.4 showing that the cell population in which the 4F1^{+} cells reside is 75% cytokeratin^{+} and with reports that 4F1 reacts with cortical epithelial cells (Kanariou *et al.,* 1989; Imami *et al.,* 1992).

Control experiments in which whole E12.5 thymus lobes or MEFs only were grafted under the kidney capsule of *nude* mice, produced the expected results: grafts recovered from recipients that received whole E12.5 thymus lobes displayed normal thymic architecture, colonisation by lymphoid cells and vascularisation, whereas

grafts of MEFs only either could not be recovered or contained cells with an adipocytic morphology and no evidence of any epithelial differentiation.

Thymic epithelial cells within the normal thymic microenvironment are surprisingly heterogeneous, with many minor subpopulations of epithelium. Progenitor cells within the MTS20/24$^+$ population were able to differentiate into MHC class II$^+$ cortical and medullary epithelium, and furthermore, the microenvironment formed in these grafts was functional. Further immunohistochemical analysis would be required to assess whether the progenitor cells within the MTS20/24$^+$ grafts have differentiated into all populations of mature thymic epithelium and generated the full complexity of the thymic microenvironment. For example, staining the grafts with antibodies against keratins 5, 14, 8 and 18 would indicate the differentiation status of the epithelial cells (Klug *et al.,* 1998). Klug and colleagues have shown that subsets of thymic epithelial cells can be defined by their pattern of cytokeratin expression: most mature cortical epithelial cells are K8$^+$K18$^+$K5$^-$K14$^-$MTS10$^-$UEA-1$^-$, most medullary epithelial cells are K8$^-$ K18$^-$K5$^+$K14$^+$MTS10$^+$UEA-1$^-$, a minor medullary epithelial subset is K8$^+$K18$^+$K5$^-$ K14$^-$MTS10$^-$UEA-1$^+$ and a further subset located at the cortico-medullary junction is K8$^+$K18$^+$K5$^+$K14$^-$MTS10$^-$UEA-1$^-$ (Klug *et al.,* 1998). Identification of these epithelial subsets within the MTS20/24$^+$ cell grafts would indicate the presence of all mature thymic epithelial cell subsets based on cytokeratin expression.

Further immunohistochemical analysis of MTS20/24$^+$ cell grafts would indicate the presence of other cell types normally found in the thymus. For example, mesenchymal cells could be identified by staining with ER-TR7 (van Vliet *et al.,* 1984) or MTS16 (Godfrey *et al.,* 1990), and expression of extracellular matrix molecules could be demonstrated with antibodies against, for example, laminin and fibronectin (Utsumi *et al.,* 1991; Lannes-Vieira *et al.,* 1993; Savino *et al.,* 1993). The presence of thymic dendritic cells and thymic macrophages, which are derived from bone marrow cells that enter the thymus through the bloodstream, could be identified

with antibodies Mac-1 and Mac-2 (Nabarra and Papiernik 1988), or ER-TR6 (van Vliet *et al.,* 1984).

Functional potential of MTS20/24$^+$ cells

Analysis of thymocyte development in MTS20/24$^+$ cell grafts supplied with CD4$^-$CD8$^-$ thymocytes demonstrated that these grafts could support the maturation of thymocytes into CD4$^+$ and CD8$^+$ SP T-cells. A normal distribution of DP and SP thymocyte subsets was observed in these grafts. Furthermore, 6/7 recipient *nude* mice that received MTS20/24$^+$ cells alone, or with fibroblasts, contained significant T-cell populations in their lymph nodes, indicating reconstitution of thymus function by these grafts in athymic recipients. These data demonstrate the functional maturity of the cells and the epithelial microenvironment formed within the MTS20/24$^+$ cell grafts. In contrast, mice that received MTS20/24$^-$ cell grafts failed to gain thymus function: distinct T-cell populations were observed in only 1 out of 6 recipient mice and these T-cell populations were small compared to those in mice grafted with MTS20/24$^+$ cells.

The numbers of MTS20/24$^+$ cells in the grafts ranged from 500 to 5000, or 0.17-1.7 embryo-equivalents. All of the mice that received just 500 MTS20/24$^+$ cells, successfully reconstituted thymus function, indicating that low numbers of MTS20/24$^+$ cells are capable of differentiating into a fully functional thymic microenvironment. In contrast, mice that received relatively high numbers of MTS20/24$^-$ cells (10,000-160,000 cells or 1.4-22.5 embryo-equivalents) were unable to reconstitute thymus function. The one MTS20/24$^-$ cell recipient mouse in which T-cell populations were observed received 10,000 MTS20/24$^-$ cells. However, the T-cell populations in this mouse were small: CD4$^+$ T-cells comprised only 4% of total lymphocytes and CD8$^+$ T-cells comprised only 5% of total lymphocytes. It is possible that successful reconstitution of this recipient resulted from the growth of a

small number of contaminating MTS20/24$^+$ cells in this graft. In all experiments, the purity of the sorted E12.5 thymus populations was greater than 95% and the MTS20/24$^-$ cell fraction was usually greater than 98% pure. However, when grafting 10,000 MTS20/24$^-$ cells, this could result in contamination of the population with up to 200 MTS20/24$^+$ cells. As grafting 500 MTS20/24$^+$ cells can successfully reconstitute thymus function, it is possible that 200 MTS20/24$^+$ cells contaminating the MTS20/24$^-$ cell graft could also reconstitute thymus function.

When cells were prepared for reaggregation prior to grafting in these experiments, total cell numbers were counted. There would therefore have been some error in the numbers of viable cells grafted, due to the presence of dead cells within the populations. This error should, however, have been similar for the MTS20/24$^+$ and MTS20/24$^-$ cell groups as the cells were treated and handled in an equivalent manner. As the dissection, dissociation and staining protocol totals 5 hours, there are likely to be a proportion of dead or dying cells within the cell preparations. However, the FACS sorting gates were set to exclude dead or dying cells, which have a particular light scatter profile. Therefore, the freshly purified cell populations were unlikely to contain significant proportions of dead cells. An error in cell numbers also arose when preparing the cells for the RTOC reaggregation method. In the last step of the protocol, the cells were collected by centrifugation and resuspended in a tiny amount of media. The cell slurry was then transferred by fine glass pipette to the filter. It was observed during these experiments that a proportion of cells always remained in the bottom of the vessel used for centrifugation and that cells adhere to the inside of the glass pipette during transfer. Therefore, fewer cells were actually placed in the reaggregate than had been counted. This indicates that, in the above experiments, even fewer than 500 MTS20/24$^+$ cells may be able to reconstitute thymus function.

Whereas 6/7 mice grafted with MTS20/24$^+$ cells contained significant T-cell populations, only 5/9 mice grafted with dissociated and reaggregated whole E12.5 thymus cells contained significant CD4$^+$ T-cell populations, while none contained significant CD8$^+$ T-cell populations. This indicates that the purified MTS20/24$^+$ cell grafts were more successful at reconstituting thymus function in athymic recipients than whole thymus cells. This was unexpected, as the whole thymus cell grafts would have contained 4F1$^+$ cortical epithelium as well as high numbers of MTS20/24$^+$ cells. The low frequency of graft success in the dissociated and reaggregated cell group may in part have been due to 8/9 of the mice in this group being grafted with cells that were reaggregated by the hanging drop culture method. As previously stated, this method did not allow the cells to reaggregate tightly and so upon grafting the cells appeared to disperse under the kidney capsule and failed to form a cohesive structure. However, this explanation is unlikely to fully account for the low success rate as 4/7 of the MTS20/24$^+$ cell grafts were also reaggregated using this method and these four grafts were all successful.

An alternative explanation is that a higher proportion of cells within the dissociated whole E12.5 thymus cell population were dead or dying cells due to the enzymatic dissociation procedure. Dead cells were not subsequently excluded from the dissociated and reaggregated cell population as they are during FACS sorting. Although the protocol for preparing dissociated cells was shorter than for preparing MTS20/24$^+$ and MTS20/24$^-$ cells, the reaggregate cultures were usually prepared altogether at the end of the total procedure, hence the dissociated cells would have been stored for several hours. This probably contributed to a higher proportion of dead cells within the dissociated thymus cell preparation, however, this is unlikely to be responsible for the low success rate of the dissociated and reaggregated grafts as large numbers of cells were grafted in these experiments (1 or 10 embryo-equivalents).

The low frequency of graft success in the dissociated and reaggregated cell group suggests that the MTS20/24$^-$ cell population may actually inhibit the proliferation and/or differentiation of the MTS20/24$^+$ cells when these populations are mixed together within the graft. However, this seems unlikely, as MTS20/24$^-$ cells comprise 70% of cells in the normal E12.5 thymus, and four of the recipient mice grafted with dissociated and reaggregated whole thymus cells did contain CD4$^+$ T-cell populations. These four recipients did not contain any CD8$^+$ T-cells, indicating that the thymic microenvironment formed in these grafts was not fully competent to select CD8$^+$ T-cells.

Another factor that could contribute to the low success rate of the dissociated and reaggregated cell grafts, is that the TEPC population within these cells had not been stimulated by MTS20 and MTS24, as it had in the MTS20/24$^+$ cell grafts. It is possible that without activation of TEPC with MTS20 and MTS24, these cells may not differentiate, or may require longer to do so. It is possible that stimulation of cells through MTS20/24 increases secretion of factors required for vascularisation of the grafts, for example, vascular endothelial growth factor (VEGF) or IL-8.

Further analysis of thymocyte development within the MTS20/24$^+$ cell grafts would determine more fully the functional capabilities of the grafts. Thymocyte development is known to proceed through many phenotypically definable stages: a recent report has shown that SP CD4$^+$ thymocytes can be divided into seven distinct stages reflecting their maturation status and based on expression of Qa-2, HSA, CD69, 3G11 and 6C10 (Ge and Chen 1999). The identification of these subsets of thymocytes in MTS20/24$^+$ cell grafts would demonstrate the ability of these grafts to generate all subsets of maturing thymocytes.

The functional potential of the T-cells from the lymph nodes of the MTS20/24$^+$ cell recipient grafted mice could be tested *in vitro* by the mixed lymphocyte reaction (MLR) assay and/or *in vivo* by the ability of the recipient

grafted mice to reject allogeneic skin grafts. The maturation status of these peripheral T-cells could also be analysed phenotypically: naïve peripheral T-cells are $CD25^{lo}CD69^{lo}CD62L^{hi}$, whereas activated T-cells show elevated levels of CD25, CD69 and CD44 and diminished levels of CD62L (Abbas *et al.*, 1997).

Thymic epithelial progenitor cells

The origins of the distinct populations of mature thymic epithelium are obscure. A dual embryonic origin for the thymic epithelium resulting in ectoderm giving rise to cortical epithelium and endoderm giving rise to medullary epithelium has been suggested (Cordier and Heremans 1975; Cordier and Haumont 1980). Other evidence, however, suggests that the thymic epithelium arises from a single endodermal embryological origin. Le Douarin demonstrated that the entire epithelium derives from pharyngeal endoderm in the chick (Le Douarin and Jotereau 1975) and earlier studies claimed that the thymus is of purely endodermal origin in man and rat (Weller 1933; Smith 1965; Cordier and Haumont 1980). The data presented in chapter three herein support an endodermal origin for the thymic epithelium in mice. Evidence that all thymic epithelial cells may originate from a common single progenitor or stem cell has come from immunohistochemical marker studies in which thymic epithelial cells were found which expressed markers of both cortical and medullary epithelium (Kendall 1991; von Gaudecker 1991; Ritter and Boyd 1993; Ritter and Palmer 1999). These 'double positive' epithelial cells have been found in human thymic tumours (Willcox *et al.*, 1987), normal human thymus (Von Gaudecker *et al.*, 1997), chicken thymus (Wilson *et al.*, 1992), rat thymus (Kendall 1991) and both adult and foetal mouse thymus (Ropke *et al.*, 1995; Ritter and Palmer 1999). Collectively, these data provide support for a common thymic epithelial progenitor cell.

A progenitor cell population for the entire thymic epithelium might reside within the E12.5 MTS20/24$^+$ or MTS20/24$^-$ cell populations. Alternatively, separate progenitors for cortical epithelium and medullary epithelium might reside in either or both of these populations. The experiments presented in this chapter have demonstrated that the MTS20/24$^+$ cell population from E12.5 thymi contains progenitor cells which can give rise to both cortical and medullary thymic epithelial cell subpopulations. This population is likely to be of endodermal origin as MTS24 staining has been observed in this area (J.Gill, Monash University Medical School, Australia, personal communication). Further immunohistochemical staining would confirm the presence of MTS20/24$^+$ cells in the endoderm and this would provide strong supporting evidence that the thymic epithelium derives from endoderm alone.

The presence of 'double positive' epithelial cells, which stain with markers of cortical and medullary epithelium, has not been demonstrated in this study, however, if they were present it is likely that they would reside within the MTS20/24$^-$ cell population, as cells marked by 4F1 are within this population. In this case, the data presented here would indicate that putative 'double positive' epithelial cells within the MTS20/24$^-$ population would not be able to give rise to mature thymic epithelium in this model system and therefore, are not progenitor cells. It is possible that a population of these 'double positive' epithelial cells resides within the E12.5 MTS20/24$^+$ cell population which has not been detected in this study. If this were the case, it could be postulated that these 'double positive' epithelial cells are progenitor cells for cortical and medullary epithelium. Alternatively, it is possible that MTS20/24$^+$ progenitor cells give rise to MTS20/24$^-$ 'double positive' epithelial cells, which then differentiate into cortical or medullary epithelium.

The experiments presented here do not directly address whether the MTS20/24$^+$ cell population contains a single progenitor for the entire thymic epithelium or whether two separate progenitor populations exist for cortical and medullary thymic epithelium, which both express MTS20 and MTS24. To address

this question, an analysis of the heterogeneity of the MTS20/24$^+$ population and a clonal analysis of the potential of individual cells within the MTS20/24$^+$ population is required. The heterogeneity of the population could be investigated by RT-PCR analysis of single cells FACS sorted from the MTS20/24$^+$ population, using the genetic markers investigated in chapter five, *Foxn1*, *Pax1*, *Pax9* and *Hoxa3*. The establishment of other markers expressed by cells within the MTS20/24$^+$ cell population would further facilitate this analysis. Possible candidate markers for cells in this population would be cytokines such as IL-7, or the Notch ligands, Jagged-1 and –2, which are expressed by thymic epithelial cells and are suggested to have essential roles in regulating early thymocyte development (Peschon *et al.,* 1994; von Freeden-Jeffry *et al.,* 1995; Oosterwegel *et al.,* 1997; Osborne and Miele 1999). Further candidate markers for cells in the MTS20/24$^+$ population might be adhesion molecules and chemokines implicated in the chemoattraction of lymphoid progenitors to the thymus, such as β1-integrin or TECK (Wilkinson *et al.,* 1999; Potocnik *et al.,* 2000), or transcription factors such as *RelB*, which is required for differentiation of some medullary epithelial cells (Burkly *et al.,* 1995; Weih *et al.,* 1995).

Conclusive evidence of a single progenitor for the thymic epithelium would come from a single cell being able to give rise to both cortical and medullary thymic epithelium. This is difficult to assess, as it is highly unlikely that one cell would form into a functional reaggregate thymus, and at present, clonal propagation of MTS20/24$^+$ cells *in vitro* is not possible. To assess the ability of low numbers of MTS20/24$^+$ cells to form a functional thymus, the experiments described in this chapter could be repeated with a dilution series of MTS20/24$^+$ cells in reaggregates otherwise made entirely of MEFs. However, it is unlikely that reaggregate thymi would form from very low numbers of cells or a single MTS20/24$^+$ cell. An alternative experiment would be to seed low numbers of labelled MTS20/24$^+$ cells into reaggregate cultures prepared with unlabelled MTS20/24$^+$ cells and supplied

with lymphoid progenitors. MTS20/24$^+$ cells could be labelled *in vitro* with a vital dye such as DiI or purified from embryonic thymi dissected from a mouse line which ubiquitously expresses green fluorescent protein (GFP) or the β-gal/*Foxn1* mouse line described in chapter three. Histological analysis, after 10-14 days *in vitro* or 3-4 weeks after grafting under the kidney capsule of *nude* mice, would determine if adjacent areas of cortex and medulla were labelled with the marker, indicating that they had developed from a single labelled cell.

In order to achieve a truly clonal analysis of these cells, we would need to propagate MTS20/24$^+$ cells *in vitro* as single proliferative clones. The potential of a particular clone of cells to give rise to both cortical and medullary thymic epithelium could then be assessed in a reaggregate culture, either *in vitro* or after grafting *in vivo*. For MTS20/24$^+$ cells to be propagated *in vitro*, appropriate cell culture conditions need to be established to support the growth of MTS20/24$^+$ cells and inhibit their differentiation *in vitro*. Preliminary experiments in this laboratory are testing extracellular matrix molecules and combinations of growth factors and cytokines which might support the proliferation of E12.5 thymus cells (C.Nowell, CGR, University of Edinburgh, personal communication). For example, extracellular matrix molecules such as laminin and fibronectin are known to be important adhesion molecules within the thymus (Utsumi *et al.,* 1991; Lannes-Vieira *et al.,* 1993), and therefore, might provide improved growth conditions for E12.5 thymus cells. Growth factors such as IGF and EGF have been shown to substitute for the influence of thymic mesenchyme on thymus development (Shinohara and Honjo 1996; Shinohara and Honjo 1997) and so might be required to support E12.5 thymic epithelial cells *in vitro*.

Chapter 7

Concluding remarks

This work aimed to test the hypothesis that the monoclonal antibodies MTS20 and MTS24 identify thymic epithelial progenitor cells (TEPC) (Blackburn *et al.,* 1996). The data presented herein demonstrate unequivocally that this hypothesis is correct: the MTS20/24^{+} cell population from the E12.5 thymic primordium contains progenitor cells that can differentiate into the major subpopulations of thymic epithelium while the MTS20/24^{-} cell population, which also contains epithelial cells, cannot. They further suggest that the thymic epithelium derives from a single origin.

Chapter three of this thesis describes early thymus organogenesis through analysis of the expression of the transcription factor *Foxn1*, which is required cell-autonomously for thymic epithelial cell development (Blackburn *et al.,* 1996). *Foxn1* was expressed in the endoderm of the third pharyngeal pouch commencing at E11.25, and subsequently, the *Foxn1*$^{+}$ cells proliferated to form the thymic primordium. In *Foxn1*$^{-/-}$ embryos, formation of the primordium was initiated but the further proliferation and differentiation of the cells was arrested at E12. These data are consistent with the *nude* phenotype (Cordier and Haumont 1980), and with previous data showing that *Foxn1* is required for the differentiation of mature thymic epithelium (Blackburn *et al.,* 1996; Nehls *et al.,* 1996). Since no *Foxn1* expression

was observed in the pharyngeal ectoderm, these data suggest that the thymus derives from a single endodermal origin in the mouse.

Chapter four describes analysis of the cellular composition of the E12.5 thymic primordium and the expression of MTS20, MTS24 and other thymus-specific markers during thymus ontogeny. Three distinct epithelial subpopulations were identified within the E12.5 thymic primordium, one of which was MTS20/24$^+$ and comprised 40% of E12.5 thymic epithelial cells. During thymus ontogeny, the proportion of MTS20/24$^+$ cells in the thymus decreased rapidly: in the late foetal and adult thymus only 1% of epithelial cells were MTS20/24$^+$. Analysis of the pharyngeal arch region at E9.5 and E10.5 revealed the presence of some MTS20/24$^+$ cells. The spatial and temporal expression pattern of MTS20/24 is therefore consistent with that expected of TEPC markers.

Chapter five describes the phenotypic characterisation of FACS purified E12.5 MTS20/24$^+$ cells. Approximately 50% of MTS20/24$^+$ cells expressed cytokeratins 5 and 8, consistent with the phenotype of putative cortical precursor cells (Klug *et al.,* 1998). MTS20/24$^+$ cells did not express 4F1 or MTS10, markers associated with mature thymic epithelium but expressed the transcription factors *Foxn1*, *Pax9*, *Pax1* and *Hoxa3*, all of which are required for thymus development. Thus, MTS20/24$^+$ cells express markers associated with thymic epithelial lineages but do not express markers of mature thymic epithelium. This is again consistent with the phenotype expected of TEPC.

Chapter six describes the direct lineage and functional analysis of MTS20/24$^+$ cells purified from E12.5 thymi. When grafted under the kidney capsule of *nude* recipients, MTS20/24$^+$ cells differentiated into cortical and medullary thymic epithelium. Furthermore, MTS20/24$^+$ cell grafts were capable of initiating vascularisation of the grafts, attracting lymphoid progenitor cells and supporting the maturation of thymocytes to single positive T-cells. MTS20/24$^-$ cells could fulfil

none of these functions. These data demonstrate unequivocally that the population of E12.5 thymus cells marked by MTS20 and MTS24 contains progenitor cells for the major populations of thymic epithelium and is sufficient to form a functional thymus *in vivo*.

MTS20 and MTS24

At present, little is known about the determinants recognised by the antibodies MTS20 and MTS24. Preliminary work on MTS24 has shown that this antibody reacts with a highly glycosylated protein with an apparent size of 70-200kDa (J.Gill, Monash University Medical School, Prahan, Australia, personal communication). Neuraminidase treatment revealed a shift in motility to 70kDa suggesting recognition of a mucin-like molecule (J.Gill, Monash University Medical School, Prahan, Australia, personal communication). Mucins are large membrane-associated or secreted glycoproteins with numerous O-linked glycans (Hassid *et al.*, 2000). A search of the literature did not reveal any mucin-like molecules with specific expression in thymic epithelial cells, however, mucin-type O-glycans have been implicated in the cell adhesion of leukocytes (Fukuda and Tsuboi 1999), and expression of an antibody against a mucin-like molecule was detected in Hassall's corpuscles in human thymus (Mattes *et al.*, 1985).

Standard expression cloning techniques (Seed and Aruffo 1987; Simmons 1993) could be employed to identify the molecules recognised by MTS20 and MTS24, as they are known to react with cell surface determinants. This involves the preparation of a cDNA library from E12.5 thymi followed by transient transfection of the library into COS cells. Subsequent rounds of immunopanning with MTS20 and MTS24 will identify cDNAs encoding the molecules recognised by these mAbs. These cDNAs can then be isolated, sequenced and identified by comparison with known sequences.

As the determinants recognised by MTS20 and MTS24 are on the cell surface, they may be receptors for receiving signals, possibly regulating the differentiation of cells by down-stream changes in transcriptional control. For example, in epidermal stem cells, β-catenin activates Tcf/Lef-mediated transcription in response to Wnt signalling through the membrane receptor frizzled (Watt and Hogan 2000). Alternatively, they could be receptors for growth or differentiation factors such as IGF, which has been implicated in thymic epithelial development *in vitro* (Shinohara and Honjo 1997). Recently, IGF-1R gene expression has been reported in the murine foetal thymus (Kecha *et al.*, 2000). Identification of the determinants recognised by MTS20 and MTS24 will allow biochemical and functional analysis of these molecules. Investigation of the function of these antigens could include over-expression or blocking of these molecules in RTOC, which may result in alterations in the differentiation potential of TEPC and the development of mature TE populations or defects in thymocyte development.

Progenitor cells or stem cells?

The MTS20/24$^+$ population purified from E12.5 thymi contains progenitor cells which are capable of giving rise to the major populations of thymic epithelium. As discussed in section 6.5, clonal analysis is required to demonstrate whether this population corresponds to a single progenitor cell for the entire epithelium or to two or more separate lineage-restricted progenitor cells for different subpopulations of epithelium, that all express MTS20/24. Molecular profiling of the TEPC population, for example, by single-cell RT-PCR or by a signal-sequence trap screen (presently underway in our laboratory), could be employed to find additional markers for TEPC or to allow identification of subpopulations of cells within the MTS20/24$^+$ population. Notwithstanding the existence of single or multiple TEPC, the MTS20/24$^+$ cell population is likely to be heterogeneous, consisting of TEPC, differentiating progenitors and possibly thymic epithelial stem cells.

Cells of the inner cell mass of a blastocyst stage embryo, embryonic stem cells, are pluripotent: when introduced into host blastocysts they can contribute to all adult tissues (Nagy *et al.,* 1993). As development proceeds, cells become progressively committed to a particular pathway of differentiation, and this is thought to lead to the establishment of stem cells for particular tissues and organs (Snyder and Vescovi 2000). The developmental commitment of cells is encoded as a combination of transcription factors (Slack 2000). The commonly accepted definition of a stem cell is its ability to self-renew and to give rise to one or more differentiated cell types (Slack 2000; Watt and Hogan 2000). Often, a stem cell will give rise to intermediate progenitor cells, termed transit-amplifying cells, which are developmentally restricted and have a limited proliferative capacity (Watt and Hogan 2000). This increases the numbers of differentiating cells arising from relatively few stem cell divisions. For example, the haematopoietic stem cell (HSC), gives rise to multipotent progenitor cells, which then give rise to lineage restricted progenitor cells, such as the common lymphoid progenitor (Weissman 2000).

It is possible that the MTS20/24$^+$ population from E12.5 thymi contains organ-specific embryonic thymic epithelial stem cells (TESC), from which all cells of the thymic epithelium can arise. The work presented here has demonstrated that cells within the MTS20/24$^+$ population are capable of generating at least two differentiated cell types. Assessment of the capacity of these cells to self-renew would indicate whether they are embryonic TESC. Self-renewal capacity could be investigated by establishing kidney capsule grafts of labelled (DiI labelled or GFP or β-gal expressing cells) MTS20/24$^+$ cells from E12.5 thymi, followed by re-purification of cells that remain MTS20/24$^+$label$^+$ from the grafts, and transfer of these cells into new RTOCs. The presence of MTS20/24$^+$ cells remaining in the grafts and the ability of these labelled cells to contribute to cortical and medullary epithelium in RTOCs would indicate the self-renewal of the MTS20/24$^+$ cells.

This thesis has concentrated on MTS20/24$^+$ cells within the E12.5 thymic primordium, which, as discussed above, would be likely to contain a high proportion of progenitor or stem cells, as well as the differentiating progeny of these cells. However, development of the thymic primordium begins earlier in the mouse embryo, at E11–E11.5, when the endoderm of the third pharyngeal pouch begins to proliferate and *Foxn1* expression commences in this tissue. Therefore, stem or progenitor cells committed to the thymic epithelial lineage may be present at E11 or even earlier in the pharyngeal endoderm. As reported in chapter four, MTS20/24$^+$ cells can be detected in the pharyngeal arch region of E9.5 and E10.5 embryos, indicating that these may be TEPC/SC. MTS24 staining has been reported in the endoderm of the third pharyngeal pouch (J.Gill, Monash University Medical School, Prahan, Australia, personal communication). Further immunohistochemical staining of the pharyngeal region of embryos between E9.5 and E11.5 would establish the location of MTS20/24$^+$ cells. In addition, novel markers that identify progenitor or stem cells within the MTS20/24$^+$ cell population identified by molecular profiling, could be used to determine the location of TEPC/SC within the pharyngeal region prior to thymus formation, by *in situ* hybridisation or immunohistochemical staining.

Developmental commitment and stem cell fate are regulated by transcription factors, with every lineage controlled by a unique combination of transcription factors (Watt and Hogan 2000). For example, in haematopoiesis, SCL is a transcription factor essential for the formation of all haematopoietic lineages in the mouse (Robb and Begley 1997). Recently, work from this laboratory has shown that within the third pharyngeal pouch, two transcription factors, *Foxn1* and *gcm2*, specify distinct domains at E10.5-E11.5 which will develop into the thymus and parathyroid respectively (Gordon *et al.,* 2001) (See Appendix 1). *Gcm2* is expressed in the ventral portion of the third pharyngeal pouch from E9.5, indicating that TESC may be specified as early as E9.5. *Foxn1* is not required for the initial formation of the thymic primordium, as the primordium forms in *Foxn1*$^{-/-}$ mice (Nehls *et al.,*

1996). This indicates that another gene upstream of *Foxn1* may be required to specify the development of the primordium and suggests that TESC do not express *Foxn1*. *Foxn1* is required for the differentiation of mature thymic epithelial populations from thymic progenitor or stem cells (Blackburn *et al.,* 1996; Nehls *et al.,* 1996). *Pax1* may also be involved in the control of TEPC differentiation, as this transcription factor is expressed in a significant fraction of TEC at E14, and in only a small number of undifferentiated cortical epithelial cells in the adult (Wallin *et al.,* 1996).

Adult stem cells

Most tissues or organs are able to regenerate and repair themselves throughout life, both as individual cells die, and following more extensive tissue damage. In some tissues, such as the haematopoietic system, stem cells remain throughout adult life and can reconstitute all haematopoietic lineages (McKay 2000). Consequently, human HSCs are in widespread clinical use, for example, for bone marrow grafting in cancer patients following myeloablative radiation and chemotherapy (McKay 2000; Weissman 2000). It is currently believed that most mature tissues and organs contain residual stem cells which remain throughout adult life. In the mouse, putative stem cells have been identified in a number of tissues, such as muscle, brain, and bone (McKay 2000), and in epithelial tissues, such as skin, intestine and liver (Slack 2000).

One of the most studied epithelial stem cells is that of the small intestine (Bach *et al.,* 2000). Multipotent stem cells reside at the base of the crypts of Lieberkuhn in the small intestine, and can give rise to all cell-types found within the crypt (Bach *et al.,* 2000). The stem cells give rise to progenitor cells called transit-amplifying cells, which occupy two-thirds of the height of the crypts and have a finite proliferative capacity before terminally differentiating (Karam 1999).

Postmitotic differentiated cells line the upper part of the crypts and villi. Studies using mutagenesis to produce a visible cell label have demonstrated that each crypt is supplied by 4 or 5 stem cells (Bjerknes and Cheng 1999).

Stem cells have also been studied extensively in the epidermis. Epidermal stem cells have unlimited self-renewal capacity and are arranged in clusters at the tips of the dermal papillae (Jensen *et al.,* 1999) in the basal layer of the epidermis (Watt 1998). These stem cells give rise to transit-amplifying cells that are committed to differentiate after a finite number of divisions (Watt 1998). The stem cells can be distinguished from the transit-amplifying population by their high level of expression of β1-integrin (Jones and Watt 1993) and β-catenin (Zhu and Watt 1999).

The transcriptional control of stem cell fate has been investigated in epidermal and intestinal stem cells: interestingly, the Wnt signalling pathway and the Tcf/Lef family of transcription factors have been implicated in both stem cell populations (Slack 2000; Watt and Hogan 2000). $Tcf4^{-/-}$ mice lack intestinal stem cells (Korinek *et al.,* 1998) and $Lef1^{-/-}$ mice have defects in hair and whisker formation (van Genderen *et al.,* 1994). In hair follicle, epidermal and intestinal stem cells, β-catenin activates TCF/LEF1-mediated transcription in response to Wnt signalling (DasGupta and Fuchs 1999; Zhu and Watt 1999). β-catenin and TCF/LEF-1 signalling are therefore necessary to maintain cells in the stem cell compartment. The importance of the Wnt signalling pathway in the regulation of these two stem cell populations may indicate a general role for this pathway in stem cell transcriptional control. Furthermore, disruption of the Wnt signalling pathway has been implicated in several types of tumour formation, again suggesting that this pathway is involved in the regulation of stem cell fate (Clevers 2000).

The precedent for epithelial stem cells in adult tissues leads to the idea of a TESC present in the adult thymus. Thymic function decreases with age as the thymus involutes (George and Ritter 1996), which is likely to be due to a decreased

requirement for naïve T-cells once the periphery is seeded with a full complement of antigen-reactive T-cells. However, studies have documented thymus tissue in adults up to 107 years of age (Steinmann *et al.*, 1985), and recently, histological studies and analysis of recent thymic emigrants have shown that thymopoiesis is ongoing throughout adult life (Bertho *et al.*, 1997; Douek *et al.*, 1998; Marusic *et al.*, 1998; Jamieson *et al.*, 1999; McFarland *et al.*, 2000). Age-related involution of the thymus does not preclude the presence of a TESC in adult thymus which can replace cells lost as a result of normal turnover or after specific damage to the thymus. Indeed, stem cells have been identified in other tissues that normally undergo very limited regeneration or turnover such as the brain (Gage 2000), liver (Alison 1998) and pancreas (Ramiya *et al.*, 2000).

MTS20/24$^+$ cells are present in the adult thymus at a very low frequency, and it is intriguing to speculate that these may be residual stem cells. This possibility could be tested by purifying the MTS20/24$^+$ cells from adult thymi and grafting them under the kidney capsule of mice to analyse their developmental potential. This experiment was attempted once during the present work: however, there were two main difficulties. In the experiment, adult thymi were collected, the cells dissociated, and thymocytes depleted from the preparation by sequential rounds of agitation and washing followed by T-cell depletion using CD4$^+$CD8$^+$ MACS beads. The remaining cells were then FACS sorted for MTS20/24$^+$ cells. The first problem is that of cell numbers: approximately 99% of cells within the adult thymus are thymocytes so purification of the 1% of epithelial cells is important. This is technically difficult, as the starting number of cells must be high to ensure a reasonable yield of epithelial cells. Furthermore, less than 1% of adult epithelial cells are positive for MTS20/24, so the population recovered after the sort was very small. The MTS20/24$^+$ population was also impure due to the limitations of the FACS sorter to purify small populations cleanly (the sorted MTS20/24$^+$ cell population was approximately 75% MTS20/24$^+$). Three weeks after grafting the adult MTS20/24$^+$ cells (reaggregated with MEFs) into

nude recipients, no evidence of any grafts remained. The second problem with this experiment was that adult thymic epithelial stem cells are likely to need a signal to activate them from their resting state. It is possible that MTS20 and MTS24 may themselves be the activators required for thymic stem cell activation, although in the above experiment the cells were FACS sorted using MTS20 and MTS24, suggesting that additional activation signals may be necessary. At present little is known about the mechanisms controlling the activation of adult epithelial stem cells. Candidate growth factors or signalling molecules, such as TGFβs, Wnts or the Notch ligand, Delta (Watt and Hogan 2000), could be added to RTOCs made with adult MTS20/24$^+$ cells to test their ability to induce proliferation and differentiation of the cells.

Therapeutic potential of TEPC/TESC

The isolation of a progenitor cell population for the thymic epithelium which can generate a functional thymus, as described here, raises new possibilities for supporting T-cell development *in vitro* or *in vivo* for clinical uses. A cell line corresponding to E12.5 MTS20/24$^+$ cells, which can be induced to differentiate under certain conditions, could be used to support the *in vitro* differentiation of T-cells. Cloning of the determinants recognised by MTS20 and MTS24 would facilitate the identification of equivalent thymic epithelial progenitor cells in human thymi. This could lead to the isolation of corresponding human thymic epithelial progenitor/stem cell lines. These could be used *in vitro* to generate normal T-cells to replace cells lost as a result of infection, chemotherapy, radiotherapy or ageing, and for the expansion of specific T-cell populations for particular clinical uses, such as CD4$^+$ T-cells for patients with HIV related immunodeficiency.

The isolation of human thymic epithelial progenitor cells also raises the possibility of restoring thymus function to athymic individuals. Various human

severe combined immunodeficiency (SCID) diseases are recognised including a mutation in the human *Foxn1* gene, which result in a severe T-cell defect (Fischer and Malissen 1998; Frank *et al.*, 1999). DiGeorge syndrome is a congenital disorder that affects the heart, thymus and parathyroid glands and results in severe T-cell deficiency (Amman *et al.*, 1982; Hong 1991). Treatments for reconstitution of the immune system have focussed on bone marrow transplantation from HLA-matched sibling or thymus transplantation (Hong 1991; Jones *et al.*, 1999). A recent report has demonstrated that bone marrow transplantation is ineffective in the long-term immune reconstitution of human nude/SCID patients (Pignata *et al.*, 2001), whilst transplantation of cultured foetal or postnatal thymus tissue into infants with DiGeorge syndrome has recently had more success in restoring immune function in these individuals (Markert *et al.*, 1997; Markert *et al.*, 1999). A graft derived from human TEPC lines may prove more successful in reconstituting T-cell immunity. The advantages of using TEPC lines are that cells can be grown in culture indefinitely, do not form tumours in animals and retain the ability to differentiate. Recent work has shown that immortalised human liver cells grafted into rats with acute liver failure can incorporate into the host tissue and keep such rats alive (Kobayashi *et al.*, 2000).

Summary

The data presented in this thesis have shown that a population of cells present in the E12.5 thymic primordium contains progenitor cells for the thymic epithelium. Figure 7.1 outlines alternative models for the development of subpopulations of thymic epithelium. As discussed above, the E12.5 MTS20/24$^+$ cell population may contain a multipotent progenitor cell which can give rise to the entire thymic epithelium. This could be via an intermediate 'double positive' epithelial cell which expresses markers of both cortical and medullary epithelium and can differentiate

Figure 7.1. Models of thymic epithelial cell development

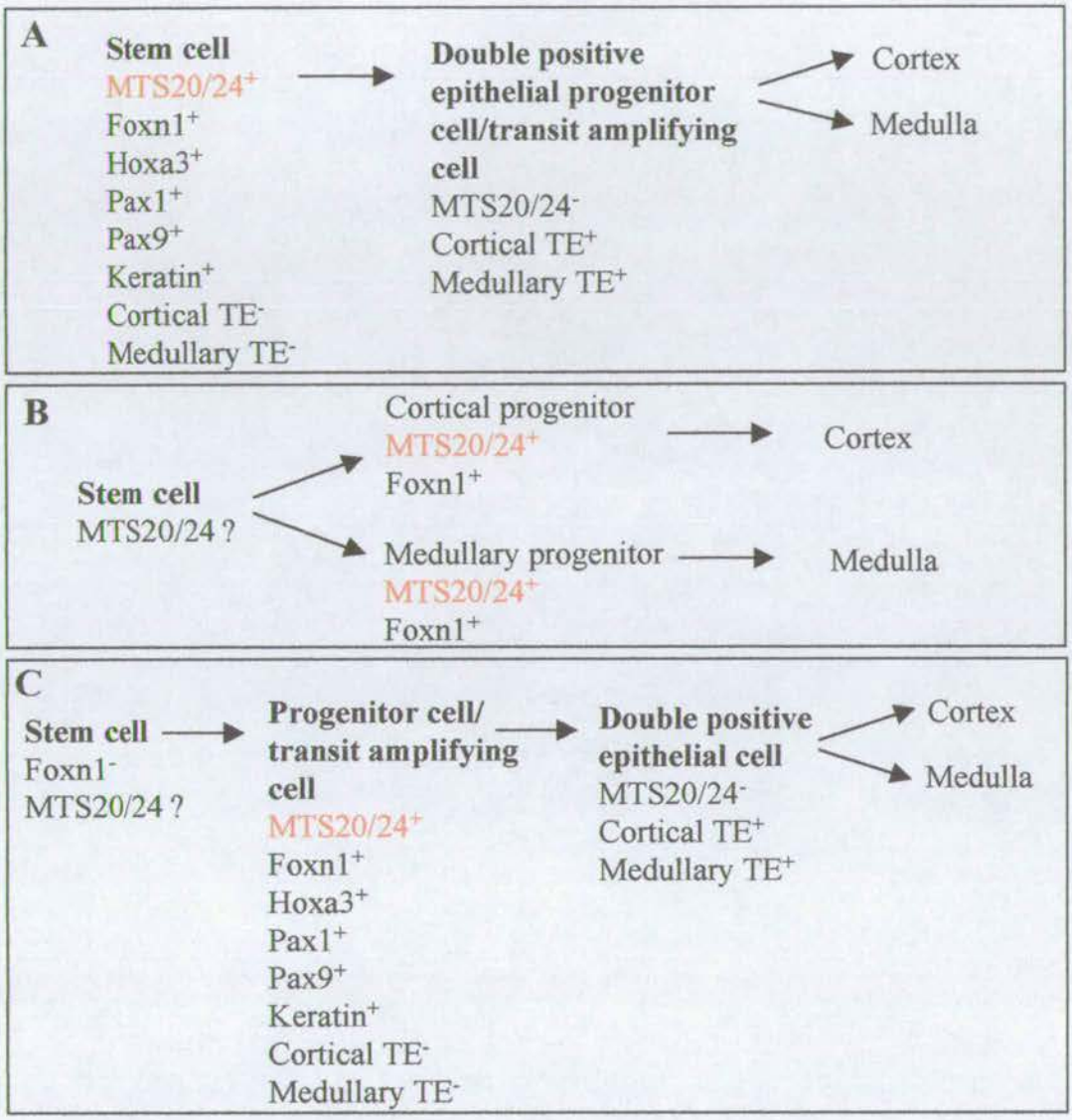

MTS20/24+ cells may be multipotent stem cells which can give rise to all TE popualtions through a progenitor or transit amplifying cell population (A). Alternatively, the MTS20/24+ population may contain separate progenitor cells restricted to the cortical or medullary epithelial lineage (B). Finally, there may be a Foxn1- stem cell which gives rise to MTS20/24+ progenitor cells which can then differntiate into all TE populations, possibly via a double positive epithelial cell population (C).

into both cell types (Figure 7.1.A,C). The multipotent MTS20/24$^+$ cells may be *Foxn1*-expressing stem cells from which all other cells can arise (Figure 7.1.A), although formation and proliferation of the thymic primordium in *Foxn1*$^{-/-}$ embryos suggests that TESC are *Foxn1*$^-$ (See Chapter 3). Alternatively, most MTS20/24$^+$ cells may be progenitor/transit-amplifying cells which have themselves arisen from a *Foxn1*$^-$stem cell (Figure 7.1.C.). Expression of *Foxn1* might promote progression of stem cells into the transit-amplifying compartment. An alternative model is that the MTS20/24$^+$ cell population contains two or more separate progenitor or stem cells, each giving rise to a different subpopulation of thymic epithelium (Figure 7.1.B).

Our data favour model C, since the morphological data presented in chapter 3 support a single origin for the entire thymic epithelium and the proliferation of the thymic primordium in *Foxn1*$^{-/-}$ mice suggests that TESC are present in the absence of *Foxn1*. This suggests that the MTS20/24$^+$ population contains both *Foxn1*$^-$ TESC and *Foxn1*$^+$ TEPC/transit-amplifying cells which can give rise to the entire thymic epithelium.

Appendix 1

Gcm2 and *Foxn1* mark early parathyroid- and thymus-specific domains in the developing third pharyngeal pouch

Julie Gordon[2,3], Andrea R. Bennett[2,3], C. Clare Blackburn[2,4], and Nancy R. Manley[1,4]

[1]Institute of Molecular Medicine and Genetics and Department of Pediatrics, Medical College of Georgia, Augusta, GA 30912 USA

[2]Centre for Genome Research / Institute of Cell, Animal and Population Biology, University of Edinburgh, King's Buildings, West Mains Road, Edinburgh, EH9 3JQ, UK.

[3,4]These authors contributed equally to this work

[4]Authors for Correspondence: c.blackburn@ed.ac.uk, and nmanley@mail.mcg.edu

Editorial inquiries should be addressed to Nancy Manley, Phone: (706) 721-0691; Fax: (706) 721-8685; E-mail: nmanley@mail.mcg.edu

Keywords: thymus, parathyroid, pharyngeal pouch, endoderm, organogenesis, *Gcm2*, *Foxn1*, *whn*, *nude*

Abstract

The thymus and parathyroids originate from a common primordium that develops from the third pharyngeal pouch in mice and humans. The molecular mechanism that specifies this primordium into distinct organ domains is not known. The *Gcm2* and *Foxn1* transcription factors are required for development of the parathyroid and thymus respectively, and are attractive candidates for this role. However, their embryonic expression patterns during pharyngeal pouch development and early thymus and parathyroid organogenesis have not been described. Here we report that *Gcm2* is expressed specifically in the developing second and third pharyngeal pouches at E9.5, and is further confined to a small domain of the third pouch endoderm by E10.5. In contrast, *Foxn1* is not expressed until after the common primordium is formed, beginning at E11.25. Our results show that *Gcm2* and *Foxn1* expression mark two complementary domains that prefigure parathyroid and thymus regions within the common primordium before morphological distinctions are present.

Results and discussion

Gcm2 is one of two mammalian homologues of the *Drosophila* gene *Glial cells missing,* and encodes a transcription factor with a novel DNA binding domain (Akiyama et al., 1996; Kim et al., 1998). Although this gene in *Drosophila* is involved in determining glial versus neuronal identity (Hosoya et al., 1995; Jones et al., 1995; Vincent et al., 1996), *Gcm2* in mice is specifically expressed in the parathyroid gland in late gestation and in adults (Kim et al., 1998). In $Gcm2^{-/-}$ mutant mice, parathyroid hormone (PTH) expression is undetectable at E11.5 (Gunther et al., 2000), indicating that *Gcm2* plays a crucial role very early in parathyroid organogenesis. However, the expression pattern for *Gcm2* during pharyngeal region development and parathyroid organogenesis has not been described.

We used whole mount *in situ* hybridization to determine the *Gcm2* expression pattern from the initial formation of the third pharyngeal pouch at E9 through early parathyroid organogenesis at E11.5. There was no detectable expression at E8.5 (Fig.1A). *Gcm2* was first expressed at E9.5 in a diffuse domain encompassing the 3rd and, at a lower level the 2nd, pharyngeal pouches (Fig. 1B). By E10.5 expression was restricted to the 3rd pouch, and appeared in whole mounts to be most strongly expressed in the cranial part of the pouch (Fig. 1C). This expression pattern was confirmed in paraffin sections, which showed strong labeling in a small domain within the cranial half of the third pharyngeal pouch endoderm (Fig 1E).

The common thymus/parathyroid primordia begin to develop from the 3rd pharyngeal pouch endoderm at E11-11.5 (Cordier and Haumont, 1980). These bilateral primordia appear morphologically uniform until E13-13.5, when each physically divides into separate parathyroid and thymus glands. At E11.5, *Gcm2* staining in whole mounts was seen exclusively in small bilateral domains in the pharyngeal region (Fig. 1D). Paraffin sectioning of these whole mounts showed that the expression was confined to the dorsal and cranial portion of the primordia developing from the 3rd pouches (Fig. 1F).

To confirm that this expression pattern corresponded to the developing parathyroid/thymus primordium, we compared it to that of a thymus-specific marker, *Foxn1* (formerly *whn/Hfh11*)(Kaestner et al., 2000). *Foxn1* is the gene mutated in the classical *nude* mouse strain, and encodes a transcription factor of the winged helix/forkhead class (Nehls et al., 1994). *Foxn1* is not required for initiation of thymus organogenesis (Nehls et al., 1996), but is required cell-autonomously for thymic epithelial cell differentiation (Blackburn et al., 1996). Therefore, *Foxn1* expression is likely to mark the thymus-specific domain in the common primordium. However, its expression pattern during early thymus organogenesis has not been described. We used a *lacZ* knock-in mouse (Nehls et al., 1996) to determine the onset of *Foxn1* expression in the pharyngeal region. In contrast to *Gcm2, Foxn1* was

not expressed in the common primordium until E11.25 (Fig.1H, I). Expression began in a subset of epithelial cells at the caudal and ventral end of the primordium, then gradually expanded to include approximately two thirds of the primordium by E11.5 (Fig. 1J). The most cranial and dorsal portion of the developing primordium did not express *Foxn1*. Therefore, the *Foxn1* expression domain appears complementary to that of *Gcm2* at E11.5. To confirm this observation, we performed dual-color *in situ* analysis for both *Gcm2* and *Foxn1* at E11.5. The two probes co-localized to the developing 3rd pouch primordium, with *Gcm2* expression and *Foxn1* immediately adjacent to each other (Fig. 1G).

Our results show that *Gcm2* is expressed in a specific region of the pharyngeal endoderm around the third pharyngeal pouch as early as E9.5. This expression pattern becomes progressively restricted in the developing third pouch before the organ primordia begin to form. In contrast, *Foxn1* expression does not begin until after the common parathyroid/thymus primordium forms. Once the primordia form, *Gcm2* and *Foxn1* are expressed in a complementary fashion in the parathyroid- and thymus-specific regions before the division into morphologically distinct organs.

Methods

Mice and genotyping

Wild type Swiss Webster embryos were collected with the day of the vaginal plug designated as E0.5. Mice carrying a lacZ insertion in exon 3 of *whn* (Nehls et al., 1996) were maintained by mating $whn^{+/-}$ males with C57BL/6 females (CGR Animal Unit): progeny were genotyped by PCR analysis of tail DNA using lacZ specific primers. All experiments were carried out with the approval of the respective institutional animal care committees.

In situ hybridization and lacZ staining

Whole mount in situ hybridizations were performed as described (Manley and Capecchi, 1995). The *Gcm2* probe was generated by PCR amplification as described (Kim et al., 1998). For single-color staining, BM-purple (Roche/BMB) was used as a chromagen to localize hybridized probe. Embryos were subsequently embedded in paraffin and 5μm sections cut for counterstaining with nuclear fast red. For dual-color labeling, embryos were hybridized simultaneously with a fluorescein-UTP *Gcm2* probe and a digoxygenin-UTP *Foxn1* probe. Antibody incubations and color reactions were carried out sequentially with Fast Red and BM-purple, with a 0.1M Glycine, pH 2.2 wash after the first color reaction. Histochemical detection of β-galactosidase was as described (Nehls et al., 1996). After lacZ staining embryos were embedded in paraffin and 7μm sections cut and counterstained with eosin.

References

Akiyama, Y., Hosoya, T., Poole, A. M., and Hotta, Y., 1996. The gcm-motif: a novel DNA-binding motif conserved in Drosophila and mammals. Proc. Natl. Acad. Sci. USA 93, 14912-6.

Blackburn, C. C., Augustine, C. L., Li, R., Harvey, R. P., Malin, M. A., Boyd, R. L., Miller, J. F., and Morahan, G., 1996. The nu gene acts cell-autonomously and is required for differentiation of thymic epithelial progenitors. Proc. Natl. Acad. Sci. USA 93, 5742-6.

Cordier, A. C., and Haumont, S. M., 1980. Development of thymus, parathyroids, and ultimobranchial bodies in NMRI and Nude mice. Am. J. Anat. 157, 227-263.

Gunther, T., Chen, Z. F., Kim, J., Priemel, M., Rueger, J. M., Amling, M., Moseley, J. M., Martin, T. J., Anderson, D. J., and Karsenty, G., 2000. Genetic ablation of parathyroid glands reveals another source of parathyroid hormone. Nature 406, 199-203.

Hosoya, T., Takizawa, K., Nitta, K., and Hotta, Y., 1995. glial cells missing: a binary switch between neuronal and glial determination in Drosophila. Cell 82, 1025-36.

Jones, B. W., Fetter, R. D., Tear, G., and Goodman, C. S., 1995. glial cells missing: a genetic switch that controls glial versus neuronal fate. Cell 82, 1013-23.

Kaestner, K. H., Knochel, W., and Martinez, D. E., 2000. Unified nomenclature for the winged helix/forkhead transcription factors. Genes Dev. 14, 142-6.

Kim, J., Jones, B. W., Zock, C., Chen, Z., Wang, H., Goodman, C. S., and Anderson, D. J., 1998. Isolation and characterization of mammalian homologs of the Drosophila gene glial cells missing. Proc. Natl. Acad. Sci. USA 95, 12364-9.

Manley, N. R., and Capecchi, M. R., 1995. The role of *hoxa-3* in mouse thymus and thyroid development. Development 121, 1989-2003.

Nehls, M., Kyewski, B., Messerle, M., Waldschütz, R., Schüddekopf, K., Smith, A. J., and Boehm, T., 1996. Two genetically separable steps in the differentiation of thymic epithelium. Science 272, 886-9.

Nehls, M., Pfeifer, D., Schorpp, M., Hedrich, H., and Boehm, T., 1994. New member of the winged-helix protein family disrupted in mouse and rat nude mutations. Nature 372, 103-7.

Vincent, S., Vonesch, J. L., and Giangrande, A., 1996. Glide directs glial fate commitment and cell fate switch between neurones and glia. Development 122, 131-9.

Acknowledgements

The authors thank T. Boehm for the *whn-lacZ* mice, and Sammy Navarre (MCG) and Jane Brennan (CGR) for technical assistance. We thank B. Condie for critical reading of the manuscript. This work was supported by: NIH grant HD35920 (NRM), the Medical Research Council (JG), the Wellcome Trust (ARB and CCB), and travel grants to JG from the British Society for Developmental Biology and the British Society for Immunology.

Figure Legend

Figure 1. Expression of *Gcm2* and *Foxn1* in the developing third pharyngeal pouch. (A,B, C, D) Views of (A) E8.5, (B) E9.5, (C) E10.5, and (D) hemisected E11.5 embryos showing Gcm2 expression in the 3rd pharyngeal pouch by whole mount *in situ* hybridization. (E) Coronal and (F) sagittal sections through the third pharyngeal pouch of (E) E10.5 and (F) E11.5 embryos following whole mount *in situ* hybridization to show Gcm2 expression. (G) Lateral view of hemisected E11.5 embryo after dual-color whole mount *in situ* hybridization showing *Foxn1* (red) and *Gcm2* (blue) expression in the organ primordium developing from the third pharyngeal pouch. Anterior is up, dorsal is to the right. (H,I,J) Sagittal sections through the third pharyngeal pouch of (H) E10.5, (I) E11.25 and (J) E11.5 embryos following whole mount lacZ staining to show *Foxn1* expression. Orientations: (A) Ventral view, anterior is up. (B-D) lateral views, dorsal is down and cranial is to the left. (E) Anterior is up. (F, G, H, I, J) Anterior is up, dorsal is to the right. H, heart. 1,2, pharyngeal arches. II,III, pharyngeal pouches. Scale bars, (A) 250μm; (B, C, G) 350μm; (E, F, H, I, J) 100μm; (D) 575μm.

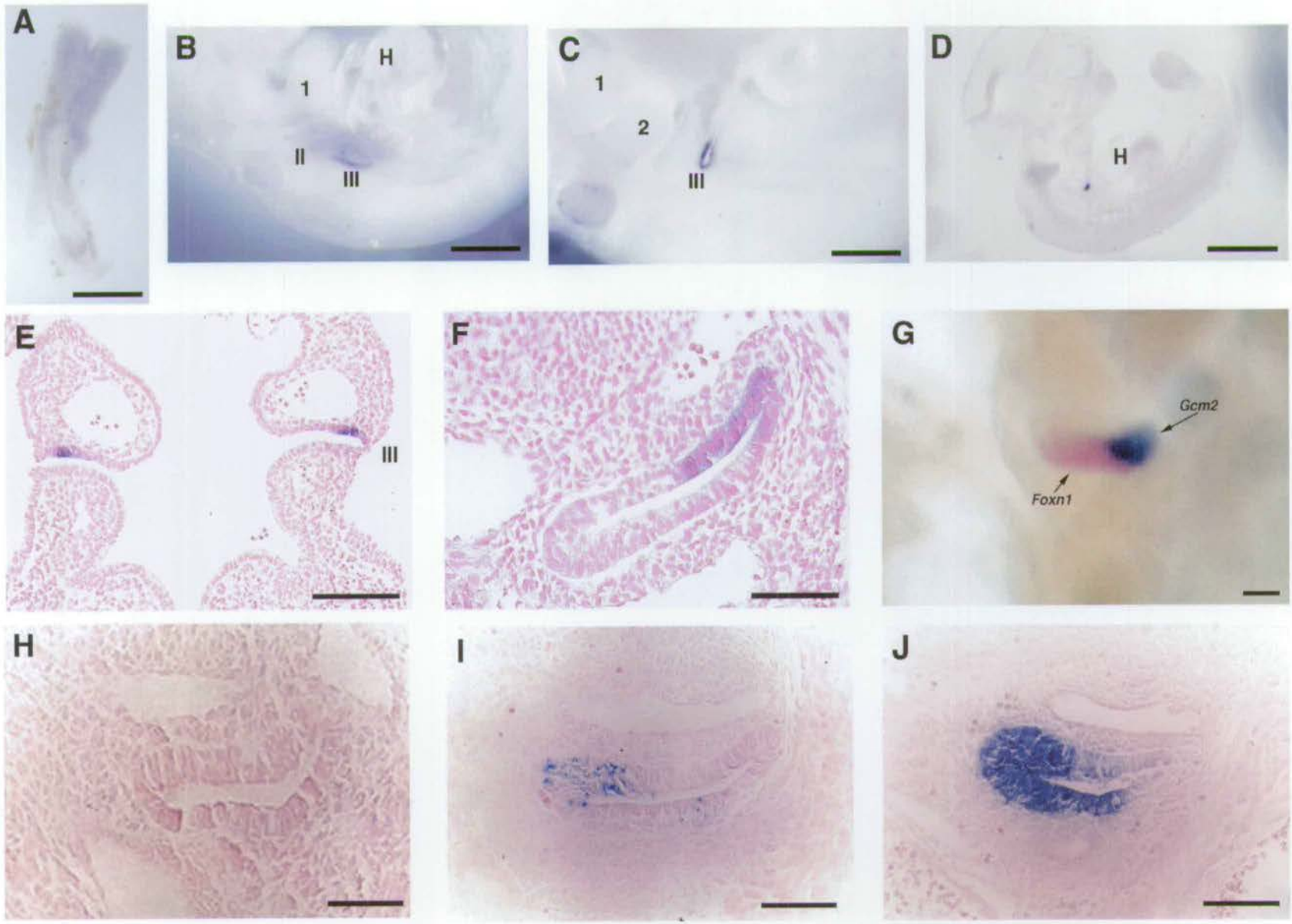
A
B
H
1
II
III
C
1
2
III
D
H
E
III
F
G
Gcm2
Foxn1
H
I
J

Abbreviations

ß-gal	ß-galactosidase
bp	base pairs
BMP	Bone morphogenetic protein
cDNA	complementary deoxyribonucleic acid
CK	Cytokeratin
CMJ	Cortico-medullary junction
CTES	Clusters of thymic epithelial staining
DC	Dendritic cell
DNA	deoxyribonucleic acid
DP	double positive thymocytes
ECM	Extracellular matrix
EGF	Epidermal growth factor
FACS	Fluorescence activated cell sorting
FGF	Fibroblast growth factor
HC	Hassall's corpuscles
HNF	Hepatocyte nuclear factor
HRP	Horse-radish peroxidase
HSC	Hematopoietic stem cell
IFN	Interferon
IL	Interleukin
IGF	Insulin-like growth factor
IRS	Inner root sheath
kDa	kiloDalton
mAb	Monoclonal antibody
MEF	Murine embryonic fibroblast
MHC	Major histocompatibility complex

MTS	Mouse thymic stromal
ORS	Outer root sheath
PVS	Perivascular space
RAG	Recombination-activating gene
RNA	ribonucleic acid
RT-PCR	reverse transcription polymerase chain reaction
RTOC	Reaggregate thymic organ culture
SCID	Severe combined immunodeficiency
SHH	Sonic hedgehog
SP	single positive thymocytes
TCR	T-cell receptor
TE	Thymic epithelium
TEC	Thymic epithelial cell
TECK	Thymus expressed chemokine
TEPC	Thymic epithelial progenitor cell
TGF	Transforming growth factor
TN	Triple negative thymocytes
TNC	Thymic nurse cell

List of figures

List of tables

References

Abbas, A.K., Lichtman, A.H. and Pober, J.S. (1997). Cellular and molecular immunology. 3rd ed. , Saunders.

Alison, M. 1998. Liver stem cells: a two compartment system. Curr. Opin. Cell Biol.l 10(6): 710-715.

Amagai, T., Itoi, M. and Kondo, Y. 1995. Limited development capacity of the earliest embryonic murine thymus. Eur. J. Immunol.l 25: 757 - 762.

Amman, A.J., Wara, D.W., Cowan, M.J., Barrrett, D.J. and Stiehm, E.R. 1982. The DiGeorge syndrome and the fetal alcohol syndrome. Am. J. Dis. Child.l 136: 906-908.

Anderson, G., Anderson, K.L., Tchilian, E.Z., Owen, J.J.T. and Jenkinson, E.J. 1997. Fibroblast dependency during early thymocyte development maps to the $CD25^+$ $CD44^+$ stage and involves interactions with fibroblast matrix molecules. Eur. J. Immunol.l 27: 1200-1206.

Anderson, G., Hare, K.J. and Jenkinson, E.J. 1999. Positive selection of thymocytes: the long and winding road. Immunol. Todayl 20(10): 463-468.

Anderson, G., Hare, K.J., Platt, N. and Jenkinson, E.J. 1997. Discrimination between maintenance- and differentiation-inducing signals during initial and intermediate stages of positive selection. Eur. J. Immunol.l 27(8): 1838-42.

Anderson, G., Harman, B.C., Hare, K.J. and Jenkinson, E.J. 2000. Microenvironmental regulation of T cell development in the thymus. Seminars in Immunolgyl 12: 457-464.

Anderson, G., Jenkinson, E.J., Moore, N.C. and Owen, J.J.T. 1993. MHC class II positive epithelium and mesenchyme cells are both required for T-cell development in the thymus. Naturel 362: 70 - 73.

Anderson, G., Moore, N.C., Owen, J.J.T. and Jenkinson, E.J. 1996. Cellular interactions in thymocyte development. Annu. Rev. Immunol.l 14: 73 - 99.

Anderson, G., Owen, J.J.T., Moore, N.C. and Jenkinson, E.J. 1994. Thymic epithelial cells provide unique signals for positive selection of $CD4^+CD8^+$ thymocytes in vitro. J. Exp. Med.l 179: 2027 - 2031.

Anderson, K.L., Moore, N.C., McLoughlin, D.E., Jenkinson, E.J. and Owen, J.J. 1998. Studies on thymic epithelial cells in vitro. Dev. Comp. Immunol.l 22(3): 367-77.

Anderson, M., Anderson, S.K. and Farr, A.G. 2000. Thymic vasculature: organizer of the medullary epithelial compartment? Int. Immunol.l 12(7): 1105-1110.

Anderson, S.J., Levin, S.D. and Perlmutter, R.M. 1993. Protein tyrosine kinase $p56^{lck}$ controls allelic exclusion of T-cell receptor β-chain genes. Naturel 365: 552-554.

Ardavin, C. 1997. Thymic dendritic cells. Immunol. Todayl 18(7): 350-61.

Ardavin, C., Wu, L., Li, C.L. and Shortman, K. 1993. Thymic dendritic cells and T cells develop simultaneously in the thymus from a common precursor population. Naturel 362(6422): 761-763.

Auerbach, R. 1960. Morphogenetic interactions in the development of the mouse thymus gland. Dev. Biol.l 2: 271 - 284.

Aurrand-Lions, M., Galland, F., Bazin, H., Zakharyev, V.M., Imhof, B.A. and Naquet, P. 1996. Vanin-1, a novel GPI-linked perivascular molecule involved in thymus homing. Immunityl 5(5): 391-405.

Bach, S.P., Renehan, A.G. and Potten, C.S. 2000. Stem cells: the intestinal stem cell as a paradigm. Carcinogenesisl 21(3): 469-476.

Bertho, J.M., Demarquay, C., Moulian, N., Van Der Meeren, A., Berrih-Aknin, S. and Gourmelon, P. 1997. Phenotypic and immunohistological analyses of the human adult thymus: evidence for an active thymus during adult life. Cell. Immunol.l 179(1): 30-40.

Berzins, S.P., Davey, G.M., Randle-Barrett, E.S., Malin, M.A., Classon, B.J., Fraser, S. and Boyd, R.L. 1999. Thymic shared antigen-2: a novel cell surface marker associated with T cell differentiation and activation. J. Immunol.l 162: 5119-5126.

Bjerknes, M. and Cheng, H. 1999. Clonal analysis of mouse intestinal epithelial progenitors. Gastroenterologyl 116(1): 7-14.

Blackburn, C.C., Augustine, C.L., Li, R., Harvey, R.P., Malin, M.A., Boyd, R.L., Miller, J.F.A.P. and Morahan, G. 1996. The *nu* gene acts cell-autonomously and is required for differentiation of thymic epithelial progenitors. Proc. Nat. Acad. Sci. USAl 93: 5742 - 5746.

Bockman, D.E. and Kirby, M.L. 1984. Dependance of thymus development on derivatives of the neural crest. Sciencel 223: 498 - 500.

Bogden, A.E., Haskell, P.M., LePage, D.J., Kelton, D.E., Cobb, W.R. and Esber, H.J. 1979. Growth of human tumour xenografts implanted under the renal capsule of normal immunocompetent mice. Exp. Cell Biol.l 47(4): 281-293.

Bosma, G.C., Custer, R.P. and Bosma, M.J. 1983. A severe combined immunodeficiency mutation in the mouse. Naturel 301: 527-530.

Boyd, R. and Chidgey, A. 2000. T-cell development and function - a downunder experience. Immunol. Todayl 21(10): 472-474.

Boyd, R.L., Tucek, C.L., Godfrey, D.I., Izon, D.J., Wilson, T.J., Davidson, N.J., Bean, A.G., Ladyman, H.M., Ritter, M.A. and Hugo, P. 1993. The thymic microenvironment. Immunol. Todayl 14(9): 445 - 459.

Brekelmans, P. and van Ewijk, W. 1990. Phenotypic characterisation of murine thymic microenvironments. Seminars in Immunologyl 2: 13 - 24.

Brissette, J.L., Li, J., Kamimura, J., Lee, D. and Dotto, G.P. 1996. The product of the mouse nude locus, Whn, regulates the balance between epithelial cell growth and differentiation. Genes and Dev.l 10(17): 2212-21.

Burkly, L., Hession, C., Ogata, L., Reilly, C., Marconi, L.A., Olson, D., Tizard, R., Cate, R. and Lo, D. 1995. Expression of relB is required for the development of thymic medulla and dendritic cells. Naturel 373(6514): 531-6.

Capone, M., Romagnoli, P., Beermann, F., MacDonald, H.R. and van Meerwijk, J.P. 2001. Dissociation of thymic positive selection and negative selection in transgenic mice expressing major histocompatibility complex class I molecules exclusively on thymic cortical epithelial cells. Bloodl 97(5): 1336-1342.

Carding, S.R., Hayday, A.C. and Bottomly, K. 1991. Cytokines in T-cell development. Immunol. Todayl 12(7): 239-45.

Chang, A.C., Wadsworth, S. and Coligan, J.E. 1993. Expression of merosin in the thymus and its interaction with thymocytes. J. Immunol.l 151(4): 1789-801.

Chen, U. and Kosco, M. 1993. Differentiation of mouse embryonic stem cells in vitro: III. Morphological evaluation of tissues developed after implantation of differentiated mouse embryoid bodies. Dev. Dyn.l 197(3): 217-226.

Chiang, C., Litingtung, Y., Lee, E., Young, K.E., Corden, J.L., Westphal, H. and Beachy, P.A. 1996. Cyclopia and defective axial patterning in mice lacking Sonic hedgehog gene function. Naturel 383(6599): 407-13.

Chisaka, O. and Capecchi, M.R. 1991. Regionally restricted devlopmental defects resulting from targeted disruption of the mouse homeobox gene hox-1.5. Naturel 350: 473 - 479.

Chou, M.Y., Chang, A.L.C., McBride, J., Dunoff, B., Gallagher, G.T. and Wong, D.T.W. 1990. A Rapid method to determine proliferation patterns of normal and malignant tissues by H3 mRNA in situ hybidisation. Am. J. Pathol.l 136(4): 729-733.

Clevers, H. 2000. Axin and hapatocellular carcinomas. Nature Geneticsl 24: 206-208.

Colic, M., Matanovic, L., Hegedis, L. and Dujic, A. 1988. Immunohistochemical characterisation of rat thymic non-lymphoid cells.I. Epithelial and mesenchymal components defined by monoclonal antibodies. Immunol.l 65: 277 - 284.

Cordier, A.C. 1974. Ultrastructure of the thymus in "nude" mice. J. Ultrastruct. Res.l 47: 26-40.

Cordier, A.C. and Haumont, S.M. 1980. Development of thymus, parathyroids and ultimo-branchial bodies in NMRI and nude mice. Amer. J. Anat.l 157: 227 - 263.

Cordier, A.C. and Heremans, J.F. 1975. Nude mouse embryo:ectodermal nature of the primordial thymic defect. Scand. J. Immunol.l 4: 193 - 196.

DasGupta, R. and Fuchs, E. 1999. Mutiple roles for activated LEF/TCF transcription complexes during hair follicle development and differentiation. Developmentl 126: 4557-4568.

DeKoning, J., DiMolfetto, L., Reilly, C., Wei, Q., Harvan, W.L. and Lo, D. 1997. Thymic cortical epithelium is sufficient for the development of mature T cells in relB-deficient mice. J. Immunol.l 158: 2558 - 2566.

Deman, J., Van Meurs, M., Claassen, E., Humblet, C., Boniver, J. and Defresne, M.P. 1996. In vivo expression of interleukin-1 beta (IL-1 beta), IL-2, IL-4, IL-6, tumour necrosis factor-alpha and interferon-gamma in the fetal murine thymus. Immunologyl 89(1): 152-7.

Douek, D.C., McFarland, R.D., Keiser, P.H., Gage, E.A., Massey, J.M., Haynes, B.F., Polis, M.A., Haase, A.T., Feinberg, M.B., Sullivan, J.L., Jamieson, B.D., Zack, J.A., Picker, L.J. and Koup, R.A. 1998. Changes in thymic function with age and during the treatment of HIV infection. Naturel 396: 690-695.

Dunon, D. and Imhof, B.A. 1993. Mechanisms of thymus homing. Bloodl 81: 1 - 8.

Dunon, D., Kaufman, J., Salomonsen, J., Skjoedt, K., Vainio, O., Thiery, J.P. and Inhof, B.A. 1990. T-cell precursor migration towards beta-2-microglobulin is involved in thymus colonization of chicken embryos. EMBO Journall 9(10): 3315 - 3322.

Dytham, C. (1999). Choosing and using statistics: A biologist's guide. , Blackwell Science.

Engelhard, V.H. 1994. How cells process antigens. Scientific Americanl 271(2): 44-51.

Fairchild, P.J. and Waldmann, H. 2000. Extrathymic signals regulate the onset of T cell repertoire selection. Eur. J. Immunol.l 30(7): 1948-1956.

Farr, A., Nelson, A., Truex, J. and Hosier, S. 1991. Epithelial heterogeneity in the murine thymus: A cell surface glycoprotein expressed by subcapsular and medullary epithelium. J Histochem. Cytochem.l 39(5): 645 - 653.

Farr, A.G. and Braddy, S.C. 1989. Patterns of keratin expression in the murine thymus. Anat. Rec.l 224: 374 - 378.

Fine, J.S. and Kruisbeek, A.M. 1991. The role of LFA-1/ICAM-1 interactions during murine T lymphocyte development. J. Immunol.l 147(9): 2852-9.

Fischer, A. and Malissen, B. 1998. Natural and engineered disorders of lymphocyte development. Sciencel 280: 237-243.

Flanagan, S.P. 1966. 'Nude', a new hairless gene with pleiotropic effects in the mouse. Genet. Res.l 8: 295.

Fontaine-Perus, J., Calman, F.M., Kaplan, C. and Le Douarin, N.M. 1981. Seeding of the 10-day mouse embryo thymic rudiment by lymphocyte precursors in vitro. J Immunol.l 126(6): 2310 - 2316.

Frank, J., Pignata, C., Panteleyev, A.A., Prowse, D.M., Baden, H., Weiner, L., Gaetaniello, L., Ahmad, W., Pozzi, N., Cserhalmi-Friedman, P.B., Aita, V.M., Uyttendaele, H., Gordon, D., Ott, J., Brissette, J.L. and Christiano, A.M. 1999. Exposing the human nude phenotype [letter]. Naturel 398(6727): 473-4.

Fukuda, M. and Tsuboi, S. 1999. Mucin-type O-glycans and leukosialin. Biochim. Biophys. Acta.l 1455(2-3): 205-217.

Gage, F.H. 2000. Mammalian neural stem cells. Sciencel 287(5457): 1433-1438.

Ge, Q. and Chen, W.-F. 2000. Effect of murine thymic epithelial cell line (MTEC1) on the functional expression of $CD4^+CD8^-$ thymocyte subgroups. Int. Immunol.l 12(8): 1127-1133.

Ge, Q. and Chen, W.F. 1999. Phenotypic identification of the subgroups of murine T-cell receptor $\alpha\beta^+CD4^+CD8^-$ thymocytes and its implications in the late stage of thymocyte development. Immunologyl 97: 665-671.

George, A.J.T. and Ritter, M.A. 1996. Thymic involution with ageing: obsolescence or good housekeeping? Immunol. Todayl 17(6): 267-271.

Godfrey, D.I., Izon, D.J., Tucek, C.L., Wilson, T.J. and Boyd, R.L. 1990. The phenotypic heterogeneity of mouse thymic stromal cells. Immunologyl 70: 66 - 74.

Godfrey, D.I., Kennedy, J., Suda, T. and Zlotnik, A. 1993. A developmental pathway involving four phenotypically and functionally distinct subsets of $CD3^-CD4^-CD8^-$ triple-negative adult mouse thymocytes defined by CD44 and CD25. J. Immunol.l 150: 4244-4252.

Goldrath, A.W. and Bevan, M.J. 1999. Selecting and maintaining a diverse T-cell repertoire. Naturel 402: 255-262.

Gordon, J., Bennett, A.R., Blackburn, C.C. and Manley, N.R. 2001. Gcm2 and Foxn1 mark parathyroid- and thymus-specific domains in the developing third pharyngeal pouch. Mechanisms of Developmentl In Press.

Gunther, T., Chen, Z.-F., Kim, J., Priemel, M., Reuger, J.M., Amling, M., Moseley, J.M., Martin, T.J., Anderson, D.J. and Karsenty, G. 2000. Genetic ablation of parathyroid glands reveals another source of parathyroid hormone. Naturel 406: 199-203.

Hammond, W.S. 1954. Origin of thymus in the chick embryo. J. Morphol.l 95: 501-521.

Hardy, M.H. 1992. The secret life of the hair follicle. Trends. Genet.l 8(2): 55-61.

Hare, K.J., Jenkinson, E.J. and Anderson, G. 1999. CD69 expression discriminates MHC-dependent and -independent stages of thymocyte positive selection. J. Immunol.l 162: 3978-3983.

Hare, K.J., Jenkinson, E.J. and Anderson, G. 1999. In vitro models of T cell development. Semin Immunoll 11(1): 3-12.

Hassid, S., Choufani, G., Delbrouch, C. and Danguy, A. 2000. Mucins and secreted factors. Acta Otorhinolaryngol Belgl 54(3): 249-254.

Haynes, B.F., Scearce, R.M., Lobach, D.F. and Hensley, L.L. 1984. Phenotypic characterisation and ontogeny of mesodermal derived and endocrine components of the human thymic microenvironment. J. Exp. Medl 159: 1149 - 1168.

Hoffmann, M.W., Allison, J. and Miller, J.F. 1992. Tolerance induction by thymic medullary epithelium. Proc. Natl. Acad. Sci. USAl 89(7): 2526-30.

Hogan, B., Beddington, R., Costantini, F. and Lacy, E. (1994). Manipulating the Mouse Embryo. Second edition. , Cold Spring Harbor Laboratory Press.

Holland, N.D., Holland, L.Z. and Kozmik, Z. 1995. An Amphioxus Pax gene, Amphipax1, expressed in the embryonic endoderm, but not in mesoderm: Implications for the evolution of class I paired box genes. Mol. marine Biol. Biotechnoll 4: 206-214.

Hollander, G.A., Wang, B., Nichogiannopoulou, A., Platenburg, P.P., van Ewijk, W., Burakoff, S.J., Gutierrez-Ramos, J.-C. and Terhorst, C. 1995. Developmental control point in the induction of thymic cortex regulated by a subpopulation of prothymocytes. Naturel 373: 350 - 353.

Hong, R. 1991. The DiGeorge anomaly. Immunodefic. Rev.l 3(1): 1-14.

Hueber, A.O., Pierres, M. and He, H.T. 1992. Sulfated glycans directly interact with mouse Thy-1 and negatively regulate Thy-1-mediated adhesion of thymocytes to thymic epithelial cells. J. Immunol.l 148(12): 3692-9.

Imami, N., Ladyman, H.M., Spanopoulou, E. and Ritter, M.A. 1992. A novel adhesion molecule in the murine thymic microenvironment: Functional and biochemical analysis. Dev. Immunol.l 2: 161 - 173.

Itoi, M. and Amagai, T. 1998. Inductive role of fibroblastic cell lines in development of the mouse thymus anlage in organ culture. Cell. Immunol.l 183(1): 32-41.

Izon, D.J., Nieland, J.D., Godfrey, D.I., Boyd, R.L. and Kruisbeek, A.M. 1994. Flow cytometric analysis reveals unexpected shared antigens between histologically defined populations of thymic stromal cells. Int. Immunol.l 6(1): 31-9.

Jamieson, B.D., Douek, D.C., Killian, S., Hultin, L.E., Scripture-Adams, D.D., Giorgi, J.V., Marelli, D., Koup, R.A. and Zack, J.A. 1999. Generation of functional thymocytes in the human adult. Immunityl 10(5): 569-75.

Jenkinson, E.J., Franchi, L.L., Kingston, R. and Owen, J.J.T. 1982. Effect of deoxyguanosine on lymphopoiesis in the developing thymus rudiment in vitro: application in the production of chimeric thymus rudiments. Eur. J. Immunol.l 12: 583-587.

Jenkinson, E.J., van Ewijk, W. and Owen, J.T.T. 1981. Major histocompatibility complex antigen expression on the epithelium of the developing thymus in normal and nude mice. J Exp. Med.l 153(2): 280 - 292.

Jensen, U.B., Lowell, S. and Watt, F.M. 1999. The spatial relationship between stem cells and their progeny in the basal layer of human epidermis: a new view based on whole-mount labelling and lineage analysis. Developmentl 126: 2409-2418.

Jiang, X., Rowitch, D.H., Soriano, P., McMahon, A.P. and Sucov, H.M. 2000. Fate of the mammalian cardiac neural crest. Developmentl 127: 1607-1616.

Jones, G.V., Botham, C.A. and Kendall, M.D. 1999. Use of cultured thymic tissues for the regeneration of the thymus. Neuroimmunomodulationl 6(1-2): 6-22.

Jones, P.H. and Watt, F.M. 1993. Separation of human epithelial stem cells from transit amplifying cells on the basis of differences in integrin function and expression. Celll 73: 713-724.

Jotereau, F., Heuze, F., Salomon-Vie, V. and Gascan, H. 1987. Cell kinetics in the fetal mouse thymus: precursor cell input, proliferation, and emigration. J. Immunol.l 138(4): 1026-30.

Jotereau, F.V., Houssaint, E. and Le Douarin, N.M. 1980. Lymphoid stem cell homing to the early thymic primordium of the avian embryo. Eur J. Immunol.l 10(8): 620-627.

Jotereau, F.V. and Le Douarin, N.M. 1982. Demonstration of a cyclic renewal of the lymphocyte precursor cells in the quail thymus during embryonic and perinatal life. J. Immunol.l 129(5): 1869 - 1877.

Juan, G., Traganos, F., James, W.M., J.M., R., Roberge, M., Sauve, D.M., Anderson, H. and Darzynkiewicz, Z. 1998. Histone H3 phosphorylation and expression of cyclins A and B1 measured in individual cells during their progression through G2 and mitosis. Cytometryl 32(2): 71-77.

Kaestner, K.H., Knochel, W. and Martinez, D.N. 2000. Unified nomenclature for the winged helix / forkhead transcription factors. Genes and Developmentl 14: 142-146.

Kampinga, J., Berges, S., Boyd, R., Brekelmans, P., Colic, M., van Ewijk, W., Kendall, M., Ladyman, H., Nieuwenhuis, P., Ritter, M., Schuurman, H.J. and Tournefier, A. 1989. Thymic epithelial antibodies: Immunohistological analysis and introduction of nomenclature. Thymusl 13: 165 - 173.

Kanariou, M., Huby, R., Ladyman, H., Colic, M., Sivolapenko, G., Lampert, I. and Ritter, M. 1989. Immunosuppression with cyclosporin A alters the thymic microevironment. Clin. Exp. Immunol.l 78: 263 - 270.

Karam, S.M. 1999. Lineage commitment and maturation of epithelial cells in the gut. Front. Biosci.l 4: D286-298.

Kaufman, M.H. (1992). The atlas of mouse development. London, Academic Press.

Kaufmann, E. and Knochel, W. 1996. Five years on the wings of fork head. Mech Devl 57(1): 3-20.

Kawamoto, H., Ohmura, K. and Katsura, Y. 1998. Presence of progenitors restricted to T, B, or myeloid lineage, but absence of multipotent stem cells, in the murine fetal thymus. J. Immunol.l 161(8): 3799-802.

Kecha, O., Brilot, F., Martens, H., Franchimont, N., Renard, C., Greimers, R., Desfresne, M.P., Winkler, R. and Geenen, V. 2000. Involvement of insulin-like growth factors in early T cell development: a study using fetal thymic organ cultures. Endocrinologyl 141(3): 1209-1217.

Kendall, M.D. 1991. Functional anatomy of the thymic microenvironment. J. Anat.l 177: 1-29.

Kendall, M.D. and Boyd, R. (1991). The diversity of thymic epithelial cells. Lymphatic tissues and in vivo immune responses. B.A. Imhof, S. Berrih-Aknin and S. Ezine, Marcel Dekker: 11 - 14.

Kendall, M.D., Schuurman, H.J., Fenton, J., Broekhuizen, R. and Kampinga, J. 1988. Implantation of cultured thymic fragments in congenitally athymic (nude) rats. Ultastructural characteristics of the developing microenvironment. Cell Tissue Res.l 254(2): 283-294.

Kim, J., Jones, B.W., Zock, C., Chen, Z., Wang, H., Goodman, C.S. and Anderson, D.J. 1998. Isolation and characterisation of mammalian homologs of the Drosophila gene glial cells missing. Proc. Natl. Acad. Sci. USAl 95: 12365-12369.

Kim, M.G., Lee, G., Lee, S.-K., Lolkema, M., Yim, J., Hong, S.H. and Schartz, R.H. 2000. Epithelial cell-specific laminin 5 is required for survival of early thymocytes. J. Immunol.l 165: 192-201.

Kinebuchi, M., Ide, T., Lupin, D., Tamatani, T., Miyasaka, M., Matsuura, A., Nagai, Y., Kikuchi, K. and Uede, T. 1991. A novel cell-surface antigen involved in thymocyte and thymic epithelial-cell adhesion. J. Immunol.l 146(11): 3721 - 3728.

Kingston, R., Jenkinson, E.J. and Owen, J.J.T. 1984. Characterization of stromal cell populations in the developing thymus of normal and nude mice. Eur. J. Immunol.l 14: 1052-1056.

Klein, L. and Kyewski, B. 2000. Self-antigen presentation by thymic stromal cells: a subtle division of labour. Curr. Opin. Immunol.l 12: 179-186.

Klug, D.B., Carter, C., Crouch, E., Roop, D., Conti, C.J. and Richie, E.R. 1998. Interdependence of cortical thymic epithelial cell differentiation and T-lineage commitment. Proc. Natl. Acad. Sci. USAl 95(20): 11822-7.

Klug, D.B., Crouch, E., Carter, C., Coghlan, L., Conti, C.J. and Richie, E.R. 2000. Transgenic expression of cyclin D1 in thymic epithelial precursors promotes epithelial and T cell development. J. Immunol.l 164: 1881-1888.

Kobayashi, N., Fujiwara, T., Westerman, K.A., Inoue, Y., Sakaguchi, M., Noguchi, H., Maiyazaki, M., Cai, J., Tanaka, N., Fox, I.J. and Leboulch, P. 2000. Prevention of acute liver failure in rats with reversibly immortalized human hepatocytes. Sciencel 287(5456): 1258-1262.

Kondo, M., Weissman, I.L. and Akashi, K. 1997. Identification of clonogenic common lymphoid progenitors in mouse bone marrow. Celll 91: 661-672.

Kopf-Maier, P., Mboneko, V.F. and Merker, H.J. 1990. Nude mice are not hairless. A morphological study. Acta. Anat.l 139(2): 178-90.

Korinek, V., Barker, N., Moerer, P., van Donselaar, E., Huls, G., Peters, P.J. and Clevers, H. 1998. Depletion of epithelial stem-cell compartments in the small intestine of mice lacking Tcf-4. Nature Geneticsl 19: 379-383.

Krumlauf, R. 1994. Hox genes in vertebrate devlopment. Celll 78: 191-201.

Kuratani, S. and Bockman, D.E. 1990. Impaired development of the thymic primordium after neural crest ablation. Anat. Rec.l 228(2): 185-90.

Kurooka, H., Segre, J.A., Hirano, Y., Nemhauser, J.L., Nishimura, H., Yoneda, K., Lander, E.S. and Honjo, T. 1996. Rescue of the hairless phenotype in nude mice by transgenic insertion of the wild-type Hfh11 genomic locus. Int. Immunol.l 8(6): 961-6.

Ladyman, H., Boyd, R.L., Brekelmans, P., Colic, M., van Ewijk, W., von Gaudecker, B., Kampinga, J., Kendall, M., Nieuwenhuis, P., Schuurman, H.-J., Tournefier, A.

and Ritter, M. 1991. Monoclonal antiepithelial antibody workshop II. Flow cytometic and bichemical analysis of thymic epithelial cell heterogeneity. Exp. Med. Biol.l 238: 15 - 20.

Lampert, I.R. and Ritter, M.A. 1988. The origin of the diverse epithelial cells in the thymus: is there a common stem cell? Thymus updatel 1: 5-25.

Lannes-Vieira, J., Chammas, R., Villa-Verde, D.M., Vannier-dos-Santos, M.A., Mello-Coelho, V., de Souza, S.J., Brentani, R.R. and Savino, W. 1993. Extracellular matrix components of the mouse thymic microenvironment. III. Thymic epithelial cells express the VLA6 complex that is involved in laminin-mediated interactions with thymocytes. Int. Immunol.l 5(11): 1421-30.

Laufer, T.M., DeKoning, J., Markowitz, J.S., Lo, D. and Glimcher, L.H. 1996. Unopposed positive selection and autoreactivity in mice expressing class II MHC only on thymic cortex. Naturel 383: 81 - 85.

Laufer, T.M., Glimcher, L.H. and Lo, D. 1999. Using thymus anatomy to dissect T cell repertoire selection. Semin. Immunol.l 11(1): 65-70.

Le Douarin, N.M. and Jotereau, F.V. 1975. Tracing of cells of the avian thymus through embryonic life in interspecific chimeras. J. Exp. Med.l 142: 17 - 40.

Lee, D., Prowse, D.M. and Brissette, J.L. 1999. Association between Mouse nude Gene Expression and the Initiation of Epithelial Terminal Differentiation. Dev. Biol.l 208(2): 362-374.

MacNeil, I., Kennedy, J., Godfrey, D.I., Jenkins, N.A., Mascianotonio, M., Mineo, C., Gilbert, D.J., Copeland, N.G., Boyd, R.L. and Zlontik, A. 1993. Isolation of a cDNA encoding thymic shared antigen-1. J.Immunol.l 151(12): 6913-6923.

Manley, N.R. 2000. Thymus organogenesis and molecular mechanisms of thymic epithelial cell differentiation. Semin. Immunol.l 12(5): 421-428.

Manley, N.R. and Capecchi, M.R. 1995. The role of Hoxa-3 in mouse thymus and thyroid development. Developmentl 121: 1989 - 2003.

Manley, N.R. and Capecchi, M.R. 1998. Hox group 3 paralogs regulate the development and migration of the thymus, thyroid, and parathyroid glands. Dev Bioll 195(1): 1-15.

Markert, M.L., Boeck, A., Hale, L.P., Kloster, A.L., McLaughlin, T.M., Batchvarova, A.M., Douek, D.C., Koup, R.A., Kostyu, D.D., Ward, F.E., Rice, H.E. and Mahaffey, S.M. 1999. Transplantation of thymus tissue in complete DiGeorge syndrome. New Engl. J. Med.l 341(16): 1180-1189.

Markert, M.L., Kostyu, D.D., Ward, F.E., McLaughlin, T.M., Watson, T.J., Buckley, R.H., Schiff, S.E., Ungerleider, R.M., Gaynor, J.W., Oldham, K.T., Mahaffey, S.M., Ballow, M., Driscoll, D.A., Hale, L.P. and Haynes, B.F. 1997. Successful formation of a chimeric human thymus allograft following transplantation of cultured postnatal human thymus. J. Immunol.l 158(2): 998-1005.

Marusic, M., Turkalj-Kljajic, M., Petrovecki, M., Uzarevic, B., Rudolf, M., Batinic, D., Ugljen, R., Anic, D., Cavar, Z., Jelic, I. and Malenica, B. 1998. Indirect demonstration of the lifetime function of human thymus. Clin. Exp. Immunol.l 111(2): 450-456.

Matsuzaki, Y., Gyotoku, J., Ogawa, M., Nishikawa, S., Katsura, Y., Gachelin, G. and Nakauchi, H. 1993. Characterization of c-kit positive intrathymic stem cells that are restricted to lymphoid differentiation. J. Exp. Med.l 178(4): 1283-92.

Mattes, M.J., Look, K., Lewis, J.L., Old, L.J. and Lloyd, K.O. 1985. Three mouse monoclonal antibodies to human differentiation antigens: reactivity with two mucin-like antigens and with connective tissue fibres. J. Histochem. Cytochem.l 33(11): 1095-1102.

McFarland, R.D., Douek, D.C., Koup, R.A. and Picker, L.J. 2000. Identification of a human recent thymic emigrant phenotype. Proc. Nat. Acad. Sci. USAl 97(8): 4215-4220.

McKay, R. 2000. Stem cells - hype and hope. Naturel 406: 361-364.

Meier, N., Dear, T.N. and Boehm, T. 1999. A novel serine protease overexpressed in the hair follicles of nude mice. Biochem. Biophys. Res. Commun.l 258(2): 374-8.

Meier, N., Dear, T.N. and Boehm, T. 1999. Whn and mHa3 are components of the genetic hierarchy controlling hair follicle differentiation. Mechanisms of developmentl 89: 215-221.

Meyers, E.N., Lewandoski, M. and Martin, G.R. 1998. An Fgf8 mutant allelic series generated by Cre- and Flp-mediated recombination. Nat Genetl 18(2): 136-41.

Miller, J.F.A.P. 1961. Immunological function of the thymus. Lancetl 2: 748 - 749.

Moll, R., Franke, W.W., Schiller, D.L., Geiger, B. and Krepler, R. 1982. The catalog of human cytokeratins: Patterns of expression in normal epithelia, tumours and cultured cells. Celll 31: 11 - 24.

Mombaerts, P., Iacomini, J., Johnson, R.S., Herrup, K., Tonegawa, S. and Papaioannou, V.E. 1992. RAG-1-deficient mice have no mature B and T lymphocytes. Celll 68: 869-877.

Montgomery, R.A. and Dallman, M.J. 1997. Semi-quantitative polymerase chain reaction analysis of cytokine and cytokine receptor gene expression during thymic ontogeny. Cytokinel 9(10): 717-26.

Moore, N.C., Anderson, G., Smith, C.A., Owen, J.J. and Jenkinson, E.J. 1993. Analysis of cytokine gene expression in subpopulations of freshly isolated thymocytes and thymic stromal cells using semiquantitative polymerase chain reaction. Eur. J. Immunol.l 23(4): 922-7.

Muller, K.M., Luedecker, C.J., Udey, M.C. and Farr, A.G. 1997. Involvement of E-cadherin in thymus organogenesis and thymocyte maturation. Immunityl 6(3): 257-64.

Muller, T.S., Ebensperger, C., Neubuser, A., Koseki, H., Balling, R., Christ, B. and Wilting, J. 1996. Expression of avian Pax1 and Pax9 is intrinsically regulated in the pharyngeal endoderm but depends on environmental influences in the paraxial mesoderm. Dev. Biologyl 178: 403-417.

Nabarra, B. and Papiernik, M. 1988. Phenotype of thymic stromal cells - an immunoelectron microscopic study with anti I-IA, anti I-Mac-1, and anti I-Mac-2 antibodies. Laboratory Investigationl 58(5): 524 - 531.

Nagy, A., Rossant, J., Nagy, R., Abramow-Newerly, W. and Roder, J.C. 1993. Derivation of completely cell culture-derived mice from early-passage embryonic stem cells. Proc. Natl. Acad. Sci USAl 90(18): 8424-8428.

Naquet, P., Naspetti, M. and Boyd, R. 1999. Development, organization and function of the thymic medulla in normal, immunodeficient or autoimmune mice. Semin. Immunol.l 11(1): 47-55.

Naspetti, M., AurrandLions, M., DeKoning, J., Malissen, M., Galland, F., Lo, D. and Naquet, P. 1997. Thymocytes and RelB-dependent medullary epithelial cells provide growth-promoting and organization signals, respectively, to thymic medullary stromal cells. Eur. J. Immunol.l 27(6): 1392 - 1397.

Nehls, M., Kyewski, B., Messerle, M., Waldschutz, R., Schuddekopf, K., Smith, A.J. and Boehm, T. 1996. Two genetically separable steps in the differentiation of thymic epithelium. Sciencel 272(5263): 886-9.

Nehls, M., Pfeifer, D., Schorpp, M., Hedrich, H. and Boehm, T. 1994. New member of the winged-helix protein family disrupted in mouse and rat nude mutations. Naturel 372(6501): 103-7.

Nelson, A.J., Dunn, R.J., Peach, R., Aruffo, A. and Farr, A.G. 1996. The murine homolog of human Ep-CAM, a homotypic adhesion molecule, is expressed by thymocytes and thymic epithelial cells. Eur. J. Immunol.l 26(2): 401-8.

Neubaser, A., Koseki, H. and Balling, R. 1995. Characterization and developmental expression of Pax9, a paired-box-containing gene related to Pax1. Dev. Biol.l 170(2): 701-716.

Nichogiannopoulou, A., Trevisan, M., Friedrich, C. and Georgopoulos, K. 1998. Ikaros in hemopoietic lineage determination and homeostasis. Seminars in Immunologyl 10: 119-125.

Nicolas, J.F., Savino, W., Reano, A., Brochier, J. and Dardenne, M. 1985. Heterogeneity of thymic epithelial cell (TEC) keratins. J. Histochem. Cytochem.l 33(7): 687 - 694.

Norment, A.M. and Bevan, M.J. 2000. Role of chemokines in thymocyte development. Seminars in Immunologyl 12: 445-455.

Oettinger, M.A., Schatz, D.G., Gorka, C. and Baltimore, D. 1990. RAG-1 and RAG-2, adjacent genes that synergistically activate V(D)J recombination. Sciencel 248: 1517-1523.

Oosterwegel, M.A., Haks, M.C., Jeffry, U., Murray, R. and Kruisbeek, A.M. 1997. Induction of TCR gene rearrangements in uncommitted stem cells by a subset of IL-7 producing, MHC class-II-expressing thymic stromal cells. Immunityl 6(3): 351-60.

Osborne, B. and Miele, L. 1999. Notch and immune system. Immunityl 11: 653-663.

Owen, J.J. and Moore, N.C. 1995. Thymocyte-stromal-cell interactions and T-cell selection. Immunol. Todayl 16(7): 336-8.

Owen, J.J.T. and Ritter, M.A. 1969. Tissue interaction in the development of thymus lymphocytes. J. Exp. Med.l 129: 431-442.

Palmer, D.B., George, A.J. and Ritter, M.A. 1997. Selection of antibodies to cell surface determinants on mouse thymic epithelial cells using a phage display library. Immunologyl 91(3): 473-8.

Palmer, D.B., Viney, J.L., Ritter, M.A., Hayday, A.C. and Owen, M.J. 1993. Expression of the alpha-beta-T-cell receptor is necessary for the generation of thymic medulla. Dev. Immunol.l 3(3): 175 - 179.

Pantelouris, E.M. 1968. Absence of thymus in a mouse mutant. Naturel 217: 370-371.

Parham, P. (2000). The immune system. , Garland publishing / Elsevier science.

Patel, D.D. and Haynes, B.F. 1993. Cell adhesion molecules involved in intrathymic T cell development. Semin. Immunol.l 5(4): 282-92.

Penit, C., Lucas, B., Vasseur, F., Rieker, T. and Boyd, R.L. 1996. Thymic medulla epithelial cells acquire specific markers by post- mitotic maturation. Dev Immunoll 5(1): 25-36.

Penit, C. and Vasseur, F. 1989. Cell proliferation and differentiation in the fetal and early postnatal mouse thymus. J. Immunol.l 142(10): 3369-77.

Peschon, J.J., Morrissey, P.J., Grabstein, K.H., Ramsdell, F.J., Maraskovsky, E., Gliniak, B.C., Park, L.S., Ziegler, S.F., Williams, D.E., Ware, C.B., Meyer, J.D. and Davison, B.L. 1994. Early lymphocyte expansion is severely impaired in interleukin 7 receptor-deficient mice. J. Exp. Medl 180: 1955-1960.

Peters, H., Doll, U. and Niessing, J. 1995. Differential expression of the chicken Pax-1 and Pax-9: in situ hybidization and immunohistochemical analysis. Dev. Dyn.l 203(1): 1-16.

Peters, H., Neubuser, A., Kratochwil, K. and Balling, R. 1998. Pax9-deficient mice lack pharyngeal pouch derivatives and teeth and exhibit craniofacial and limb abnormalities. Genes and Developmentl 12: 2735 - 2747.

Pignata, C., Gaetaniello, L., Masci, A.M., Frank, J., Christiano, A., Matrecano, E. and Racioppi, L. 2001. Human equivalent of the mouse Nude/SCID phenotype: long term evaluation of immunological reconstitution after bone marrow transplantation. Bloodl 97(4): 880-885.

Pitari, G., Malergue, F., Martin, F., Philippe, J.M., Massucci, M.T., Chabret, C., Maras, B., Dupre, S., Naquet, P. and Galland, F. 2000. Pantetheinase activity of membrane-bound vanin-1: lack of free cysteamine in tissues of vanin-1 deficient mice. FEBS lettersl 483(2-3): 149-154.

Potocnik, A.J., Brakebusch, C. and Fassler, R. 2000. Fetal and adult hematopoietic stem cells require ß1 integrin function for colonizing fetal liver, spleen, and bone marrow. Immunityl 12: 653-663.

Prowse, D.M., Lee, D., Weiner, L., Jiang, N., Magro, C.M., Baden, H.P. and Brissette, J.L. 1999. Ectopic expression of the nude gene induces hyperproliferation and defects in differentiation: Implications for the self-renewal of cutaneous epithelia. Dev. Biol.l 212: 54-67.

Ramiya, V.K., Maraist, M., Arfors, K.E., Schatz, D.A., Peck, A.B. and Cornelius, J.G. 2000. Reversal of insulin-dependent diabetes using islets generated in vitro from pancreatic stem cells. Nature Medicinel 6(3): 278-282.

Randle, E.S., Waanders, G.A., Masciantonio, M., Godfrey, D.I. and Boyd, R.L. 1993. A lymphostromal molecule, thymic shared Ag-1, regulates early thymocyte development in fetal thymus organ culture. J. Immunol.l 151(11): 6027-6035.

Randle-Barrett, E.S. and Boyd, R.L. 1995. Thymic microenvironment and lymphoid responses to sublethal irradiation. Dev. Immunol.l 4(2): 101-16.

Reecy, J.M., Yamada, M., Cummings, K., Sosic, D., Chen, C.-Y., Eichele, G., Olson, E.N. and Schwatz, R.J. 1997. Chicken Nkx-2.8: A novel homeobox gene expressed in early heart progenitor cells and pharyngeal pouch-2 and -3 endoderm. Dev. Biol.l 188: 295-311.

Reza, J.N. and Ritter, M.A. 1994. Differential expression of adhesion molecules within the human thymus. Dev. Immunol.l 4(1): 55-64.

Ritter, M.A. and Boyd, R.L. 1993. Development in the thymus: it takes two to tango. Immunol. Todayl 14(9): 462 - 469.

Ritter, M.A. and Palmer, D.B. 1999. The human thymic microenvironment: new approaches to functional analysis. Semin. Immunol.l 11(1): 13-21.

Ritter, M.A., Schuurman, H.J., MacKenzie, W.A., de Maagd, R.A., Price, K.M., Broehuizen, R. and Kater, L. 1985. Heterogeneity of human thymus epithelial cells revealed by monoclonal anti-epithelial cell antibodies. Adv. Exp. Med. Biol.l 186: 283-288.

Robb, L. and Begley, C.G. 1997. The SCL/TAL1 gene: roles in normal and malignant haematopoiesis. Bioessaysl 19(7): 607-613.

Ropke, C., van Soest, P., Platenburg, P.P. and van Ewijk, W. 1995. A common stem cell for murine cortical and medullary thymic epithelial cells? Dev. Immunol.l 4: 149 - 156.

Rouse, R.V., van Ewijk, W., Jones, P.P. and Weissman, I.L. 1979. Expression of MHC antigens by mouse thymic dendritic cells. J. Immunol.l 122: 2508 - 2515.

Savino, W. and Dardenne, M. 1988. Developmental studies on expression of monoclonal antibody defined cytokeratins by thymic epithelial cells from normal and autoimmune mice. J. Histochem. Cytochem.l 36: 1123 - 1129.

Savino, W., Villa-Verde, D.M. and Lannes-Vieira, J. 1993. Extracellular matrix proteins in intrathymic T-cell migration and differentiation? Immunol. Todayl 14(4): 158-61.

Sawada, M., Nagamine, J., Takeda, K., Utsumi, K., Kosugi, A., Tatsumi, Y., Hamaoka, T., Miyake, K., Nakajima, K., Watanabe, T., Sakakibara, S. and Fujiwara, H. 1992. Expression of VLA-4 on thymocytes. Maturation stage-associated transition and its correlation with their capacity to adhere to thymic stromal cells. J. Immunol.l 149(11): 3517-24.

Schlake, T., Schorpp, M., Maul-Pavicic, A., Malashenko, A.M. and Boehm, T. 2000. Forkhead/winged-helix transcription factor whn regulates hair keratin gene expression: molecular analysis of the nude skin phenotype. Dev. Dyn.l 217(4): 368-376.

Schlake, T., Schorpp, M., Nehls, M. and Boehm, T. 1997. The nude gene encodes a sequence-specific DNA binding protein with homologs in organisms that lack an anticipatory immune system. Proc. Natl. Acad. Sci. USAl 94(8): 3842-7.

Schmidt-Ullrich, R., Memet, S., Lilienbaum, A., Feuillard, J., Raphael, M. and Israel, A. 1996. NF-κB activity in transgenic mice: developmental regulation and tissue specificity. Developmentl 122: 2117-2128.

Schorpp, M., Hofmann, M., Dear, T.N. and Boehm, T. 1997. Characterization of mouse and human nude genes. Immunogeneticsl 46(6): 509-15.

Schuddekopf, K., Schorpp, M. and Boehm, T. 1996. The whn transcription factor encoded by the nude locus contains an evolutionarily conserved and functionally indispensable activation domain. Proc. Natl. Acad. Sci. USAl 93(18): 9661-4.

Schuler, W., Weiler, I.J., Schuler, A., Philips, R.A., Rosenberg, N., Mak, T.W., Kearney, J.F., Perry, R.P. and Bosma, M.J. 1986. Rearrangement of antigen receptor genes is defective in mice with severe combined immunodeficiency. Celll 46: 963-972.

Seed, B. and Aruffo, A. 1987. Molecular cloning of the CD2 antigen, the T-cell erythrocyte receptor, by a rapid immunoselection procedure. Proc. Natl. Acad. Sci. USAl 84: 3365 - 3369.

Segre, J.A., Nemhauser, J.L., Taylor, B.A., Nadeau, J.H. and Lander, E.S. 1995. Positional cloning of the nude locus: genetic, physical, and transcription maps of the region and mutations in the mouse and rat. Genomicsl 28(3): 549-59.

Shinkai, Y., Rathbun, G., Lam, K.-P., Oltz, E.M., Stewart, V., Mendelsohn, M., Charron, J., Datta, M., Young, F., Stall, A.M. and Alt, F.W. 1992. RAG-2-deficient mice lack mature lymphocytes owing to inability to initiate V(D)J rearrangements. Celll 68: 855-867.

Shinohara, T. and Honjo, T. 1996. Epidermal growth factor can replace thymic mesenchyme in induction of embryonic thymus morphogenesis *in vitro*. Eur. J. Immunol.l 26: 747-752.

Shinohara, T. and Honjo, T. 1997. Studies in vitro on the mechanism of the epithelial/mesenchymal interaction in the early fetal thymus. Eur. J. Immunol.l 27: 522 - 529.

Shores, E.W., van Ewijk, W. and Singer, A. 1991. Disorganisation and restoration of thymic medullary epithelial-cells in T-cell receptor-negative SCID mice - evidence that receptor-bearing lymphocytes influence maturation of the thymic microenvironment. Eur. J. Immunol.l 21(7): 1657 - 1661.

Shores, E.W., Van Ewijk, W. and Singer, A. 1994. Maturation of medullary thymic epithelium requires thymocytes expressing fully assembled CD3-TCR complexes. Int. Immunol.l 6(9): 1393-1402.

Shortman, K. and Wu, L. 1996. Early T lymphocyte progenitors. Annu. Rev. Immunol.l 14: 29 - 47.

Simmons, D.L. (1993). Cloning cell surface molecules by transient expression in mammalian cells. Cellular interactions in development. D.A. Hartley, IRL Press: 93-127.

Slack, J.M.W. 2000. Stem cells in epithelial tissues. Sciencel 287: 1431-1433.

Smith, C. 1965. Studies on the thymus of the mammal XIV. Histology and histochemistry of embryonic and early postnatal thymuses of C57Bl/6 and AKR strain mice. Am. J. Anat.l 116: 611-630.

Snyder, E.Y. and Vescovi, A.L. 2000. The possibilities/perplexities of stem cells. Nature Biotech.l 18: 827-828.

Steinmann, G.G., Klaus, B. and Muller-Hermelink, H.K. 1985. The involution of the ageing human thymic epithelium is independent of puberty. A morphometric study. Scand. J. Immunol.l 22(5): 563-575.

Su, D.-M. and Manley, N.R. 2000. Hoxa3 and Pax1 transcription factors regulate the ability of fetal thymic epithelial cells to promote thymocyte development. J. Immunol.l 164: 5753-5760.

Sugimura, I., Adachi-Yamada, T., Nishi, Y. and Nishida, Y. 2000. A Drosophilia winged-helix nude (Whn)-like transcription factor with essential functions throughout development. Develop. Growth Differ.l 42: 237-248.

Sun, T.-T., Shih, C. and Green, H. 1979. Keratin cytoskeletons in epithelial cells of internal organs. Proc. Natl. Acad. Sci. USAl 76(6): 2813 - 2817.

Suniara, R.K., Jenkinson, E.J. and Owen, J.J. 1999. Studies on the phenotype of migrant thymic stem cells. Eur. J. Immunol.l 29(1): 75-80.

Suniara, R.K., Jenkinson, E.J. and Owen, J.J.T. 2000. An essential role for thymic mesenchyme in early T cell development. J. Exp. Med.l 191(6): 1051-1056.

Surh, C.D., Ernst, B. and Sprent, J. 1992. Growth of epithelial cells in the thymic medulla is under the control of mature T cells. J. Exp. Med.l 176(2): 611-6.

Surh, C.D., Gao, E.K., Kosaka, H., Lo, D., Ahn, C., Murphy, D.B., Karlsson, L., Peterson, P. and Sprent, J. 1992. Two subsets of epithelial cells in the thymic medulla. J. Exp. Med.l 176(2): 495-505.

Thomson, A.W., Pugh-Humphreys, R.G.P. and Woo, J. 1991. The influence of FK506 on the thymus - Implications of drug-induced injury to thymic epithelial cells. Transplantation proceedings.l 23(1): 947 - 948.

Ting, C.-N., Olson, M.C., Barton, K.P. and Leiden, J.M. 1996. Transcription factor GATA-3 is required for development of the T-cell lineage. Naturel 384: 474-478.

Tseng, S.C.G., Jarvinen, M.J., Nelson, W.G., Huang, J.-W., Woodcock-Mitchell, J. and Sun, T.-T. 1982. Correlation of specific keratins with different types of epithelial differentiation: Monoclonal antibody studies. Celll 30: 361 - 372.

Tucek, C.L. and Boyd, R.L. 1990. Surface expression of CD4 and Thy-1 on mouse thymic stromal cells. Int. Immunol.l 2: 593 - 601.

Utsumi, K., Sawada, M., Narumiya, S., Nagamine, J., Sakata, T., Iwagami, S., Kita, Y., Teraoka, H., Hirano, H., Ogata, M. and et al. 1991. Adhesion of immature thymocytes to thymic stromal cells through fibronectin molecules and its significance for the induction of thymocyte differentiation. Proc. Natl. Acad. Sci. USAl 88(13): 5685-9.

van de Wijngaert, F.P., Kendall, M.D., Schuurman, H.J., Rademakers, L.H.M.P. and Kater, L. 1984. Heterogeneity of human thymus epithelial cells at the ultrastructural level. Cell Tiss Res.l 237: 227 - 237.

van Ewijk, W. 1991. T-cell differentiation is influenced by thymic microenvironments. Annu. Rev. Immunol.l 9: 591 - 615.

van Ewijk, W., De Kruif, J., Germeraad, W.T.V., Berendes, P., Ropke, C., Plantenburg, P.P. and Logenberg, T. 1997. Subtractive isolation of phage-displayed single-chain antibodies to thymic stromal cells by using intact thymic fragments. Proc. Natl. Acad. Sci. USAl 94: 3903 - 3908.

van Ewijk, W., Hollander, G., Terhorst, C. and Wang, B. 2000. Stepwise development of thymic microenvironments in vivo is regulated by thymocyte subsets. Developmentl 127: 1583-1591.

van Ewijk, W., Rouse, R.V. and Weissman, I.L. 1980. Distribution of H-2 microenvironments in the mouse thymus. Immunoelectron microscopic identification of I-A and H-2K bearing cells. J. Histochem. Cytochem.l 28: 1089 - 1099.

van Ewijk, W., Shores, E.W. and Singer, A. 1994. Crosstalk in the mouse thymus. Immunol. Todayl 15(5): 214 - 217.

van Ewijk, W., Wang, B., Hollander, G., Kawamoto, H., Spanopoulou, E., Itoi, M., Amagai, T., Jiang, Y.F., Germeraad, W.T., Chen, W.F. and Katsura, Y. 1999. Thymic microenvironments, 3-D versus 2-D? Semin. Immunol.l 11(1): 57-64.

van Genderen, C., Okamura, R.M., Farinas, I., Quo, R.G., Parslow, T.G., Bruhn, L. and Grosschedl, R. 1994. Development of several organs that require inductive epithelial-mesenchyml interations is impaired in LEF-1-deficient mice. Genes Dev.l 8(22): 2691-2703.

van Vliet, E., Jenkinson, E.J., Kingston, R., Owen, J.J.T. and van Ewijk, W. 1985. Stromal cell types in the developing thymus of the normal and nude mouse embryo. Eur. J. Immunol.l 15: 675-681.

van Vliet, E., Melis, M. and van Ewijk, W. 1984. Monoclonal-antibodies to stromal cell-types of the mouse thymus. Eur. J. Immunol.l 14(6): 524 - 529.

Vicari, A., Abehsira-Amar, O., Papiernik, M., Boyd, R.L. and Tucek, C.L. 1994. MTS-32 monoclonal antibody defines CD4+8- thymocyte subsets that differ in their maturation level. lymphokine secretion and selection patterns. J. Immunol.l 152: 2207 - 2213.

von Boehmer, H. 1988. The developmental biology of T lymphocytes. Ann. Rev. Immunol.l 6: 309 - 326.

von Freeden-Jeffry, U., Vieira, P., Lucian, L.A., McNeil, T., Burdach, S.E.F. and Murray, R. 1995. Lymphopenia in Interleukin (IL)-7 gene-deleted mice identifies IL-7 as a nonredundant cytokine. J. Exp. Med.l 181: 1519-1526.

von Gaudecker, B. 1991. Functional histology of the human thymus. Anat. Embryol.l 183(1): 1-15.

Von Gaudecker, B., Kendall, M.D. and Ritter, M.A. 1997. Immuno-electron microscopy of the thymic epithelial microenvironment. Microsc. Res. Tech.l 38(3): 237-49.

Wadsworth, S., Halvorson, M.J., Chang, A.C. and Coligan, J.E. 1993. Multiple changes in VLA protein glycosylation, expression, and function occur during mouse T cell ontogeny. J. Immunol.l 150(3): 847-857.

Wall, N. and Hogan, B.L.M. 1995. Expression of bone morphogenetic protein-4 (BMP-4), bone morphogenetic protein-7 (BMP-7), fibroblast growth factor-8 (FGF-8) and sonic hedgehog (SHH) during branchial arch development in the chick. Mechanisms of developmentl 53: 383-392.

Wallin, J., Eibel, H., Neubuser, A., Wilting, J., Koseki, H. and Balling, R. 1996. Pax1 is expressed during development of the thymus epithelium and is required for normal T-cell maturation. Developmentl 122: 22 - 30.

Wang, B., Biron, C., She, J., Higgins, K., Sunshine, M.-J., Lacy, E., Lonberg, N. and Terhorst, C. 1994. A block in both early T lymphocyte and natural killer cell development in transgenic mice with high-copy numbers of the human CD3ε gene. Proc. Natl. Acad. Sci. USAl 91: 9402-9406.

Watt, F.M. 1998. Epidermal stem cells: markers, patterning and the control of stem cell fate. Philos. Trans. R. Soc. Lond. B. Biol. Scil 353(1370): 831-837.

Watt, F.M. and Hogan, B.L.M. 2000. Out of eden: Stem cells and their niches. Sciencel 287: 1427-1430.

Weih, F., Carrasco, D., Durham, S.K., Barton, D.S., Rizzo, C.A., Ryseck, R.P., Lira, S.A. and Bravo, R. 1995. Multiorgan inflammation and hematopoietic abnormalities in mice with a targeted disruption of RelB, a member of the NF-kappa B/Rel family. Celll 80(2): 331-40.

Weissman, I.L. 2000. Translating stem and progenitor cell biology to the clinic: barriers and opportunities. Sciencel 287: 1442-1446.

Wekerle, H., Ketelsen, U.-P. and Ernst, M. 1980. Thymic nurse cells: Lymphoepithelial cell complexes in murine thymuses: Morphological and serological characterisation. J. Exp. Medl 151: 925 - 944.

Wekerle, H. and Ketelsen, U.P. 1980. Thymic nurse cells - Ia-bearing epithelium involved it T-lymphocyte differentiation? Naturel 283: 402 - 404.

Weller, G.L. 1933. Development of the thyroid, parathyroid, and thymus glands in man. Carnegie Inst. Wash. Publ.n. 443 Contrib. Embryol.l 24: 93-143.

Wilkinson, B., Owen, J.J. and Jenkinson, E.J. 1999. Factors regulating stem cell recruitment to the fetal thymus. J. Immunol.l 162(7): 3873-81.

Wilkinson, R.W., Anderson, G., Owen, J.J.T. and Jenkinson, E.J. 1995. Positive selection of thymocytes involves sustained interactions with the thymic microenvironment. J. Immunol.l 155: 5234 - 5240.

Willcox, N., Schluep, M., Ritter, M.A., Schuurman, H.J., Newsom-Davis, J. and Christensson, B. 1987. Myasthenic and nonmyasthenic thymoma. An expansion of a minor cortical epithelial cell subset? Am. J. Pathol.l 127(3): 447-460.

Wilson, T.J., Davidson, N.J., Boyd, R.L. and Gershwin, M.E. 1992. Phenotypic analysis of the chicken thymic microenvironment during ontogenic development. Dev. Immunol.l 2: 19 - 27.

Winnier, G., Blessing, M., Labosky, P.A. and Hogan, B.L. 1995. Bone morphogenetic protein-4 is required for mesoderm formation and patterning in the mouse. Genes Devl 9(17): 2105-16.

Wolfer, A., Bakker, T., Wilson, A., Nicolas, M., Ioannidis, V., Littman, D.R., Wilson, C.B., Held, W., MacDonald, H.R. and Radtke, F. 2001. Inactivation of Notch1 in immature thymocytes does not perturb CD4 or CD8 T cell development. Nature Immunologyl 2(3): 235-241.

Wu, L., Antica, M., Johnson, G.R., Scollay, R. and Shortman, K. 1991. Developmental potential of the earliest precursor cells from the adult mouse thymus. J. Exp. Med.l 174(6): 1617-27.

Wu, L., Kincade, P.W. and Shortman, K. 1993. The CD44 expressed on the earliest intrathymic precursor population functions as a thymus homing molecule but does not bind to hyaluronate. Immunol. Lett.l 38: 69-75.

Wu, L., Scollay, R., Egerton, M., Pearse, M., Spangrude, G.J. and Shortman, K. 1991. CD4 expressed on earliest T-lineage precursos cells in the adult murine thymus. Naturel 349: 71-74.

Young, I.T. 1977. Proof without prejudice: use of the kolmogorov-smirnov test for the analysis of histograms from flow systems and other sources. J. Histochem. Cytochem.l 25(7): 935-941.

Zhu, A.J. and Watt, F.M. 1999. Beta catenin signalling modulates proliferative potential of human epidermal keratinocytes independently of intercellular adhesion. Developmentl 127: 2285-2298.

Zinkernagel, R.M., Althage, A., Waterfield, E., Kindred, B., Welsh, R.M., Callahan, G. and Pincetl, P. 1980. Restriction specificities, alloreactivity, and allotolerance expressed by T cells from nude mice reconstituted with H-2-compatible or - incompatible thymus grafts. J. Exp. Med.l 151: 376-399.